CHARACTERISING THE PHENOTYPE AND FUNCTION OF NATURAL KILLER CELLS IN PATIENTS WITH PROSTATE CANCER

SIMON HOOD

A thesis submitted in partial fulfilment of the requirements of Nottingham Trent University for the degree of Doctor of Philosophy

December 2016

Acknowledgements

After four long, hard years I have finally reached the point where so many PhD students that have gone before me have reached: The submission of the thesis! It's done! It's written! Victory celebration for me! Celebration now over I would now like to take this opportunity to thank everybody at the John van Geest Cancer Research Centre for all the support they have given me over the years. It is truly appreciated.

Firstly, I would like to thank my supervisors Prof A. Graham Pockley and Prof Robert Rees for giving me the opportunity to work on this project. After attending many interviews for PhD projects over the years I'm really glad that I ended up with this one. I truly think this was the right PhD project for me and enjoyed working it. Thank you for giving me the freedom but yet guidance to develop the project using my ideas. On this basis, a special thank you to my third supervisor Dr Stéphanie McArdle for all the technical support you have given me and the freedom to have theoretical chats and debates with you, they have been a positive influence on this project.

I would also like to thank Mr Masood Khan and Mr Shady Nafie, not only for the clinical samples but also for the clinical knowledge that you have given me in regards to prostate cancer. On a number of occasions I have bombarded you both with questions in regards to the clinical aspects of the project and you have always patiently answered them.

Thank you to all the staff at the John van Geest Cancer Research Centre for making this such a fun supportive place to work. Thank you to the research fellows Dr Jayakumar Vadakekolathu and Dr Gemma Foulds for both the scientific support and just as important non-scientific support and conversations that we have had. I very much enjoy working alongside you both. Thank you to the Senior Research Fellows, Dr Amanda Miles and in particular Dr David Boocock and Dr Tarik Regad for your support, political conversations and career advice over the years. Notes have been taken!

A special thanks to the technical team Stephen Reeder, Anne Schneider, Catherine Johnson and Clare Coveney for your support. This Centre does not function without you. Thank you to Steve for processing those last minute orders that you hate so much before you go on holiday. I really did appreciate it. Thank you to Anne for keeping the labs so well stocked and clean (and encouraging me not to fall into bad habits by pinching plastic ware from other labs). Thank you to Cathy for your help with the flow cytometry work and helping me to stay organised. All your efforts made a real difference to how easily I could do my lab work, I really appreciate it.

To my fellow PhD students, for each one of us there has been good times and bad times, but always we stand united, supporting each other and I thank you for being there for me. Special recognition goes to Matthew Nicklin, Devika Agarwal, Magdalena Buczek, and Divya Nagarajan as we have been together the longest.

Finally, but by no means least, a very very special thank you to my partner Dr Jessica Dale for all your support, patience, guidance and, when I deserve, it love. I really appreciate all the patience you have shown when staying sometimes very late at work waiting for me to finish my lab work. It's not easy living with someone who is a PhD student, often you have to give a lot of support and sometimes compromise on other aspects of life and you have ended up doing that more for me than I did for you in the past. I'm lucky to have you. Hopefully now we will see the fruits of our labours!

Abstract

Background: The detection and diagnosis of prostate cancer was greatly improved with the introduction of the prostate specific antigen (PSA) test and the transrectal ultrasound prostate (TRUS) biopsy. However, PSA levels above the normal range in the blood are not necessarily indicative of prostate cancer and the TRUS biopsy, which provides limited access to the prostate outside of the peripheral zone, only delivers a positive detection rate of ~30 %. Although the recently developed transperineal biopsy (TP) method, which is capable of detecting cancer in all regions of the prostate, has improved the positive detection rate to ~60 %, this technique is expensive and not widely available. The development of new, non-invasive approaches for detecting the presence of prostate cancer would greatly inform and assist the management of individuals who are suspected of having prostate cancer.

Aim and hypothesis: Evading immune destruction is one of the emerging hallmarks of cancer, as part of which tumours create an immunosuppressive microenvironment which has the potential to modify the phenotype and function of immune cells such as natural killer (NK) cells. The aim of the study is to assess whether alterations in the phenotype and function of NK cells induced by the presence of prostate cancer can be detected in the periphery and be used as parameters for aiding diagnosis and assessing disease progression. The underlying hypothesis of this study was that the presence of prostate cancer would induce detectable changes in the phenotype and function of NK cells in the periphery and that the detection of these would improve the diagnosis and prognosis of prostate cancer.

Methods: Samples were obtained from two cohorts of patients. Patients in the 'TRUS' cohort (n=92) were diagnosed using the TRUS biopsy only, whereas patients in the TP cohort (n=72) were biopsy naïve, had a PSA level of <20ng.ml^{-1} and underwent simultaneous TRUS (12 cores) and TP biopsies (36 cores). Peripheral blood mononuclear cells (PBMCs) from patients who were defined as having benign disease (Benign, HGPIN, ASAP) or Gleason Grades 6 to 9 disease were analysed for the expression of antigens defining T, B and NK cells (CD3, CD8, CD19, CD56), and NK cell inhibitory (CD85j, NKG2A, LAIR-1) and activation (DNAM-1, NKG2D, NKp30, NKp44, NKp46, 2B4) receptors by flow cytometry.

The influence of prostate cancer on NK cell functional potential was determined by comparing the phenotypes of NK cells that had been 'primed' by co-incubation with CTV-1 human leukaemic cells (a process which was shown to enhance the capacity of NK cells from healthy individuals to kill NK cell 'resistant PC3 prostate cancer cells) from patients with Gleason grades 6 or 9 disease with those of NK cells from individuals with benign disease and volunteers with no known disease. All of these studies were supported by extensive methodology development.

Results and conclusions: Compared to Gleason 6 patients, a reduced expression of NK cell activating receptors (NKp30, NKp46, 2B4) was observed as the Gleason grade of the patients increased. These patients could not be phenotypically distinguished from patients with benign disease. This suggests that these markers may only have potential for use as biomarkers of progression, not diagnosis. Limited investigations into the ability of NK cells from patients to be primed only found phenotypic differences between healthy volunteers and patients in general (regardless of the presence of disease). Priming of NK cells from patients induced a lower induction of CD137 and CRTAM expression, and a greater down-regulation of NKp46 and CD96 expression compared to that which was observed following the priming of NK cells from healthy volunteers. Although further investigation is needed, no evidence of an immunosuppressive effect by prostate cancer on the phenotype and function of peripheral NK cells was observed in this study.

Table of Contents

List of Figures

List of Tables

Abbreviations

ADAM	A Disintegrin and Metalloproteinase
ADCC	Antibody dependent Cell-mediated Cytotoxicity
ADT	Androgen Deprivation Therapy
AML	Acute Myeloid Leukaemia
ASAP	Atypical Small Acrinar Proliferation
ATP	Adenosine Triphosphate
B-CLL	B cell Chronic Lymphocytic Leukaemia
BiKEs	BiSpecific Killer cell Engagers
CCL	C-C motif ligand
CD	Cluster of Differentiation
cDNA	complement Deoxyribose Nucleic Acid
CRTAM	Cytotoxic and Regulatory T cell Molecule
CSF	Colony Stimulating Factors
CXCL	C-X-C motif Chemokine
DMSO	Dimethyl Sulphoxide
DNA	Deoxyribose Nucleic Acid
DNAM-1	DNAX Accessory Molecule 1
DRE	Digital Rectal Examination
EBRT	External Beam Radiation Therapy
ELISA	Enzyme Linked Immunosorbant Assay
FAP	Fibroblast Growth Factor
FBS	Fetal Bovine Serum
FcR	Fc Recptor
FGF	Fibroblast Growth Factor
FL	Fluorescence
FSc	Forward Scatter
GITR	Glucocorticoid-induced TNFR related protein
H&E	Hematoxylin and Eosin
HGF	Hepatocyte Growth Factor
HGPIN	High Grade Prostatic Intraepithelial Neoplasia
HLA	Human Leukocyte Antigen
ICAM	Intracellular Adhesion Molecule
IDO	Indoleamine Pyrrole 2,3-dioxygenase
IFN-γ	Interferon Gamma
IGF	Insulin Growth Factor
IL	Interleukin
IMRT	Image guided Intensity Modulated Radiation Therapy
KIR	Killer-cell Immunoglobulin-like Receptor
LAIR-1	Leukocyte-associated immunoglobulin-like receptor 1
LAMP	Lysosome asscociated Membrane Protein
LFA	Lymphocyte function-associated antigen
L-Glut	L-Glutamine
M-CSF	Macrophage Colony Stimulating Factor
MDSCs	Myeloid Derived Suppressor cells
MFI	Median Fluorescence Intensity
MHC	Major Histocompatibility Complex
MICA	MHC class I polypeptide-related sequence A

MICB	MHC class I polypeptide-related sequence B
MIP1α	Macrophage Inflammatory Protein 1-alpha
MIP1β	Macrophage Inflammatory Protein 1-Beta
MMPs	Matrix Metalloproteinases
MRI	Magnetic Resonance Imaging
MTG	Mitotracker Green dye
MTOC	Microtubule Organising Centre
NCAM	Neural Cell Adhesion Molecule
NCR	Natural cytotoxicity Receptor
NF-κB	Nuclear Factor-κB
NK	Natural Killer
NKG2	Natural killer group 2
NKp	Natural killer protein
NOD SCID	Nonobese diabetic severe combined immunodeficiency
NOS	Nitric oxide Synthase
PBMC	Peripheral Blood Mononuclear Cell
PBS	Phosphate Buffered Saline
PCNA	Proliferating Cell Nuclear Antigen
PD-1	Program Death Receptor 1
PDGF	Platelet derived Growth Factor
PGE_2	Prostaglandin E_2
PI	Propidium Iodide
PSA	Prostate specific Antigen
RANTES	Regulated on Activation Normal T cell Expressed and Secreted
RT	Room Temperature
SARMs	Selective Androgen Receptor Modulators
SD	Standard deviation
SHP	Src homology region 2 domain-containing phosphatase
SSc	Side Scatter
STAT3	Signal Transducer annd Activator of Transcription
STDs	Sexually Transmitted Infections
TAF	Tumour Associated Fibroblasts
TAM	Tumour Associated Macrophages
TAN	Tumour Associated Neutrophils
TGF-β	Transforming Growth Factor Beta
TNFRSF	Tumour Necrosis Factor Receptor Superfamily
TNF-α	Tumour Necrosis Factor Alpha
TP	Transperineal
TPTPB	Transperineal Template Prostate Biopsy
TRAIL	TNF-related Apoptosis inducing Ligand
Tregs	Regulatory T cells
TriKEs	TriSpecific Killer cell Engagers
TRUS	Transrectal Ultrasound guided prostate
UTIs	Urinary Tract Infections
VEGF	Vascular Endothelial Growth Factor
3D-CRT	Three Dimensional Conformal Radiation Therapy

1. Introduction

1.1 Prostate cancer

1.1.1 The prostate gland and its function

The prostate is a gland which surrounds the prostatic urethra and is located underneath the bladder. Initially the prostate grows slowly until puberty starts, at which time it grows rapidly. Between the ages of 30 and 45, the size of the prostate remains relatively stable, after which point it may progressively enlarge with time. The prostate secretes a milky, slightly acidic fluid which makes up about 25 % of the volume of semen, and this seminal fluid contributes to sperm motility and viability. Prostate secretions contain several important substances such as citric acid (used by sperm to produce ATP), proteolytic enzymes such as prostate-specific antigen (PSA) and acid phosphatase (Tortora and Grabowski, 2003).

1.1.2 Incidence of Prostate Cancer

According to the most update information, prostate cancer is the second most common cancer in men worldwide with an estimated 1.1 million new cases in 2012 (Torre et al., 2015). In the more developed countries, prostate cancer is the most frequently diagnosed cancer in men (Torre et al., 2015). In Europe, 417,000 new cases of prostate cancer was diagnosed in 2012 and the incidence in the UK was the 17th highest in Europe (CRUK., 2013). Based on the latest World Health Organisation (WHO) statistics, 45,406 men were diagnosed with prostate cancer with 12,082 men dying from the disease (WHO, 2014). The incidence of prostate cancer rose by 155 % between 1979 and 2013 (CRUK., 2013). Although this is, in part at least, due to improved diagnostic techniques, even within the last decade prostate cancer incidence has risen by 5 % (CRUK., 2013). Prostate cancer appears to be an age-related disease, with the age-specific incidence rates increasing sharply from the age group 50-54 yrs, to peak within the 75-79 age group. This has resulted in more than half of newly diagnosed cases (54 %) being in men aged over 70 yrs. Overall, 1 in 8 men will develop prostate cancer in their lifetime. However, black men of African / Caribbean heritage are at a higher risk of developing prostate cancer (1 in 4 men will be diagnosed), with age standardised rates for black men at 120.8 to 247.9 per 100,000, in contrast to that of 96-99.9 per 100,000 for Caucasian men. Furthermore, the disease in black men also appears to be more aggressive, as twice as many black men die of prostate cancer than their Caucasian counterparts (CRUK., 2013). The age-standardised rates appear to be the lowest in Asian men at 28.7 to 60.6 per 100,000 (CRUK., 2013).

1.1.3 Types of prostate cancer

Although prostate cancer is typically a slow growing disease, it presents as a more aggressive disease and can grow more quickly in a small percentage of patients (CRUK., 2013). The most common type of prostate cancer is acinar adenocarcinoma, with this form of the disease being present in 90 % of patients. Although there are architectural and cytological variations of acinar adenocarcinoma such as atrophic, pseudohyperplastic, foamy gland, colloid and signet-ring, oncocytic and lymphoepithelioma, these pathologic variants have no known prognostic significance (Mazzucchelli et al., 2008). Unusual histological prostatic carcinomas which include small cell carcinoma, ductal adenocarcinoma, sarcomatoid carcinoma, basal cell, squamous cell, adenosquamous carcinoma and urothelial carcinoma make up the rest of the detected prostate carcinomas. These are aggressive variants of prostate cancer and are associated with poor prognosis (Mazzucchelli et al., 2008).

1.1.4 Diagnosis and Grading of Prostate Cancer

1.1.4.1 Digital Rectal Examination

Prior to the development of the Prostate-Specific Antigen (PSA) test and the Trans Rectal Ultrasound guided prostate (TRUS) biopsy technique, both of which are described in more detail below, the digital rectal examination (DRE) was the most widely used screening test to detect prostate cancer, with 40 – 50 % of all palpable, 'suspicious' prostates harbouring biopsy-detected cancer (Chodak et al., 1989) However, the ability to detect prostate cancer via the DRE depends on the skill and experience of the examiner, with variabilities across different examiners having been reported (Smith and Catalona, 1995). The inclusion of the DRE test in prostate cancer screening has been the subject of debate (Yossepowitch, 2008). Studies have shown that the DRE test has a low positive predictive value in men with low PSA levels <4 ng/ml. The argument is that if cancer is indeed present in these patients, then it is often non-aggressive and non-life threatening with the DRE test itself being unpleasant and potentially unnecessary (Schröder et al., 1998). However, other studies have shown that a significant proportion of patients with abnormal DRE results and a PSA level < 4 ng/ml had Gleason grade >7 cancer (see below) (Gosselaar et al., 2008, Okotie et al.). It is thought that patients with abnormal DRE results are at higher risk of harbouring high-grade disease and some clinicians argue that the DRE test should be used in conjunction with PSA test (Gosselaar et al., 2008, Yossepowitch, 2008).

1.1.4.2 Gleason score and overall grade

The Gleason grading system was devised by Dr Donald Gleason in 1974 who, at the time, was Chief of Pathology at the Veterans Hospital in Minnesota (Gleason and Mellinger, 1974). Based on a study of roughly 5000 patients, Dr Gleason created a grading system for prostate cancer which was based on different histologic patterns, as could be identified using Haematoxylin & Eosin (H&E) stained prostatic tissue sections. He identified five prognostic patterns, and identified that most tumours had two histologic patterns. He therefore decided to add the two most common grades together to create a composite score which correlated with clinical stage, metastatic progression and overall survival. Although the Gleason scores originally ranged between 2 and 10 (Gleason and Mellinger, 1974, Gordetsky and Epstein, 2016, Humphrey, 2004), the grading system has undergone numerous revisions, with the most recent revision following the 2014 International Society of Urological Pathology Consensus Conference on Gleason Grading or Prostatic Carcinoma (Epstein et al., 2016). Currently, the original Gleason grade patterns 1 and 2 are now no longer assigned based on needle biopsy due to poor reproducibility and poor correlation with radical prostatectomy grade. The consequence of this revision is that Gleason scores 2 to 5 are no longer reported. Gleason score 6 is now recommended as the lowest Gleason score to be assigned to prostate biopsies, and is associated with the best prognosis (Gordetsky and Epstein, 2016). Current histological patterns are summarised in Table 1.1. In contrast to the original Gleason grading system, the Gleason score is now calculated as the grade of the most common cancer added to the highest Gleason grade of the remaining cancer (Gordetsky and Epstein, 2016).

Table 1.1 Current Gleason grades and their associated histological pattern.

Gleason grade	Histological pattern determined by H&E staining of prostate biopsy sections
3	Well-formed, individual glands of various sizes including branching glands. The glands should form discrete units. Small glands are acceptable providing as they are well formed and not fused.
4	Poorly formed, fused and cribriform glands. Glomeruloid morphology characterised by dilate glands containing intraluminal cribriform structures with a single point of attachment, resembling a renal glomerulus.
5	Sheets of tumour, individual cells and cords of cells. Solid nests of cells with vague microacinar or only occasional gland space formation. Includes uncommon morphological patterns consisting of comedonecrosis within solid nests or cribriform glands.

Information taken from (Gordetsky and Epstein, 2016)

If histologically-defined cancer is not found in the prostate, then the tissue is referred to as being 'benign'. However, this does not necessarily mean the tissue is normal. Instead, it could mean that there are tissue abnormalities, but that these abnormalities are not considered to be cancerous / malignant. Two abnormalities that are commonly recorded are high grade prostatic intraepithelial neoplasia (HGPIN) and atypical small acinar proliferation (ASAP). HGPIN is essentially where the epithelial cells lining the acini and ducts become abnormal, but crucially remain intact (unlike in prostate cancer). ASAP is the proliferation of usually small acini with features highly suggestive, but not diagnostic for carcinoma (www.harvardprostateknowledge.org). The current recommendation is to re-biopsy patients diagnosed with ASAP, as studies have shown that 51.9 % of patients have cancer upon repeat biopsy, as compared to 21.9 % of patients with HGPIN (Amin et al., 2007, El-Hakim and Moussa, 2010).

1.1.4.2.1 TNM stages of prostate cancer

The staging of cancer is based on the TNM classification system which is used globally (AJCC, 2009). The TNM classification system for prostate cancer is applied as follows:

The T stage measures the stage of the tumour:

T1 = the cancer cannot be felt by DRE or seen by MRI scan and can only be seen under a microscope following a needle biopsy

T2 = the cancer can be felt by DRE / seen by MRI and is contained within the prostate.

T2a = the tumour is in only half of one of the lobes of the prostate.

T2b = the tumour is in more than one half of one of the lobes of the prostate.

T2c = the tumour is in both lobes but is still within the prostate.

T3 = the cancer can be felt / seen breaking though the prostate capsule, but has not spread to other organs.

T3a = the tumour has broken through the prostate capsule, but has not spread to the seminal vesicles.

T3b = the tumour has broken through the prostate capsule and has spread to the seminal vesicles

T4 = the cancer has spread to nearby organs e.g. bladder, rectum, muscles or the sides of the pelvic cavity

The N stage indicates if the cancer has spread to the lymph and is measured using a MRI or CT scan:

NX = the lymph nodes cannot be checked

N0 = cancer has not spread to lymph nodes

N1 = cancer has spread to the lymph nodes

The M stage indicates whether the cancer has metastasised to other parts of the body e.g. bones.

M0 = cancer has not spread outside of the pelvis

M1 = cancer has spread outside of the pelvis

M1a = cancer cells in lymph nodes outside of the pelvis

M1b = cancer cells present in the bone

M1c = cancer cells have spread to other areas of the body

Based on the staging of the prostate cancer within the patient using the above criteria, clinicians refer to the location of the prostate cancer by stating whether it is localised prostate cancer (cancer contained within the prostate), locally-advanced prostate cancer (cancer has broken through the prostate capsule), or metastatic prostate cancer (cancer has spread to other parts of the body e.g. lymph nodes) (CRUK., 2013, PCUK, 2013)

1.1.4.2.2 D'Amico classification system

The D'Amico classification system (D'Amico et al., 1998) is used to reflect the likelihood that the cancer will reoccur following treatment. There are three groups:

Low risk – patients who have a PSA 10 ng/ml or less **plus** a Gleason score of 6 or less **and** have a stage T1 or T2a cancer.

Intermediate risk – patients who have a PSA between 10 and 20ng/ml **or** a Gleason score of 7 **or** a T2b to T2c stage cancer.

High risk – patients who a PSA of 20ng/ml or higher **or** a Gleason score of 8 or higher **or** a T3 to T4 stage cancer.

1.1.4.3. Prostate-specific antigen (PSA) test

The prostate-specific antigen (PSA) test was developed by Kuriyama et al in 1980 and is an enzyme immunoassay (ELISA) that measures PSA circulating in the blood (Kuriyama et al., 1980). PSA is a serine protease that cleaves high molecular weight clotting proteins into smaller peptides and results in the liquification of the seminal fluid in order to allow sperm to swim freely. It is specifically found in the prostate (Kuriyama et al., 1980, Westdorp et al., 2014). The PSA test was introduced into clinical use in 1986 and studies showed that it had a better positive predictive value for prostate cancer than the DRE test alone (Catalona et al., 1991, Nafie et al.,

2014a). Normal PSA levels measured in the serum of the blood can vary between individuals, with PSA levels naturally increasing with age. Generally, as an approximate guideline, PSA levels ≤3 ng/ml is considered normal for men aged < 60 yrs old. Normal PSA levels are considered ≤4 ng/ml in men aged between 60 and 69 yrs, whereas PSA levels ≤5 ng/ml are considered normal for men aged over 70. However, the PSA test is not sufficiently reliable to be used on its own, as studies have shown that 21 % of patients with PSA <4 ng/ml had prostate cancer, whereas patients suffering from non-cancerous diseases such as benign prostatic hyperplasia or prostatitis can have elevated PSA levels (Catalona et al., 1991, Hudson et al., 1989, Stamey et al., 1987). Although PSA levels typically increase with advancing cancer, reports have shown that there is a substantial overlap of PSA levels with difference stages of prostate cancer (Hudson et al., 1989).

1.1.4.4 Trans Rectal Ultrasound guided prostate (TRUS) biopsy

Although the Trans Rectal Ultrasound guided prostate (TRUS) biopsy was developed by Watanabe and colleagues in 1971 (Watanabe et al., 1971), it was not incorporated into routine clinical practice until the mid-1980s when high resolution ultrasound scanners became commonly available (Lee et al., 1989). Using an ultrasound to visualise the prostate, a needle is inserted into the prostate through the rectal wall. One limitation of the TRUS biopsy as a technique is that it can only biopsy the peripheral zone and is poor at sampling the apical and anterior zones of the prostate. Typically, 10 to 12 biopsies are taken from the peripheral zone (Chang et al., 2013, Nafie et al., 2014b). It is a technique that is quick and efficient to perform with readily available equipment. However, the TRUS biopsy is associated with a risk of potentially life-threatening sepsis and urinary tract infections because of the nonsterile 'transfaecal' method. Therefore, prophylactic antibiotics are routinely prescribed. Unfortunately, this practice is leading to increased incidence of antibiotic-resistant microorganisms (reviewed by (Chang et al., 2013)). Studies have shown that the prostate cancer detection rate upon initial biopsy is between 26 and 33 % (Aganovic et al., 2011, Naughton et al., 2000, Welch et al., 2007, Yuasa et al., 2008). Upon repeat biopsy, studies have shown the detection rate is between 18 to 35.7 % (Aganovic et al., 2011, Yuasa et al., 2008). Attempts to improve the detection rate of the TRUS biopsy using a saturation biopsy technique (increasing the number of biopsies taken to 23) have only slightly increased the prostate cancer detection rate to between 34 and 43 % (Lane et al., 2008, Stewart et al., 2001).

1.1.4.5 Transperineal template prostate (TP) biopsy

The technique was developed by adapting the template grid which was used to assist transrectal ultrasound guided brachytherapy (Demura et al., 2005). Although the technique is performed

slightly differently by different clinicians, it is basically a technique that can take biopsy samples from all areas of the prostate gland (peripheral, apical and anterior zones), with between 17 and 36 biopsy cores taken (Dimmen et al., 2012, Mabjeesh et al., 2012, Nafie et al., 2014b, Pal et al., 2012).

In a study directly comparing the detection rate of the TRUS and TP biopsy techniques in biopsy naïve men with a PSA < 20 ng/ml and a benign feeling DRE, the prostate cancer detection rate of the TP biopsy was 60 % compared to the 28 % detection rate of the TRUS biopsy (Nafie et al., 2014a). Studies have shown that the TP biopsy has a cancer detection rate of 26 to 68 % in men who have had a previous set of negative TRUS biopsies despite rising PSA levels. The grade of cancer obtained from positive cores ranged between Gleason 6 and 9, with a median Gleason grade of 7 (Mabjeesh et al., 2012, Nafie et al., 2014b, Pal et al., 2012). Overall, the TP biopsy improves the detection rate of prostate cancer, particularly in patients with a normal feeling prostate by DRE (Demura et al., 2005). Demura et al found that in DRE positive patients, the positive carcinoma rate was higher in the posterior region (77 %) compared to the anterior region. In the repeat biopsy, DRE negative patients, the positive carcinoma rate was higher in the anterior region (60 %). A typical observation is that the carcinoma positive cores are equally distributed throughout the prostate in DRE negative patients (Demura et al., 2005). It has been suggested that the TP biopsy should be used to biopsy patients with elevated PSA levels and benign feeling prostate , whereas patients that are DRE positive should continue to undergo a TRUS biopsy which is unlikely to miss the presence of cancer (Nafie et al., 2014a). However, it should be noted that the TP biopsy requires more expensive equipment, facilities and resources which are less freely available and also requires patients to undergo general anaesthesia.

Despite its greater demand on resources and increased risks due to general anaesthesia, the benefits of the TP biopsy are that the technique is more comfortable for the patient and can be performed in an aseptic environment. Providing the patient urine is sterile, then there is no need for prophylactic antibiotic pre-treatment (reviewed by (Chang et al., 2013)).

1.1.4.6 Emerging genomic biomarkers and assays with the potential to aid prostate cancer diagnosis and inform treatment.

There is now a need to identify new biomarkers of prostate cancer that can help determine the aggressive nature of a patient's cancer and / or indicate when a repeat biopsy might be necessary. This would allow for improved stratification of patients into treatment groups, thereby enabling clinicians to improve the treatment and quality of life of their patients while reducing the incidence of over-treatment (Narayan et al., 2017, Shen and Abate-Shen, 2010).

Table 1.2 Common genomic alterations detected in patients with prostate cancer.

Gene	Chromosome Location	Type of genomic aberration	Comments
Androgen Receptor	Xq11	Amplification Mutation	Only present in 58 % of castration-resistant prostate cancer cases. Associated with castration resistance. Mutated in 10% of patients.
TMPRSS2-ERG	Chr21	Gene Fusion	Probable early event. Present in 50 % of localised and metastatic prostate cancers.
NKX3.1	8p21	Deletion	Early event. Present in up to 78 % of metastatic prostate cancer cases.
PTEN	10q23	Deletion Mutation	Early event. Up to 40 % loss in copy number. Most frequent homozygous deletion.
C-Myc	8q24	Amplification	Commonly amplified. Chromosomal region contains multiple genes involved in prostate cancer.
TP53	17p31	Deletion Mutation	Role in the transcription of genes involved in apoptosis. P53 alterations associated with recurrence after radiation and androgen suppression. Variable frequency in localised prostate cancer (5 – 40 %).
CHD1	5q21	Deletion	Identified in 10 – 17 % prostate tumour samples. Associated with increased invasiveness in prostate cancer cell lines.
RB1	13q14	Deletion	Present in 34 % of primary cases compared to 74 % of metastatic cases.
FOXA1	6q21	Deletion	Androgen receptor transcription modulator
NCOA2	8q13	Amplification Mutation	Co-activator of the androgen receptor. Amplification in ~8 % of primary cancers compared to 37 % of metastatic cancers.
SPOP		Mutation	Frequent mutation in castration resistant prostate cancer (15 %)
N-Myc	2p24	Amplification	Occurs in 40 % of cancers with neuroendocrine differentiation and in 5 % of primary prostate cancer cases.
Aurora Kinase A	20q13	Amplification	Associated with Neuroendocrine differentiation.

Adapted from Lorente and De Bono (Lorente and De Bono, 2014)

As reviewed by Lorente and De Bono (Lorente and De Bono, 2014), molecular studies have now be carried out on prostate cancer. Following an extensive search of the literature using Pubmed the authors identified what they considered to be potentially relevant genomic alterations in human prostate cancer, some of which are linked to key regulatory genes. The challenge now is to identify which genomic alterations can been incorporated into a clinical test that is relevant, reliable and cost effective. Summarised in Table 1.3 is a list of molecular and genomic tests identified by Narayan and colleagues (Narayan et al., 2017) which they consider to be currently the most relevant, novel tests available to be used in the clinical assessment of prostate cancer.

Table 1.3 Summary of novel genomic test available to aid clinical assessment of prostate cancer.

Biomarker Assay (Commercial company)	Source material	What the assay measures	Comments
Early diagnosis and screening 4Kscore (OPKO Laboratory, USA)	Blood	Panel of 4 proteins: Total PSA, free PSA, Single-chain PSA and human kallikrein 2.	Predicts the likelihood that a patient will have Gleason ≥ 7 grade cancer detected upon needle biopsy.
Prostate Health Index (Beckman Coulter, USA)	Blood	Formula calculation using PSA, free PSA and p2PSA measurements.	Predicts the likelihood of finding prostate cancer on a repeat biopsy.
PCA3/Progensa (Hologic, USA)	Urine	PCR test measuring the concentration of PCA3 and PSA RNA in post DRE specimens.	Scores <25 are associated with lower likelihood of positive biopsy. Score ≥ 25 associated with higher likelihood of positive biopsy.
ConfirmMDx (MDxHealth, USA)	Biopsy Tissue	Quantifies the DNA hypermethylation of three genes (GSTP1, APC, RASSF1) associated with prostate cancer.	Performed on previous negative biopsies. DNA changes suggest present of nearby cancer missed by the biopsy.
Staging and primary treatment selection Prolaris (Myriad Genetics, USA)	Biopsy Tissue	Measures mRNA expression of CCP genes which are thought to indirectly measure the growth rate and potential aggressiveness of tumour cells.	CCP score predicts the likelihood of biochemical reoccurrence if patients were to undergo radical prostatectomy.
Oncotype DX Prostate Cancer Test (Genomic Health, USA)	Biopsy Tissue	RT-PCR based assay that measures the expression of 12 cancer related genes involved in androgen signalling, cellular organisation, stromal response and cell proliferation.	Genomic prostate score ranging from 0 to 100. Predicts likelihood of favourable pathology after radical prostatectomy.
Post Treatment risk stratification Decipher (GenomeDx Biosciences, USA)	Biopsy Tissue	Measures 22 genes involved in cell proliferation, migration, tumour motility, androgen signalling, and immune system evasion.	Predicts the likelihood of clinical disease recurrence 5 years' post prostatectomy in men whose cancer has adverse pathological features and who might benefit from adjuvant radiation.
CellSearch Circulating Tumour Cell Test (Janssen Diagnostics BVBA, Belgium)	Blood	Measures epithelial cell-specific adhesion markers to distinguish circulating tumour cells.	Markers of cancer progression potentially aiding estimation of overall survival and prognosis thereby guiding treatment decisions in metastatic patients.

TMPRSS2:ERG	Urine	Measures recurrent chromosomal rearrangements that are characteristic of malignancies.	Maybe used in both prognosis and diagnosis when combined with other clinical parameters.

Adapted from Narayan et al (Narayan et al., 2017)

1.1.5 Treatment of prostate cancer

Prostate cancer primarily affects older men and the cancer develops slowly in most cases. Post mortems of men who have died from other causes have been shown to provide evidence of prostate cancer of which the individual was not aware due to the absence of symptoms (McNeal, 1969). It is therefore the case that that most men die with, rather than of, the disease. Recent developments in the detection of prostate cancer have meant that the disease is being diagnosed earlier, and clinicians may wish to wait and see if the cancer develops before giving treatment in order to avoid unnecessary treatment associated side-effects. These side-effects can seriously affect the patient's quality of life. Active surveillance is offered to patients with very low risk cancer for whom curative treatment may be unnecessary – these patients are only monitored for signs of cancer progression (Heidenreich et al., 2014a). In well-selected patients, studies have shown that active surveillance is associated with low progression rate and low cancer-specific death (Klotz, 2010, Klotz et al., 2010). Treatment with curative intent only begins if cancer progression, or a threat of progression occurs (Heidenreich et al., 2014a, Klotz et al., 2010). Monitoring of patients in the first year involves PSA tests every 3 to 4 months, a DRE every 6 to 12 months and another TRUS biopsy at the end of 12 months. Beyond the first year, patients are monitored just by PSA tests every 3 to 6 months and by DRE tests every 6 to 12 months (NICE, 2014). The current National Institute of Clinical and Care Excellence (NICE) Guidelines for the management of individuals with Gleason grade 6 disease is to 'watch and wait'.

If the cancer has not spread beyond the prostate, then radical prostatectomy (surgical removal of the prostate) can be used with curative intent, and studies have shown survival benefit in a subset of patients (Heidenreich et al., 2014a, Holmberg et al., 2012). Radiotherapy can also be used to cure cancer that has not spread beyond the prostate. Internal radiotherapy, known as brachytherapy, is a safe effective form of treatment to cure localised prostate cancer that is low risk and involves placing between 80 and 120 radioactive seeds into the prostate (Ash et al., 2000). External beam radiation therapy (EBRT) can be used to treat localised cancers (Heidenreich et al., 2014a). Three dimensional conformal radiation therapy (3D-CRT) is considered the gold standard in external beam radiation therapy with an optimised version known as image-guided intensity modulated radiation therapy (IMRT) now recommended for the treatment of localised prostate cancers (Bauman et al., 2012, Heidenreich et al., 2014a).

Hormone therapy, also known as Androgen Deprivation Therapy (ADT), can be used in conjunction with radiotherapy for the treatment of high risk localised cancer and for prostate cancer that is advanced, relapsed or become castration resistant (Fitzpatrick et al., 2014, Heidenreich et al., 2014b, Heidenreich et al., 2014a). Examples are:

- Luteinising hormone blockers
- Gonadotrophin releasing hormone blocker
- Anti-androgens

1.2. Cancer and its microenvironment

1.2.1. Hallmarks of cancer

Research has shown that cancer is a highly complex disease, with a great deal of work having been undertaken in order to elucidate the complex mechanisms involved in the transformation of normal cells into a neoplastic state. Hanahan and Weinberg proposed that the complex nature of cancer could be condensed into a set of underlying principles that govern the transformation of normal human cells into malignant cancers. They believed that all different types of cancer shared molecular, biochemical and cellular traits / acquired capabilities. These ideas were conceptualised as 'The Hallmarks of Cancer' in 2000 (Hanahan and Weinberg, 2000). In this, they defined 6 hallmarks of cancer which neoplastic cells would have to acquire to enable them to become tumorigenic and ultimately malignant. In 2011, Hanahan and Weinberg updated the hallmarks of cancer to include two emerging hallmarks and two enabling cancer characteristics which facilitate normal cells to acquire the hallmarks of cancer (Hanahan and Weinberg, 2011). The concepts surrounding the 'Hallmarks of Cancer' were derived from the analysis and interpretation of an extensive number of reviews which themselves were based on an extensive number of primary publications. Since my PhD is primarily focused on the effects of prostate cancer on innate immunity in the context of natural killer (NK) cell phenotype and function, I am only going to briefly summarise the hallmarks and emerging characteristics of cancer, as defined in the Hanahan and Weinberg reviews:

The original 6 hallmarks of cancer were:

1. Sustaining proliferative signalling – This refers to the ability of cancer cells to sustain chronic proliferation. Normal tissues use growth factors to control the entry of cells into, and their progression through the cell growth and division cycle. This control ensures homeostasis of cell number and maintains the architecture and function of the tissue. Cancer cells appear to be able to control their own cell cycle through a number of mechanisms that include:

releasing and subsequently responding to their own growth factor ligands in an autocrine fashion, stimulating healthy cells to release growth factors and maintaining mutations in genes such as Ras that compromise negative feedback mechanisms designed to attenuate proliferative signalling.

2. Evading Growth Suppressors - Cancer cells must evade powerful intracellular mechanisms that negatively regulate cell growth and proliferation via the actions of tumour suppressor genes. Two key proteins described are the retinoblastoma associated (RB) protein and the TP53 protein. Cancer cells have defects in the RB pathway which receives signals from intracellular and extracellular sources and decides whether the cell should proceed through its growth and division cycle. The TP53 protein receives inputs from stress and abnormality sensors that measure factors such as genome damage, levels of nucleotides, oxygen and glucose and can halt cell-cycle progression or even trigger apoptosis if the damage is irreversible. This leads on to the 3rd hallmark of cancer.

3. Resisting Cell Death – Apoptosis is triggered in response to various physiological stresses during tumourigenesis. Cancer cells are able to reduce or evade the mechanisms allowing the cell to progress to high grade malignancy and resist therapies. Apoptosis can be regulated by both external signals e.g. Fas / Fas ligand, and by intracellular mechanism both of which activates the caspase program.

4. Enabling Replicative Immortality – The majority of normal cell lineages can only undergo a limited number of growth and division cycles. This limitation is in association with 'senescence' which is an irreversible entrance into a non-proliferative, but viable state and 'crisis', in which the majority of cells in a population die. Cancer cell lines possess the ability to proliferate in culture in the absence of senescence or crisis and are therefore deemed to be immortalised. Telomeres protect the ends of chromosomes and progressively shorten as a result of proliferation, eventually losing their ability to protect the ends of chromosomal DNA from fusing with the ends of other chromosomes. Telomerase adds telomere repeat segments to telomeric DNA. This enzyme is virtually absent from non-immortalised cells, but is expressed by up to ~ 90 % of spontaneously immortalised cells, thereby countering the telomere erosion mechanism associated with proliferation.

5. Inducing Angiogenesis – Like normal tissues, cancer cells require nutrients and oxygen and must also be able to eradicate and remove metabolic waste and carbon dioxide. Cancer cells are able to switch on and maintain angiogenesis which promotes the growth of new

vasculature vessels which, in turn, helps to sustain the growth of the tumour. In normal tissues, angiogenesis is switched off and is only transiently switched on during physiological process such as wound healing and the female reproductive cycle.

6. Activating Invasion and Metastasis – Research has shown that carcinomas arising from epithelial tissue progress to higher grades of malignancy, gain increased local invasion and can gain metastatic abilities. This is the result of cancer cells altering both their shape and their ability to attach to other cells and the extracellular matrix. This is thought to occur through the alteration in the expression of cell-to-cell adhesion molecules such as E-cadherin. A multistep schematic of the process of invasion and metastasis stating the processes involved from local invasion by cancer cells, to their entry into the lymphatic and hermatogenous systems and then subsequent escape into the parenchyma of distant tissues and subsequent colonising in these tissues allowing the formation of metastasis has been developed.

Recently described, emerging hallmarks of cancer and enabling characteristics are:

Emerging hallmark: Reprogramming energy metabolism – Due to uncontrolled replication, cancer cells must alter their energy metabolism in order to fuel cell growth and division. Normal cells can either generate ATP through anaerobic glycolysis or generate ATP via mitochondrial oxidative phosphorylation. Cancer cells gain the ability to reprogramme their energy metabolism largely towards glycolysis even when oxygen is present. Glycolytic fuelling has been associated with the activation of oncogenes and mutant tumour suppressors.

Emerging hallmark: Evading immune destruction – This hallmark is associated with the observation that, in solid tumours, cancer cells avoid detection by the various arms of the immune system and thus evade being killed by the immune system. This hallmark of cancer is of particular relevance to this PhD and will be discussed further in subsequent sections.

Enabling characteristic: Genome instability and mutation – The ability to acquire the capabilities described in the above hallmarks of cancer is in part dependent on mutations in the genome. These mutations are not repaired by the surveillance systems that normally monitor and maintain genomic integrity. The surviving genomic mutations may give the cell a selective advantage and allow it to outgrow and dominate in the local tissue environment.

Enabling characteristic: Tumour promoting inflammation – Research has shown that tumours are densely infiltrated by cells of both the innate and adaptive immune system, thereby promoting inflammatory conditions and environments. It was originally thought that the dense infiltration of cells reflected an immune response against the tumour. However, research has shown the immune infiltrate can have the opposite effect and enhance tumourigenesis and progression. This will also be further discussed in subsequent sections.

1.2.2 The Tumour Microenvironment

1.2.2.1 Genomic instability and inflammation

The tumour microenvironment is a complicated network of interactions between tumour cells, stromal cells and resident or recruited immune cells. Initial acute inflammatory responses within the tumour microenvironment become skewed towards chronic inflammatory responses that favour tumour formation and evasion of the host immune response (Vitale et al., 2014). There is a connection between the two recently described cancer enabling characteristics 'genome instability and mutation' and 'tumour promoting inflammation' (Hanahan and Weinberg, 2011). This connection can be considered as involving two pathways: an extrinisic pathway or an intrinsic pathway (Mantovani et al., 2008). The extrinsic pathway is associated with the generation of an inflammatory milieu, sometimes a consequence of unknown processes that destabilise the cellular genome and increase the risk of cell transformation towards cancer. The inflammatory milieu may induce DNA damage, affect DNA repair mechanisms or dysregulate cell cycle checkpoints (Mantovani et al., 2008, Vitale et al., 2014). The formation of prostate cancer is thought to occur via an extrinsic pathway. The inflammatory conditions needed to promote prostate cancer are still being investigated. In a study of 68,000 men the risk of developing prostate cancer was increased with a history of prostatitis (a bacterial infection of the prostate) and increased duration of symptoms. Furthermore, an increased risk of prostate cancer has been associated with a history of sexually transmitted diseases (STDs) in some ethnic groups of men (Cheng et al., 2010). Interestingly, the incidence and mortality rates for prostate cancer is lower in East Asia compared to the United States and Western Europe. However, the relocation of Chinese and Japanese men to the United States increases the incidence of prostate cancer in these men, thereby suggesting that environmental factors e.g. diet, may influence the development of prostate cancer (Hsing et al., 2000). Taken together, evidence suggests that the development of prostate cancer appears to be linked to environmental factors which promote inflammatory conditions within the prostate. If these inflammatory conditions are long term, reoccurring or even chronic, then there is an increased risk of developing prostate cancer.

The intrinsic pathway is associated with genetic alterations that drive inflammation and transformation of cells (Mantovani et al., 2008). An example of where genetic alterations drive the development of an inflammatory microenvironment is in human papillary thyroid carcinoma. The gene encoding the RET protein tyrosine kinase becomes rearranged as a result of chromosomal inversions or translocations. The altered RET becomes activated and induces the expression of genes encoding colony stimulating factors (CSFs), inflammatory cytokines e.g. IL-1β, chemokines (e.g. CXCL8, which promotes angiogenesis), matrix degrading enzymes (e.g. metalloproteases (MMPs)) and adhesion molecules (e.g. L-selectin) (Borrello et al., 2005). Both tumour cells and inflammatory cells appear to abnormally activate transcription factors such as nuclear factor-κB (NFκB), signal transducer and activator of transcription 3 (STAT3) and hypoxia-inducible factor 1α. In turn, activation of these factors promotes the expression of genes involved with the induction of inflammatory mediators promoting cell survival, proliferation and angiogenesis (Karin, 2006, Yu et al., 2007).

1.2.2.2 Tumour residing immune cell populations

Tumours induce the recruitment and / or activation of immune cells within the microenvironment. In addition to attracting immunosuppressive cells, the inflammation which is orchestrated by tumours is capable of polarising many types of inflammatory immune cells towards an immunosuppressive phenotype (Vitale et al., 2014). Below are brief descriptions of immune cells and non-immune cells found in the tumour microenvironment:

Tumour associated fibroblasts (TAFs) – In response to tumour-derived factors such as fibroblast growth factor (FGF), transforming growth factor-β (TGF-β) and platelet derived growth factor (PDGF), TAFs secrete factors that promote tumour cell transformation and proliferation e.g. TGF-β, insulin growth factor (IGF) and hepatocyte growth factor (HGF). TAFs also gain the ability to secrete extracellular matrix remodelling enzymes which favour tumour invasion (e.g MMPs, fibroblast activation protein (FAP), vascular endothelial growth factor (VEGF)) and inflammation promoting chemokines e.g. CXCL12, CXCL8 and IL-6 (reviewed by (Servais and Erez, 2013)).

Tumour associated macrophages (TAMs) – TAMs originate from circulating monocytes and are recruited into the tumour microenvironment through the secretion of CCL2 (Nesbit et al., 2001). Exposure to tumour-derived cytokines such as IL-4, IL-10, IL-13 and M-CSF polarises the macrophages towards an M2 phenotype which secrete immunosuppressive cytokines (e.g. IL-10, TGF-β), extracellular matrix remodelling enzymes (e.g. MMPs), and growth factors that

promote tumour proliferation and angiogenesis (e.g. EGF, VEGF) (reviewed by (Biswas and Mantovani, 2010)).

Dendritic cells – Dendritic cells (DCs) play an important role in presenting antigens to T cells and thereby triggering antigen-specific adaptive immunity. However, their differentiation can be skewed towards an immature / tolerogenic phenotype by the presence of VEGF, PGE2 and IL-10 (secreted by TAMs and TAFs). The immature / tolerogenic DCs produce TGF-β and Indoleamine-pyrrole 2,3-dioxygenase (IDO) and become poor at activating T cells (reviewed by (Zitvogel et al., 2006)). The production of TGF-β by DCs has been reported to inhibit NK cell function (Sarhan et al., 2015).

Tumour associated neutrophils (TANs) – Mature neutrophils are recruited to the tumour by chemokines such as CXCL8 which can be secreted by both the tumour and TAMs. Cytokines such as TGF-β can induce neutrophil polarisation towards a more pro-tumoural phenotype. TANs secrete arginase and proangiogenic factors that promote tumour growth and progression (reviewed by (Fridlender and Albelda, 2012)).

Regulatory T cells (Tregs) – T cells that are attracted to the tumour site appear to be mostly made up of TH2 $CD4^+$ T cells (T cells which release cytokines that promote humoral immune responses) and Tregs (reviewed by (Whiteside, 2008)). Tregs have been shown to be capable of suppressing the proliferation of other T cells via secretion of IL-10 and TGF-β. Tregs expressing membrane bound TGF-β have also been shown to inhibit NK cell cytotoxic functions (Ghiringhelli et al., 2005, Strauss et al., 2007).

Myeloid derived suppressor cells (MDSC) – MDSCs are defined as immature myeloid progenitor cells of monocytes, dendritic cells and granulocytes that have immunosuppressive functions. Currently, there is some confusion in the literature regarding what markers define MDSCs in humans. MDSCs have a variety of mechanisms to suppress innate and adaptive immune responses. MDSCs consume L-arginine and L-cysteine, thereby depleting T cells of vital nutrients for their function (reviewed by (Gabrilovich et al., 2012)). Cell-to-cell contact between MDSCs and NK cells can result in suppression of NK cell function via the downregulation of NKp30 (Hoechst et al., 2009). MDSCs can also generate oxidative stress through the production of NOS and reactive nitrogen species (which additionally promote the activation and expansion of Tregs) (reviewed by (Gabrilovich et al., 2012)).

1.2.2.3 Immune populations present in the prostate of cancer patients

Assessing tumour infiltrating leukocytes in prostate cancer is difficult. Research has been limited to immunohistochemical analysis of prostatectomy and prostate needle biopsies, thereby making it difficult to fully characterise the phenotype of the tumour infiltrating lymphocytes (Strasner and Karin, 2015). A range of immune cells including T cells, B cells, NK cells, macrophages (including TAMs), MDSCs and neutrophils are present in the prostate of prostate cancer patients. However, for many of the immune populations, whether their presence is associated with a good or bad prognosis, results have been conflicting, reviewed by (Strasner and Karin, 2015). An increased presence of macrophages (including TAMs), Tregs and MDSCs has generally been associated with prostate cancer progression (Ebelt et al., 2009, Gollapudi et al., 2013, Idorn et al., 2014, Lanciotti et al., 2014, Valdman et al., 2010). As a consequence, prostate cancer progression appears to be associated with immunosuppressive immune populations that, as described above, are capable of inhibiting NK cell and T cell responses. NK and T cell responses may therefore be inhibited within the prostate of prostate cancer patients.

1.2.2.4. The cancer immunoediting hypothesis

The cancer immunoediting hypothesis was described by Dunn et al based on previous work from the same group showing that the immune system may promote the emergence of primary tissues that were capable of escaping immune recognition and destruction (Dunn et al., 2004a, Shankaran et al., 2001). A subsequent review by Dunn et al described the three phases of the cancer immunoediting hypothesis (Dunn et al., 2004a). Cancer immunoediting can be conceptualised into the elimination phase, equilibrium phase and the escape phase.

The elimination phase is essentially the concept of cancer immunosurveillance whereby lymphocytes e.g. T cells and NK cells, survey host tissues and eradicate cancer cells via cytotoxic killing and the release of interferon-gamma (IFN-γ). Inhibition of these functional processes permits the formation of tumours. Although the immune cells involved in the cancer immunosurveillance process eradicate the majority of transformed cells due to the unstable genomic and heterogeneous nature of cancer cells, eventually cells that can start to withstand / tolerate the immunological pressure put on them emerge. This is where the equilibrium phase starts. The equilibrium phase is a dynamic interaction between cancer and the immune system whereby the immune system selects tumour cells that can survive within the immunocompetent host due to their increasing low immunogenicity. The host immune response continues to eradicate the higher immunogenic cancer cells, ultimately leaving the low immunogenic cancers alive which then have the chance to mutate and lower even further their immunogenicity. This process leads to the escape phase whereby the growth of the tumour is no longer restrained by

the immune response and can continue to grow to the point of clinical detection. It is thought that the specific processes / changes that allow or promote tumour escape may be mechanistically different in different tissues (Dunn et al., 2004a).

1.2.2.5 The discontinuity theory

A new theory called 'The discontinuity theory' has emerged. This proposes 'that immune cells induce an effector response when there is a discontinuity in the molecular motifs with which their receptors interact, whereas they tend to become tolerant to continuously expressed motifs.' (Pradeu et al., 2013). This theory applies to all immune cells whereby they will respond to non-self-antigens / motifs that suddenly appear (microorganisms) or self-antigens / motifs that suddenly appear or increase (tumours). Upon chronic exposure to these antigens, innate immune cells such as macrophages and NK cells become hyporesponsive and decrease their level of functional responses, whereas adaptive immune cells i.e. T cells and B cells, become anergic via negative feedback pathways e.g. PD-1 (Pradeu et al., 2013).

1.3 Natural killer (NK) cells

1.3.1 Discovery of NK cells

Natural killers were first described in the 1970s as lymphoid cells that could lyse allogenic tumour cell lines (Herberman et al., 1975a, Herberman et al., 1975b, Rosenberg et al., 1972). Subsequent studies showed these cells were devoid of T cell and B cell surface antigens, as a consequence of which they were referred to as 'null cells' (Herberman and Ortaldo, 1981, Ozer et al., 1979). Further studies were focussed on discovering markers that specifically identified NK cells and established that lymphocytes mediating non MHC-restricted cytotoxicity expressed CD16 (Lanier et al., 1983, Perussia et al., 1983a, Perussia et al., 1983b, Rumpold et al., 1982) and NKH-1 antigens (Griffin et al., 1983, Hercend et al., 1985).

Antibodies generated against CD56 were first described in the 1980s, but were known at the time as being reactive against NKH-1 and N901 (Griffin et al., 1983, Hercend et al., 1985). It was later demonstrated that a new antibody against Leu-19 which was developed by Becton Dickinson recognised a different epitope of the NKH-1 antigen to the one which the already available anti-NKH-1 antibodies recognised (Lanier et al., 1986). Leu-19 and NKH-1 were reclassified as CD56 and further studies revealed that the anti-CD56 antibodies recognised the neural cell adhesion molecule (N-CAM) glycoprotein, thereby revealing that CD56 was, in fact, an isoform of N-CAM (Lanier et al., 1989). This led to the suggestion that CD56 acted as an adhesion molecule on NK cells. Around the same time, two independent effector-target cell

binding pathways were discovered: CD2 on effector cells binding to LFA-3 (CD58) on target cells and LFA-1 (CD11a/CD18) on effector cells binding to ICAM-1 (CD54) on target cells. These two binding pathways were first discovered on T cells (Shaw and Luce, 1987) and then on NK cells (Ritz et al., 1988). Nitta et al demonstrated that CD56 served as a third effector-target binding pathway, but only when the target cells themselves expressed N-CAM (Nitta et al., 1989).

The antibody to CD16 was first described in 1983 and was referred to as anti-Leu11 (Lanier et al., 1983). Studies by Lanier and colleagues revealed that anti-CD16 was expressed on large granular lymphocytes i.e. NK cells, neutrophils and basophils, but was not present on B cells, T lymphoblasts or resting T cells. In the same study, it was recognised that anti-Leu11 bound to the Fc receptor on NK cells. Although the binding of anti-Leu11 inhibited the binding of aggregated IgG complexes, it did not inhibit antibody-dependent cell-mediated cytotoxicity (ADCC) activity. Further studies revealed that other antibodies such as B73.1, 3G8, Leu-11b and VEP13 also recognised CD16 (Perussia et al., 1984). However, the Leu11a, Leu11b and VEP13 antibodies recognised a different epitope to the B73.1 antibody which also recognised a different epitope to that recognised by the 3G8 antibody which was the most efficient antibody at inhibiting FcR-dependent functional activities e.g ADCC. This suggested the presence of three distinct antigenic determinants and different isoforms of CD16 (Perussia et al., 1984).

1.3.2 Characterisation of NK cell subsets

Although it had been described that NK cells expressed CD56 and CD16, it was not known if differential expression of these markers described subsets with differing or unique functions. Studies in the mid-1980s were therefore focussed on describing the phenotype and function of lymphocytes that differentially expressed CD16 and CD56 (Lanier et al., 1986).

Using a combination of immunofluorescence and flow cytometry, $CD3^{+}CD56^{+}$ NK-T cells were distinguished from $CD3^{-}CD19^{-}CD56^{+}$ NK cells, and it was noted that this NK cell population could be further segregated into $CD56^{bright}CD16^{-}$ and $CD56^{dim}CD16^{+}$ subsets. Although both NK cell subsets could kill the NK cell sensitive human erythroleukaemic cell line K562, the $CD56^{bright}CD16^{-}$ population, which could be morphologically both agranular and granular, were less efficient at killing K562 cells than $CD56^{dim}CD16^{+}$ cells which were morphologically only granular. The same study also noted that a minor population of granular NK cells that were $CD3^{-}CD56^{dim}$, lacked CD16 expression, but had comparable ability to kill K562 as $CD56^{dim}CD16^{+}$ NK existed. The authors hypothesised that $CD56^{dim}CD16^{+}$ NK cells may lose CD16 expression (Lanier et al., 1986). In 1989 it was formally recognised that three distinct NK cell subsets existed: $CD56^{dim}CD16^{bright}$, $CD56^{bright}CD16^{dim}$ and $CD56^{bright}CD16^{neg}$ (Nagler et al., 1989). All three NK cell subsets could kill K562, with the $CD56^{dim}CD16^{bright}$ subset exhibiting the highest level of K562

cytolysis, followed by the $CD56^{bright}CD16^{dim}$ subset and then the $CD56^{bright}CD16^{neg}$ subset, which exhibited the lowest capacity to kill K562 cells. It was also shown that the NK cell subsets expressing CD16 had low levels of cytotoxicity against Daudi cells. Although none of the three subsets showed cytotoxicity against NK cell-resistant cells lines Colo-205, SB and BDMel-1 (Nagler et al., 1989), incubation of all three NK subsets in 800U/ml of recombinant IL-2 for 18 hrs induced the ability of these NK cell subsets to lyse the NK cell-resistant tumour cell lines (Nagler et al., 1989). This is a characteristic that had also been described by other studies (Itoh et al., 1985, Lanier et al., 1985, Phillips and Lanier, 1986, Trinchieri et al., 1984).

Both the $CD56^{dim}$ subset and the two $CD56^{bright}$ NK cell subsets express the low affinity p75 IL-2 receptor, whereas the two $CD56^{bright}$ subsets additionally express CD25 (the p55 IL-2R alpha subunit) (Nagler et al., 1989). Nagler et al revealed that in addition to the increased cytotoxicity against K562 and NK cell-resistant tumour cell lines, IL-2 induced NK cell proliferation. The two $CD56^{bright}$ NK cell subsets exhibited a 5 to 60 fold greater degree of proliferation then the $CD56^{dim}$ NK cell subset. Furthermore, IL-2 stimulation increased the expression of CD56 on the $CD56^{dim}CD16^{+}$ subset to a level which was equivalent across all three NK subsets. Interestingly, although CD16 expression did not significantly change, all three subsets were morphologically large granular lymphocytes with numerous cytoplasmic extensions (Nagler et al., 1989). Therefore, in cultures containing all three NK cell subsets incubated in the presence of IL-2, Nagler et al suggested that the NK cell population is predominately made up of the two $CD56^{bright}$ subsets due to their greater proliferative capacity. This was in contrast to general hypothesis at the time that $CD56^{dim}$ NK cells predominated and that CD16 was down-regulated following IL-2 stimulation (Nagler et al., 1989).

As described above, the $CD56^{dim}$ NK cell subset exhibits the greatest, constitutive cytotoxic potential against K562 target cells. In addition to this function, it was shown that $CD56^{dim}$ NK cells can also produce IFN-γ and TNF-α in response to stimulation, either via IL-2 stimulation or as a consequence of contact with tumour cells (Anegon et al., 1988, Cuturi et al., 1989, Degliantoni et al., 1985, Nagler et al., 1989, Peters et al., 1986, Procopio et al., 1985, Timonen et al., 1980, Trinchieri et al., 1984). Increasingly, it was recognised that NK cells in general can produce cytokines and also respond to cytokines (Cooper, 2001). However, it began to emerge that although the $CD56^{dim}$ subset was generally the more cytotoxic NK cell subset, the $CD56^{bright}$ subset primarily produced cytokines following cytokine stimulation, in addition to an increase in their cytotoxic killing ability (Cooper, 2001, Cooper et al., 2001).

Two studies recognised that $CD56^{bright}$ NK cells expressed significantly more of the type I cytokines IFN-γ and TNF-β than $CD56^{dim}$ NK cells when stimulated with different cytokine combinations (IL-12, IL-15, IL-18 and IL-1β) (Cooper, 2001, Fehniger et al., 1999). Interestingly,

both NK cell subtypes only secreted type 2 cytokines when IL-15 was used as a co-stimulus, whereas the combination of IL-12 + IL-15 induced NK cells to produce IL-10, IL-15 + IL-1β or IL-15 + IL-18 stimulation induced IL-13 production (Cooper, 2001, Fehniger et al., 1999). It was also noted that the chemokines MIP-1α and MIP-1β were also secreted by NK cells when stimulated with IL-12 + IL-18, but that the secretion of these was greater following stimulation with IL-15 + IL-12 (Fehniger et al., 1999).

1.3.3 Cytokine and chemokine secretion

In summary, NK cell populations can be split into two general subsets on the basis of their expression of CD56 ($CD56^{dim}$ and $CD56^{bright}$). The $CD56^{dim}$ subset is considered to be the more cytotoxic subset which produces only low levels of cytokines, whereas the $CD56^{bright}$ subset is considered to be the more immunoregulatory subset and has the capacity to produce high levels of cytokines. However, these cells are poorly cytotoxic (Cooper et al., 2001, Vivier et al., 2008). Although this NK cell subset concept has been largely accepted, it is a basic / simplistic concept at best, with more recent studies having shown that the functions of NK cell subsets overlap.

A comprehensive study by Yenan Bryceson's group which examined cytokine and chemokine secretion following contact stimulation of NK cells with K562 and Drosophila cells expressing specific combinations of NK cell ligands showed that, in fact, $CD56^{dim}$ cells are major producers of cytokines and chemokines upon target cell recognition and produce more cytokines and chemokines than $CD56^{bright}$ NK cells (Fauriat et al., 2010). Therefore, this study suggested that the pathways for cytokine and chemokine production for $CD56^{dim}$ cells and $CD56^{bright}$ cells are different. $CD56^{dim}$ NK cells express more cytokines and chemokines than $CD56^{bright}$ NK cells upon target cell recognition, whereas $CD56^{bright}$ NK cells express more cytokines and chemokines when stimulated by exogenous cytokines then $CD56^{dim}$ NK cells (Fauriat et al., 2010).

Kinetic studies revealed that upon incubation of NK cells with K562 cells, the secretion of the chemokines MIP-1α, MIP-1β and RANTES could be detected within 1 hour. Interestingly, IFN-γ and TNF-α cytokine secretion could not be detected until 3 hours of co-incubation and their expression did not peak until 6 hours of co-incubation. Chemokine secretion also peaked at 6 hours' co-incubation and their levels remained stable for the rest of the time course (12-hour time course). However, the expression levels of the cytokines decreased following their peak at 6 hours' co-incubation. Overall, it was concluded that chemokine secretion appears to occur early in an NK cell response and is triggered by relatively weak activating signals, whereas degranulation and cytokine production requires greater stimulation. The production of cytokines such as IFN-γ and TNF-α is stringently controlled and requires greater receptor cooperation then chemokine production (Fauriat et al., 2010).

1.3.4 Mechanisms associated with NK cell function

As described above, NK cells exhibit three main functions: 1) cytotoxic killing, 2) antibody dependent cell cytotoxicity (ADCC) and 3) immunoregulatory functions via the secretion of cytokines and chemokines. Certainly, the binding of cytokines to cytokine receptors expressed on the NK cell surface is one method of activating and stimulating NK cells. ADCC operates via the binding of the FcR receptor CD16 to the Fc region of antibodies that are bound to their antigen targets and this sends a stimulating signal to the NK cell to degranulate. However, how do NK cells become activated by target cell recognition following cell-to-cell contact? What are the mechanisms behind this function? Furthermore, how do all three activation mechanisms coordinate and influence each other? These questions have yet to be fully answered.

1.3.4.1 'Missing-self' hypothesis

Whilst writing his own thesis, Klas Kärre was struggling to summarise what was known about NK cell target specificity in comparison to T cell specificity. It was already known that NK cells were able to kill some tumour cells and virally-infected cells, but were not able to kill uninfected or healthy cells. There were already known examples of cell lines that were resistant to T cell killing, yet sensitive to NK cell killing and *vice versa*. It had been shown that cell lines that were NK cell resistant, yet sensitive to T cells expressed more MHC class I molecules than cell lines that were sensitive to NK cells (Karre, 2008). This prompted the idea that there were NK cell receptors that detected MHC class I molecules, which, when bound, induced an inhibitory signal that prevented the NK cells from killing the target (Ljunggren and Karre, 1985). The 'missing self' hypothesis which arose from these concepts simply states that NK cells will kill tumours with low or no MHC class I expression (Ljunggren and Karre, 1985).

1.3.4.2 NK cell inhibitory receptors

As shown in Table 1.4, many inhibitory receptors have now been identified, but the two most recognised inhibitory receptors are the Killer Ig-like Receptors (KIR) receptors and the CD94/NKG2A receptor complex.

The Killer Ig-like Receptors (KIR) were among the first NK cell receptors to be identified. Two antibodies, termed GL183 and EB6, were capable of detecting KIR receptors and were produced by immunising 5-week old BALB/c mice with NK cell clones. Splenocytes from the mice were isolated and fused with P3U1 myeloma cells to produce hybridomas. The supernatants of the hybridomas were then screened for being able to modulate cytotoxic activity of NK cell clones against human cell lines in ^{51}Chromium release cytotoxic assays. Hybridomas that secreted antibodies that increased cytolytic activity were further subcloned using limiting dilution, and

Table 1.4 Types of NK cell receptors and their respective ligands

Type of Receptor	Name	Cluster of differentiation	Ligands
Inhibitory	LIR/ILT2	CD85j	HLA-1
	KIR2DL1	CD158a	HLA-C2
	KIR2DL2/3	CD158b	HLA-C1
	KIR2DL4[a]	CD158d[a]	HLA-G
	KIR3DL1	CD158e1	HLA-Bw4
	KIR2DL5	CD158f	?
	KIR3DL2	CD158k	HLA-A*03 and *11, CpG-ODN
	NKG2A	CD159a/CD94	HLA-1
	IRp60	CD300a	?
	P75 /AIRM1 (Siglec7)	C328	A2,8-linked disialic acid
	TIGIT		Nectin-2 (CD112), CD155 (PVR). Nectin-3 (CD113)
	LAIR-1	CD305	Collagen
Activating	FcγRIIIa	CD16a	IgG
	KIR2DS1	CD158h	HLA-C2
	KIR2DS2/3	CD158j	?
	KIR2DL4a	CD158d[a]	HLA-G
	KIR3DS1	CD158e2	HLA-Bw4(?)
	KIR2DS5	CD158f	?
	KIR2DS4	CD158i	HLA-A*11 and some HLA-C alleles
	NKG2C	CD159c/CD94	HLA-E
	NKG2E	CD159e/CD94	HLA-E
	NKRP-1	CD161	LLT-1
	DNAM-1	CD226	Nectin-2 (CD112), CD155 (PVR)
	2B4	CD244	CD48
	NKG2D	CD314	MICA, MICB, ULBPs
	NKp46	CD355	?, Viral HA
	NKp44	CD336	?, Viral HA
	NKp30	CD337	B7-H6, pp65, Bat-3
	NTB-A	CD352	NTB-A
	NKp80		AICL
	TACTILE	CD96	CD155 (PVR), Nectin-1 (CD111)
	TNFRSF7	CD27	CD70
Adhesion / costimulatory	LFA-1	CD11a/CD18	ICAM-1, ICAM-2, ICAM-3
	LFA-2	CD2	CD58, CD48
	LFA-3	CD58	CD2
	αMβ2	CD11b/CD18	C3bi, fibrinogen, x factor, ICAM-4
	αXβ2	CD11c/CD18	C3bi, fibrinogen, ICAM-1
	N-CAM	CD56	?
	Human NK-1	CD57	?
	L-selectin	CD62L	GLyCAM-1, MadCAM-1
	CRTAM	CD355	Necl-2
	OX40	CD134	OX40L
	(TNFRSF4)	CD137	CD137L

	4-1BB (TNFRSF9) GITR (TNFRSF18)	CD357	GITRL
Death Receptors and ligands	Fas or Apo-1 Fas ligand CD40L TRAIL	CD95 CD95L CD154 CD253	CD95L CD95 CD40 DR4 (TRAIL-R1), DR5 (TRAIL-R2)
Degranulation receptors	LAMP-1 LAMP-2	CD107a CD107b	E-Selectin P-selectin, galectins E-Selectin P-selectin, galectins

Adapted from Montaldo et al (Montaldo et al., 2013)

this led to the production of antibodies GL183 and EB6 (Moretta et al., 1990a, Moretta et al., 1990b). Further experiments revealed that these two antibodies recognised allotypic molecules expressed by HLA class I (HLA-C) alleles. As reviewed by Montaldo et al (Montaldo et al., 2013), a whole superfamily of KIRs were described, including KIRs that were activating instead of inhibitory receptors. Inhibitory KIRs have been characterised by a long intracytoplasmic tail capable of recruiting and activating phosphatases SHP1 and SHP2, whereas activating KIRs have been characterised by short intra cytoplasmic tails coupled to ITAM bearing signalling peptides DAP12. KIRs are encoded by a cluster of genes that are polymorphic in nature, similar to the genes that encoded MHC class I molecules that the KIR detect (Trowsdale, 2001).

The NKG2 group of receptors were identified following the generation of cDNA libraries (Houchins et al., 1990). Further investigation into this group of receptors revealed that this group could be further subdivided into 4 distinct groups of transcripts referred to as NKG2 A, B, C, and D. NKG2A is a type II membrane protein with only an 18 amino acid difference to NKG2B (Houchins et al., 1991). NKG2A binds with CD94 to form a receptor complex that recognises HLA-E expressed on target cells and transduces an inhibitory signal which, in some cases, is sufficient to inhibit NKG2A+ NK cells from lysing target cells expressing HLA-E (Braud et al., 1998, Perez-Villar et al., 1997). Similar to the inhibitory KIR receptors, inhibitory signals are transduced by the phosphorylation of ITIM sequences in the intracytoplasmic domain, thereby enabling the binding of protein tyrosine phosphatases SHP1 and SHP2 (Le Drean et al., 1998)

Interestingly, a study analysing the expression of activating and inhibitory receptors on NK cells using mass cytometry has revealed that the expression of inhibitory receptors is primarily determined by genetics. NKG2A was found to be expressed on 40 of the top 50 NK cell phenotypes alongside CD94. In comparison, the expression of the KIR receptors was much more diverse, with many different NK cell subpopulations, comprising of only a few cells, expressing different combinations of KIR receptors (Horowitz et al., 2013).

1.3.4.3 NK cell activating receptors

Similar to the inhibitory receptors, many activating receptors have been described (Table 1.4). Herein, I describe the discovery of the most commonly considered and studied activating receptors:

Natural cytotoxicity receptors (NCRs): Three natural cytotoxicity receptors (NCRs) have been identified: NKp30 (Pende et al., 1999), NKp44 (Vitale et al., 1998) and NKp46 (Sivori et al., 1997). All three NCRs were identified using a similar approach to that which was used to identify inhibitory receptors, and these receptors are considered as classic activating receptors. Monoclonal antibodies were generated by immunising BALB/c mice with NK cell clones and hybridomas were created from the splenocytes of those mice. The monoclonal antibodies contained in the hybridoma supernatants were selected for their ability to induce lysis in redirected killing assays against FcγR+ P815 target cells, of which the magnitude was comparable to the CD16 monoclonal antibody control. Both NKp46 and NKp30 were found to be expressed on freshly isolated, resting NK cells, whereas NKp44 was only detected on IL-2 activated NK cells after at least 3 days of culture. All three receptors require efficient cross-linking to induce NK cell triggering, and blocking experiments using antibodies resulted in inhibition of cytolytic activity which was maximal when all three receptors were blocked at the same time (Pende et al., 1999, Sivori et al., 1997, Vitale et al., 1998). Interestingly, experiments focusing on signal transduction revealed that, like CD16, NKp46 and NKp30 transduce activating signals via association with the ITAM-containing CD3ζ polypeptides that become tyrosine phosphorylated upon cell stimulation. In contrast, NKp44 induced activating signals via KARAP/DAP12 tyrosine phosphorylated molecules similar to activating KIR (Pende et al., 1999, Vitale et al., 1998).

Currently, little is known about the ligands to which the three NCRs bind, and it is thought that they bind more than one ligand (Horton and Mathew, 2015). NKp46 and NKp44 have both been shown to bind the hemagglutinin protein expressed by the influenza virus (Arnon et al., 2001, Mandelboim et al., 2001). NKp30 has been shown to bind B7-H6 which has been found to be expressed by a range of tumour cells such as lymphomas, myeloid leukaemias, melanomas etc. (Brandt et al., 2009). The ligation of the NCRs with their respective ligands were all found to trigger cytotoxicity. More recently, it has been shown that both NKp44 and NKp30 can bind ligands that transduce inhibitory signals. Binding of Proliferating Cell Nuclear Antigen (PCNA) to NKp44 resulted in inhibition of NK cell cytotoxic function and IFN-γ secretion (Rosental et al., 2011). Interestingly, the ligand BAT3 has been described to be able to both activate and inhibit NK cell cytotoxicity (Binici et al., 2013, Pogge von Strandmann et al., 2007).

NKG2D was discovered as a consequence of further analysis of NKG2 cDNA transcripts. It was found to be distantly, but significantly, related to NKG2A, sharing a 21 % amino acid homology (Houchins et al., 1991). The upregulation of the NKG2D ligands MICA and MICB is associated with cellular stress and further experiments involving γδ T cells revealed that these molecules may regulate protective immune responses (Groh et al., 1996, Groh et al., 1998). Studies aiming to find the immune receptor that recognises MICA revealed that NKG2D recognised MICA and likely the same receptor also recognised MICB (Bauer et al., 1999). Functional studies involving γδ T cells and blocking antibodies to NKG2D revealed that blocking NKG2D resulted in decreased tumour cell lysis, thereby confirming that NKG2D was an activating receptor (Bauer et al., 1999). Sutherland et al later revealed that, in addition to binding MICA and MICB, NKG2D could also bind ULBP 1, 2 and 3, to resulting in the transduction of activating signals (Sutherland et al., 2002). Signalling through NKG2D occurs via a pathway involving DAP10 which has a SH2 binding domain, in which the p85 subunit PI3-kinase binds (Wu et al., 1999).

DNAM-1: Using methods similar to those used to generate antibodies against the NCRs, but with the difference that mice was immunised with a $CD8^+$ T cell clone, led to the discovery of the DNAX accessory molecule 1 (DNAM-1), termed DX11 (Shibuya et al., 1996). DNAM-1 was found to be expressed on both T cells, NK cells and a subset of B cells, and it is involved in both cell-to-cell adhesion as well as inducing cytolytic activity by recognising and binding to its ligands CD155 (poliovirus receptor) and nectin 2 (Shibuya et al., 1996).

1.3.4.4 Adhesion / Co-stimulatory receptors

Evidence that adhesion and co-stimulatory receptors play important roles in the function of NK cells is also emerging. LFA-1 is an adhesion receptor made up of two subunits (CD11a and CD18) which binds the intercellular adhesion molecules (ICAM) 1, 2 and 3 (Fawcett et al., 1992, Rothlein et al., 1986, Rothlein and Springer, 1986, Staunton et al., 1989). The CD2 receptor was shown to be another example of an adhesion receptor (Vollger et al., 1987). In addition to their roles as adhesion molecules, both LFA-1 and CD2 also play a role in cell signalling (Barber et al., 2004, Denning et al., 1988). In T cells, LFA-1 was shown to strengthen its adhesion to ICAMs through conformational changes upon activation of the T cell following the ligation of other receptors e.g. CD2, to their ligands (Dustin and Springer, 1989, van Kooyk et al., 1989). This type of signalling is known as 'inside out' signalling. For NK cells, signalling through LFA-1 was shown to be one of the minimal requirements for induction of cytotoxicity and, in conjunction with signalling through CD2, is recognised as one of the early signals that is needed in the formation of a lytic immunological synapse between an NK cell and its target (Bryceson et al., 2009, Mace et al., 2014). Signalling through LFA-1 has been shown to induce the reorganisation of the NK

cell actin cytoskeleton and, following co-ligation of NKG2D, lytic granules are polarised towards to the immunological synapse (Mace et al., 2009).

NK cell stimulation with cytokines upregulates additional adhesion and co-stimulatory molecules. The class I restricted T cell associated molecule (CRTAM) was first identified from cDNA libraries that were generated following activation of thymocytes (Kennedy et al., 2000). CRTAM has been found to be expressed on activated NK cells as a dimer. Although it is debatable whether CRTAM promotes cytotoxicity following ligation with its ligand necl2, the receptor does play a role in cellular adhesion (Arase et al., 2005, Boles et al., 2005).

TNF receptors without death domains e.g. OX40, CD137, GITR, are known co-stimulatory receptors that are expressed on T cells and which enhance their responses (Croft, 2003). These receptors have also been shown to induce reverse signalling transduction, which means that the cell expressing the ligand receives a signal following receptor ligand ligation. In the case of CD137L, reverse signalling has been shown to induce secretion of pro-inflammatory cytokines (TNF, IFN-γ, IL-6, IL-8 and IL-12) by human monocytes, up-regulate their expression of ICAM-1 and promote monocyte proliferation (Ju et al., 2009, Ju et al., 2003, Langstein et al., 1998). Resting NK cells do not express the receptor CD137 and express only a low level of the receptor GITR. Upon stimulation with IL-2 or IL-15, the expression of CD137 and GITR is up-regulated (Baessler et al., 2010, Baltz et al., 2007). Ligation of CD137 and GITR on NK cells with their respective ligands expressed on leukaemic cell lines (e.g.AML, B-CLL) and adherent cells lines (e.g. MCF-7, HCT116) respectively results in inhibition of NK cytotoxicity and IFN-γ secretion. In turn, the leukaemic cells secrete immunosuppressive cytokines such as TNF, IL-8, IL-10 (leukaemic cells) and TGF-β (adherent cell lines) which can suppress both NK and T cell immune responses (Baessler et al., 2010, Baltz et al., 2007)

1.3.4.5. Chemokine receptor expression

The term used to describe the movement of immune cells towards a chemical attractant is called chemotaxis. The chemical attractants, known as chemokines, bind to chemokine receptors expressed on the surface of the immune cell to promote the tethering and rolling of leukocytes on endothelial cells that are mediated by transient selectin interactions (Lawrence and Springer, 1991). A list of chemokine receptors expressed by NK cells and the chemokines that they bind is shown in Table 1.5.

Table 1.5 Chemokine receptors expressed on NK cell subsets and the chemokines they recognise

Chemokine Receptor	Expression on NK cell subsets	Chemokines recognised
CXCR1	$CD56^{dim}$ NK only	CXCL8 (IL-8) CXCL6
CXCR2	$CD56^{dim}$ NK only (low level)	CXCL1, CXCL2, CXCL3, CXCL5, CXCL6, CXCL7 and CXCL8
CXCR3	$CD56^{dim}$ NK (low level) $CD56^{bright}$ NK (high level)	CXCL9 (MIG), CXCL10 (IP-10), CXCL11 (I-TAC)
CXCR4	$CD56^{bright}$ (high level)	CXCL12
CX3CR1	$CD56^{dim}$ (High level) $CD56^{bright}$ (very low level)	CX3CRL1, CCL26 (Eotaxin-3)
CCR5	$CD56^{bright}$ (high level)	CCL3 (MIP-1α), CCL4 (MIP-1β) CCL5 (RANTES), CCL8 CCL13, CCL16
CCR7	$CD56^{bright}$ (high level)	CCL19, CCL21

References (Campbell et al., 2001, Griffith et al., 2014)

1.3.4.6 Dynamic Equilibrium theory and receptor co-ordination

Since it was discovered that NK cells have both activating and inhibitory receptors it was realised that the 'missing self' hypothesis proposed by Ljunggren and Karre (Ljunggren and Karre, 1985) only partially described the function of NK cells. A new hypothesis known as the 'dynamic equilibrium theory' was proposed. This stated 'that the integration of opposing signals from activating and inhibitory receptors determines the functional outcome of NK cell activity' (Sabry and Lowdell, 2013). This theory is generally accepted, but at best it is a basic overview of a very complicated mechanistic process. In a series of studies, Bryceson et al discovered that when NK cell activating receptors were stimulated in pairs using cross-linking monoclonal antibodies, there was a greater influx of Ca^{2+} when compared to single receptor stimulation alone, with the Ca^{2+} influx correlating with degranulation. In redirected killing assays against the mouse FcR+ cell line P815, human resting NK cells were able to kill P815 cells when using cross-linking antibodies, but not (or very little) when using antibodies that bound only one activating receptor (Bryceson et al., 2006)). Furthermore, in experiments involving the expression of NK cell ligands on Drosophilia S2 cells, Bryceson determined that the minimal requirements to stimulate resting NK cells to kill S2 cells required co-engagement of the LFA-1, 2B4, and NKG2D receptors with their respective ligands. They went on to show that NKG2A can inhibit the activating signals of NKG2D, 2B4, but particularly LFA-1 resulting in reduced degranulation (Bryceson et al., 2009).

Interestingly, it appears that cytotoxicity is controlled by more than the coordination of activating and inhibitory signals transmitted by receptors recognising different ligands. It is starting to emerge that in some cases both activating and inhibitory receptors recognise and compete for the same ligands. The activating receptor DNAM-1 competes with the inhibitory

receptor TIGIT and with the activating / inhibitory receptor CD96 for the same ligands i.e. CD155 and CD112 (Chan et al., 2014, Stanietsky et al., 2009, Yu et al., 2009). Furthermore, it has been shown that TIGIT has a higher binding affinity for CD155 than both DNAM-1 and CD96, thereby suggesting that TIGIT may out compete DNAM-1 and CD96 for the CD155 stress ligand (Yu et al., 2009). It appears that both DNAM-1 and TIGIT have roles in the formation of both lytic and regulatory immunological synapses, reviewed by (Martinet and Smyth, 2015). Further work is required in order to elucidate the exact roles of DNAM-1 and TIGIT in the formation of regulatory synapses with dendritic cells (DCs). During the formation of the lytic synapse it has been shown that DNAM-1 works together with LFA-1 during the process of actin cytoskeleton re-organisation (Shibuya et al., 1999), whereas TIGIT has been shown to disrupt the polarisation of the microtubule organising centre (Liu et al., 2013b). Future experiments to observe how DNAM-1, TIGIT and CD96 interact at immunological synapses are needed.

1.3.4.7 'Priming' and 'Triggering' of NK cell responses

As described above, both NK cell subsets can be stimulated to kill cancer cell lines that are otherwise resistant to being killed by resting NK cells by cytokines such as IL-2 (Nagler et al., 1989). Studies have also shown that co-incubation of NK cells with the leukaemic cell line CTV-1 results in the 'priming' of NK cells via the ligation of the CD2 receptor on the NK cells with CD15 receptor on the CTV-1 cells (North et al., 2007, Sabry et al., 2011). Although the primed NK cells were not able to kill the CTV-1 cells themselves, they were able to kill other NK cell-resistant cell lines such as Raji, DU145 and ARH77. Furthermore, primed NK cells up-regulated expression of CD69 and CD25 and down-regulated their expression of NKG2D and NKp46. Although the up-regulated CD69 receptor was subsequently shown to act as a triggering receptor, it was concluded that it was unlikely to be the only one (North et al., 2007, Sabry et al., 2011). It was postulated that the stimulation of NK cells to kill cancer cells can be split into two distinct stages: 'priming' and 'triggering' (North et al., 2007, Sabry and Lowdell, 2013). The priming signal can be either in the form of cytokine stimulation or stimulation following cell-to-cell contact with a target cell expressing the appropriate combination and intensity of ligands for the NK cell activating receptors expressed. The triggering signal is delivered by an additional ligation of at least one activating receptor with its stress ligand expressed on the target, thereby preventing auto-reactivity with healthy cells (Sabry and Lowdell, 2013). This theory fits with the widely accepted dynamic equilibrium hypothesis and also potentially describes how cytokines can be used to stimulate NK cells to kill tumour cells, yet spare healthy cells.

1.3.5 NK cell recognition of cancer cells

Studies have shown that different activating receptors and / or the extent of their involvement in the recognition of different cancer cell lines appears to differ from cell line to cell line, even when they are from the same type of cancer. The studies used antibody blocking experiments involving cytokine-stimulated NK cells targeted against NK cell-resistant tumour cells. They analysed the effects of blocking specific activating receptors on the ability of the NK cells to kill various cancer cell lines. These studies revealed that the most important NK cell activating receptors involved in the recognition of different breast cancer cells was NKG2D and DNAM-1. The activating receptors NKp46 and NKp30 were also involved in the recognition of breast cancer cell lines, but to a lesser extent (Mamessier et al., 2011a). In a study of melanoma cells lines, El-Sherbiny et al showed that cytotoxic killing of three melanoma cell lines was dependent on the DNAM-1 receptor. However, one melanoma cell line lacked expression of DNAM-1 ligands and the cytotoxic killing of this cell line was NKG2D and NKp46 dependent (El-Sherbiny et al., 2007). Recognition of prostate cancer cell lines appear to primarily involve NKG2D, DNAM-1, NKp46 and, to a lesser extent, NKp30 (Pasero et al., 2015). Furthermore, a study measuring the ability of NK cells to target colon cancer showed that allogeneic NK cells could kill cancer initiating cells much more effectively than their differentiated counterparts. Cancer initiating cells were shown to express higher levels of NKp30 and NKp44 ligands, but lower levels of MHC class I molecules than the differentiated colon cancer cells (Tallerico et al., 2013).

Overall, the ability of cytokine stimulated NK cells to kill NK cell-resistant tumour cells lines is heavily dependent on the level of expression of NK cell activating and inhibitory ligands by that cell line. As a consequence, the expression requirement for activating receptors by the NK cells in order to kill the cell line is different between cell lines. A study analysing the range of NK cell phenotypes within an individual has shown that there are up to 30,000 different NK cell phenotypes within one person. Expression of the activating receptors NKG2D and NKp46 was only found on 28 and 25 of the top 50 phenotypes, with the top 50 phenotypes only accounting for about 15 % of the total NK cell population (Horowitz et al., 2013). These results suggest that only specific NK cell subpopulations having the correct combination of activating and inhibiting receptors are capable of killing specific cell lines.

1.3.6 Cleavage of stress ligands

As already discussed above, both tumours and recruited tumour associated immune cells e.g. TAM, TAFs, Tregs etc secrete immunosuppressive cytokines (e.g. TGF-β, IL-10, TNF) into the tumour microenvironment which can inhibit NK cell function by down-regulating NK activating receptors such as NKp44, NKp30 and DNAM-1 (Balsamo et al., 2009, Li et al., 2012).

Furthermore, recruited Tregs and MDSCs can also down-regulate the expression of activating receptors (e.g. NKG2D, NKp30) following cell-to-cell contact due to these cells (i.e. Tregs) expressing membrane bound TGF-β (Ghiringhelli et al., 2005, Hoechst et al., 2009). An additional evasion mechanism used by cancer cells to avoid the NK cell immune responses is to cleave off NK cell ligands from the cancer cell surface. The most common example is the shedding of NKG2D ligands e.g. MICA and MICB which has been shown to occur on a range different types of cancer, including pancreatic (Panc89, PancTu-I), breast (MDA-MB231) and prostate cancer (PC3) cell lines (Chitadze et al., 2013). In the case of T cells, the binding of soluble MICA has been shown to down-regulate NKG2D expression by endocytosis and degradation of the NKG2D receptor (Groh et al., 2002). High levels of soluble MIC (the assay used in these studies could not distinguish between MICA and MICB) have been detected in the serum of patients with advanced prostate cancer. Incubation of healthy NK cells in the serum of patients containing soluble MIC was associated with a down-regulation of NKG2D resulting in inhibition of NK cell cytotoxic function and IFN-γ secretion (Wu et al., 2004). Elevated levels of soluble MIC has also been observed in patients with pancreatic cancer, and this also resulted in decreased NKG2D expression and inhibition of the cytotoxic function of both γδ T cells and NK cells (Marten et al., 2006).

Shedding of MICA and MICB ligands from the surface of cancer cells has been shown to be mediated by either matrix metalloproteinases (e.g. MMP9 and MMP14) or by 'a disintegrin and metalloproteinases' (ADAM) (e.g. ADAM 10 and 17) (Chitadze et al., 2013, Liu et al., 2013a, Sun et al., 2011). Interestingly, although MICB is cleaved from the cell surface of PC3 cells by ADAM10 and ADAM 17, MICA is secreted in a truncated form from the cancer cell via exosomes (Chitadze et al., 2013). HeLa (cervical cancer) cells are also capable of secreting MICA via exosomes which has been shown to down-regulate NKG2D expression on NK cells and inhibit their cytotoxic function (Ashiru et al., 2010).

1.3.7 Immunological synapses and their functions

The contact between an immune cell e.g. NK cell or T cell, with a cell of interest is termed an 'immunological synapse'. Research has shown that NK cells can form three different types of immunological synapses upon contact with a cell of interest: 1) a lytic synapse, 2) an inhibitory synapse or 3) a regulatory synapse. The type of immunological synapse formed by the NK cell and the cell of interest is dependent on the expression level of stress ligands and MHC class I molecules by the target cell, the clustering of NK cell activating and inhibitory receptors at the immunological synapse, actin reorganisation and polarisation by either the NK cell or target cell and, finally, the polarisation of the microtubule reorganising centre and lytic granules towards the immunological synapse, reviewed by (Mace and Orange, 2011). Described in further detail

in Chapter 4, NK cells form lytic synapses when more activating signals are received by the NK cell than inhibitory signals. The NK cell reorganises its actin cytoskeleton at the synapse and polarises its microtubule organising centre and lytic granules towards the immunological synapse (Mace and Orange, 2011, Orange, 2008). The lytic granules contain perforin and granzyme B (Peters et al., 1991) which are released into the cleft of the immunological synapse following complete fusion of the lytic granule membrane with the cell plasma membrane (Liu et al., 2009, Orange, 2008). Inhibitory synapses are formed when inhibitory signals predominate over activating signals and / or when actin reorganisation and polarisation of the microtubule organising centre to the immunological synapse is blocked (reviewed by (Mace and Orange, 2011)).

Regulatory synapses between NK cells and dendritic cells have also been studied. In contrast to lytic synapses, the dendritic cell reorganises its actin cytoskeleton allowing for clustering of MHC class I molecules at the synapse, thereby preventing the formation of lytic synapse. Furthermore, dendritic cells polarise IL-12 and IL-15 cytokines towards the regulatory synapse, whereas NK cells polarise IL-12 and IL-15 receptors. It is thought that these interactions promote NK cell survival, proliferation and also prime them (Barreira da Silva et al., 2011, Borg et al., 2004, Brilot et al., 2007).

1.4 Aims and Hypothesis of the PhD study

There is a need to improve the ability of clinicians to diagnosis prostate cancer and better determine patient prognosis. Better diagnosis and improved prognosis has the potential to lead to better patient care, as the clinicians will be able to make more informed choices regarding what treatment plan to put their patients on, thereby allowing them to maintain a good quality of life. The formation of prostate cancer is thought to occur as a result of inflammation within the prostate. Tumours promote chronic inflammation and the secretion of immunosuppressive cytokines and factors as a mechanism to evade the NK immune response via the down-regulation of NK cell activating receptors, subsequently inhibiting NK cell immune function.

The aim of this PhD project is to characterise the phenotype and function of peripheral NK cells isolated from patients with prostate cancer in order to determine whether these reflect the presence and severity of disease. If so, then it might be possible to use these measurements to improve prostate cancer diagnosis and better determine patient prognosis.

The study is based on the hypothesis that, in comparison to individuals with benign disease, the presence of prostate cancer down-regulates the expression of NK cell activating receptors and has the potential to inhibit NK cell function, and that these effects are reflected in the phenotype and functional potential of NK cells in the peripheral circulation. If this is the case, then changes

in NK cell phenotype and function can then be used to distinguish patients with and without cancer and those patients with an increased risk of progression.

2: Materials and Methods

2.1 Patients, patient groups and ethics

Patients with suspected prostate cancer attending the Urology Clinic at Leicester General Hospital (University Hospitals of Leicester NHS Trust) were examined by Mr Masood Khan (Consultant Urologist) and Mr Shady Nafie (Registrar in Urology).

Samples were obtained from two cohorts of patients, termed the 'TRUS' and 'TP' cohorts. Patients in the TRUS cohort were diagnosed using the TRUS biopsy only, whereas patients in the TP cohort were selected on the basis of them meeting the criteria of being biopsy naïve, with a PSA level of <20ng.ml^{-1} and agreeing to undergo simultaneous TRUS biopsy (12 cores) and TP biopsy (36 cores) procedures under general anaesthetic. Demographics for both patient cohorts are described in chapter 3 (Tables 3.1 to 3.4).

The TP cohort samples were collected from 24th October 2012 to 15th August 2014. This cohort comprised samples from 72 males who had previously had a TRUS-guided biopsy and then underwent a transperineal template prostate biopsy (TPTPB). The mean age for this cohort was 66 years old (age range of 50 to 84 years old). Given the more definitive diagnostic power of this approach (Nafie et al., 2014a, Nafie et al., 2014b), samples that were considered as being from patients with benign disease were obtained from this cohort.

The TRUS cohort samples were collected from 24th October 2012 to 15th August 2014. This cohort comprised samples from 92 males who had been diagnosed on the basis of a TRUS biopsy alone. The mean age for this cohort was 66 years old (age range of 50 to 84 years old). For both cohorts, patients were recruited and treated as described previously (Nafie et al., 2014a)

The Research Protocols were registered and approved by the National Research Ethics Service Committee of East Midlands and by the Research and Development Department in the University Hospitals of Leicester NHS Trust. All participants were given information sheets explaining the nature of the study and they all signed their informed consent forms.

Ethical approval for the collection and use of samples from the TRUS cohort (Project title: *A pilot study to identify gene fusions in Prostate Cancer)* was given by NRES Committee East Midlands – Derby 2 (NREC Reference number: 09/H0401/92; UHL 10856).

Ethical approval for the collection and use of samples from the TP cohort (Project Title: *Defining the role of Transperineal Template-guided prostate biopsy*) was given by NRES Committee East Midlands – Derby 1 (NREC Reference number: 11/EM/3012; UHL11068).

Peripheral blood (60 ml) was collected from all patients using standard NHS procedures. Aliquots (30 ml) were transferred into two 50 ml polypropylene (Falcon) tubes containing 300 µl of sterilised Heparin (1000 U/ml, Sigma). Anti-coagulated samples were immediately transferred by taxi to the John van Geest Cancer Research Centre at Nottingham Trent University and were processed immediately upon receipt (as described below) within 3 hours of collection.

Approval for the collection of peripheral blood from healthy volunteers was obtained from the Nottingham Trent University College of Science and Technology Human Ethics Committee (Application numbers 165 and 412). Samples were collected by standard procedures by suitably qualified individuals.

2.1.1 Collection of plasma from blood

Plasma was collected from a total of 4 ml of anticoagulated blood by centrifuging four aliquots at 300g for 15 mins at room temperature (RT). The separated plasma was then aliquoted and frozen at -80°C. The four remaining pellets were retained and frozen at -80°C.

2.1.2 Isolation of peripheral blood mononuclear cells (PBMCs) from blood

Prior to sample arrival, Leucosep® tubes (Greiner Bio-One) containing 15 ml of Ficoll-Paque (GE Healthcare Life Sciences) were centrifuged at 400g for 1 min. The centrifugation enabled the Ficoll-Paque to pass through the specially designed filter that prevents added blood mixing with the Ficoll-Paque prior to centrifugation, thereby enabling a quicker setup time.

Peripheral blood mononuclear cells (PBMCs) were isolated from the remaining blood by mixing 20 ml of blood with 10 ml phosphate-buffered saline (PBS, Lonza) and layering this into the previously-prepared Leucosep® tube. Following centrifugation at 800g for 30 mins at RT with the brake off, the PBMC fraction was transferred into a separate tube, washed with PBS, centrifuged at 600g for 10 min at RT and then washed again with PBS followed by centrifugation at 400g for 10 mins at RT. Following centrifugation, the pellet was re-suspended in 5 ml of fetal bovine serum (FBS, Hyclone) the viable PBMCs counted using a haemocytometer and trypan blue dye exclusion (0.1 % v/w Trypan Blue, Santa Cruz). The PBMCs were re-suspended in freeze medium (90% v/v FBS (Hyclone) and 10% v/v DMSO (Santa Cruz)) and frozen down at 10 x 10^6 cells/ml per cryovial (Sarstedt). For this, vials were placed in a Coolcell™ freezing container (Biocision) and frozen at -80°C overnight before being transferred to liquid nitrogen until phenotypic and functional analysis.

2.1.3 Thawing of PBMCs

At the time of analysis, an appropriate number of cryovials was removed from liquid nitrogen, defrosted using a hair dryer and 1-2 ml of PBMCs were pipetted into a 15 ml conical Falcon tube

(BD Biosciences), to which was slowly added an equal volume of RT Thaw solution (90 % v/v RPMI (Lonza), 10 % v/v CTL wash™ solution (Cellular Technology Limited) plus 10 µl of Benzonase (Novagen®)). Vials were washed with 1 ml of Thaw solution, the contents of which were added to the 15 ml Falcon tube. Additional thaw solution was added to make the volume up to 12 ml. Samples were then centrifuged at 400g for 5 min at RT and then re-suspended in RPMI containing 10% v/v FBS and 1% v/v/ L-glutamine (Lonza). The PBMCs were then allowed to rest at 37 °C for 1 hr before the number of viable cells was determined by trypan blue dye exclusion.

2.2 Flow cytometry setup

2.2.1 Flow cytometry

The phenotype of the peripheral natural killer (NK) cells within the PBMC populations that had been previously isolated from the blood of each patient was determined by flow cytometry using a Beckman Coulter Gallios™ instrument which is capable of measuring 10 fluorescent channels. The lasers and filters specifications are shown in Table 2.1.

Table 2.1 Beckman Coulter Gallios laser and filter specifications

Laser	Excitation Wavelength	Channel	Emission Wavelength Range
Blue	488nm	FL1	525/40
		FL2	575/30
		FL3	620/30
		FL4	695/30
		FL5	755LP
Red	638nm	FL6	660/20
		FL7	725/20
		FL8	755LP
Violet	410nm	FL9	450/40
		FL10	550/40

2.2.2 Flow cytometer and protocol setup

Flow-Check™ and Flow-Set™ fluorospheres (Beckman Coulter) were routinely used to align the lasers. The Gallios™ is somewhat different to other flow cytometers in that the protocol file is combined with the FCS data file in order to create an LMD file. For each antibody panel, the voltages and gains for the forward scatter (FSc) and side scatter (SSc) were adjusted to enable the cell populations being measured to be viewed in the FSc *versus* SSc dot plot. For each antibody panel, the appropriate lasers and FL channels were switched on. The voltage settings for each FL channel were adjusted and the compensation settings calculated and applied as described in Section 2.2.3. The linear time of flight setting was enabled in order to measure

doublets so they could be excluded during analysis. Settings for each of the antibody panels were saved and used throughout the study.

2.2.3 Compensation for spectral overlap

A compensation tube for each antibody or fluorescent dye present in the antibody panel was set up in order to establish and correct for spectral overlap between fluorescence channels. For this, one drop of OneComp eBeads (eBioscience) was added to a 12x75 mm polycarbonate flow cytometry tube containing 50 µl of Wash Buffer (PBS + 2% w/v BSA + 0.02% w/v sodium azide (Sigma)) and the appropriate amount of antibody. The bead-antibody mix was then incubated in the dark for 15 mins at RT.

All experiments included a viability stain in order to exclude non-viable cells from the analysis. For this a Live/Dead™ Fixable Violet dead stain (Thermo Fisher Scientific) was used, further details on which are provided below. The spectral overlap of the Fixable dead stain was determined using ArC™ Amine Reactive Compensation Bead Kit (Thermo Fisher Scientific). For this, one drop of positive ArC™ beads was added to each 12x75 mm flow cytometry tube for each fluorophore used.

All tubes were incubated in the dark for 30 mins at RT. Following incubation, 1 ml of wash buffer was added and the tubes were then centrifuged at 400g for 5 min at RT. The supernatant was then removed and the beads, with dye or antibody bound, were re-suspended in 500µl of Isoton™ II diluent (Beckman Coulter). One drop of the negative ArC™ beads was added to viability stain tube.

PBMCs were defrosted as previously described (section 2.1.4) and 500,000 cells were added to two 12x75 mm tubes followed by 1 ml of Wash buffer. The cells were then centrifuged at 400g for 5 min at RT, after which the supernatant was removed. For one tube, the PBMCs were re-suspended in 500µl of Isoton™ II diluent. The PBMCs in the second tube were stained with the antibodies and dyes described in the antibody panel (method described in section 2.3.1).

Compensation was achieved following the automated program on the Beckman Coulter Gallios™. Briefly, histograms for each FL channel were drawn and the unstained PBMCs run on the flow cytometer. The voltage for each FL channel were adjusted so that the peaks for the unstained PBMCs were within the 1st log decade of the x axis on the histogram. Using the same voltage settings, Beckman Coulter Flow-Set™ beads were then run on the flow cytometer and the mean fluorescence recorded. The automated compensation program on the Beckman Coulter Gallios™ was then applied and the mean fluorescence values for the Flow-Set™ beads added. During the automated program, the fluorescence of each antibody and dye stained beads

were run and measured in order to allow the amount of compensation to add for each possible antibody and dye combination to be calculated. Each antibody and dye combination were then examined manually and the compensation settings adjusted so that the mean fluorescence values for Q1 and Q3 and Q3 and Q4 were comparable

Once the compensation settings had been established, they were then added to the protocol for the antibody panel. Compensation was undertaken for each antibody panel for which there was a difference in the fluorochromes used or the company that made the antibody. Once the compensation settings were added to the protocol, PBMCs stained with the full antibody panel were then run on the flow cytometer and later analysed using the Beckman Coulter Kaluza™ 1.2 software. Again, each possible antibody / dye combination was analysed using density plots gated on single cells, and the compensation manually adjusted if necessary.

2.3 Determining the phenotype of natural killer (NK) cells in the peripheral blood of patients with prostate cancer using thawed PBMCs

2.3.1 Staining protocol

One vial of patient or control PBMCs was defrosted, as previously described (section 2.1.4). Following counting, 1 x 10^6 PBMCs were then aliquoted into three 12x75 mm flow cytometry tubes per patient and washed with 1 ml of Wash buffer, centrifuged at 400g for 5 mins at RT, after which cells were re-suspended in 100 µl of Wash buffer. The PBMCs were then stained in the dark for 15 min at RT with the antibody panels 1 to 3 (one antibody panel per tube), as described in Table 2.2. Following incubation, the PBMCs were washed with PBS and then re-suspended in 1 ml Live/Dead™ Fixable Violet solution and incubated in the dark for 30 min at RT. Following incubation, the PBMCs were then pelleted at 400g for 5 mins, washed and re-suspended in 500 µl Isoton™ II diluent. The PBMCs were analysed immediately. Patient PBMC samples were stained and analysed on the flow cytometer in batches of four plus one control PBMC sample. Data were analysed using the Beckman Coulter Kaluza™ software, using the gating strategy shown in Figure 2.1.

2.3.2 'Fluorescent minus one' controls

As shown in Figure 2.1, for some of the antibodies (e.g. NKp46 and NKp30) distinct positive and negative populations for those antibodies could not be clearly seen. As a consequence, fluorescent minus one experiments were carried out for each activating and inhibitory NK cell receptor antibody in order to determine where the positive and negative staining gates should be placed for each antibody. For this, cells were stained as previously described in section 2.3.1, but omitting the antibody for which the negative staining gate was being measured. Following

data acquisition on the flow cytometer, the data were again analysed using Beckman Coulter Kaluza™ software (Table 2.2).

Table 2.2: Antibody panels for measuring the phenotype of patient Natural Killer cells

FL Channel & Wavelength	Antibody	Fluorochrome /dye	Clone	Manufacturer	Vol per tube
Panel 1					
FL1 525/40	DNAM-1	FITC	11A8	BioLegend	5 µl
FL2 575/30	NKG2D (CD314)	PE	1D11	eBioscience	5 µl
FL3 620/30	CD56	ECD (PE-Texas Red)	N901	Beckman Coulter	2.5 µl
FL4 695/30	CD16	PerCP-Cy5.5	3G8	BioLegend	5 µl
FL5 755LP	NKp46 (CD335)	PE-Cy7	9E2	BioLegend	5 µl
FL6 660/20	NKp30 (CD337)	Alexa Fluor 647	P30-15	BioLegend	5 µl
FL7 725/20	CD3	Alexa Fluor 700	UCHT1	BioLegend	2 µl
FL7 725/20	CD19	Alexa Fluor 700	HIB19	BioLegend	1 µl
FL8 755LP	CD8	APC-Cy7	SK1	BioLegend	2.5 µl
FL9 450/40	Live/Dead™	Dye (violet)		Thermo Fisher Scientific	1 µl in 1 ml
Panel 2					
FL1 525/40	CD85j	FITC	GHI/75	Miltenyi biotec	10 µl
FL2 575/30	LAIR-1	PE	DX26	BD Biosciences	20 µl
FL3 620/30	CD56	ECD (PE-Texas Red)	N901	Beckman Coulter	2.5 µl
FL4 695/30	CD16	PerCP-Cy5.5	3G8	BioLegend	5 µl
FL5 755LP	NKG2A	PE-Cy7	Z199	Beckman Coulter	10 µl
FL6 660/20	NKp44	Alexa Fluor 647	P44-8	BioLegend	5 µl
FL7 725/20	CD3	Alexa Fluor 700	UCHT1	BioLegend	2 µl
FL7 725/20	CD19	Alexa Fluor 700	HIB19	BioLegend	1 µl
FL8 755LP	CD8	APC-Cy7	SK1	BioLegend	2.5 µl
FL9 450 / 40	Live/Dead™	Dye (violet)		Thermo Fisher Scientific	1 µl in 1 ml
Panel 3					
FL1 525/40	2B4 (CD244.2)	FITC	C1.7	BioLegend	5 µl
FL3 620/30	CD56	ECD (PE-Texas Red)	N901	Beckman Coulter	2.5 µl
FL4 695/30	CD16	PerCp-Cy5.5	3G8	BioLegend	5 µl
FL7 725/20	CD3	Alexa Fluor 700	UCHT1	BioLegend	2 µl
FL7 725/20	CD19	Alexa Fluor 700	HIB19	BioLegend	1 µl
FL8 755LP	CD8	APC-Cy7	SK1	BioLegend	2.5 µl
FL9 450/40	Live/Dead™	Dye (violet)		Thermo Fisher Scientific	1 µl in 1 ml

2.4 Priming of NK cells using the CTV-1 human leukemic cell line

2.4.1 CTV-1 cell culture

The CTV-1 cell line (a T cell leukemic cell line) was purchased from the DSMZ (ACC 40) and was cultured using RPMI supplemented with 10% v/v FBS and 1% v/v L-Glut, as recommended by the DSMZ. Cultures were split twice a week when the medium looked exhausted or when the cells were used for an experiment. Cultures were split within the range of 1 in 5 and 1 in 10 by

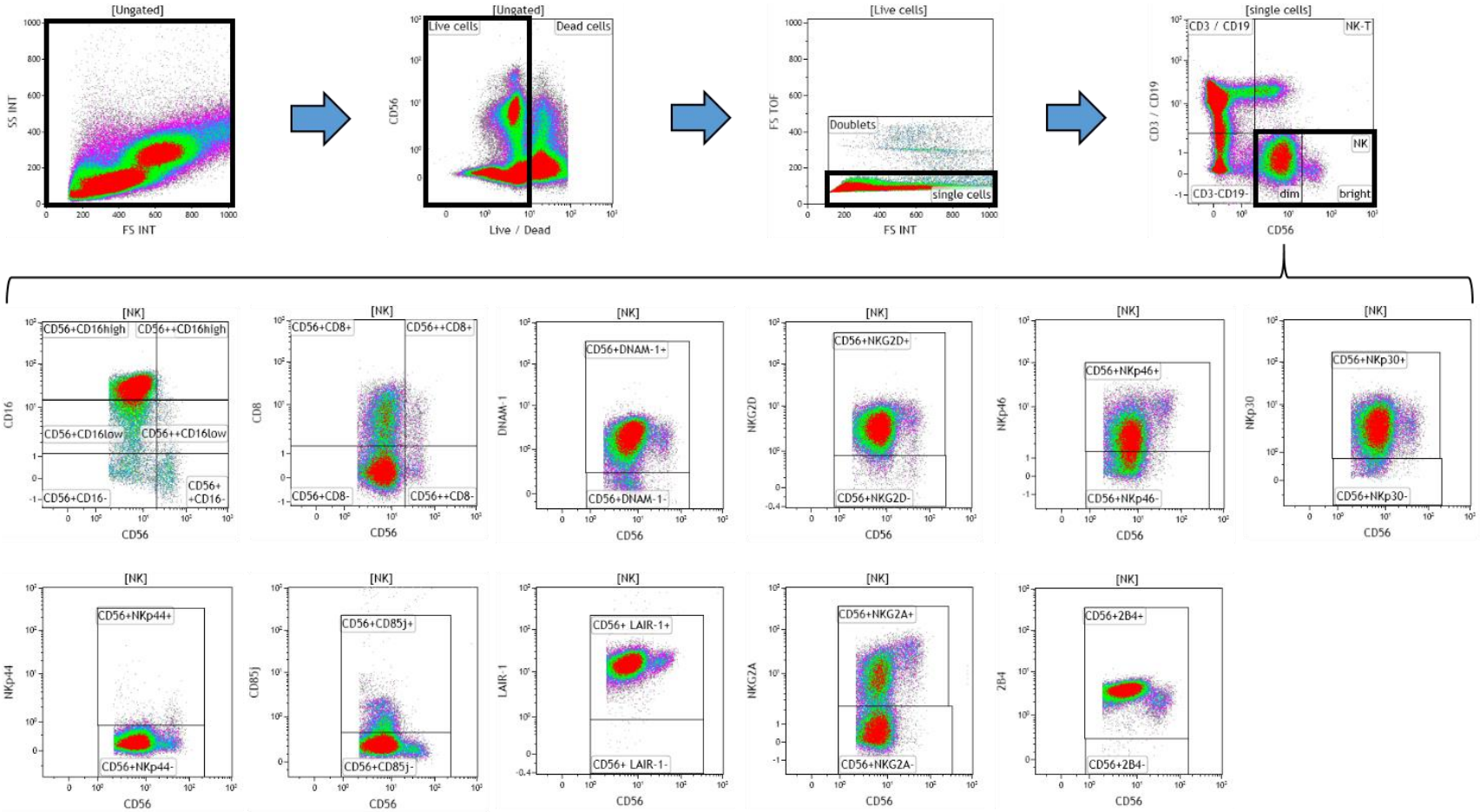

Figure 2.1: Gating strategy for analysing the expression of activating and inhibitory receptors on patient NK cells.

Using density plots the NK cells were analysed by first gating on 'live cells' from the cells acquired in the forward scatter (FSc) linear vs side scatter (SSc) linear density plot and then gating on single cells (determined by FSc Linear vs FS time of flight). Cells where then gated on the NK cell population that were $CD3^{-}CD19^{-}CD56^{+}$. Analysis of the expression of each activating and inhibitory receptor on patient NK cells was done by gating on the NK population and then looking for positive and negative expression of each receptor on cells expressing CD56. Gates were set using FMO controls. The expression of each NK receptor was measured using the 'Logical' setting.

adding an aliquot of the cell culture to a fresh flask and adding between 40 and 50 ml of RPMI supplemented with 10% v/v FBS and 1% v/v L-Glut.

2.4.2 NK cell priming

Cultured CTV-1 cells were transferred into a 50 ml Falcon conical tube and then centrifuged at 400g for 5 mins. Following centrifugation, the cell pellet was re-suspended in 1 to 3 ml of RPMI supplemented with 10% v/v FBS and 1% v/v L-Glut (RPMI complete medium), depending on the size of the cell pellet. The viable cell count was determined using trypan blue exclusion and a haemocytometer. In order to inhibit the growth of CTV-1 cells during NK cell priming, CTV-1 cells were treated with Mitomycin C. For this, a vial of Mitomycin C (2 mg) (Sigma) was re-suspended in 6 ml ddH_20 to give a concentration of 333 µg/ml. To 900 µl of CTV-1 cell suspension ($\leq 7 \times 10^6$ CTV-1 cells/ml) in a 15 ml Falcon conical tube was added 100µl of Mitomycin C to give a final concentration of Mitomycin C at 33 µg/ml per $\leq 7 \times 10^6$ CTV-1 cells. The CTV-1 cells were incubated with Mitomycin C for 2 hrs in the dark at 37°C, after which cells were centrifuged at 400g for 5 min at RT and the supernatant discarded. The CTV-1 cells were then washed using 13 ml of PBS, centrifuged and the supernatant discarded. The CTV-1 cells were washed a further two times before finally being re-suspended in RPMI complete medium and counted as before.

During the CTV-1 incubation with Mitomycin C, the appropriate number of PBMC vials were removed from liquid nitrogen and thawed, as previously described in section 2.1.4. Following resting for at least 1 hr and counting, NK cells were isolated from the PBMC using an EasySep™ Human NK Cell Enrichment Kit for the negative selection of NK cells following the manufacturer's instructions (STEMCELL Technologies). For this, unwanted cells are targeted for removal with Tetrameric Antibody Complexes recognising non-NK cells and dextran-coated magnetic particles. The labelled cells are separated using an EasySep™ magnet without the use of columns. Desired cells are poured off into a new tube. Isolated NK cells were centrifuged at 400g for 5 min at RT, re-suspended in 500 µl of complete medium and counted using a haemocytometer. The isolated NK cells were then co-incubated with the mitomycin C treated CTV-1 cells in a 15 ml Falcon conical tube at an NK : CTV-1 ratio of 1 : 2 for 17 hrs at 37°C, unless otherwise stated in the experimental protocol. A control tube containing isolated NK cells alone in RPMI complete medium which served as a 'non-primed' NK cell control was always set up.

2.4.3 Phenotypic analysis of non-primed and primed NK cells

The phenotype of non-primed and primed NK cells was determined by flow cytometry using the same protocol as described in section 2.3.1, but with the following differences: 100,000 isolated NK cells were added wherever possible to each 12x75 mm flow cytometry tube and cells were stained using the antibody panels shown in Table 2.3. To determine the position

Table 2.3: Antibody panels used to measure the phenotype of Natural Killer cells before and after priming

FL Channel Wavelength	Antibody	Fluorochrome /dye	Clone	Manufacturer	Vol per tube
Panel 1					
FL1 525/40	2B4 (CD244.2)	FITC	C1.7	BioLegend	5 µl
FL2 575/30	NKG2D (CD314)	PE	1D11	eBioscience	5 µl
FL3 620/30	CD56	ECD (PE-Texas Red)	N901	Beckman Coulter	2.5 µl
FL4 695/30	CD16	PerCP-Cy5.5	3G8	BioLegend	5 µl
FL5 755LP	NKp46 (CD335)	PE-Cy7	9E2	BioLegend	5 µl
FL6 660/20	NKp30 (CD337)	Alexa Fluor 647	P30-15	BioLegend	5 µl
FL7 725/20	CD3	Alexa Fluor 700	UCHT1	BioLegend	2 µl
FL7 725/20	CD19	Alexa Fluor 700	HIB19	BioLegend	1 µl
FL8 755LP	CD8	APC-Cy7	SK1	BioLegend	2.5 µl
FL9 450/40	Live/Dead™	Dye (violet)		Thermo Fisher Scientific	1 µl in 1 ml
Panel 4					
FL1 525/40	CD2	FITC	TS1/8	BioLegend	5 µl
FL2 575/30	NKp80	PE	5D12	BioLegend	5 µl
FL3 620/30	CD56	ECD (PE-Texas Red)	N901	Beckman Coulter	2.5 µl
FL4 695/30	CD16	PerCP-Cy5.5	3G8	BioLegend	5 µl
FL5 755LP	CD25	PE-Cy7	M-A251	BioLegend	5 µl
FL6 660/20	CD69	APC	FN50	BioLegend	5 µl
FL7 725/20	CD3	Alexa Fluor 700	UCHT1	BioLegend	2 µl
FL7 725/20	CD19	Alexa Fluor 700	HIB19	BioLegend	1 µl
FL8 755LP	CD8	APC-Cy7	SK1	BioLegend	2.5 µl
FL9 450 / 40	Live/Dead™	Dye (violet)		Thermo Fisher Scientific	1 µl in 1 ml
Panel 5					
FL1 525/40	OX40	FITC	BerACT35	BioLegend	5 µl
FL2 575/30	CD96	PE	NK92.39	Biolegend	5 µl
FL3 620/30	CD56	ECD (PE-Texas Red)	N901	Beckman Coulter	2.5 µl
FL4 695/30	CD16	PerCp-Cy5.5	3G8	BioLegend	5 µl
FL5 755LP	4-1BB (CD137)	PE-Cy7	4B4-1	BioLegend	5 µl
FL6 660/20	CRTAM	APC	FN50	BioLegend	5 µl
FL7 725/20	CD3	Alexa Fluor 700	UCHT1	BioLegend	2 µl
FL7 725/20	CD19	Alexa Fluor 700	HIB19	BioLegend	1 µl
FL8 755LP	CD8	APC-Cy7	SK1	BioLegend	2.5 µl
FL9 450/40	Live/Dead™	Dye (violet)		Thermo Fisher Scientific	1 µl in 1 ml
Panel 6					
FL1 525/40	DNAM-1 (CD226)	FITC	11A8	BioLegend	5 µl
FL2 575/30	TIGIT	PE	MBSA43	eBioscience	5 µl
FL3 620/30	CD56	ECD (PE-Texas Red)	N901	Beckman Coulter	2.5 µl
FL4 695/30	CD16	PerCP-Cy5.5	3G8	BioLegend	5 µl
FL6 660/20	GITR	APC	ebioAITR	eBioscience	5 µl
FL7 725/20	CD3	Alexa Fluor 700	UCHT1	BioLegend	2 µl
FL7 725/20	CD19	Alexa Fluor 700	HIB19	BioLegend	1 µl
FL8 755LP	CD8	APC-Cy7	SK1	BioLegend	2.5 µl
FL9 450/40	Live/Dead™	Dye (violet)		Thermo Fisher Scientific	1 µl in 1 ml

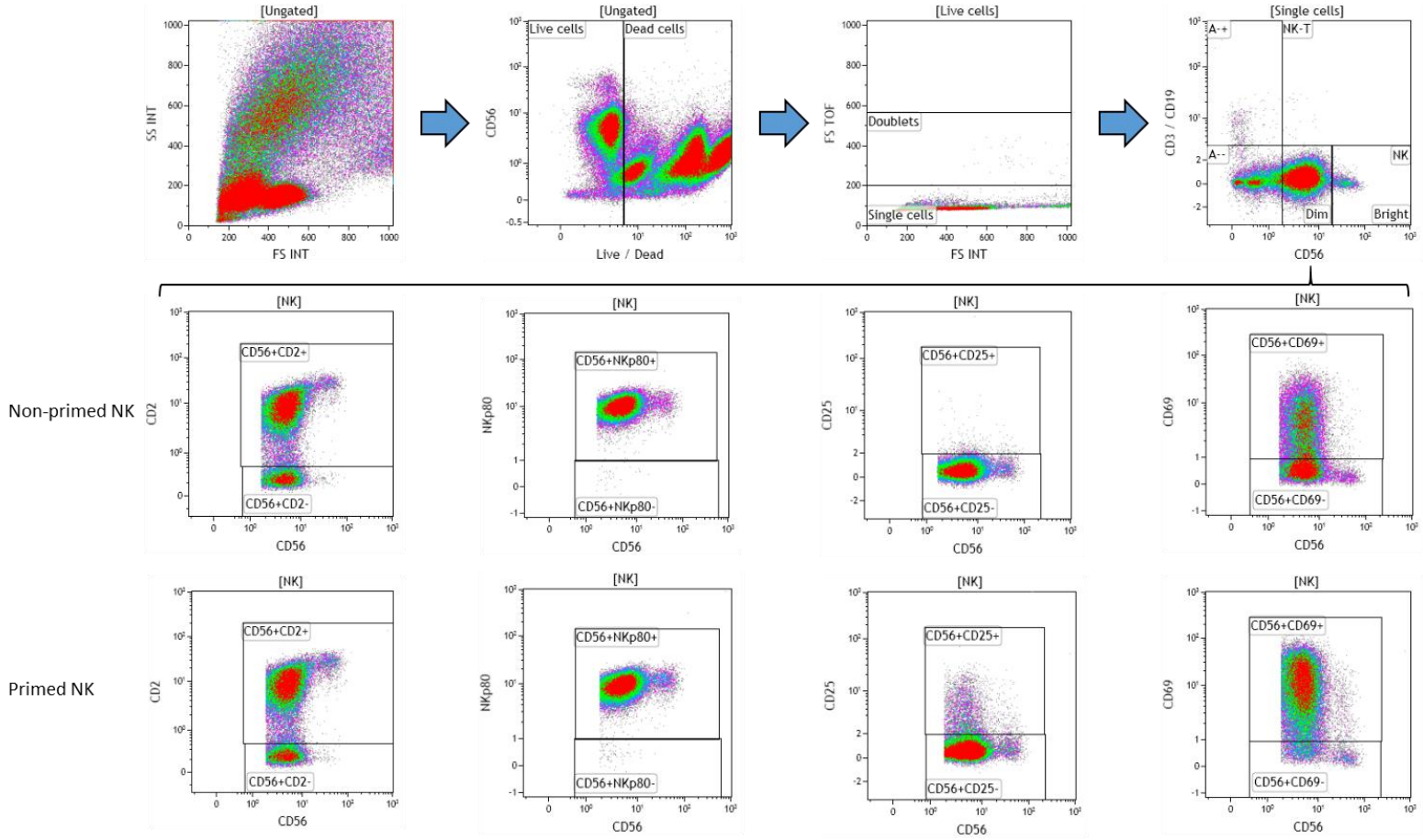

Figure 2.2 Gating strategy for analysing the expression of receptors CD2, NKp80, CD25 and CD69 on CTV-1 primed NK cells and non-primed NK cells.
Using density plots the NK cells were analysed by first gating on 'live cells' from the cells acquired in the forward scatter (FSc) linear vs side scatter (SSc) linear density plot and then gating on single cells (determined by FSc Linear vs FS time of flight). Cells where then gated on the NK cell population that were $CD3^{-}CD19^{-}CD56^{+}$. Analysis of the expression of receptors CD2, NKp80, CD25 and CD69 on healthy volunteer and patient NK cells was done by gating on the NK population and then looking for positive and negative expression of each receptor on cells expressing CD56. Gates were set using control NK stained for NK defining antibodies (CD3, CD19, CD56, CD16 and CD8) only. The expression of each NK receptor was measured using the 'Logical' setting.

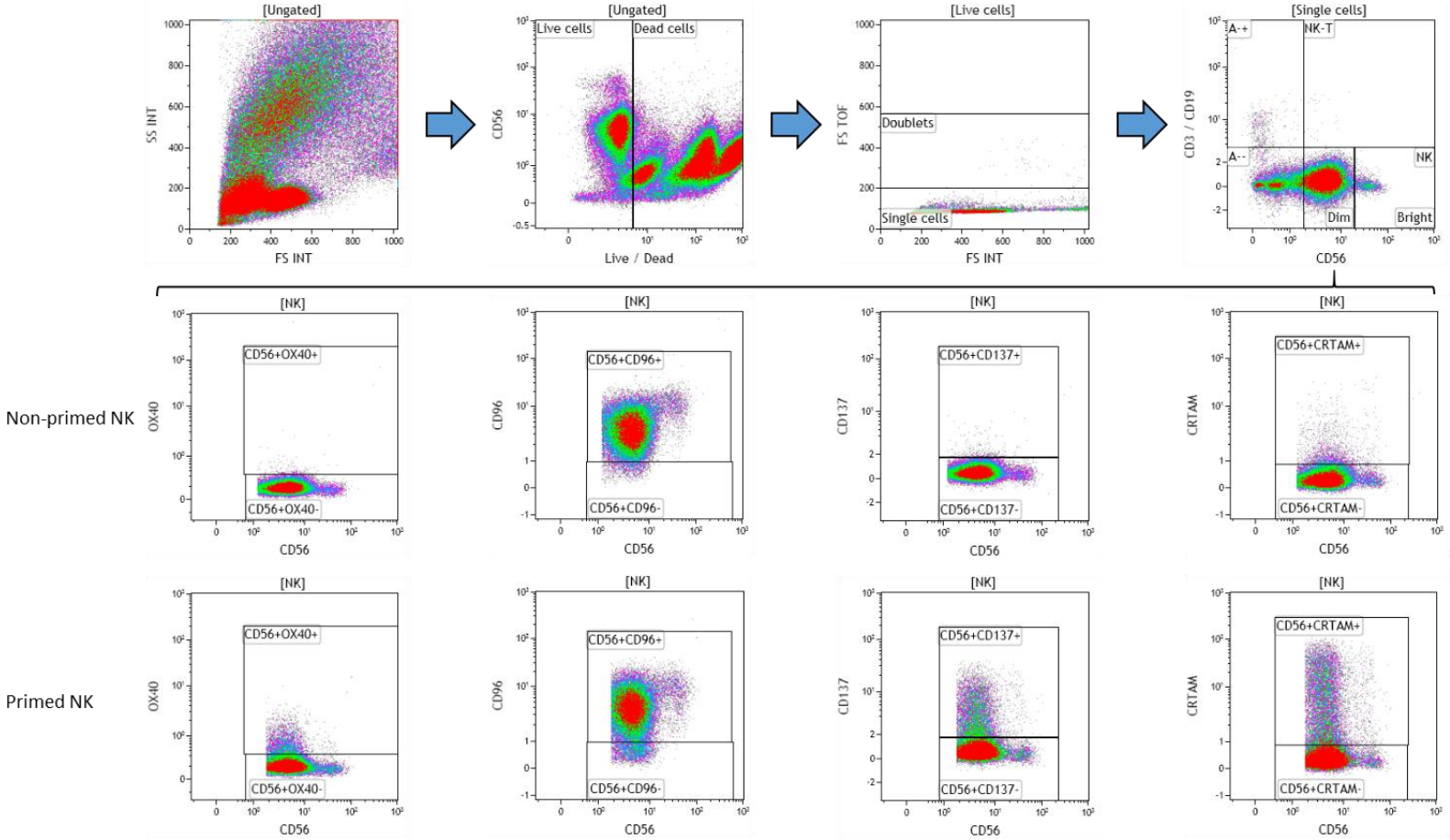

Figure 2.3: Gating strategy for analysing the expression of receptors OX40, CD96, CD137, CRTAM on CTV-1 primed NK cells and non-primed NK cells.
Using density plots the NK cells were analysed by first gating on 'live cells' from the cells acquired in theforward scatter (FSc) linear vs side scatter (SSc) linear density plot and then gating on single cells (determined by FSc Linear vs FS time of flight). Cells where then gated on the NK cell population that were $CD3^{-}CD19^{-}CD56^{+}$. Analysis of the expression of receptors OX40, CD96, CD137, CRTAM on healthy volunteer and patient NK cells was done by gating on the NK population and then looking for positive and negative expression of each receptor on cells expressing CD56. Gates were set using control NK stained for NK defining antibodies (CD3, CD19, CD56, CD16 and CD8) only. The expression of each NK receptor was measured using the 'Logical' setting.

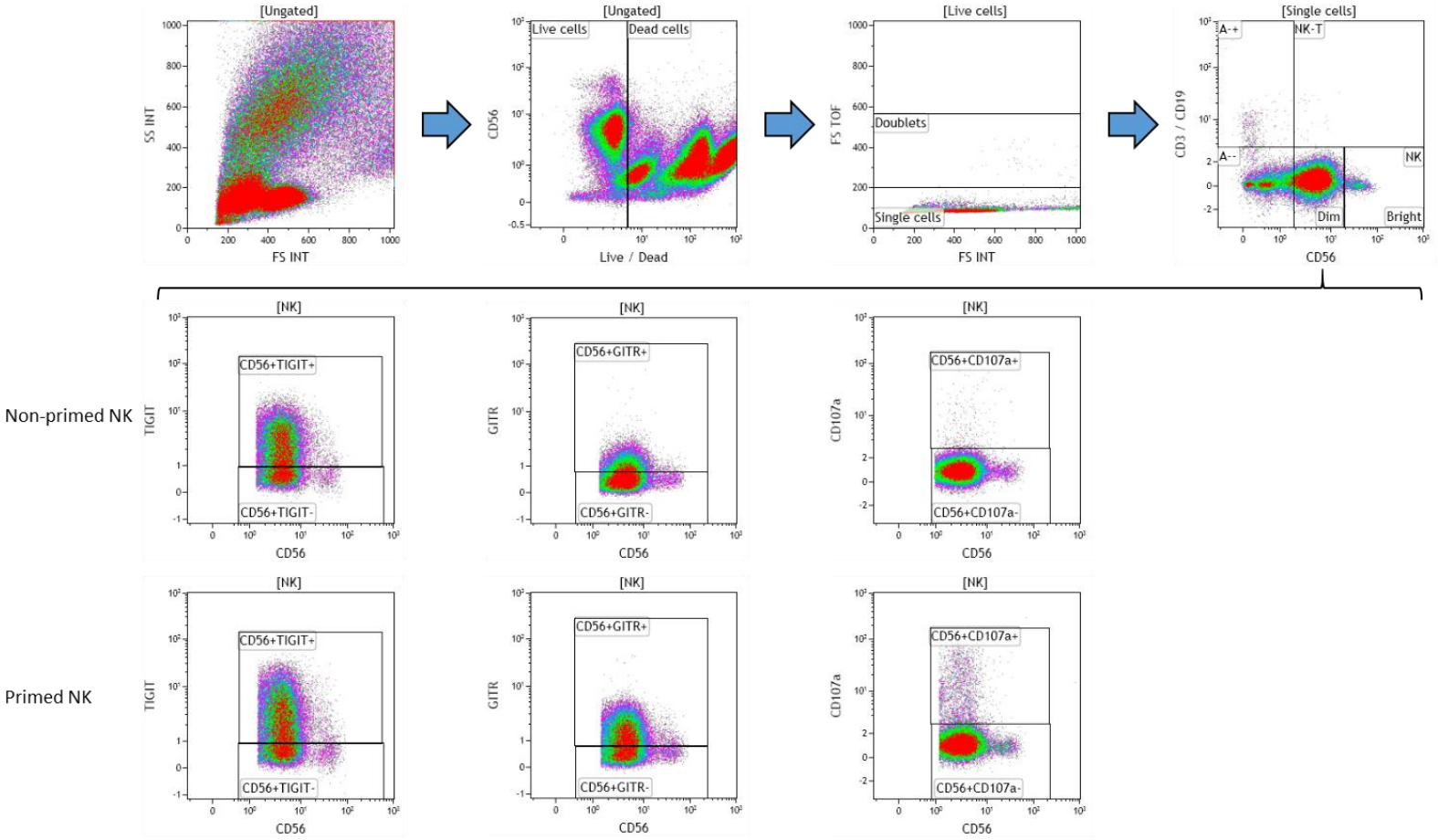

Figure 2.4: Gating strategy for analysing the expression of receptors TIGIT, GITR, CD107a CTV-1 primed NK cells and non-primed NK cells.
Using density plots the NK cells were analysed by first gating on 'live cells' from the cells acquired in the forward scatter (FSc) linear vs side scatter (SSc) linear density plot and then gated on single cells (determined by FSc Linear vs FS time of flight). Cells where then gated on the NK cell population that were $CD3^{-}CD19^{-}CD56^{+}$. Analysis of the expression of receptors TIGIT, GITR, CD107a on healthy volunteer and patient NK cells was done by gating on the NK population and then looking for positive and negative expression of each receptor on cells expressing CD56. Positive and negative gates were set using control NK stained for NK defining antibodies (CD3, CD19, CD56, CD16 and CD8) only. The expression of each NK receptor was measured using the 'Logical' setting.

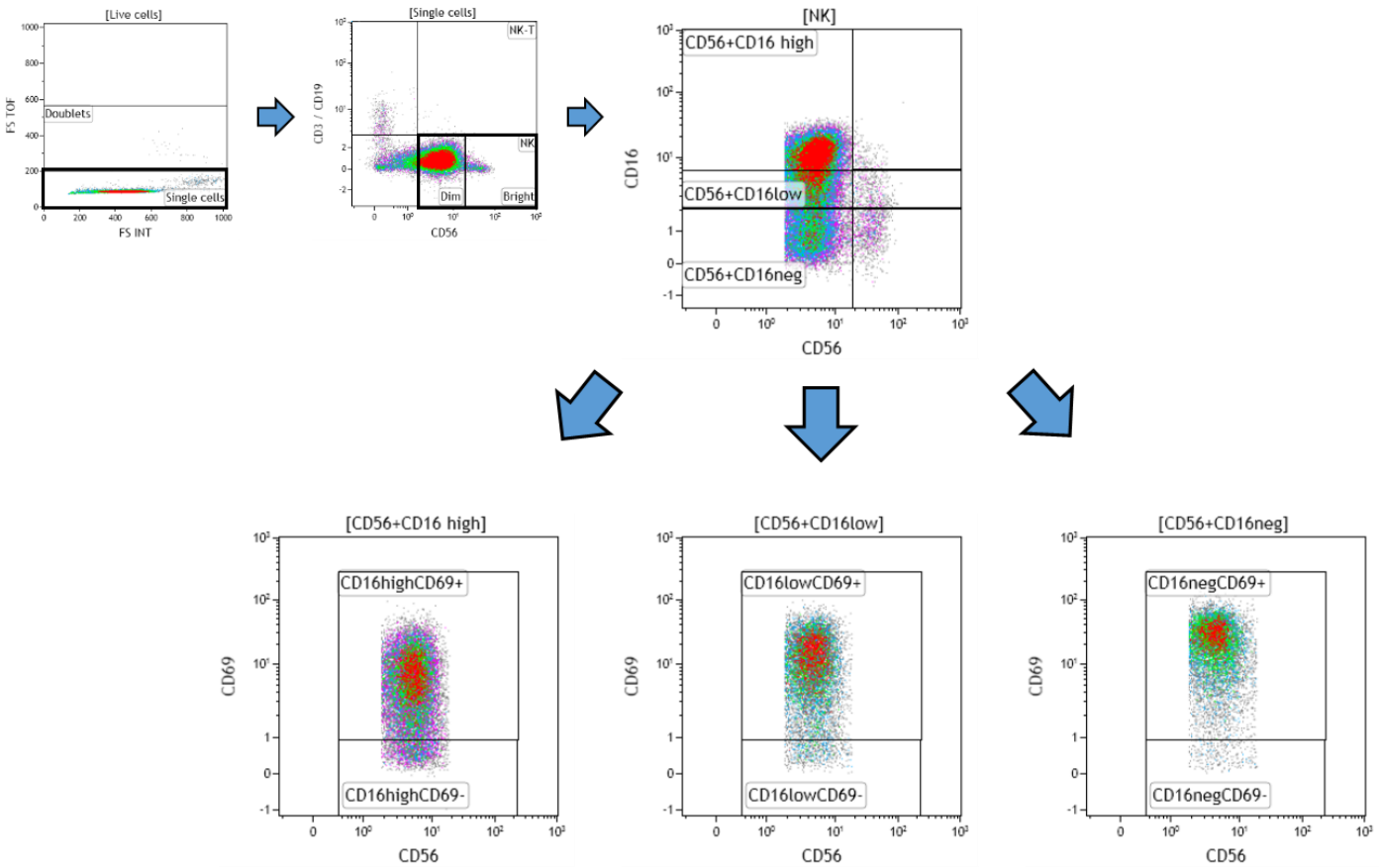

Figure 2.5: Representative gating strategy for measuring the expression of activating and adhesion / co-stimulatory receptors on the $CD56^{dim}CD16^{high}$, $CD56^{dim}CD16^{low}$ and $CD56^{dim}CD16^{neg}$ NK subpopulations.

Using density plots the NK cells were analysed by first gating on 'live cells' from the cells acquired in the forward scatter (FSc) linear vs side scatter (SSc) linear density plot and then gating on single cells (determined by FSc Linear vs FS time of flight). Cells where then gated on the NK cell population ($CD3^{-}CD19^{-}CD56^{+}$) and then subdivided into subpopulations based on CD56 and CD16 expression. Positive and negative expression of each activating and adhesion / co-stimulatory receptor was measured on the $CD56^{dim}CD16^{high}$, $CD56^{dim}CD16^{low}$ and $CD56^{dim}CD16^{neg}$ NK subpopulations by gating the on $CD56^{+}CD16^{high}$, $CD56^{+}CD16^{low}$ and $CD56^{+}CD16^{neg}$ gates. Positive and negative gates were set using control NK stained for NK defining antibodies (CD3, CD19, CD56, CD16 and CD8) only. The expression of each NK receptor was measured using the 'Logical' setting.

of positive and negative staining gates control tubes were set up for each antibody panel. For this, 100,000 NK cells were added to a 12x75 mm flow cytometry tube and were only stained with NK cell defining antibodies (CD3, CD19, CD56, CD16, CD8) using same protocol as previously described in section 2.3.1. Data were again analysed using the Beckman Coulter Kaluza™ software. Gating strategies for the positive and negative expression of each receptor on total NK cells are shown in Figures 2.2 to 2.4. A representative gating strategy for the positive and negative expression of each receptor on three NK cell subpopulations ($CD56^{dim}CD16^{high}$, $CD56^{dim}CD16^{low}$ and $CD56^{dim}CD16^{neg}$) is shown in Figure 2.5.

2.5 Measurement of NK cell cytotoxic function against human K562 erythroleukaemic and PC3 prostate cancer cells

2.5.1 K562 cell culture

The K562 cell line is an HLA class I negative, human erythroleukemic suspension cell line which was obtained from American Type Culture Collection (ATCC). Cryovials were defrosted using the same methods described in section 2.1.4 and cells were cultured in Iscove's Modified Dulbecco's Medium (IMDM) supplemented with 10% v/v FBS (Hyclone) (complete medium) in T75 flasks. On reaching confluence, cells were split in the range of 1 in 10 and 1 in 50 by adding the desired volume of K562 cell suspension to a new T75 flask and adding the appropriate volume of fresh medium.

2.5.2 PC3 cell culture

The PC3 cell line is an HLA Class I positive adherent epithelial cell line isolated from metastatic prostate cancer in the bone which was obtained from the American Type Culture Collection (ATCC). Cryovials containing previously frozen PC3 cells were defrosted using the same methods described in section 2.1.4 and cultured in F-12K Nut mix (Kaighn's modification) medium (Gibco, Thermo Fisher Scientific) supplemented with 10% v/v FBS (F-12K nut mix complete medium) in T175 flasks. Upon reaching confluence, PC3 cells were split between 1 in 5 and 1 in 12. For this, adherent cells were washed with 13 ml of PBS which was then discarded. The cells were then incubated in 10 ml of trypsin for 6 min at 37°C. Following the incubation, 13 ml of fresh medium was added to the flask to neutralise the trypsin. The detached PC3 cells were pelleted in a 50 ml Falcon tube at 300g for 5 min at RT and then re-suspended in 1 ml of fresh medium. The desired volume of re-suspended PC3 cells were then added to a fresh T175 flask containing 30 ml of fresh medium.

For the ^{51}chromium release cytotoxicity assay, K562 cells were pelleted in a 50 ml Falcon conical tube and incubated with 1.85MBq of ^{51}chromium in the residual RPMI complete medium in a water bath at 37°C for 1 hr. The K562 cells were then washed in serum-free RPMI medium and

centrifuged at 300g for 5 min. The supernatant was decanted, the cell pellet re-suspended in 1 ml of RPMI complete medium and incubated at 37 °C for 1 hr. Cells were washed in serum-free RPMI and re-suspended in 1 ml of complete medium. Cells were counted using trypan blue dye exclusion and diluted to a concentration of 1 x 10^5 viable cells/ml. Effector cells that were used were either PBMCs or isolated NK cells.

PBMCs were either isolated from fresh blood (see section 2.1.3) or thawed following being previously frozen using the method described in section 2.1.4. If isolated NK cells were to be used, then they were isolated from PBMCs using a Beckman Coulter MoFlow™ cell sorter following staining with CD45, CD3 and CD56 antibodies for 15 min in the dark at RT. Isolated effector cells were counted using a haemocytometer and trypan blue and diluted: PBMCs were diluted to 5 x 10^6 cells/ml in RPMI complete medium and isolated NK cells were diluted to 1 x 10^6 cells/ml. In a round-bottomed 96-well plate, 200 µl of effector cells were added to wells A, B, C, and D of column 1. To the rest of the wells was added 100 µl of RPMI complete medium. The cells were then serially diluted 1 in 2 from an effector to target ratio of 50 : 1 to an effector to target ratio of 1.5625 : 1. Then to each well containing effector cells 100 µl of target cells was added. To 4 separate wells, not containing effector cells, 100 µl of target cells were added and left on their own to measure spontaneous release of ^{51}chromium. To another 4 wells, again not containing effector cells, 100 µl of target cells were added and incubated in 1 % w/v SDS in order to determined maximum release of ^{51}chromium. Plates were incubated at 37 °C for 4 hours, after which 50 µl of supernatant from each well was transferred to a Luma plate containing dried scintillant. The plate was left to dry and then read on a Top Count machine (PerkinElmer®).

2.5.3 Calculation of target cell lysis for the ^{51}chromium release assay

To calculate the percentage of target cell lysis from the ^{51}chromium release assay, counts obtained by the Top Count machine the following calculation was used:

$$\left[\frac{\text{Average Test well count} - \text{Average Spontaneous release count}}{\text{Average Maximum release count} - \text{Average Spontaneous release count}}\right] \times 100 = \%\ \text{of Target cell lysis}$$

The test well count, spontaneous release count and maximum release count used in the calculation was an average of 4 repeats.

2.5.4 Flow cytometry-based cytotoxicity assay

2.5.4.1 Mitotracker® Green and propidium iodide cytotoxic assay

The principle of this flow cytometry assay is that target cells are labelled using the mitochondrial dye Mitotracker® Green (MTG) and their loss of viability following incubation with appropriate effector cells is determined by staining the cells using the viability dye propidium iodide (PI) (Hopkinson et al., 2007). The flow cytometric analysis of the stained cytotoxicity cell preparation on a two dimensional dot plot reveals four possible populations: $MTG^{pos}PI^{neg}$ (viable target cells), $MTG^{pos}PI^{pos}$ (non-viable, i.e. killed target cells), $MTG^{neg}PI^{neg}$ (viable effector cells) and $MTG^{neg}PI^{pos}$ (non-viable effector cells).

For the assay, Mitotracker® Green FM dye (Thermo Fisher Scientific) was prepared by re-suspending the lyophilised dye in 74.4 µl of dimethyl sulphoxide (DMSO, Santa Cruz) to a concentration of 1 mM which was aliquoted and stored at -20°C. In accordance with the manufacturer's instructions, an aliquot of the Mitotracker® Green was diluted to 200 nM in RPMI only and warmed at 37°C.

The target cells for this cytotoxic assay were either the K562 cell line or the PC3 cell line. If PC3 cells were the target of choice, then these cells were first washed with PBS, which was then discarded and cells detached from the T175 flask by incubating with 10 ml of Accutase™ Cell Detachment Solution (Innovative Cell Technologies) at RT for 3 min followed by a further 3 min at 37°C. Following the incubation, 13 ml of F-12K medium (supplemented with 10% v/v FBS) was added to the detached PC3 cells. The cells were then pelleted in a 50 ml Falcon conical tube at 300g for 5 min at RT, followed by re-suspension in 2 ml of fresh F-12K medium (supplemented with 10% v/v FBS). Cells were then counted using trypan blue and a haemocytometer. The required number of PC3 cells were then added to a 15 ml Falcon conical tube and incubated in 200 nM Mitotracker® Green solution at a concentration of 2×10^6 cells per ml for 20 min at 37°C in the dark. Following the incubation, the Mitotracker® Green stained PC3 cells was washed with 13 ml of PBS, pelleted and the supernatant discarded. The PC3 cells were washed twice more before being re-suspended in 1 ml of F-12K medium (supplemented with 10% v/v FBS) and counted using trypan blue and a haemocytometer. The PC3 cells were then re-suspended at 2×10^5 cells per ml.

The effector cells for this cytotoxic assay were either fresh PBMCs / isolated NK cells (prepared as described in section 2.1.3) or thawed PBMCs / resting isolated NK cells (prepared as described 2.1.3) or non-primed / primed NK cells (prepared as described in section 2.4.2). NK cells were isolated using either the Beckman Coulter MoFlow™ cell sorter or the EasySep™ Human NK Cell Enrichment Kit (STEMCELL Technologies). The prepared effectors cells were counted using a

haemocytometer and diluted to a concentration of 1 x 10^6 cells per ml in RPMI supplemented with 10% v/v FBS and 1% v/v L-glutamine.

The cytotoxic assay was setup in accordance with the experimental plan. In all experiments there was a time point 0 hr 'control' tube and a 'cytotoxic tube' for each sample or condition being measured. Depending on the experiment, the effector to target ratio was either 50 : 1, 25 : 1 or 5 : 1, with the number of target cells added always being 20,000 cells. For the control tube, the desired number of effector cells (depending on the effector target ratio) and 20,000 target cells were aliquoted into separate 12x75 mm flow cytometry tubes and the volume for each tube was made up to 100 µl (for non-primed control NK cells and primed NK cells the final volume was 200 µl to prevent the medium from becoming exhausted). The tubes were then incubated at 37°C in the dark for 2.5 hrs if using PC3 cells as targets, or 3.5 hrs if using K562 cells, unless the experiment was a time course over 1 to 4 hrs. Immediately prior to being measured on the flow cytometer, the effector and target cells were added together in a 12x75 mm flow cytometry tube, 10 µl of propidium iodide (50 µM/ml) added and the overall volume made up to 500 ul with PBS. The control tube indicated the degree of background target cell death.

For the 'cytotoxic tube', the desired number of effector cells and 20,000 target cells were co-incubated in 12x75 mm flow cytometry tubes in a total volume of 200 µl per tube at 37°C in the dark for the same length of time as the control tube. Immediately prior to being measured on the flow cytometer, 10 µl of propidium iodide (50 µM/ml) was added and the total volume in the tube made up to 500 µl with PBS. The 'control' tubes and the 'cytotoxic' tubes were then analysed by flow cytometry using the appropriate protocol which had been previously setup and compensated, as previously described in sections 2.2.2 and 2.2.3. For each tube measured, 6000 target cell (K562, PC3) events were acquired. Following acquisition, the data were analysed using the Beckman Coulter Kaluza™ software. The gating strategies are shown in Figure 2.6 (PBMCs targeted against K562 cells), Figure 2.8 (non-primed NK cells and primed NK cells targeted against PC3 cells) and Figure 2.9 (non-primed NK cells and primed NK cells targeted against K562 cells).

2.5.4.2 Calculation of target cell lysis

The flow cytometry data were analysed using the Beckman Coulter Kaluza™ software. Different gating strategies and total target cell lysis calculation methods were used depending on the effector and target cells that were used in the Mitotracker® Green and propidium iodide cytotoxicity assays.

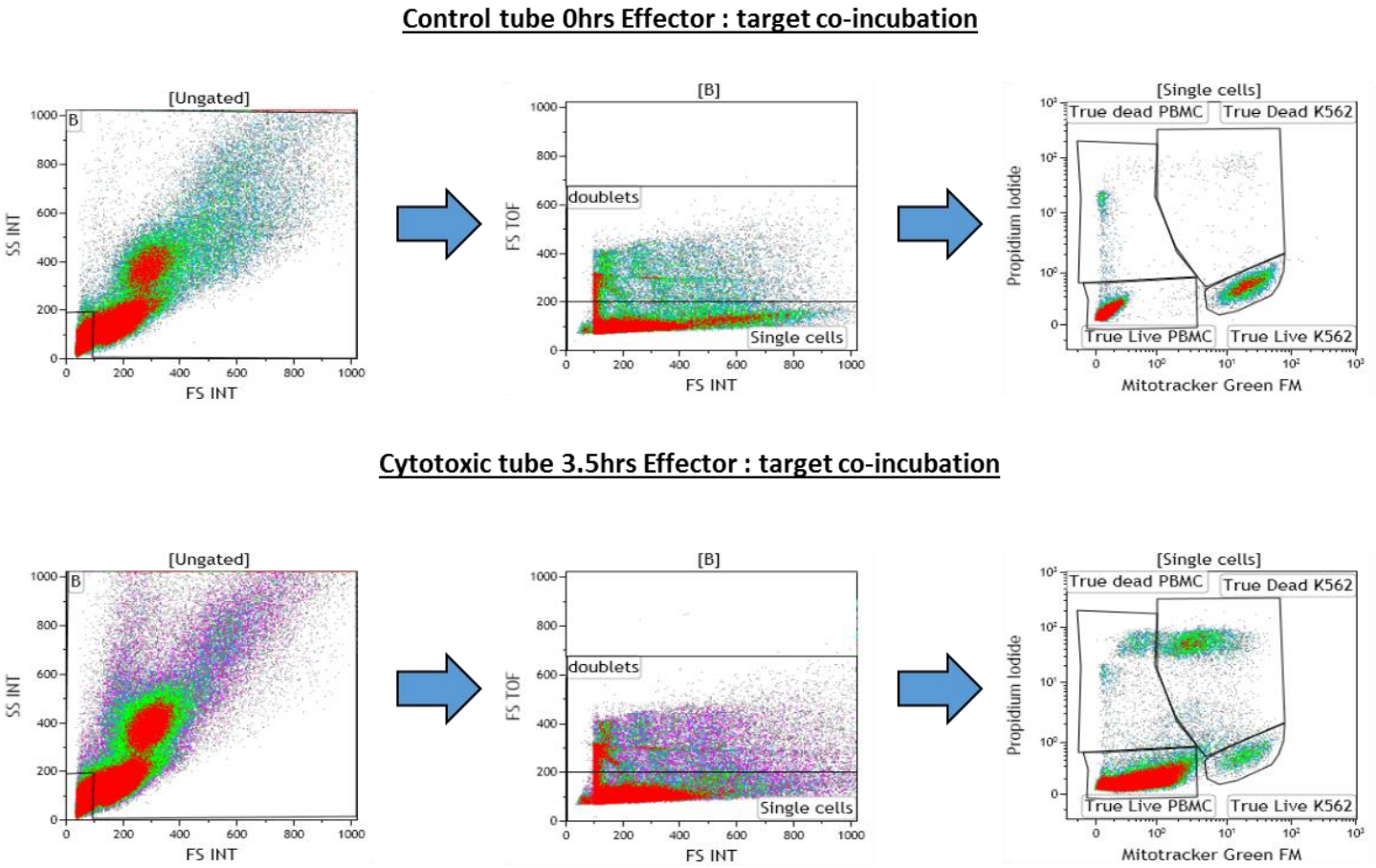

Figure 2.6: Gating strategy for determining the percentage of lysed K562 cells by PBMC using the flow cytometry based Mitotracker® Green and Propidium Iodide cytotoxic assay.

Using density plots the cells were gated on 'single cells' using the Forward scatter (FSc) linear and the FSc time or flight channels from cells acquired in the forward scatter (FSc) linear vs side scatter (SSc) linear density plot. The single cells were then further subdivided into 'True Dead PBMC', 'True Dead K562', 'True Live PBMC' and 'True Live K562' subsets based on their expression of Mitotracker® Green and Propidium Iodide both measured using the 'logical' setting. This gating strategy was used for data acquired from both the 'control' tube and the 'cytotoxic' tube.

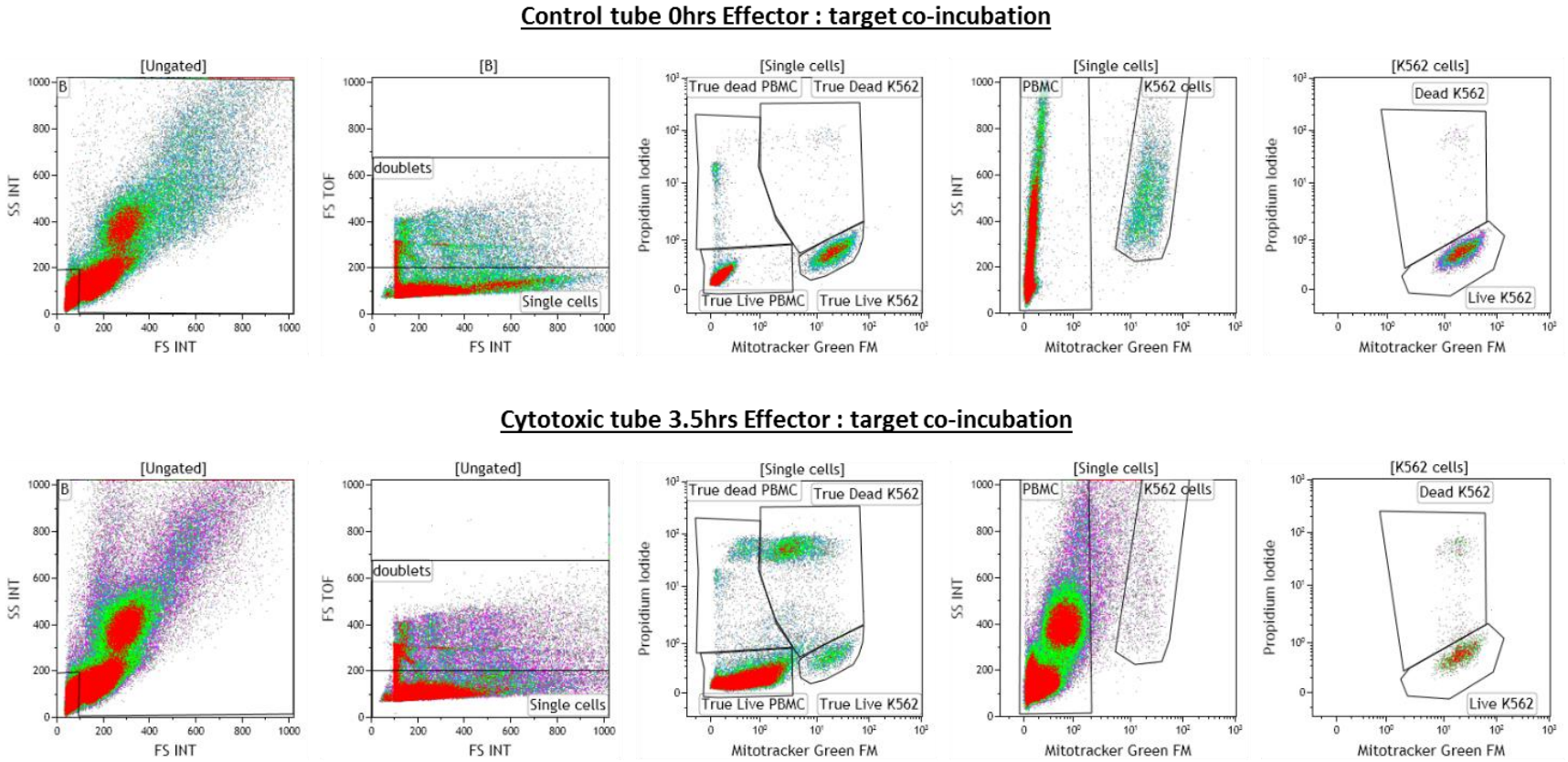

Figure 2.7: Alternative gating strategy for determining the percentage of lysed K562 cells by PBMC using the flow cytometry based Mitotracker® Green and Propidium Iodide cytotoxic assay.

Using density plots the cells were gated on 'single cells' (using the Forward scatter (FSc) linear and the FSc time or flight channels) from cells acquired in the forward scatter (FSc) linear vs side scatter (SSc) linear density plot. The 'single cells' were then further subdivided into 'True Dead PBMC', 'True Dead K562', 'True Live PBMC' and 'True Live K562' subsets based on their expression of Mitotracker® Green and Propidium Iodide both measured using the 'logical' setting. An additional density plot gated on 'single cells' was set up to measure the expression of Mitotracker® Green by K562 cells. Gating on the 'K562 cells' gate a further density plot was set up to measure the percentage of K562 cells that were dead within the 'K562 cells' gate based on their expression of Mitotracker® Green and Propidium Iodide. This gating strategy was used for data acquired from both the 'control' tube and the 'cytotoxic' tube.

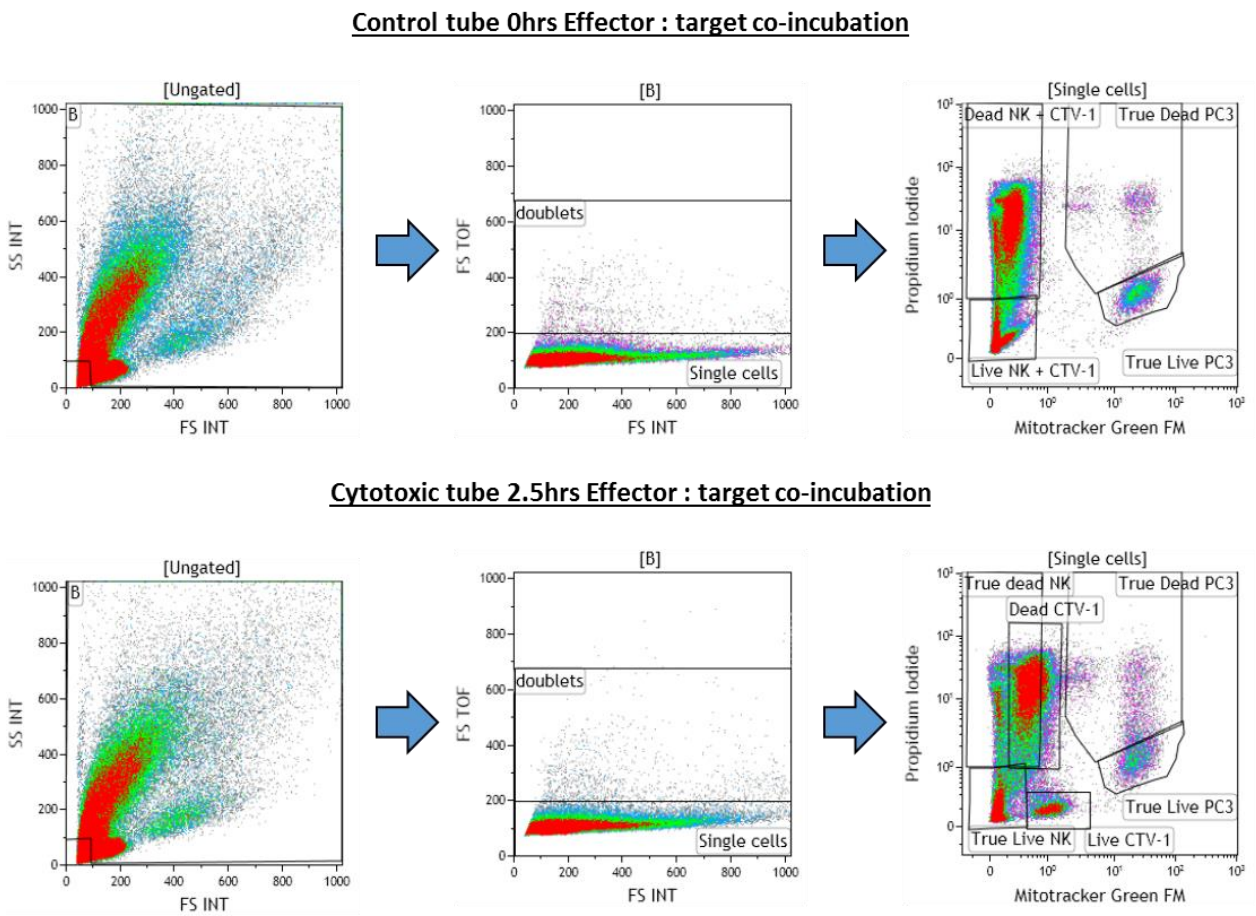

Figure 2.8: Gating strategy for determining the percentage of lysed PC3 cells by CTV-1 primed NK and non-primed NK using the flow cytometry based Mitotracker® Green and Propidium Iodide cytotoxic assay.

Using density plots the cells were gated on 'single cells' using the Forward scatter (FSc) linear and the FSc time or flight channels from cells acquired in the forward scatter (FSc) linear vs side scatter (SSc) linear density plot. The single cells were then further subdivided into 'True Dead NK', 'True Dead PC3', 'True Live NK' and 'True Live PC3' subsets based on their expression of Mitotracker® Green and Propidium Iodide both measured using the 'logical' setting. This gating strategy was used for data acquired from both the 'control' tube and the 'cytotoxic' tube.

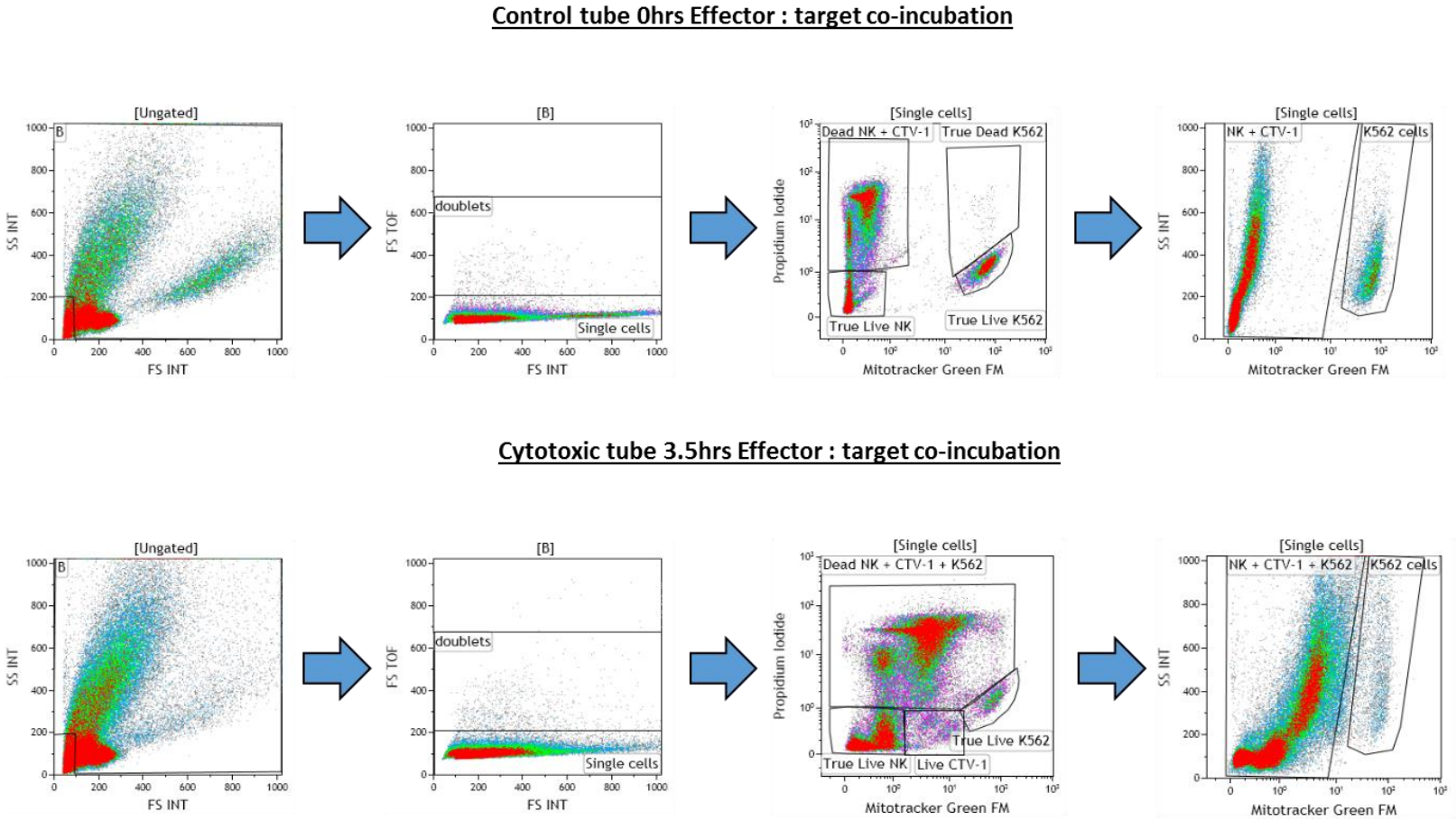

Figure 2.9: Gating strategy for determining the percentage of lysed PC3 cells by CTV-1 primed NK and non-primed NK using the flow cytometry based Mitotracker® Green and Propidium Iodide cytotoxic assay.

Using density plots the cells were gated on 'single cells' using the Forward scatter (FSc) linear and the FSc time or flight channels from cells acquired in the forward scatter (FSc) linear vs side scatter (SSc) linear density plot. The single cells were then further subdivided into 'True Dead NK', 'True Dead PC3', 'True Live NK' and 'True Live PC3' subsets based on their expression of Mitotracker® Green and Propidium Iodide both measured using the 'logical' setting. This gating strategy was used for data acquired from both the 'control' tube and the 'cytotoxic' tube.

2.5.4.2.1 Calculation of cytotoxicity when using resting PBMCs or isolated NK cells as effector cells against K562 target cells

Two calculation methods were initially used to determine the percentage of K562 target cell lysis:

Calculation method 1

Using the gating strategy illustrated in Figure 2.6. The following calculation method was used:

$$\text{Stage 1} \quad \left[\frac{\%\text{ True dead K562 (cytotoxic)} - \%\text{ True dead K562 (control)}}{\%\text{ True Live K562 (Control)}}\right] \times 100 = \%\text{ of cytotoxic killing}$$

$$\text{Stage 2} \quad \%\text{ True Live K562} + \%\text{ True Dead K562} = \%\text{ of Total K562}$$

$$\text{Stage 3} \quad \left[\frac{\%\text{ Total K562 (control)} - \%\text{ Total K562 (cytotoxic)}}{\%\text{ of Total K562 (control)}}\right] \times 100 = \%\text{ of missing K562}$$

$$\text{Stage 4} \quad \%\text{ of cytotoxic killing} + \%\text{ of missing K562} = \%\text{ of Total K562 Lysis}$$

Stage 1 of the calculation uses the percentage values from the 'True Live K562' and 'True Dead K562' gates. It was noted that the total percentage of K562 in the cytotoxic tube was always less than in the control tube. It was concluded that the 'missing K562 cells' may have been totally lysed and no longer detectable in the 'True Dead K562 cell' gate. Therefore, in stage 3 of the calculation, the percentage of 'missing' K562 cells was calculated and added to the calculated percentage of cytotoxic killing to give the percentage of total K562 cell lysis.

To confirm the accuracy of the results, an alternative way of calculating the percentage of total K562 lysis using the gating strategy shown in Figure 2.7 was also used. In theory, the calculated values for the percentage of total K562 cell lysis should be comparable using both calculation methods, assuming that the 'missing K562 cells' really are K562 cells that can no longer be detected in the 'True dead K562' gate . As shown in the 'K562 cells' gates of Figure 2.7 when K562 cells die they lose expression of Mitotracker® Green. The alternative calculation method was therefore based on the movement of 'dying' K562 cells out of the 'K562 cell' gate that was initially drawn around live K562 cells on the density plot of the control tube. Any K562 cells that are no longer detectable due to being completely lysed will not be present in the 'K562 cell' gate of the cytotoxic tube. The alternative calculation works as follows

$$\text{Stage 1} \quad \%\text{ of K562} - \left[\frac{\%\text{ dead K562}}{\%\text{ K562}} \times 100\right] = \text{Calculated \% of Live K562}$$

$$\text{Stage 2} \quad \left[\frac{\text{Calculated \% Live K562 (control)} - \text{Calculated \% dead K562 (cytotoxic)}}{\%\text{ True Live K562 (Control)}}\right] \times 100 = \%\text{ of Total K562 Lysis}$$

2.5.4.2.2 Calculation of cytotoxicity when using primed, isolated NK cells as effector cells against PC3 target cells

Adherent cancer cell lines present a different challenge to non-adherent cancer lines, as some cell lines such as the human prostate cancer cell line DU145 adhere to the 12x75 mm flow cytometry tubes, whereas others do not (e.g. PC3). However, because the PC3 cells do not adhere to the 12x75 mm flow cytometry tubes, they may be vulnerable to cell death when they are the only cell line in the tube. In contrast to the K562 cells, when using PC3 cells as targets it was often observed that the cytotoxic tube contained a slightly greater percentage of total PC3 cells (i.e. % True Live PC3 + % True Dead PC3) than the control tube. Although there is currently no explanation for this effect, the presence of NK cells might support the viability of a proportion of PC3 cells. As a consequence of this observed phenomenon, the calculation method had to be changed in order to take this account. The gating strategy for this calculation is shown in Figure 2.8 and the calculation method used to calculate percentage of total PC3 cell lysis is shown below:

Calculation method 2

$$\left[\frac{\%\text{ True dead PC3 (cytotoxic)} - \%\text{ True dead PC3 (control)}}{\%\text{ Total PC3 (cytotoxic)} - \%\text{ True dead PC3 (control)}}\right] \times 100 = \%\text{ Total PC3 lysis}$$

2.5.4.2.3 Calculation of cytotoxicity when using primed, isolated NK cells as effector cells against K562 target cells

It was not possible to remove the CTV-1 cells from the primed NK cells following NK priming, and it appeared that dead CTV-1 cells in the effector cell populations absorbed the Mitotracker® Green that had leaked out of the dead / dying K562. As a consequence, the two populations (i.e. the dead CTV-1 and the dead / dying K562) overlapped and made it impossible to gate around the dead / dying K562 accurately. As a consequence, it was necessary to alter the approach for calculating the percentage of K562 lysis. Using the gating strategy in Figure 2.9 calculation method 3 shown below was used to calculate the '% of total K562 lysis' value:

Calculation method 3

$$\left[\frac{\%\text{ True Live K562 (control)} - \%\text{ True Live K562 (control)}}{\%\text{ True Live K562 (Control)}}\right] \times 100 = \%\text{ of Total K562 Lysis}$$

2.5.5. CD107a degranulation assay.

The CD107a degranulation assay was setup in the same way as the Mitotracker® Green and Propidium Iodide cytotoxic assay in section 2.5.4, but with the following differences. For the 'Time Point 0hr' tube for each sample or condition, the effector and target cells were aliquoted into the same 12x75 mm flow cytometry tube, stained with one of the antibody panels shown in Table 2.4 and immediately measured following setup of the assay. The CD107a antibody was either added to the 'cytotoxic' tubes prior to co-incubation at 37°C in the dark for the desired length of time, or following co-incubation as part of the antibody panel. Propidium Iodide was not used to measure cell death in the CD107a degranulation assay, instead Live/Dead™ was used as part of the antibody panel. Only in the experiments observing the effect of GolgiStop™ (BD, Biosciences), 0 to 4 µl of GolgiStop™ were added to the 'cytotoxic' tubes after 1 hr initial co-incubation with the total time of co-incubation being 4 hrs in those experiments. Following these experiments it was apparent that the addition of GolgiStop™ was no longer required as it was found to hinder CD107a up-regulation. As a consequence, GolgiStop™ was no longer added to the 'cytotoxic' tubes in subsequent CD107a degranulation experiments

Following co-incubation at 37°C for up to 4 hrs (depending on the experiment), the 'cytotoxic' tubes were stained using one of the antibody panels in Table 2.4. The staining protocol for all tubes (both 'control' and 'cytotoxic') was as follows:

Cells were washed with 1 ml of wash buffer (PBS supplemented with 2% w/v BSA + 0.02% w/v Sodium Azide), after which they were centrifuged at 400g for 5 min at RT. The supernatant was discarded and the cells were re-suspended in 100µl of wash buffer. The cells were then stained with one of the CD107a antibody panels described in Table 2.4, with or without the CD107a antibody, depending on whether it had already been previously added to the tube prior to co-incubation at 37°C. The antibodies were incubated for 15 min in the dark at RT. Following incubation, cells were washed with PBS and re-suspended in 1 ml of the Live/Dead™ viability dye and incubated for 30 min in the dark at RT. After incubation, cells were centrifuged, the supernatant discarded, washed with wash buffer and finally re-suspended in 400 µl of Isoton™ II diluent. All tubes were then analysed by flow cytometry using the appropriate CD107a antibody panel protocol which had been previously setup and compensated in the same manner as previously described in sections 2.2.2 and 2.2.3. Measurement of the tubes was stopped following the acquisition of 40,000 NK cells or after 300 seconds in the event of low sample volume. Following acquisition, the data were analysed using the Beckman Coulter Kaluza™ software and a gating strategy similar to that shown in Figure 2.4.

Table 2.4: Antibody panels used to measure CD107a degranulation by Natural Killer cells and characterise their phenotype.

FL Channel & Wavelength	Antibody	Fluorochrome /dye	Clone	Manufacturer	Vol per tube
Panel 1					
FL1 525/40	Mitotracker™ Green FM	Dye (Green)		Thermo Fisher Scientific	200 nM
FL2 575/30	CD107a	PE	H4A3	BioLegend	5 µl
FL3 620/30	CD56	ECD (PE-Texas Red)	N901	Beckman Coulter	2.5 µl
FL4 695/30	CD16	PerCP-Cy5.5	3G8	BioLegend	5 µl
FL5 755LP	4-1BB (CD137)	PE-Cy7	4B4-1	BioLegend	5 µl
FL6 660/20	CRTAM (CD337)	APC	FN50	BioLegend	5 µl
FL7 725/20	CD3	Alexa Fluor 700	UCHT1	BioLegend	2 µl
FL7 725/20	CD19	Alexa Fluor 700	HIB19	BioLegend	1 µl
FL8 755LP	CD8	APC-Cy7	SK1	BioLegend	2.5 µl
FL9 450/40	Live/Dead™	Dye (violet)		Thermo Fisher Scientific	1 µl in 1 ml
Panel 2					
FL1 525/40	Mitotracker Green FM	Dye (Green)		Thermo Fisher Scientific	200 nM
FL3 620/30	CD56	ECD (PE-Texas Red)	N901	Beckman Coulter	2.5 µl
FL4 695/30	CD16	PerCP-Cy5.5	3G8	BioLegend	5 µl
FL5 755LP	CD107a	PE-Cy7	H4A3	BioLegend	5 µl
FL7 725/20	CD3	Alexa Fluor 700	UCHT1	BioLegend	2 µl
FL7 725/20	CD19	Alexa Fluor 700	HIB19	BioLegend	1 µl
FL8 755LP	CD8	APC-Cy7	SK1	BioLegend	2.5 µl
FL9 450 / 40	Live/Dead™	Dye (violet)		Thermo Fisher Scientific	1 µl in 1 ml

2.6 Graphical Representation of Data and Statistical Analysis

GraphPad Prism v6 software was used to create graphs and determine statistical significances in the cell phenotypic and cytotoxicity data between the experimental groups. Depending on whether there was one or two variables between groups of phenotypic data, a one-way or two-way ANOVA statistical test was used in conjunction with a comparisons test. The initial ANOVA, whether parametric or non-parametric, only determined whether there was a statistical difference between the mean values of each of the three or more groups of data. Based upon the significance, it then provides a P value. To find out which groups within a dataset were significantly different, a comparisons test must be performed. It should be noted that it is possible for the ANOVA to indicate a statistically significant difference, implying that the mean values of the 3 or more groups are significantly different, which is not observed using the comparisons test.

2.6.1 Statistical approach for examining differences in the phenotype of NK cells in patients with prostate cancer (Chapter 3)

A non-parametric Kruskal-Wallis test was used (non-parametric version of the one-way ANOVA) to determine differences in the expression of receptors by NK cells from patients with benign disease and patients with different Gleason grades of prostate cancer. This test was used due to the fact that the patient group was the only variable and the data points within each Gleason group exhibited a non-Gaussian distribution, as measured using the D'Agostino & Pearson normality test. The only comparisons test made available by the GraphPad Prisim v6 software following a non-parametric Kruskal- Wallis test was the Dunns multiple comparison test.

2.6.2 Statistical approach for examining the influence of priming on NK cell phenotype (Chapter 4)

A one-way ANOVA (parametric test) was used to examine differences in the expression of each NK cell receptor on total NK cells following NK cell priming at different NK : CTV-1 ratios, despite the data exhibiting a non-Gaussian distribution. A one-way ANOVA was used because the only variable was the level of NK cell priming and there were very few data points within each data group. Despite a non-parametric test usually being used in this situation, the non-parametric test was found not to be sufficiently powerful to accurately measure significant differences between data groups due to the low number of data points within each group. As a consequence, the more powerful parametric test was used to improve the accuracy of detecting significant differences between data groups.

A two-way ANOVA was used to examine differences in the expression of NK cell receptors on $CD56^{dim}CD6^{high}$, $CD56^{dim}CD16^{low}$, $CD56^{dim}CD16^{neg}$ populations following NK cell priming. This was because there were two variables: one variable was the different degree of NK cell priming and the second variable was the expression of the specific receptor on different $CD56^{dim}CD16$ subpopulations. The two-way ANOVA was carried out twice using the Tukey's comparison test to separately identify the significant differences between data groups based on each variable.

2.6.2 Statistical approach for examining the differential influence of priming on the phenotype of NK cells from healthy volunteers *versus* patients with prostate cancer (Chapter 5)

A two-way ANOVA was used to examine the differential influence of priming on the phenotype of NK cells from healthy volunteers *versus* patients with prostate cancer. This test was used because there were two variables and there were a limited number of data points within each data group. One variable was whether the NK cells were primed or non-primed and the second variable was comparing non-primed NK cell and primed NK cell data groups between the healthy volunteers and the three cancer patient groups. Comparison tests were again used to determine

between which data groups there was a significant difference. A Tukey's comparison test was used to compare NK cell receptor expression between healthy data groups and cancer patient data groups. A Fisher's least significant difference (Fisher's LSD) comparisons test was used to compare NK cell receptor expression between non primed and primed NK cells within each healthy volunteer, benign patient groups or cancer patient group. The differences between the Tukey's comparison test and the Fisher's LSD test is explained below.

2.6.2.1 Tukey's comparison test

The Tukey's comparison test is used to compare the group mean with every other group mean. When comparing the mean of group A to the mean of group C, the test compares the difference between the two means to the amount of scatter quantified using information from all the groups, not just groups A and C. This gives the test more power to detect differences, and the test assumes that all data are sampled from populations with the same standard deviation even if the means are different (reference GraphPad Prism v6 statistical test help guide).

2.6.2.2 Fisher's Least Significant Difference (LSD) comparison test

In simple terms, this test is a set of t tests that does not correct for multiple comparisons. The difference between the Fisher's LSD test and a set of t tests is that the t tests compute the pooled standard deviation from only the two groups being compared. The Fisher's LSD test computes the pooled standard deviation from all the groups, which gains power (reference GraphPad Prism v6 statistical test help guide).

Chapter 3 - RESULTS

Expression of NK cell activating and inhibitory receptors on peripheral blood NK cells from patients with prostate cancer, individuals with benign disease and healthy controls

3.1 Introduction

As reviewed by Vivier et al (Vivier et al., 2008), natural killer (NK) cells were first recognised as being large lymphocytes having natural cytotoxicity against tumour cell lines (Trinchieri, 1989). NK cells express two primary types of receptors; activating receptors and inhibitory receptors (Lanier, 2005, Parham, 2005). Healthy cells that have either become infected by virus or have transformed into cancerous cells, up-regulate stress-induced self-ligands on their cell surface, whereas the expression of MHC class I is often down-regulated. NK cells recognise stress ligands via activating receptors and the presence of MHC class I (and other inhibitory ligands) via the relevant inhibitory receptors (Lanier, 2005, Parham, 2005).

It is proposed that the net balance of signals received via the activating and inhibitory receptors dictate the activation status and thereby the functional response of the NK cell. This concept is known as the 'Dynamic Equilibrium' hypothesis (Brumbaugh et al., 1998). Therefore, host cells that are becoming cancerous or have been virally infected up-regulate stress ligands, concomitant with a potential downregulation of MHC class I molecules. This provides the NK cell with more activating signals then inhibitory signals, thereby promoting their activation and cytotoxic potential against the relevant target cell. Healthy cells express few or no stress ligands and maintain MHC class I expression. As a consequence, more inhibitory signals than activating signals are received by the NK cell, preventing activation of the NK cell and thus no cytotoxic function is exerted against the healthy cell.

Increasing evidence suggests that the microenvironment surrounding solid tumours can exert immunosuppressive and inhibitory effects on NK cells which can manifest as an inhibition of cytotoxic function (Hasmim et al., 2015, Vitale et al., 2014). The location of tumours has been associated with the presence of chronic inflammation, with this occurring either prior to the formation of the tumour or being caused by the activation of oncogenes (Mantovani et al., 2008). Studies have shown that tumours are able to secrete immunosuppressive cytokines such as TGF-β and other immunosuppressive soluble factors such as indoleamine pyrrole 2,3-dioxygenase (IDO) and prostaglandin E_2 (PGE2) into the microenvironment. TGF-β down-regulates the expression of NKp30 and alters NK cell chemokine receptor expression, whereas IDO and PGE2 have been shown to downregulate the expression of NKp30, NKp44 and NKG2D on NK cells (Castriconi et al., 2013, Pietra et al., 2012). In addition, activated inflammatory and

immunosuppressive cells such as tumour-associated fibroblasts (TAFs) and macrophages (TAMs), myeloid-derived suppressor cells (MDSCs), immunoregulatory T cells (Treg) and neutrophils are also recruited to the tumour microenvironment and contribute to its suppressive nature by secreting immunosuppressive cytokines (e.g. IL-10, TGF-β) and factors (e.g. IDO, PGE2), as well as growth factors (e.g. IGF, HGF) and extracellular-matrix remodelling enzymes (MMPs, FAP and VEGF), reviewed by (Vitale et al., 2014). This immunoregulatory microenvironment favours tumour invasion. TAFs have been shown to down-regulate NK cell expression of DNAM-1 through cell-to-cell contact and down-regulate NKp44 and NKp30 expression via the release of PGE2 and IDO in a melanoma model and a hepatocellular carcinoma (Balsamo et al., 2009, Li et al., 2012). *In vitro*, Treg cells and MDSCs have been shown to down-regulate NKG2D expression upon cell-to-cell contact via their expression of membrane bound TGF-β (Ghiringhelli et al., 2005, Li et al., 2009)

In addition to suppressing NK cell and adaptive immune responses, tumours also modulate the microenvironment around them in order to aid their proliferation and survival by promoting angiogenesis and tumour metastasis (Hasmim et al., 2015, Mantovani et al., 2008, Vitale et al., 2014). A deeper understanding of the immunoregulatory environment of the tumour and its effects on key elements of the protective immune system would inform the development of diagnostic and therapeutic approaches. However, access to the tumour can be difficult in some instances, and so studies have investigated whether the phenotype of NK cells in the peripheral blood reflect the phenotype of tumour infiltrating NK cells (Carlsten et al., 2009, Mamessier et al., 2011b, Platonova et al., 2011). To date, the results have been mixed and it appears that only in some forms of cancer does the phenotype of peripheral NK cells reflect the phenotype of tumour infiltrating NK cells.

A series of papers published by Mamessier et al in 2011 (Mamessier et al., 2011a, Mamessier et al., 2011b) revealed that the phenotype of peripheral blood NK cells was altered in patients with invasive breast cancer compared to that of NK cells in the periphery of patients with non-invasive disease and healthy controls. NK cells in patients with invasive breast cancer displayed a decrease in the intensity (MFI) of NKp30, NKG2D, DNAM-1 and 2B4 expression compared to the controls. These decreases in receptor expression were also associated with a decreased ability to degranulate and kill the NK cell sensitive cell line K562. Their ability to secrete cytokines such as IFN-γ and TNF-α in response to K562 was also impaired (Mamessier et al., 2011b). In an attempt to assess how well the phenotype of peripheral NK cells reflects the phenotype of tumour infiltrating NK cells, NK cells were isolated from large localised and locally advanced tumours from which sufficient numbers could be extracted, and the phenotype of these cells was compared to the phenotype of NK cells in the peripheral blood. Although the phenotype of

tumour-infiltrating NK cells was heterogeneous, patients with poor prognosis exhibited a decreased expression of nearly all of the primary NK cell receptors (Mamessier et al., 2011b). Overall, positive correlations between the intensity (MFI) of NKp30, CD16, NKG2D and NKG2A expression on tumour-infiltrating NK cells and peripheral blood NK cells were found. It was concluded that tumour infiltrating NK cells recirculate in the peripheral blood and therefore the phenotype of peripheral NK cells reflect the phenotype of tumour-infiltrating NK cells. However, it was noted that the alterations in phenotype of peripheral NK cells were reduced in comparison to tumour-infiltrating NK cells, and that the NK cells within the tumour expressed a higher intensity of CD56. The authors could not distinguish whether this increased expression of CD56 reflected a more immature phenotype, and therefore associated with the $CD56^{bright}$ NK cell subset, or whether it reflected an activation phenotype which is similar to that which characterises cytokine-activated NK cells (Mamessier et al., 2011b). In a separate study, Mamessier and colleagues did establish, using peripheral NK cells and breast cancer cell lines, that NK cells recognise breast cancer cells mainly through their NKG2D and DNAM-1 receptors, with the receptors NKp30 and NKp46 playing a lesser role. Therefore, taken together, these findings suggest that invasive breast tumours develop mechanisms that down-regulate the expression of NK receptors that recognise them, thereby suppressing the immune response of the NK cells that infiltrate the tumour and that this suppression to some extent is reflected in peripheral NK cells (Mamessier et al., 2011a).

Although peripheral blood NK cells, to some degree at least, reflect the phenotype of tumour infiltrating NK cells in breast cancer, the phenotype of peripheral NK cells does not reflect the phenotype of tumour infiltrating NK cells in other cancers such as lung cancer and ovarian cancer (Carlsten et al., 2009, Platonova et al., 2011). In a study involving patients suffering from lung carcinoma, the phenotype of peripheral, intratumoural and nontumoural NK cells was measured and compared to that of the peripheral blood NK cells of healthy donors. It was observed that the phenotype of the peripheral blood NK cells did not reflect the phenotype of the intratumoural NK cells in the cancer patients, as the percentage of intratumoural NK cells expressing NK activating receptors NKp30, NKp80, CD16 and DNAM-1 was significantly down-regulated compared to their expression on peripheral NK cells. Additionally, the expression of NKp44 was significantly up-regulated on the intratumoural NK cells compared to the peripheral blood NK cells. Furthermore, the percentage of intratumoural NK cells expressing these receptors was significantly different compared to nontumoural NK cells, whereas there was no significant difference between the phenotype of peripheral blood NK cells from healthy donors compared to peripheral blood NK cells from patients (Platonova et al., 2011). Similar findings were found in a study of patients with ovarian cancer, in whom the phenotype of peripheral

blood NK cells from healthy donors was comparable to the phenotype of NK cells in the peripheral blood of patients. No significant differences in the expression of any of the NK cell activating receptors that were measured were observed. However, a comparison of the phenotype of peripheral blood NK cells from patients with that of tumour-associated NK cells (from peritoneal effusions) revealed that the intensity (MFI) of expression of the NK cell receptors DNAM-1, 2B4 and CD16 was decreased, whereas the intensity of expression of the NK cell receptors NKG2D and NKp46 was increased (Carlsten et al., 2009).

Currently, very few studies have examined NK cell phenotype and function in patients with prostate cancer. It was only relatively recently that NK cell receptors involved in prostate cancer recognition were identified (Pasero et al., 2015). For these studies, Pasero et al assessed the capacity of NK cells from healthy donors that had been activated with IL-2 to kill prostate cancer cell lines in the presence or absence of blocking antibodies. Blocking the activating receptors NKG2D, DNAM-1, NKp46 and NKp30 decreased the level of NK cell degranulation in response to the prostate cancer cell lines PC3, DU145 and LNCaP. They also found significantly higher levels of NKp30, NKp46 and DNAM-1 expression on NK cells from patients with metastatic prostate cancer that took > 18 months to become castrate-resistant compared to the levels of the same receptors expressed on NK cells by patients who became castrate resistant in < 18 months. Patients with high levels of NKp30 and NKp46 expression were linked to increased probability of survival at 3 years compared to patients with a low expression of NKp30 and NKp46. The study concluded that NKG2D, DNAM-1, NKp46 and, to a lesser extent NKp30, were the NK cell receptors that are involved in the recognition prostate cancer, and suggested that peripheral blood NK cells may represent the intratumoural NK cell phenotype. They concluded that peripheral blood NK cells in prostate cancer patients have prognostic value and hypothesised that the screening of NK cell markers could be used for routine diagnosis (Pasero et al., 2015).

3.2 Aims and Hypothesis

The aims of this part of the study was to determine the expression of NK cell activating and inhibitory receptors on peripheral blood NK cells from patients with different Gleason grades of prostate cancer, and compare the expression profiles with those on NK cells from the peripheral blood of individuals that were diagnosed with benign disease. The NK cell phenotype profiles were then correlated with patient clinical data e.g. Gleason grade in order to determine whether the phenotype of peripheral blood NK cells correlates with disease status. Ultimately, the data could be used to monitor disease progression and patient prognosis.

It was hypothesised that the presence of prostate cancer would exert a suppressive effect on NK cells that is detectable in the periphery and that the down-regulation of specific NK receptors would correlate with increased Gleason grade of prostate cancer.

3.3 Results

3.3.1 Patient cohorts

Peripheral blood was obtained from two patient cohorts; the so-called TRUS cohort and Transperineal (TP) cohort. Only 56 out of the 92 TRUS patients and 71 out of 72 TP patients have been included in the analysis, as only the NK cells from these patients were phenotyped by flow cytometry. The clinical details for the patients in the TRUS patient cohort are shown in Table 3.1, and those for the TP cohort are shown in Tables 3.2 and 3.3. All patients received a digital rectal examination (DRE), underwent a TRUS biopsy and their levels of PSA determined using standard techniques. The patients in the TP cohort had additional TP biopsies taken in order to observe whether this technique improved prostate cancer detection and diagnosis, and only individuals having peripheral PSA levels < 20 ng/ml were included. Peripheral blood was obtained for analysis of peripheral blood immune cell populations by multi-parameter flow cytometry. For both patient cohorts, patients were grouped according to the overall Gleason grade of the biopsy tissue which had been collected from their tumours.

3.3.1.1 Patient Age

The age of the patients within the TRUS group ranged between 53 and 88 yrs old (Table 3.1). Although the ages of the patients overlapped for each patient group, the median age of each group was significantly higher (P = 0.0015) as the Gleason grade of the group increased (Figure 3.1A and Table 3.1).

Table 3.1: TRUS patient cohort clinical details

TRUS Gleason grade	TRUS Gleason score	Number of patients	Age Mean (yrs)	Group Age Range (yrs)	Group PSA range (ng/ml)	Group DRE range
Benign	Benign	13		53 - 73	1.5 - 83	Benign - T2
Gleason 6	3+3	12		55 - 88	3.9 - 19	Benign - T2
Gleason 7	3+4	9		66 - 86	3.0 - 76	Benign - T2
	4+3	8		63 - 85	7.8 - 248	Benign - T4
Gleason 8	4+4	2		70 - 74	7.9 - 12	T2
Gleason 9	4+5	10		67 - 88	11 - 2617	Benign - T4
	5+4	2		69 - 84	40 - 118	T4

Table 3.2: TP patient cohort clinical details

TP Gleason Grade	TP Gleason score	Number of patients	Age Mean (yrs)	Group Age range (yrs)	Group PSA range (ng/ml)	Group DRE range
Benign	Benign	6		64 - 71	5.3 to 14.4	N/A
	HG pin	9		58 - 70	5.1 - 12	
	ASAP	8		62 - 70	5.3 - 15	
	HG Pin + ASAP	8		50 - 76	4.7 - 19	
Gleason 6	3+3	14		55 - 71	4.7 - 11	T1 - T2a
Gleason 7	3+4	18		53 - 80	4.7 - 13	T2a -T2c
	4+3	6		54 - 77	5.1 - 19	T2a -T2c
Gleason 9	4+5	2		65 - 75	6.3 - 18	T2b - T2c

The median age of the TRUS benign and Gleason 6 patients was 66 yrs and 68 yrs respectively. The median age of patients with Gleason 7 and Gleason 9 disease (72 yrs and 78.5 yrs respectively) was significantly higher than that of patients with benign disease. Although only two patients had Gleason 8 disease, their ages were similar to those with Gleason 7 disease.

Similar to TRUS patients, the age range of the TP patients was between 50 and 80 yrs old (Table 3.2). The age range within each of the TP patient groups was similar and no significant differences in the median age was observed between individuals with benign disease (median age 66 yrs) and those with Gleason 6 (median age 63.50 yrs), Gleason 7 (median age 66 yrs) or Gleason 9 (median age 70 yrs) disease (Figure 3.1B).

3.3.1.2 Patient PSA levels (ng/ml)

Similar to patient age, the PSA levels for each TRUS patient group also significantly increased as the Gleason grade increased (Figure 3.2A and Table 3.1). The PSA levels for the patients in the benign disease and Gleason 6 group were comparable (medians of 8.2 ng/ml and 8.3 ng/ml respectively). Gleason 9 patients were found to have significantly higher levels of PSA (median 54 ng/ml) in their blood than individuals with benign disease and those with Gleason 6. There were no significant differences in the levels of PSA in patients with Gleason 7 or Gleason 8 disease patients and those with benign and Gleason 6 patients, despite median PSA levels for the Gleason 7 patient group being 16 ng/ml.

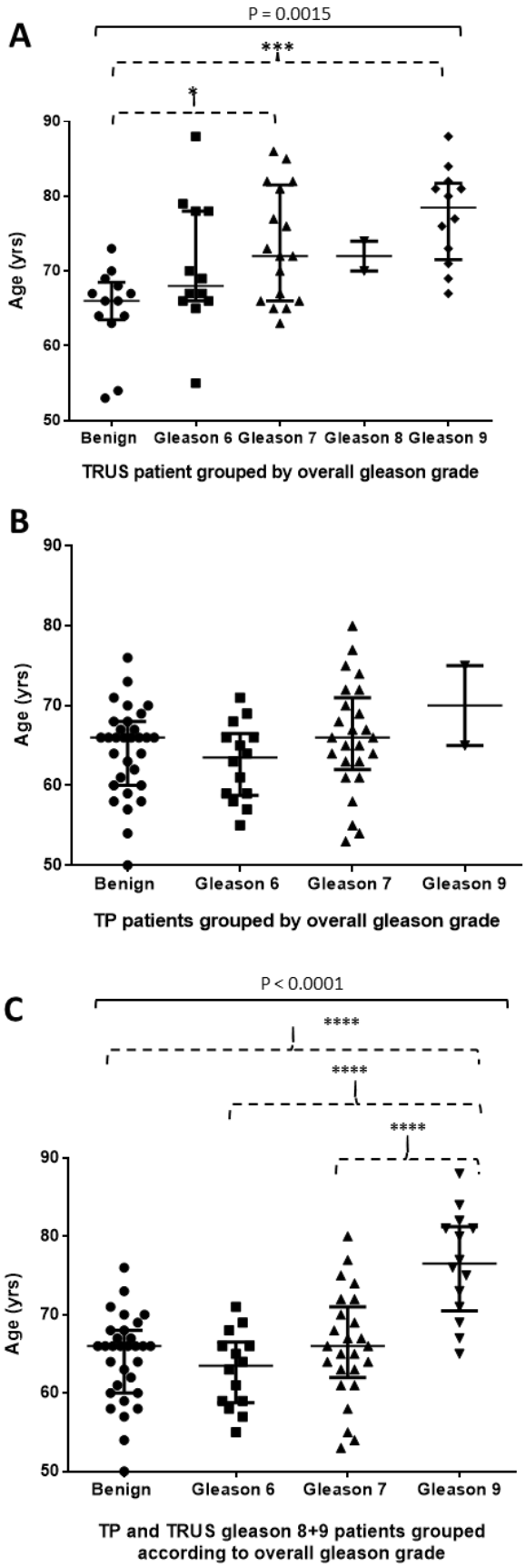

Figure 3.1: Age range of the patient groups within the TRUS and TP cohorts.
Grouped according to Gleason grade the age of each patient in the (A) TRUS cohort, (B) TP cohort, (C) TP and TRUS (Gleason 8 and Gleason 9 patients only) are plotted. Statistical analysis according to Kruskal-Wallis test (solid line) and Dunns multiple comparison test (dashed line). *P≤0.05, **P<0.005, ***P≤0.0005, ****P≤0.00005

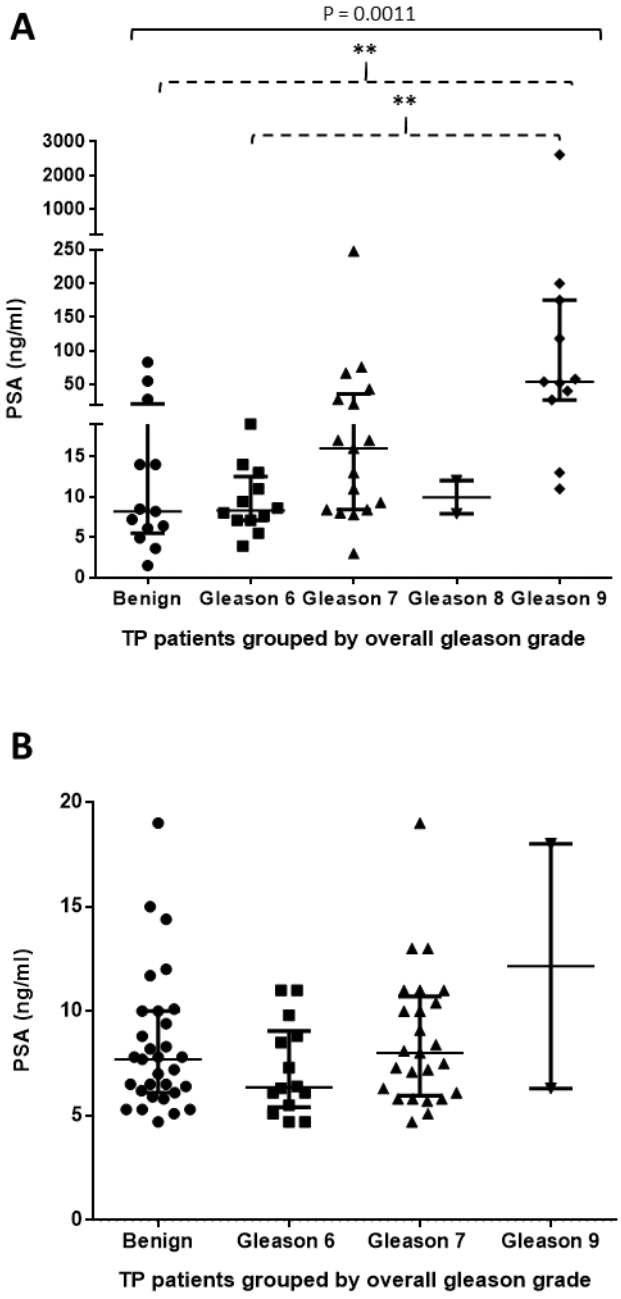

Figure 3.2: PSA range of the patient groups within the TRUS and TP cohorts.
Grouped according to Gleason grade the PSA value (ng/ml) in the blood of each patient in the (A) TRUS cohort, (B) TP cohort, (C) TP and TRUS (Gleason 8 and Gleason 9 patients only) are plotted. Statistical analysis according to Kruskal-Wallis test (solid line) and Dunns multiple comparison test (dashed line). *P≤0.05, **P<0.005.

In contrast to the TRUS cohort, the PSA levels for the TP patient groups were comparable and no significant differences were observed (Figure 3.2B and Table 3.2). The selection criterion for this cohort was that all TP patients had a PSA levels < 20 ng/ml.

3.3.1.3 Patient DRE results

Analysis of the digital rectal examination (DRE) results for the TRUS cohort revealed that, within each Gleason group, a proportion of patients were detected as having benign disease. The majority of the patients within the benign group (as diagnosed by TRUS biopsy) were diagnosed as being benign on the basis of the DRE, with one patient diagnosed with stage 2 cancer. The majority of the Gleason 6 group patients were also diagnosed as having benign disease on the basis of the DRE, with only three patients presenting with stage 2 cancer. Within the Gleason 7 group, on the basis of DRE four patients were diagnosed with stage 2 cancer, one with stage 3 cancer and one with stage 4 cancer, with the remainder having benign disease. The two patients within the Gleason 8 patient group were diagnosed with benign and stage 2 cancer respectively, on the basis of the DRE, whereas the patients within the Gleason 9 patient group were diagnosed with either stage 3 cancer (n=5), stage 4 cancer (n=4), or as having benign disease (n=2) (Table 3.1)

In the TP cohort, all benign patients were diagnosed as having benign disease on the basis of the DRE. Four patients within the Gleason 6 patient group had stage 1 cancers, with the rest having stage 2 cancers. All patients with Gleason 7 and Gleason 9 disease had stage 2 cancer (Table 3.2).

3.3.1.4 Patient Gleason grade

As shown in Table 3.1, there were 56 patients within the TRUS cohort. The number of patients within each Gleason group was different. There were only 13 patients with benign disease and 12 patients with Gleason 6 disease. Out of the 17 patients with Gleason 7, 9 patients had a Gleason score of 3+4 and 8 patients had a Gleason score of 4+3. There were two Gleason 8 patients and 12 patients with Gleason 9, with 10 patients having been diagnosed with a Gleason score 4+5 and two patients diagnosed with a Gleason score of 5+4.

In the TP cohort, patients were grouped according to the overall Gleason grade, and the number of patients with each Gleason score recorded for biopsies using both techniques is shown in Table 3.3.

Figure 3.3 highlights the discrepancies in Gleason grade and score, as detected using the TRUS biopsy (A and C) and the TP biopsy (B and D). As detected by TRUS biopsy, 73.7 % of the patients were diagnosed with benign disease, whereas the rest of the patients were positive for prostate cancer; Gleason 6: 4.2 %, Gleason 7: 4.2 %, Gleason 9: 1.4 % (Table 3.3 and Figure 3.3A). Using the more sensitive TP biopsy, the percentage of patients diagnosed with benign disease fell to 43.1 %, with the rest of the patients within the cohort being diagnosed as being positive for prostate cancer; Gleason 6: 22.3 %, Gleason 7: 32 %, Gleason 9: 2.8% (Table 3.3 and Figure 3.3B).

As shown in Table 3.3, the TRUS biopsy misdiagnosed 39 % of the patients, in that 30.6 % of the patients were diagnosed as having benign disease using the TRUS biopsy when in fact they

Table 3.3: The discrepancies in diagnosis of prostate cancer between the TRUS biopsy and the TP biopsy methods in the TP cohort.

Patient diagnosis by biopsy method		Number of Patients	PSA Range (ng/ml)	Percentage of TP cohort
Gleason grade by TRUS biopsy	Gleason grade by TP biopsy			
Benign	Benign	31	5.1 - 19	43.1
Benign	3+3	10	4.7 - 11	13.9
Benign	3+4	9	4.7 - 10.4	12.5
Benign	4+3	3	10 - 19	4.2
3+3	3+3	4	4.7 - 8.5	5.6
3+3	3+4	2	5.8 - 7.3	2.8
3+3	4+5	1	6.3	1.4
3+4	3+4	6	5.7 - 13	8.3
3+4	3+3	2	5.8 - 11	2.8
4+3	4+3	2	5.1 - 9.1	2.8
4+3	3+4	1	11	1.4
4+5	4+5	1	18	1.4

had Gleason 6 and 7 grade cancers, as detected by TP biopsy. Only 4.2 % of the patients diagnosed as having Gleason 6 disease using the TRUS biopsy were misdiagnosed. The TP biopsy diagnosed these individuals as either having Gleason 7 or Gleason 9 grade cancers.

The 31 TP patients (30.9 %) that were diagnosed as having benign disease were further subcategorised into subgroups based on evidence of abnormal, but not cancerous looking tissue; benign, high grade HG PIN, ASAP and HG PIN + ASAP. Six patients (19.4 %) were benign with normal-looking tissue, 9 (29 %) patients showed evidence of HG PIN only, 8 patients (25.8 %) showed evidence of ASAP only and 8 patients (25.8 %) showed evidence of both HG PIN and ASAP.

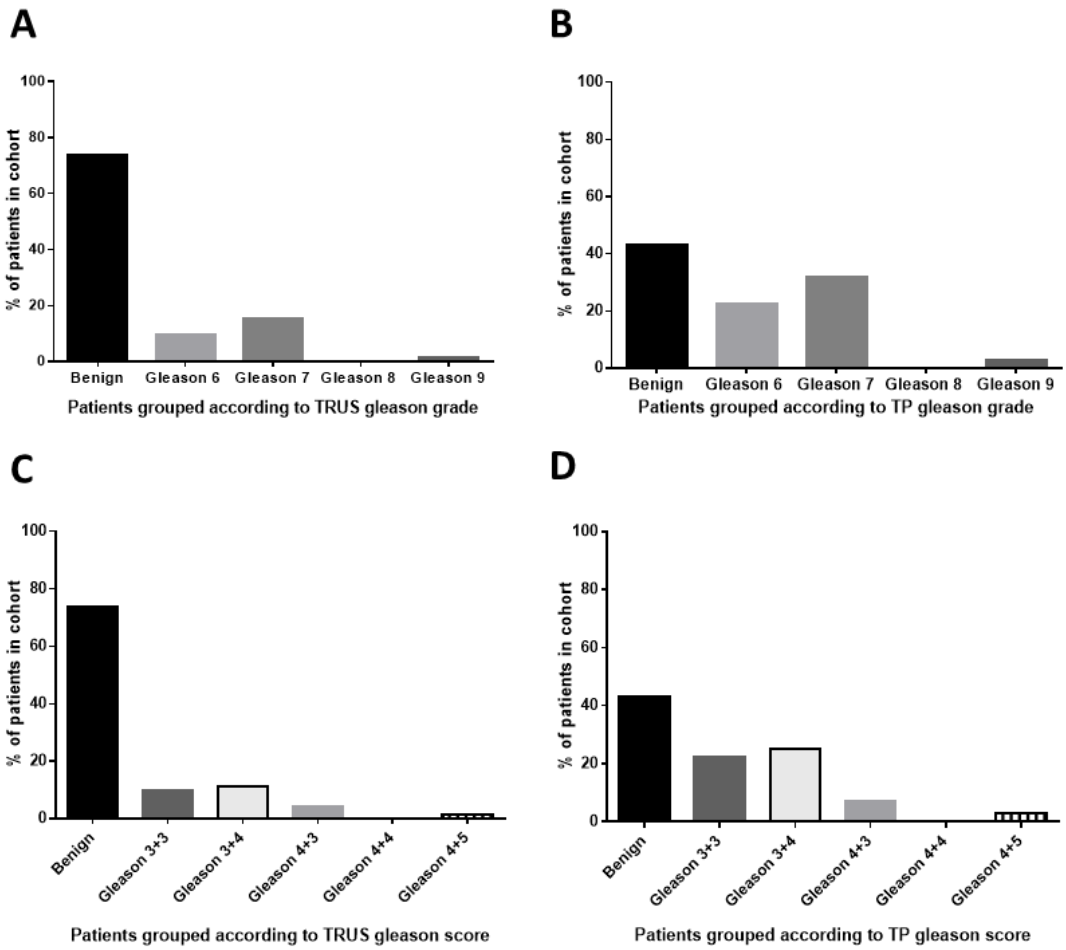

Figure 3.3: The effect of biopsy method on the diagnosis of patients suspected of having prostate cancer within the TP cohort.
Comparison of the diagnosis of prostate cancer in patients that made up the TP cohort, as determined by either TRUS or TP biopsy. A and B) Patients grouped according to their Gleason grade diagnosed by TRUS biopsy or TP biopsy respectively. C and D) Patients grouped according to their Gleason score diagnosed by TRUS biopsy or TP biopsy respectively.

3.3.2 Comparison of the phenotype of NK cells within each patient group

In order to determine any differences between the phenotype of NK cells from patients with different grades of prostate cancer and benign disease, patients would need to be accurately diagnosed. The TP cohort represented the most accurately diagnosed patients and therefore were chosen for this analysis. However, the number of patients with advanced cancer (Gleason 9) was limited. Although the Gleason 8 and Gleason 9 patients from the TRUS cohort were diagnosed using the TRUS biopsy only, the fact that these patients already had advanced cancer that was predominately made of grade 4 cancer with evidence of grade 5 cancer (Gleason 9 patients only) meant that these patients were likely to have been accurately diagnosed. This was further supported by the fact only 3 out of 19 TP patients initially diagnosed with prostate cancer by TRUS biopsy had a higher grade cancer detected by the TP biopsy (Figure 3.3). Therefore, the

TRUS Gleason 8 and Gleason 9 patients were included in the analysis in order to contribute to the dataset on the phenotype of peripheral blood NK cells in patients with advanced disease. It should be noted that this increased the median age of the Gleason 8+9 group to 76.5 yrs which was found to be significantly higher than the median age of the other patient groups (Figure 3.1C). The clinical details of the patients for each Gleason group that were included in the NK cell phenotypic analysis cohort are shown in Table 3.4.

Table 3.4: Clinical characteristics of the combined TP and TRUS (Gleason 8 and 9 patients only) NK phenotypic analysis cohort used to analyse differences in NK cell phenotype in correlation with severity of disease.

Overall Gleason grade	Overall Gleason Score	Number of patients	Group Age range (yrs)	Group PSA range (ng/ml)	Group DRE range
Benign	Benign	6	64 - 71	5.3 to 14.4	N/A
	HG pin	9	58 - 70	5.1 - 12	
	ASAP	8	62 - 70	5.3 - 15	
	HG Pin + ASAP	8	50 - 76	4.7 - 19	
Gleason 6	3+3	14	55 - 71	4.7 - 11	T1 - T2a
Gleason 7	3+4	18	53 - 80	4.7 - 13	T2a -T2c
	4+3	6	54 - 77	5.1 - 19	T2a -T2c
Gleason 8	4+4	2	70 - 74	7.9 - 12	T2
Gleason 9	4+5	13	65 - 88	4.3 - 2617	T2 - T4
	5+4	2	69 - 84	40 -118	T4

3.3.2.1 Prevalence of $CD56^{dim}$ and $CD56^{bright}$ NK cell subsets

The percentage of NK cells within the PBMCs from each patient group is shown in Figure 3.4A. There was no significant difference in the percentage of NK cells between the four groups that were examined. The percentage of NK cells in the PBMCs of individuals with benign disease ranged between 0.23 % and 27.49 %, whereas the range in patients with cancer was between 2.07 % to 35.89 %. (Figure 3.4A). The percentage of $CD56^{dim}$ and $CD56^{bright}$ NK cells that made up the patient NK cell population also did not significantly differ between patient groups. Whether positive or negative for prostate cancer, > 90 % of NK cells were the $CD56^{dim}$ phenotype in the majority of patients (Figure 3.4C). Although there was no difference in the intensity of the expression of CD56 on $CD56^{dim}$ NK cells, the intensity of CD56 expression on $CD56^{bright}$ NK cells

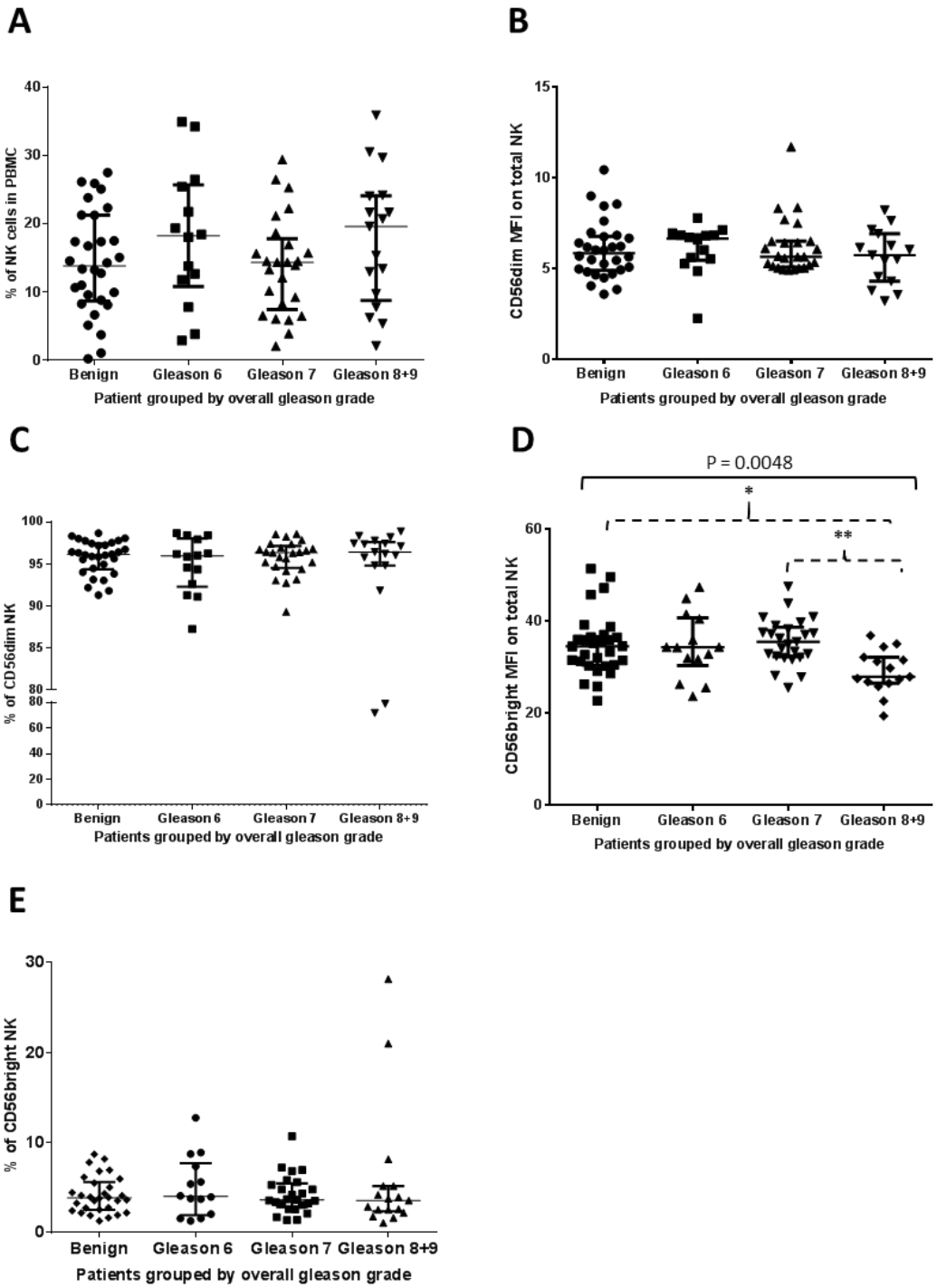

Figure 3.4: The prevalence of CD56^{dim} and CD56^{bright} NK subsets in the peripheral blood of patients. Analysis of patient CD56^{dim} and CD56^{bright} NK cell subsets with patients grouped according to overall Gleason graded diagnosed by TRUS and TP biopsy methodologies. A) The percentage of NK cells within patient PBMC. B) The median intensity fluorescence (MFI) of the CD56 receptor on patient CD56^{dim} NK subsets. C) Percentage of the patient NK cells that were CD56^{dim}. D) The MFI of the CD56 receptor on patient CD56^{bright} NK subsets. E) Percentage of patient NK cells that were CD56^{bright}.expression of CD56 on CD56^{dim} NK cells, the intensity of CD56 expression on CD56^{bright} NK cells was significantly different amongst the patient groups (P = 0.0048), with CD56^{bright} NK cells in patients with Gleason 8+9 disease, on average, expressing lower intensities of CD56 than those in patients with Gleason 7 and benign disease (Figure 3.4D). Statistical analysis according to Kruskal-Wallis test (solid line) and Dunns multiple comparison test (dashed line). *P≤0.05, **P<0.005.

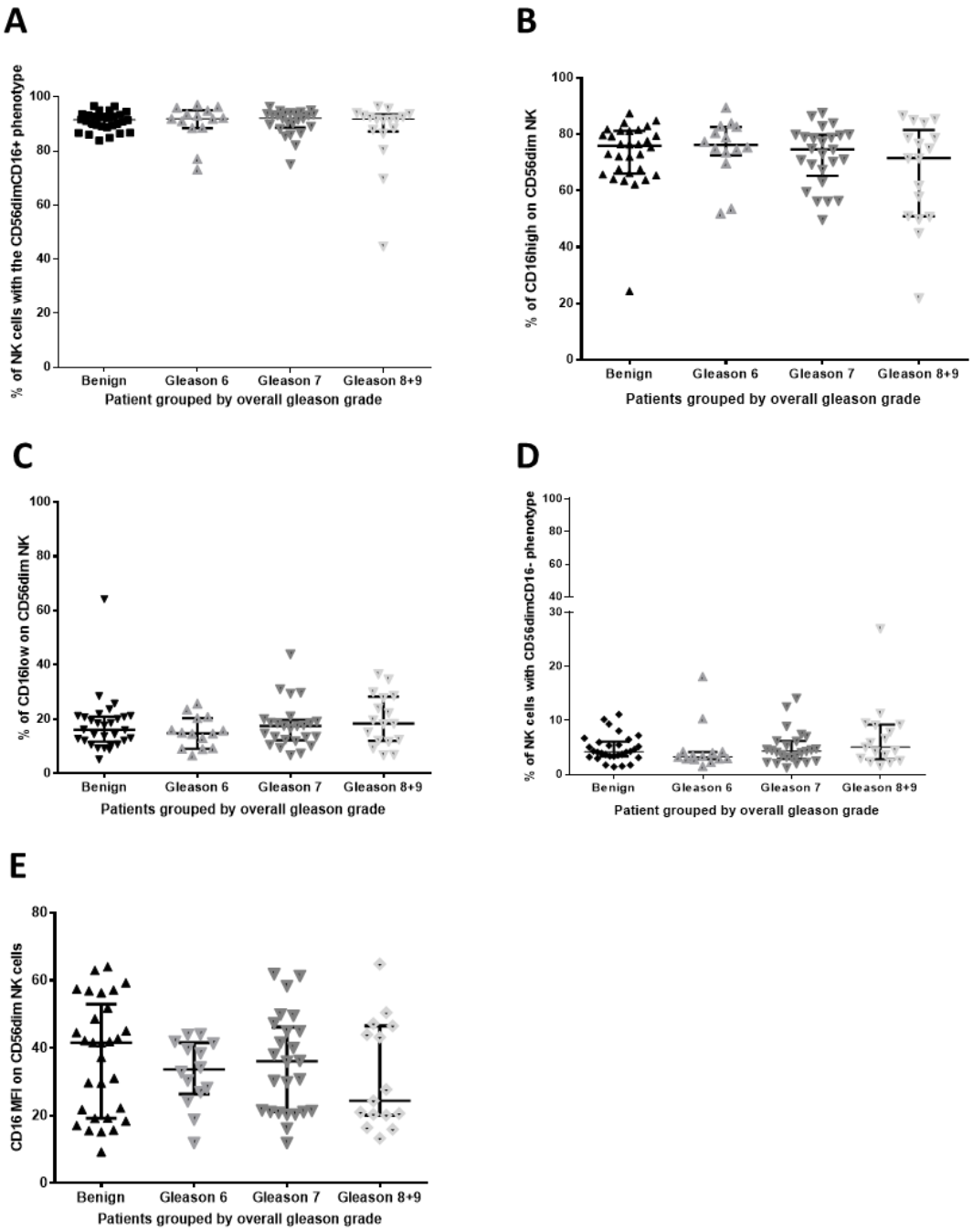

Figure 3.5: Analysis of expression of the CD16 receptor on patient CD56^{dim} NK cells.
The expression of CD16 on patient CD56dim NK cells when patients were grouped according to overall Gleason grade diagnosed by TRUS and TP biopsy methodologies. A) Percentage of the patient NK population that were CD56^{dim}CD16^{+}. B) The percentage of patient CD56dim NK cells with high CD16 expression. C) The percentage of patient CD56^{dim} NK cells with low CD16 expression. D) The percentage of patient CD56^{dim} NK cells that were negative for CD16 expression. E) The median fluorescence intensity (MFI) of CD16 expression on patient CD56dim NK cell subset population.

was significantly different amongst the patient groups (P = 0.0048), with CD56^{bright} NK cells in patients with Gleason 8+9 disease, on average, expressing lower intensities of CD56 than those in patients with Gleason 7 and benign disease (Figure 3.4D).

3.3.2.2 CD16 expression on the CD56^{dim} NK cell subset

The percentage of NK cells that were CD56^{dim}CD16^{+} did not significantly differ between the patient groups, with > 80 % of the NK cells displaying this phenotype for the majority of patients, irrespective of whether they were positive for prostate cancer or not (Figure 3.5A).

The median percentage of NK cells displaying a CD56^{dim}CD16^{high} or CD56^{dim}CD16^{low} phenotype was also the same across the four patient groups (Figure 3.5 B and C). Interestingly though, the median fluorescence intensity (MFI) of expression for CD16 on the CD56^{dim} NK cells progressively reduced as the Gleason grade of the patient increased. Although the range in MFI expression of CD16 for all four groups was comparable, the median expression decreased from an MFI value of 41.56 for individuals with benign disease to an MFI value of 33.66 and 36.06 for the Gleason 6 and 7 patient groups. The median expression then decreased again to a MFI value of 24.37 for the Gleason 8+9 patient group. Despite the visible decrease in median MFI values for the patient groups as the Gleason grade of cancer increased, the differences in the MFI of CD16 expression on CD56^{dim} NK cells was not found to be significantly different between the patient groups (Figure 3.5E).

3.3.2.3 Expression of activating receptor and receptor CD8 on patient NK cells

The results for the expression of activating receptors NKp30, NKp46, NKG2D, DNAM-1, 2B4 and the CD8 receptor are shown in Figures 3.6. and 3.7.

There was no significant difference in the percentage of NK cells expressing NKG2D, nor was there a significant difference in the intensity of NKG2D expression between patient groups (Figures 3.6 G and H). A similar pattern of expression was observed for the expression of the CD8 receptor (Figures 3.6 A and B). The median percentage of patient NK cells expressing NKG2D within in each patient group was approximately 95 % for each group. For CD8 expression, the median percentage of patient NK cells expressing that receptor for each patient group ranged between 42.2 % and 37.7 %.

In contrast to the expression of NKG2D and CD8, differences in the expression of the NKp30 and NKp46 receptors on NK cells from patients in the different groups were observed. As shown in Figure 3.6C, the percentage of NK expressing NKp30 was significantly different between the four patient groups. There was a broad range of expression for NKp30 on the NK cells of the individuals with benign disease. The percentage of NK cells expressing NKp30 ranged between 96.74 % and 40.69 % and there appeared to be two defined groups; in one group, >90 % of

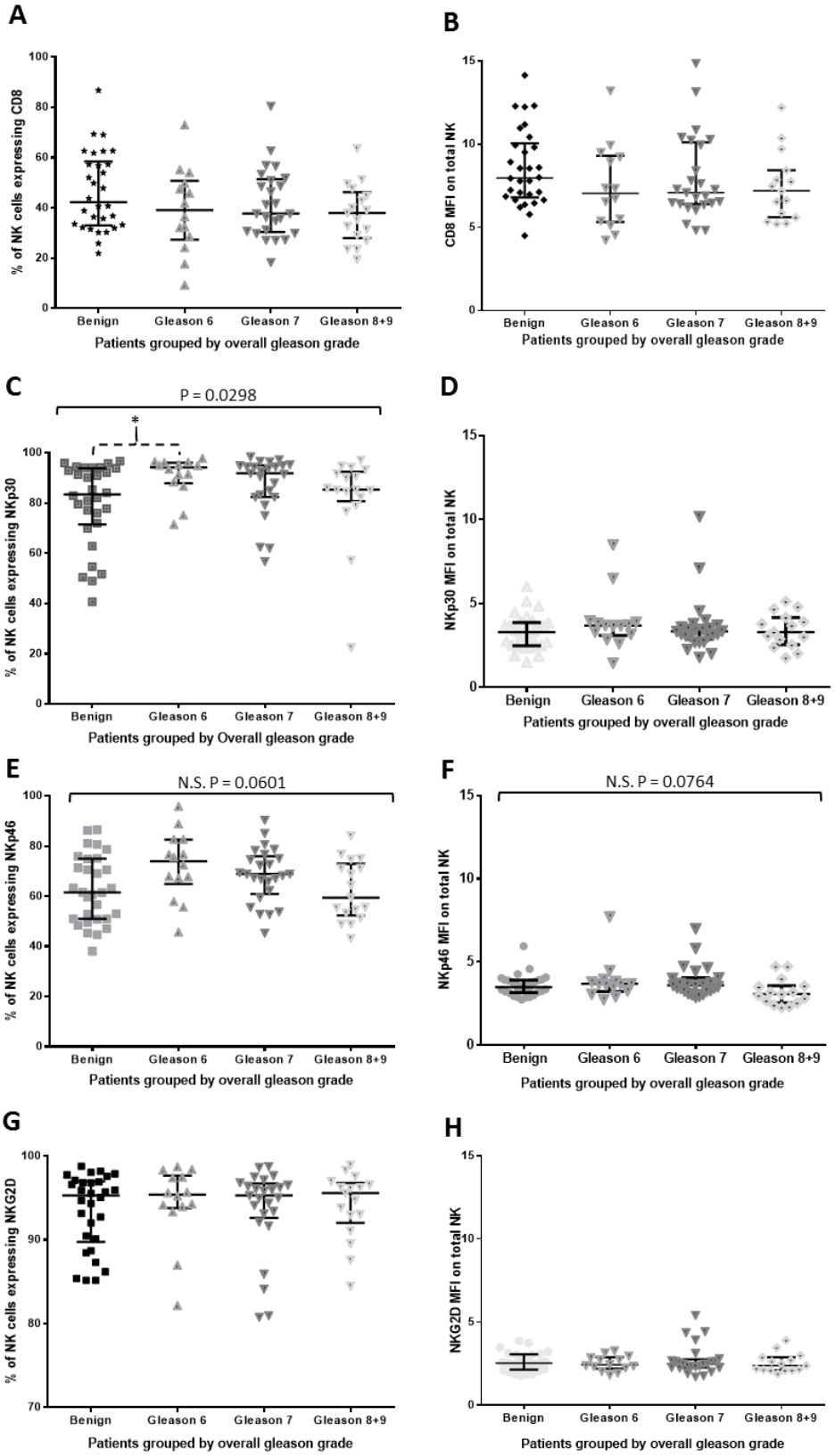

Figure 3.6: Expression of CD8 and activating receptors NKp30, NKP46 and NKG2D on patient NK cells.

Expression of receptors CD8, NKp30, NKp46 and NKG2D on patient NK cells with patients grouped according to overall Gleason grade diagnosed by TRUS and TP biopsy methodologies. A and B) Percentage and median fluorescence (MFI) intensity of CD8 expression. C and D) Percentage and MFI of NKp30 expression. E and F) Percentage and MFI of NKp46 expression. G and H) Percentage and MFI of NKG2D expression. Statistical analysis according to Kruskal-Wallis test (solid line). *P≤0.05.

NK cells were expressing NKp30, whereas in the other the range of NKp30 expression variably ranged between 40 and 90 % of NK cells. The percentage of NK cells expressing NKp30 for the majority of Gleason 6 patients ranged between 86% and 98 %, with the data being tightly grouped. The mean percentage of NK cells expressing NKp30 for Gleason 6 patients was significantly different to the benign group. Although the majority of the data points were also tightly grouped for the Gleason 7 and Gleason 8+9 patients, no significant differences in the medians were observed.

It can be clearly seen in Figure 3.6E that the median percentage of NK cells expressing NKp30 increases to 94.12 % for the Gleason 6 patient group compared to 83.47 % for the benign group. In comparison to the Gleason 6 patients, the median was slightly lower for the Gleason 7 patients (91.83 %) and the Gleason 8+9 patients (85.29 %). Despite changes in the median percentage of NK expressing NKp30 between the four patient groups, no significant difference in the MFI of NKp30 expression was observed between the four groups, with the median MFI value being maintained at around 3.

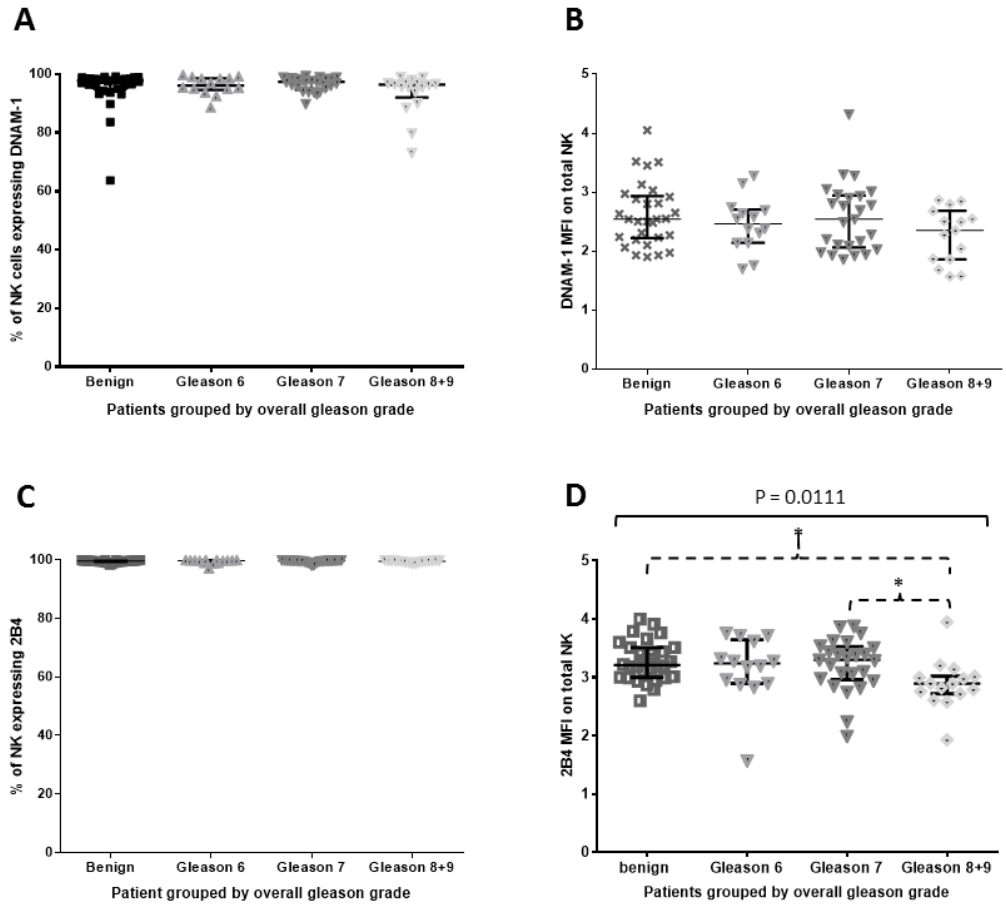

Figure 3.7: Expression of activating receptors DNAM-1 and 2B4 on patient NK cells.
Expression of receptors DNAM-1 and 2B4 on patient NK cells with patients grouped according to overall Gleason grade diagnosed by TRUS and TP biopsy methodologies. A and B) Percentage and median fluorescence (MFI) intensity of DNAM-1 expression. C and D) Percentage and MFI of 2B4 expression. Statistical analysis according to Kruskal-Wallis test (solid line) and Dunns multiple comparison test (dashed line). *P≤0.05.

Overall, the patient groups exhibited a pattern of NKp46 expression which was comparabale to that of NKp30 expression. The median percentage of NK cells expressing NKp46 was 73.95 % for Gleason 6 patients compared to 61.53 % for individuals with benign disease. Compared to the Gleason 6 patients the median percentage of NK cells expressing NKp46 was lower in the Gleason 7 patients (68.89 %) and Gleason 8+9 patients (59.45 %). Despite the differences in median percentage of NK cells expressing NKp46 between the four groups, these were not of statistical significance (P = 0.0601). It should be noted that the spread in data for all four patient groups was greater for the expression of NKp46 than for NKp30. Although there was no significant difference (P = 0.0764) between the MFI expression of NKp46 for the four patient groups, the median MFI of NKp46 expression for the Gleason 8+9 patient group is slightly lower than the other three patient groups, for which the median MFI expression for NKp46 was comparable (Figure 3.6F).

The percentage of NK cells expressing DNAM-1 was >90 % for the majority of patients, irrespective of their prostate cancer status (Figure 3.7A), and no significant difference in the intensity of DNAM-1 expression was observed between the patient groups (Figure 3.7B). A similar level of expression was observed for the 2B4 receptor on NK cells. Greater than 98 % of NK cells in each patient tested expressed 2B4 (Figure 3.7C). However, the intensity of 2B4 expression did significantly differ between patient groups (P = 0.0111), with the mean MFI expression of 2B4 for the Gleason 8+9 group being significantly different to the Gleason 7 and benign patient groups (Figure 3.7D).

3.3.2.4 Expression of inhibitory receptors on NK cells from patients with prostate cancer

No significant differences in the expression of the inhibitory receptors CD85j, LAIR-1 and NKG2A between the four patient groups was observed (Figure 3.8). The percentage of NK cells expressing LAIR-1 was >98 % for the majority of patient NK cells, irrespective of whether the patient had prostate cancer or not. The percentage of NK cells expressing NKG2D and CD85j was highly variable, and again this was irrespective of whether the patients had prostate cancer or not. The spread of data for the percentage of patient NK cells expressing CD85j, irrespective of patient group, ranged between 14.21 % and 91.59 %, whereas the percentage of NK cells expressing the NKG2A receptor ranged between 9.90 % and 80.52 %.

3.3.2.5 Expression of NKp30 and NKp46 on NK cells in patients having PSA levels <20 ng/ml

The selection criteria for the TRUS patients meant that there was no restriction on the PSA level of the patients included in the cohort. However, for TP patients there was a restriction and the PSA level for these patients was <20 ng/ml. This meant that in the NK cell receptor phenotypic analysis, the PSA levels for the Gleason 8+9 patients were significantly higher (P<0.0005) than

the PSA levels for each of the other patient groups (Figure 3.9C). The potential relationship between PSA

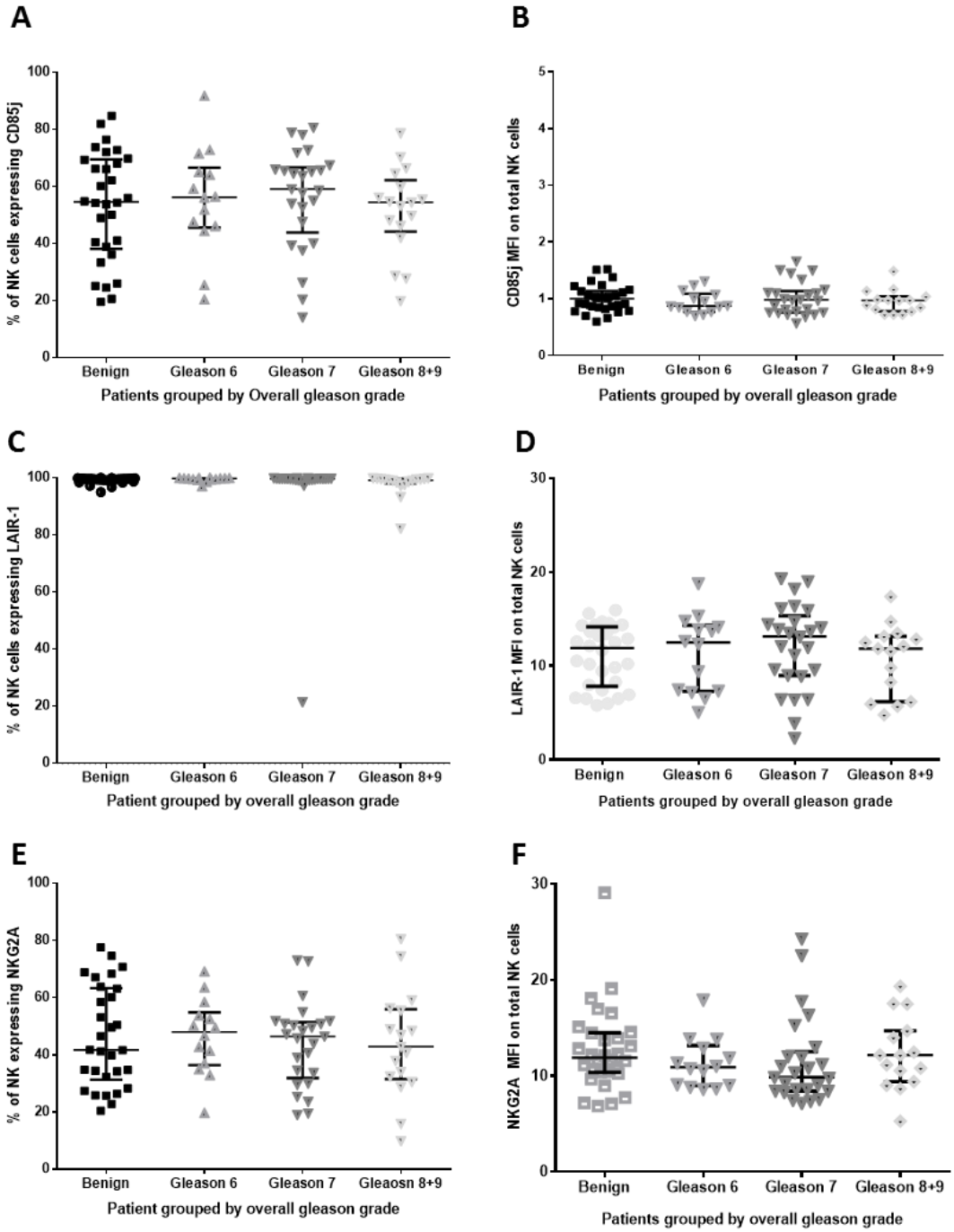

Figure 3.8: Expression of inhibitory receptors CD85j, LAIR-1 and NKG2A on patient NK cells
Expression of receptors CD85j, LAIR-1 and NKG2A on patient NK cells with patients grouped according to overall Gleason grade, as diagnosed by TRUS and TP biopsy methodologies. A and B) Percentage and median fluorescence (MFI) intensity of CD85j expression. C and D) Percentage and MFI of LAIR-1 expression. E and F) Percentage and MFI of NKG2A expression.

levels on NKp30 and NKp46 expression in terms of the percentage of NK cells expressing these receptors was assessed by excluding TRUS patients from the Gleason 8+9 group that had PSA levels >20 ng/ml from the analysis. Expression remained comparable to the pattern of

expression before the removal of these TRUS Gleason 8+9 patients (Figure 3.9A and B). The differences observed in the percentage of NK cells expressing NKp30 across the four patient groups remained significant (P = 0.0470).

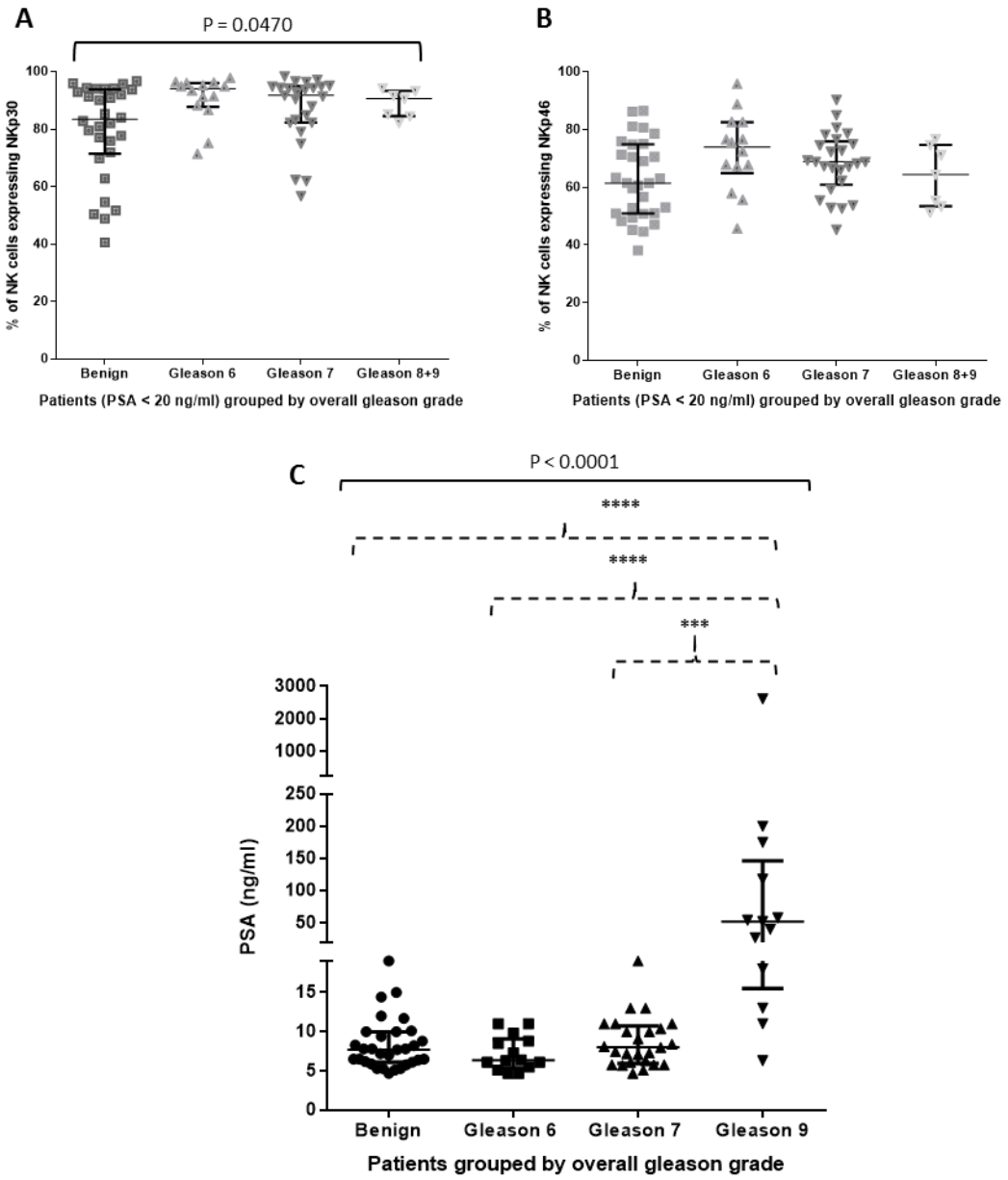

Figure 3.9: Analysis of NKp30 and NKp46 expression on patient NK cells in the NK phenotypic analysis cohort taking into account PSA level (ng/ml).
In order to assess whether patient PSA levels had any effect on NKp30 and NKp46 expression on patient NK cells within the Gleason 8+9 patient group, TRUS patients with a serum PSA level >20 ng/ml were removed from the analysis. A and B) Re-analysis of the percentage of patient NK cells expressing NKp30 and NKp46 respectively. C) Serum PSA levels (ng/ml) of each patient within the cohort grouped by overall Gleason grade. Statistical analysis according to Kruskal-Wallis test (solid line) and Dunns multiple comparison test (dashed line). *P≤0.05, **P<0.005, ***P≤0.0005, ****P≤0.00005.

3.3.2.6 What is the effect of TRUS misdiagnosis on the pattern of NKp30 and NKp46 NK cell receptor expression?

The NKp30 and NKp46 receptor expression data were reanalysed in order to observe whether the differences between the percentage of NK cells expressing NKp30 and NKp46 is altered when using the TRUS Gleason grade for the TP patients compared to the TP Gleason grade. As shown in Figure 3.10A and C, when the TRUS biopsy results were used to group TP patients, the median percentage of NK cells expressing NKp30 and NKp46 was higher in the Gleason 7 group, as opposed to the Gleason 6 group when the TP biopsy data were used to group the patients.

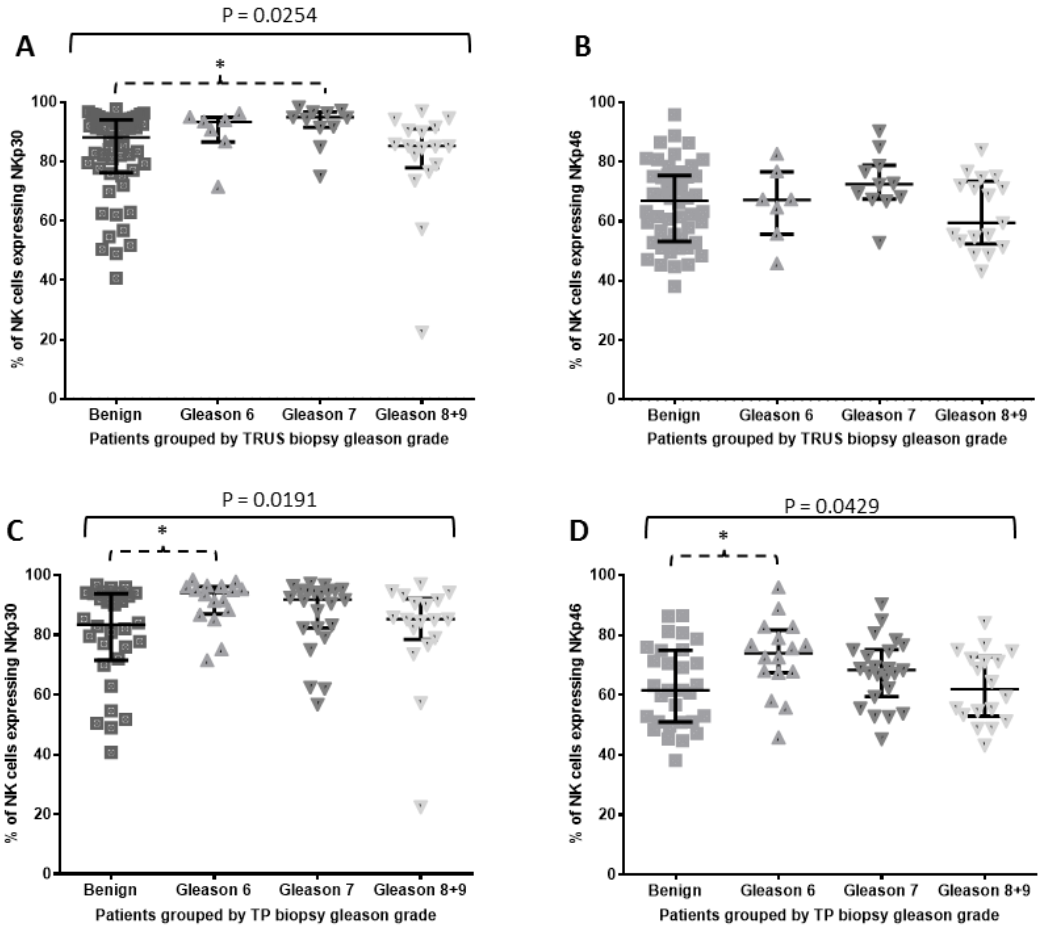

Figure 3.10: Comparison of NKp30 and NKp46 expression on patient NK cells when TP patients were diagnosed by either TRUS biopsy or TP biopsy and grouped according to Gleason grade.
The data was re-analysed to explore whether the biopsy method used to diagnose the TP patients could affect the pattern and statistical significance of NKp30 and NKp46 expression on patient NK cells when patients were grouped according to Gleason grade. A and B) Percentage of NK cells expressing NKp30 and NKp46 respectively when TP patients were grouped according to their TRUS biopsy diagnosis. C and D) Percentage of NK cells expressing NKp30 and NKp46 respectively when TP patients were grouped according to their TP diagnosis. Statistical analysis according to Kruskal-Wallis test (solid line) and Dunns multiple comparison test (dashed line). *P≤0.05.

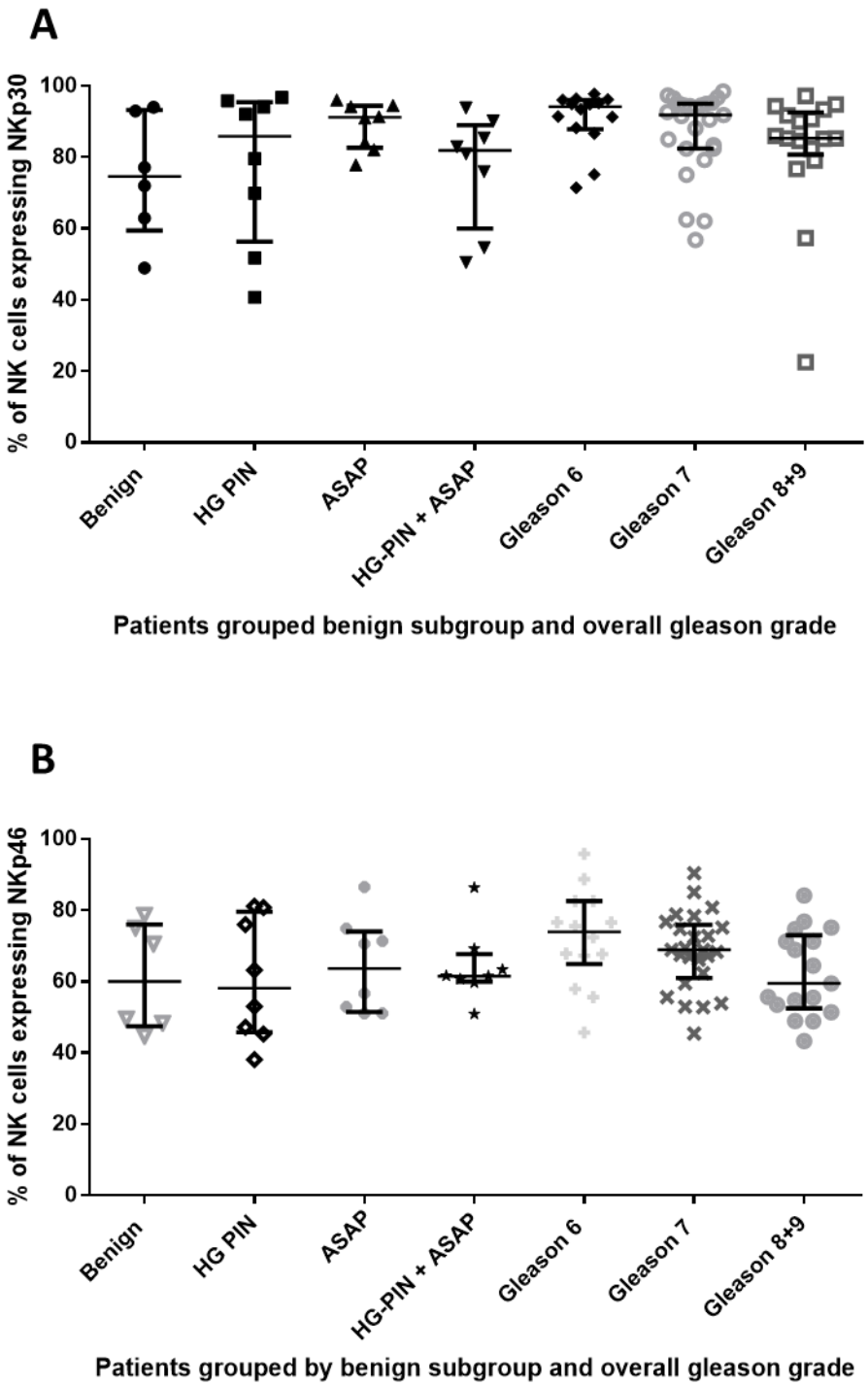

Figure 3.11: In depth analysis regarding the expression of activating receptors NKp30 and NKp46 on patient NK cells when prostate cancer patients were grouped according to Gleason grade and benign patients further sub-grouped on the basis of tissue abnormalities.
Re-analysis of the data with the benign disease patient grouped further subgrouped regarding tissue abnormalities in order to assess whether the percentage of patient NK cells expressing NKp30 and NKp46 could identify patients with increased risk of developing prostate cancer. A) Percentage of patient NK cells expressing NKp30. B) Percentage of patient NK cells expressing NKp46

Irrespective of whether the TRUS biopsy or TP biopsy data were used to group patients, the differences in the percentage of NK cells expressing NKp30 remained significant (TRUS P =

0.0254 and TP P = 0.0191). Interestingly, the differences in the percentage of NK cells expressing NKp46 between the four groups became significant when using the TP biopsy data to group patients (P = 0.0429), with a significant difference in the mean percentage of NK cells expressing NKp46 being observed between the benign and Gleason 6 patient groups. Using just the TP biopsy data to group the patients, two patients moved from the Gleason 7 group to the Gleason 6 group (Figure 3.10B and D).

3.3.2.7 Expression of NKp30 and NKp46 on peripheral blood NK cells when individuals are grouped into benign disease subgroups and overall cancer Gleason grade

Individuals with benign disease were further subgrouped according to benign pathologic abnormalities observed in the prostate tissue which are not classed as being cancerous, but were different to normal tissue. The spread of data for the percentage of NK cells expressing NKp30 in the ASAP group was tightly grouped, with a high median value of 91.14 % which was comparable to patients with Gleason 6 cancer, whereas individuals with benign disease exhibited a lower median of 74.56 %. Even within the group of patients displaying ASAP and High Grade PIN, the majority of the data were skewed towards higher percentages of NK cells expressing NKp30 (median value 81.92 %). In contrast, the spread of data for the benign (normal tissue) group and high grade PIN was greater compared to both the ASAP group and the High Grade PIN + ASAP group (Figure 3.11A).

Analysis of the pattern of NKp46 expression on the benign subgroups in terms of the percentage of NK cells expressing NKp46 revealed no significant differences, with the spread of data across the four benign subgroups being comparable (Figure 3.11B).

3.4 Discussion

In this study, patients were grouped according to the Gleason grade of their cancer, as detected by either TRUS or TP biopsy. As observed in the TRUS cohort, the PSA levels of the four patient groups heavily overlapped, thereby confirming reports that PSA levels do not reliably predict the Gleason grade of patients with prostate cancers (Catalona et al., 1991). Similarly, the digital rectal examination also failed to accurately detect prostate cancer, therefore demonstrating the importance of a biopsy to confirm the presence of prostate cancer. However, studies have shown that the detection rate of prostate cancer by TRUS biopsy is only ~ 32 % (Nafie et al., 2014a, Welch et al., 2007), as a consequence of which there is a significant risk of mis-diagnosis i.e. a patient being told he has benign disease when in fact the TRUS biopsies missed the cancer present in their prostate. One of the aims of this part of the study was to observe whether the TP biopsy could improve the diagnosis of prostate cancer compared to the standard TRUS biopsy. One conundrum that clinicians are faced with is why a proportion of patients experience

a continued rise of PSA levels in the absence of detectable prostate cancer when assessed using the TRUS biopsy (Nafie et al., 2014a). The TRUS biopsy is limited in its ability to biopsy the prostate. The TRUS biopsy is only able to take biopsies from the peripheral zone on the posterior side of the prostate which is closest to the rectal wall. In contrast, the TP biopsy is able to take biopsies from all regions of the prostate, including the apical and anterior zones of the prostate that is poorly sampled by TRUS biopsy (Nafie et al., 2014b). Multiple studies have shown that in patients with elevated PSA levels and previous negative biopsies, 26 to 68 % of these patients have prostate cancer, with 44 to 83 % of the cancers being found on the anterior side of the prostate (Dimmen et al., 2012, Mabjeesh et al., 2012, Pal et al., 2012).

In this study, a cohort of 70 patients with PSA <20 ng/ml were biopsied using both TRUS and TP biopsy. Twenty two individuals (31.4 %) were diagnosed as having benign disease on the basis of the TRUS biopsy, but were positive for prostate cancer. The TP cohort contained 29 biopsy naïve patients and 41 patients that had a previous set of TRUS biopsies that indicated benign disease, but were experiencing rising PSA levels. Out of the 41 patients who were previously diagnosed as benign, 15 patients (36.6 %) were again diagnosed as benign by the TRUS biopsy but were diagnosed with cancer by the TP biopsy. The TRUS biopsy only diagnosed 5 patients (12.1 %) with prostate cancer, and this was confirmed by the TP biopsy. The results suggest that there is about a 34 % misdiagnosis rate within the cohort by TRUS biopsy, thereby highlighting that the TP biopsy is superior at detecting prostate cancer. Furthermore, patients with a Gleason grade of 8 or 9 prostate cancer were more likely to be older and have higher PSA levels than patients who had Gleason 6 or 7 cancer, or individuals who were found to have benign disease.

Analysis of the receptor phenotype expressed on the NK cells from patients with prostate cancer was focused on using PBMCs isolated from patients that had undergone the TP biopsy and patients that were diagnosed as having Gleason 8 and 9 disease on the basis of the TRUS biopsy. These patients were as accurately diagnosed as possible and represent patients for almost the full spectrum of Gleason grades possible. The expression of activating receptors (NKG2D, DNAM-1, 2B4, NKp30, NKp46 and NKp44) and inhibitory receptors (CD85j, NKG2A and LAIR-1) in addition to CD8 and the receptors that define the NK cell populations (CD56 and CD16) on the NK cells from these patients was determined. The proportion of $CD56^{dim}$ and $CD56^{bright}$ cells within the patient NK cell population was not altered, with >90 % of the peripheral NK cells displaying a $CD56^{dim}$ phenotype, and the remainder of the NK cells being $CD56^{bright}$. These findings are consistent with the literature (Cooper et al., 2001). Curiously, the intensity of CD56 expression on $CD56^{bright}$ NK cells from patients with Gleason 8+9 disease was significantly lower than that on $CD56^{bright}$ NK cells from individuals with benign disease and patients with Gleason 7 disease. This was a surprising finding, as the intensity of CD56 expression on $CD56^{dim}$ NK cells

was comparable for all patient groups. The reason for the down-regulation in CD56 expression on the Gleason 8+9 patient $CD56^{bright}$ NK cells is unclear, as CD56 is typically not one of the major cell adhesion molecules which is involved in cytotoxicity (Nitta et al., 1989).

Analysis of the activating and inhibitory receptor expression revealed that only the expression of NKp30 and 2B4 significantly differed amongst the four patient groups. Consistent with the literature, the 2B4 receptor was uniformly expressed on 100 % of NK cells for each patient, irrespective of whether they had prostate cancer or not (Mathew et al., 2009). However, on average, NK cells from patients in the Gleason 8+9 patient group expressed significantly less 2B4 on their cell surface compared to NK cells from patients in the other three patient groups. In humans, 2B4 functions as an activating receptor and so the down-regulation of 2B4 on the Gleason 8+9 patients may represent immunosuppression by prostate cancer (Tangye et al., 2000).

In contrast to 2B4, the significant differences in the expression of NKp30 was associated with the percentage of NK cells expressing the receptor, not its intensity. The intensity (MFI) of NKp30 expression remained unchanged. Surprisingly, the median percentage of NK cells from patients with Gleason 6 disease expressing NKp30 was higher than that in individuals with benign disease. This increased median percentage of NK cells expressing NKp30 appeared to be maintained in Gleason 7 patients, with lower levels being present in Gleason 9 patients. This pattern suggests that the Gleason 6 patients may be exhibiting an NK cell immune response to early stage prostate cancer. Grouping the benign patients into abnormality subgroups i.e. benign (normal morphology), High grade PIN and ASAP (atypical small acinar proliferation) revealed that patients with signs of ASAP tended to exhibit an increased percentage of NK cells expressing NKp30 which was comparable to that which was present in Gleason 6 patients. Although these results did not reach statistical significance, they suggest that an NK cell response may start prior to the formation of prostate cancer, and that the measurement of the percentage of NK cells expressing NKp30 in patients with benign disease might indicate patients that are at increased risk of progression to early stage cancer. Further investigation with increased patient numbers is needed to test this observation. The decrease in the percentage of NK cells expressing NKp30 in Gleason 8+9 patients may suggest that, as a patient develops more advanced prostate cancer, the cancer may be exerting a greater immunosuppressive effect on patient NK cells.

Although the pattern of expression for NKp46 was similar compared to the pattern of expression for NKp30, there was no statistically significant pattern when the TP patients were grouped according to overall Gleason grade (combination of both TP and TRUS Gleason grades). However, when the TP patients were grouped according to only their TP Gleason grade, the differences in the percentage of NK cells expressing NKp46 across the four patient groups

became significant. This change in significance was driven by two patients moving from the Gleason 7 group to the Gleason 6 group when patients were grouped according to TP Gleason grades only. In contrast to NKp30, the median intensity of NKp46 expression for the Gleason 8+9 patient group was lower than for the other three patient groups, although this finding did not quite reach statistical significance. Taken together, these results suggest that, similar to NKp30, the percentage of NK cells expressing NKp46 is also up-regulated in response to early stage cancer, thereby indicating an NK cell immune response which is gradually suppressed by advanced prostate cancer. This is suggested by the decrease in the percentage of NK cells expressing NKp46 in Gleason 8+9 patient and the decrease in the intensity of this expression.

The median intensity of the CD16 receptor expression for each of the patient groups appeared to decrease as the Gleason grade of the patient groups increased. Although the relationship did not reach statistical significance, a pattern of decreased intensity of CD16 expression for the majority of Gleason 8+9 patients compared to the patients in the other three groups was observed. Perhaps greater patient numbers would increase the significance of this result. Down-regulation of CD16 has been reported to be associated with NK cell activation and, to some extent, NK cell cytotoxic function (Grzywacz et al., 2007). Therefore, overall the results in this study suggest that prostate cancer patients do appear to mount an NK cell immune response against their cancer.

In one of the few studies that have assessed NK cell phenotype in prostate cancer, Pasero et al found that high intensity of NKp30 and NKp46 expression was associated with increased survival in patients with metastatic disease and also that these two receptors, in addition to NKG2D and DNAM-1, regulated NK cell recognition of prostate cancer cells (Pasero et al., 2015). The increase and decrease in the percentage of NK cells expressing NKp30 and NKp46 observed in this study suggested that these receptors may play a role in NK cell recognition / immune response towards prostate cancer, which is in line with the findings of Pasero et al. Surprisingly, given that NKG2D is commonly thought to be involved in the recognition of a range cancers and a target for down-regulation by cancer induced immunosuppressive mechanisms, we did not see a change in the expression of NKG2D between patient groups (Mamessier et al., 2011a, Mamessier et al., 2011b, Morgado et al., 2011, Platonova et al., 2011, Wilson et al., 2011). The decrease in the MFI of 2B4 expression on NK cells from patients with Gleason 8+9 prostate cancer compared to the three patient groups suggests that 2B4 may also play some role in the recognition of prostate cancer. Although we saw differences in the median expression of NKp30 and NKp46 associated with increased grade of prostate cancer, the spread of data within the four patient groups heavily overlapped, meaning that these NK cells markers cannot be used to differentiate patients with and without prostate cancer. Therefore, in contrast to the hypothesis

of this part of the study (and also suggested by Pasero et al), the expression of NKp30 and NKp46 cannot be used as markers to aid routine diagnosis of prostate cancer. However, as suggested by Pasero et al, these markers could potentially be used to measure progression to advanced prostate cancer, since the median percentage of NK cells expressing NKp30 and NKp46 was lower in the Gleason 8+9 patient grouped compared to the Gleason 6 and 7 patient groups. Further investigations would be needed to prove this hypothesis, and this would only be true for patients who were not undergoing treatment at the time of sampling.

Unfortunately, since we did not have access to intratumoural NK cells we could not assess how well the peripheral NK cell phenotype of prostate cancer patients reflects their intratumoural NK cell phenotype. The significant increase and decrease in the percentage of NK cells expressing NKp30 is in contrast to the gradual decrease in the MFI of expression of this receptor and other activating receptors seen in breast cancer (Mamessier et al., 2011b). Although a decrease in the median percentage of NK cells expressing NKp30 and NKp46 in patients with Gleason 8+9 disease compared to those with Gleason 7 disease was observed and thought to be due to immunosuppression, further investigation of immune suppressive cytokine levels e.g. TGF-β in patient plasma / serum needs to be performed in order to confirm immunosuppression. There are reports that expression of NKp30 and NKp46 on NK cells decrease with age, as a consequence of which the decrease in the percentage of Gleason 8+9 patient NK cells expressing NKp30 and NKp46 compared to Gleason 7 patients could also be due to the fact that the TRUS Gleason 8+9 patients were on average older than the TP patients (Almeida-Oliveira et al., 2011, Hazeldine et al., 2012). Again, this possibility needs to be explored in future studies.

Chapter 4 - RESULTS

NK cell priming and the optimisation of NK cell cytotoxicity assays

4.1 Introduction

In the previous chapter, it was suggested that the presence of prostate cancer may down regulate the expression of the NK cell activating receptors NKp30 and NKp46 on NK cells in the peripheral circulation. However, measuring the expression of these receptors on NK cells in the peripheral blood could not be used to distinguish patients with prostate cancer from individuals who had benign disease in a diagnostic setting. Furthermore, since patients were only diagnosed with prostate cancer following the development of symptoms or the detection of a rising PSA level, it was only possible to measure the expression of NK cell activating and inhibitory receptors at the point of diagnosis as a group, and there is no pre-diagnostic data that would indicate the expression of these receptors prior to cancer developing. Therefore, on the basis of these data, it is not possible to prove that the down-regulation of NKp30 and NKp46 on patient NK cells was truly the result of prostate cancer-related effects, nor could the significance of these effects on prognosis be evaluated.

Direct measurements of NK cell cytotoxic function may be a better indicator of NK cell function and their ability to fight against prostate cancer and therefore provide important prognostic information. Unlike T cells, NK cells contain pre-formed lytic granules when resting (Orange, 2008). Lytic granules (also known as cytotoxic granules) are specialised secretory lysosomes that have been shown to contain granzyme B, perforin, granulysin and cathespins. The low pH and calcium concentrations within the lysosome prevent the granzyme B and perforin from harming the lysosomal membrane (Raja et al., 2002). During the cytotoxic process, an immunological synapse is formed between the NK cell and its target cell prior to the release of the lytic granule content (Davis et al., 1999). Lytic granules fuse with the plasma membrane of the NK cells and their contents are exocytosed into the cleft of the immunological synapse (Peters et al., 1991, McCann et al., 2003). This process, known as degranulation, results in the human lysosomal membrane glycoproteins CD107a (LAMP-1), CD107b (LAMP-2) and CD63 (LAMP-3) becoming exposed on the surface of the NK cell. CD107a has also been shown to be up-regulated on both activated platelets and lymphocytes, and it was originally thought to play a role in the adhesion of these cells to vascular endothelium via binding of CD107a to selectins on endothelial cells (Peters et al., 1991). CD107a is a highly glycosylated protein and in addition to its adhesion function it has been widely suggested that CD107a also protects the NK cells from being harmed by the lytic granules contents it had just released (Peters et al., 1991, Febbraio and Silverstein, 1990). In this context, the expression of CD107a on engineered plasma membranes has been

shown to protect cells from being lysed by NK cells and from purified lytic granules. Furthermore, knock down of CD107a increases of apoptosis in the presence of degranulating NK cells (Cohnen et al., 2013).

Currently, two main methods of measuring the NK cell cytotoxic function have been utilised:

1) The direct detection of lysed target cells following co-incubation with NK cells using a variety of readouts
2) The detection of CD107a on the NK cell surface following degranulation

For a long time, the standard method for measuring NK cell cytotoxic responses towards target cells has been the ^{51}chromium Release assay. This involves staining target cells (e.g. MHC class I-deficient K562 human erythroleukaemic cell line) with radioactive ^{51}chromium and measuring the release of ^{51}chromium from these cells following contact with NK cells (Brunner et al., 1968). In an attempt to move away from the use of radioactive materials, cytotoxic assays involving the use of a flow cytometer and fluorescent dyes for the labelling of viable and non-viable (i.e. killed) target cells have now been developed (Hopkinson et al., 2007). The detection of CD107a on the cell surface of the NK cells following degranulation using flow cytometry has also been used to indirectly measure NK cytotoxic killing. This method was first developed for detecting the presence of CD107a on $CD8^+$ T cells. Monensin was added to the co-culture of $CD8^+$ T cells with their target cells. The concept is that monensin retains the expression of CD107a on the cell surface, thereby preventing it from being re-internalised and allowing CD107a to be stained with fluorochrome conjugated monoclonal antibodies (mAbs) and its expression to be analysed using a flow cytometer (Betts et al., 2003). The same method has been shown to be capable of detecting NK cell degranulation (Alter et al., 2004).

A commonly used target cell for the measurement of NK cell-mediated cytotoxic activity is the K562 human lymphoblastic cell line. Originally described as a granulocytic lymphoblast isolated from 53-year-old female with chronic myelogenous leukemia in terminal blast crises, it was later reclassified as being an MHC class I negative erytholeukaemic cell line (Andersson et al., 1979). The absence of MHC class I expression renders K562 cells resistant to killing by $CD8^+$ T cells, but susceptible to NK cell killing due to the absence of key inhibitory signals. Although a commonly used target cell, the absence of MHC class I expression casts doubt on the relevance of K562 as a target cell for measuring NK cell cytotoxic potential in patients with prostate cancer, given that prostate cancer and prostate cancer cell lines such as PC3 and DU145, are both MHC class I positive and thereby typically resistant to being killed by resting NK cells (Sabry et al., 2011).

Until relatively recently, the only way to induce NK cells to kill NK cell-resistant tumour cells has been considered to be stimulation with IL-2, which increases the cytotoxic capacity of both $CD56^{dim}$ and $CD56^{bright}$ cells. Although IL-2 is primarily known to promote the proliferation of T lymphocytes, it can also induce the proliferation of NK cells, with the rate of proliferation of the $CD56^{bright}$ cell subset being 5 to 60 times greater than $CD56^{dim}$ NK cells. The $CD56^{bright}$ NK cells have been shown to express the IL-2 receptor alpha subunit (CD25), the expression of which was absent on $CD56^{dim}$ NK cells. These data suggest that the $CD56^{bright}$ NK cells may express the high affinity IL-2 receptor enabling them to proliferate faster than $CD56^{dim}$ NK cells. As a consequence, IL-2 stimulation not only increases the cytotoxic capabilities of both subsets, but also increases the relative proportion of the $CD56^{bright}$ NK subset (Nagler et al., 1989).

A series of studies has now shown that NK cells can also become 'activated' by specific cancer cell lines, the consequence of which alters the phenotype of the NK cell and increases its ability to kill NK cell-resistant cancer cell lines (North et al., 2007, Sabry et al., 2011). It has now been suggested that NK cells require priming (S1) and triggering signals (S2) to kill. Cancer cells evade NK cell killing by down-regulating either the priming signal or triggering signal from their cell surface. It has been suggested that K562 cells are susceptible to NK cell killing because they provide both S1 and S2 signals, whereas the NK cell resistant cell line Raji is resistant as it does not deliver the S1 priming signal. The S1 signal can be provided by either stimulating the NK cells with cytokines or co-incubating them with cells that can deliver such a signal, an example of which is the human leukaemic T cell line CTV-1. Activating NK cells via cytokine stimulation or CTV-1 co-incubation increases their ability to kill Raji cells. Interestingly activated NK cells are unable to kill CTV-1 cells and it is thought this is because CTV-1 cells do not provide the S2 signal (North et al., 2007, Sabry and Lowdell, 2013).

Lowdell et al have developed a method to artificially provide the S1 signal by incubating NK cells with CTV-1 cells, thereby enabling the NK cell to kill a range of NK cell-resistant cell lines (North et al., 2007, Sabry and Lowdell, 2013). Stimulation of isolated NK cells with CTV-1 cells (a T cell lymphoblast from a patient suffering with acute lymphoblastic leukaemia) for up to 20 hrs has been shown to result in a form of activation (referred to as 'priming'), as demonstrated by the up-regulation of CD69 (a marker of early activation) and CD25 (IL-2 alpha subunit), whereas the expression of CD16, NKp46 and NKG2D are all down-regulated. Primed NK cells exhibit an increased ability to lyse a range a NK cell-resistant cell lines; Raji (Burkitts Lymphoma), RPMI8226 (myeloma B lymphoblast), ARH77 (EBV transformed B lymphoblast) and DU146 (metastatic epithelial prostate cancer), when compared to non-primed NK cells (North et al., 2007, Sabry et al., 2011). The mechanism behind priming NK cells using CTV-1 cells has been shown to be cell-cell contact dependent and to involve ligation of the CD2 receptor on NK cells with the CD15

receptor expressed by the CTV-1 cells (North et al., 2007, Sabry et al., 2011). Interestingly, other CD15 positive cancer cells e.g. MV411 (lymphoblast, macrophage lineage) and SEM (lymphoblast, B cell precursor lineage) have also been shown to able to prime NK cells and increase their ability to kill NK cell-resistant Raji cells, whereas CD15 negative cell lines such as PF-382 and MOLT16 (both T cell lymphoblasts from patients with acute lymphoblastic leukaemia, ALL) are unable to prime NK cells, nor increase their ability to kill Raji cells beyond non-primed levels. Although K562 cells are also CD15 positive and blocking this receptor substantially inhibits K562 lysis, K562 cells are unable to prime NK cells. This suggested that other NK cell:CTV-1 interactions in addition to CD2:CD15 are required for NK cell priming (North et al., 2007, Sabry et al., 2011). Recently, the results of a Phase I clinical trial into the use of primed NK cells as an immunotherapeutic treatment to treat patients with acute myeloid leukaemia (AML) demonstrated that of 7 patients, four had HLA mismatched primed NK cells that survived and expanded *in vivo* without host immunosuppression and anti-leukaemic effects were reported (Kottaridis et al., 2015).

The central theme aim of this PhD study was to investigate whether measuring the phenotype and function of peripheral blood NK cells from patients with prostate cancer could provide insight into the presence / absence of disease and its severity. As reported in the previous chapter, significant differences and trends in the expression of activating receptors NKp30, NKp46 and 2B4 on NK cells from patients with prostate cancer were apparent. However, the expression of these receptors could not distinguish patients with different grades of prostate cancer or distinguish patients with prostate cancer from patients with benign disease. It was therefore concluded that single measurements cannot inform patient diagnosis / prognosis. However, it might be that measuring NK cell function provides additional information and improves our ability to define prostate cancer patients into groups and inform diagnosis and or prognosis.

Given the questionable relevance of measuring NK cell cytotoxic function using the K562 cell line as the target, a better measure might be to examine the capacity of NK cells from patients with prostate cancer and benign disease to be primed, and the functional consequence of priming on their cytotoxic potential against relevant, prostate cancer cell lines. This proposition is reasonable given that priming NK cells by co-incubation with CTV-1 cells has already been shown to increase the ability of the NK cells to kill the metastatic prostate cancer line DU145 by up to about 60% (Sabry et al., 2011). Measuring patient NK cell function using this CTV-1 priming method would allow for the measurement of two key NK cell parameters:

1) The ability of the patient NK cells to become primed, and the influence of priming on their phenotype.
2) The ability of the primed NK cells from patients with prostate cancer to lyse prostate cancer cell lines (with the lysis of K562 cells used as a comparison).

These studies will also provide insight into the autologous NK cell priming as a potential immunotherapeutic approach for the treatment of patients with prostate cancer.

4.2 Aims and hypothesis

The aim of this part of the study was to use peripheral blood samples from healthy volunteers to:

1. Optimise the approach for NK cell priming using CTV-1 cells
2. Better define the phenotype of NK cells that have been primed using CTV-1 cells
3. Optimise a flow cytometry based cytotoxic assay based on a previously published method in order to measure NK cytotoxic function against K562 and PC3 cells.
4. Optimise a previously published CD107a degranulation assay in order to directly measure NK cytotoxic function and reveal which NK subsets are responsible for lysing K562 or PC3 target cells.

4.3 Results

4.3.1 Optimisation of the NK cell priming method using mitomycin C treated CTV-1 cells

4.3.1.1 Optimising the NK cell : CTV-1 co-incubation period, as determined on the basis changes in NK cell phenotype

The original published method co-incubated isolated NK cells with irradiated (30 Gy) CTV-1 cells for up to 20 hrs (North 2007). In order to determine if irradiation could be replaced by mitomycin C treatment, the optimal co-incubation period for the priming of isolated healthy NK cells by mitomycin C (final concentration 33 µg/ml) treated CTV-1 cells was determined. For this, thawed PBMCs from two healthy volunteers were co-incubated for 16, 18 or 20 hrs at 37°C with mitomycin C treated CTV-1 at a 2 : 1 PBMC : CTV-1 ratio. Control PBMCs were incubated under the same conditions, but in the absence of CTV-1 cells. PBMCs were then stained with NK cell antibody panels 1 and 4 and receptor expression analysed by multi-parameter flow cytometry. Expression of CD25, CD69, NKG2D, NKp30 and NKp46 was determined on the entire $CD3^{-}CD56^{+}$ NK cell population using the gating strategies shown in Figures 2.1 to 2.2?

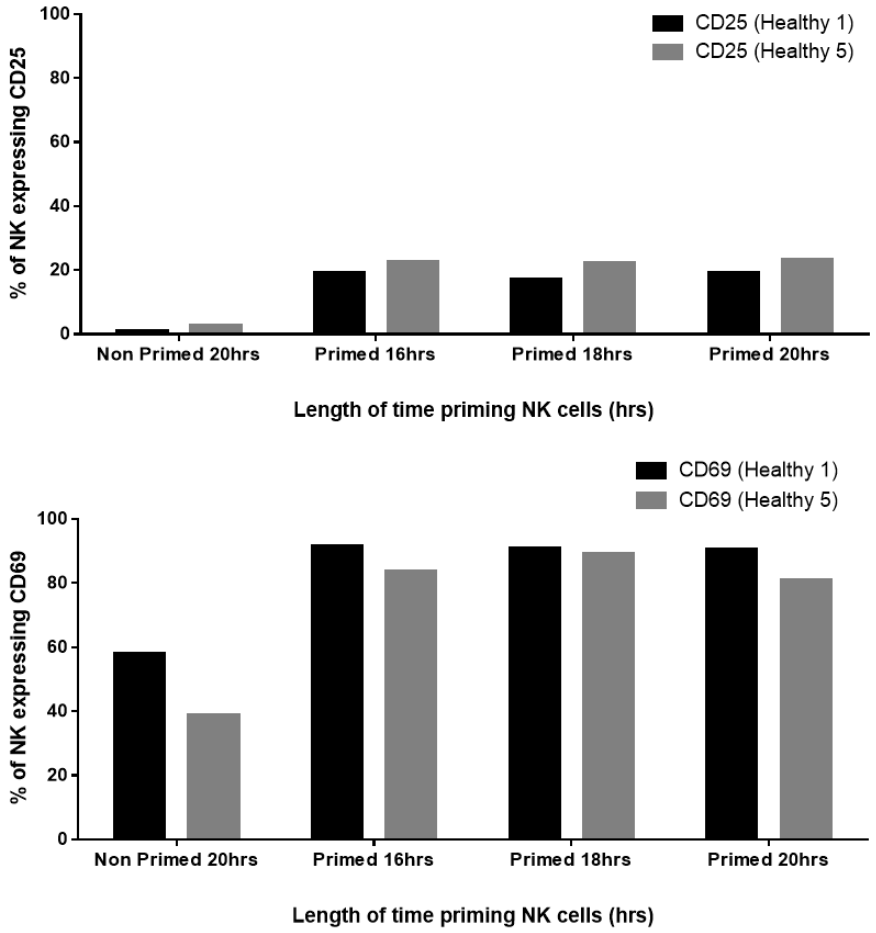

Figure 4.1: Up-regulation of CD25 and CD69 expression on NK cells following priming with CTV-1 over the course of 16 to 20 hrs.
Thawed PBMC were primed by co-incubating them with mitomycin C treated CTV-1 cells at a 2 : 1 PBMC : CTV-1 ratio for 16, 18 and 20 hrs. Expression of CD25 (top graph) and CD69 (bottom graph) was measured by flow cytometry. The expression of CD25 and CD69 on primed NK cells was compared to non-primed NK cells that were incubated in media only for 20 hrs.

As indicated in Figure 4.1, priming increases the proportion of NK cells expressing CD69 and CD25 by between 20 to 50 % and 18 to 20% respectively. Increasing the co-incubation period from 16 to 20 hrs had no impact on the expression of these antigens. In contrast, priming had no effect on the proportion of NK cells expressing NKp30 and NKp46, whereas the expression of NKG2D was variable, in that expression decreased for one donor and did not change for the other (Figure 4.2). Based on these results, all future experiments used a co-incubation period of 17 hrs.

4.3.1.2 Identifying the optimal NK : CTV-1 priming ratio, as determined on the basis of changes in NK cell phenotype

The influence of priming at different NK : CTV-1 ratios (ranging from 4:1 to 1:4) on the phenotype of NK cells was determined. For this, PBMCs isolated from 5 healthy volunteers which had been stored in liquid nitrogen were thawed, the NK cells isolated and primed at NK : CTV-1 ratios

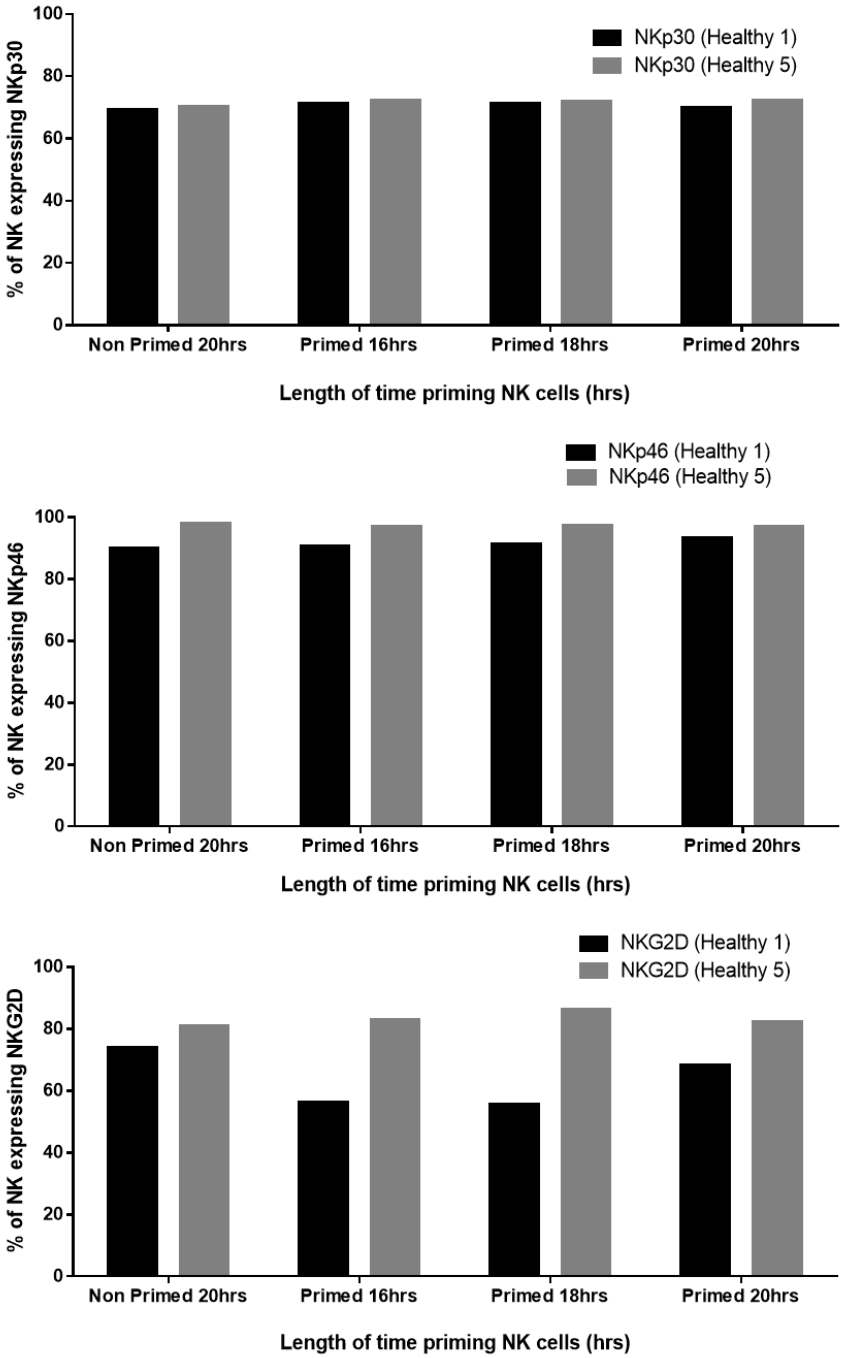

Figure 4.2: Expression of activating receptors NKp30, NKp46 and NKG2D expression on NK cells following priming with CTV-1 over the course of 16 to 20 hrs.
NK cells were primed by co-incubating them with mitomycin C treated CTV-1 cells at a 2 : 1 PBMC : CTV-1 ratio for 16, 18 and 20 hrs. Expression of NKp30 (top graph) NKp46 (middle graph) and NKG2D (bottom graph) were measured by flow cytometry. The expression of these receptors on primed NK cells were compared to non-primed NK cells that were incubated in media only for 20 hrs.

ranging from 4:1 to 1:4 (except for volunteer healthy 1 who was not tested at the 4:1 priming ratio). Non-primed NK cells were used as a control. Both non-primed and primed NK cells were then stained for the expression of the following receptors; inhibitory receptors (CD85j, LAIR-1, NKG2A), activating receptors (CD16, NKp30, NKp44, NKp46, NKG2D, DNAM-1 and 2B4) and

adhesion / co-stimulatory or co-inhibitory receptors (OX40, GITR, CD137, CRTAM, TIGIT and CD96). Results were analysed using the gating strategies shown in Figures 2.1 to 2.4., and the optimal NK cell priming ratio was considered as the ratio which resulted in the highest expression of co-stimulatory receptors. Statistical analyses were only undertaken on receptor expression data for NK cell priming ratios 2 : 1 to 1 : 4 (NK : CTV-1) due to incomplete data for the expression of NK receptors at the 4 : 1 priming ratio.

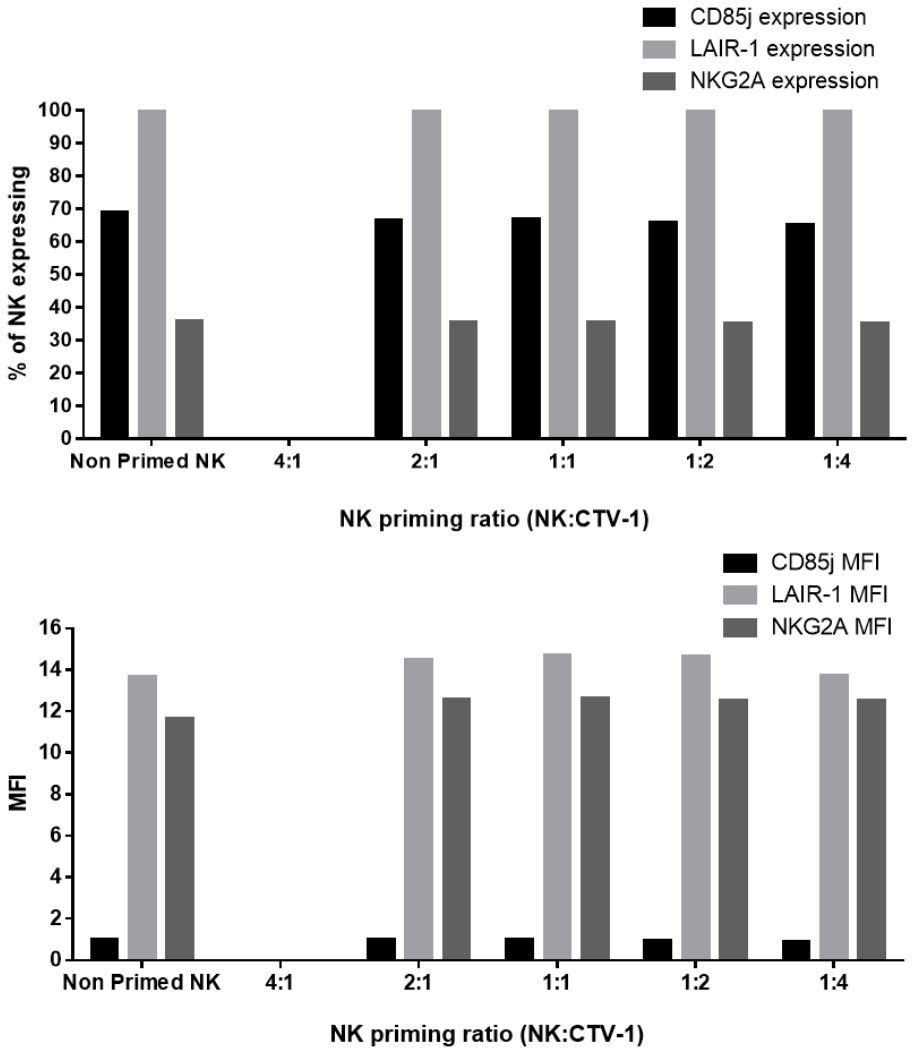

Figure 4.3: Expression of inhibitory receptors CD85j, LAIR-1 and NKG2A expression on NK cells following priming with CTV-1 at different.

NK cells were primed by co-incubating them with mitomycin C treated CTV-1 cells for 17 hrs at NK : CTV-1 ratios 2 : 1, 1 : 1, 1 : 2 and 1 : 4. Expression of receptors CD85j, LAIR-1 and NKG2A were measured by flow cytometry. The expression of these receptors on primed NK cells were compared to non-primed NK cells that were incubated in media only for 17 hrs. Data on the percentage of NK cells expressing these receptors (top graph) and the median fluorescence intensity (MFI) of that expression (bottom graph) are shown.

4.3.1.2.1 Influence of priming on the expression of inhibitory receptors by CD56^{+} NK cells

Only the NK cells from volunteer healthy 1 were analysed for CD85j, LAIR-1 and NKG2A expression. As shown in Figure 4.3, priming the NK cells at NK : CTV-1 priming ratios of 2 : 1 to 1 : 4 had no effect on the percentage of NK cells expressing these receptors, nor did it have any apparent effect on the intensity of their expression. For these reasons, and in order to reduce the number of antibody panels that the NK cells were being stained for, NK cells were not stained using the inhibitory receptor panel in subsequent NK cell priming experiments.

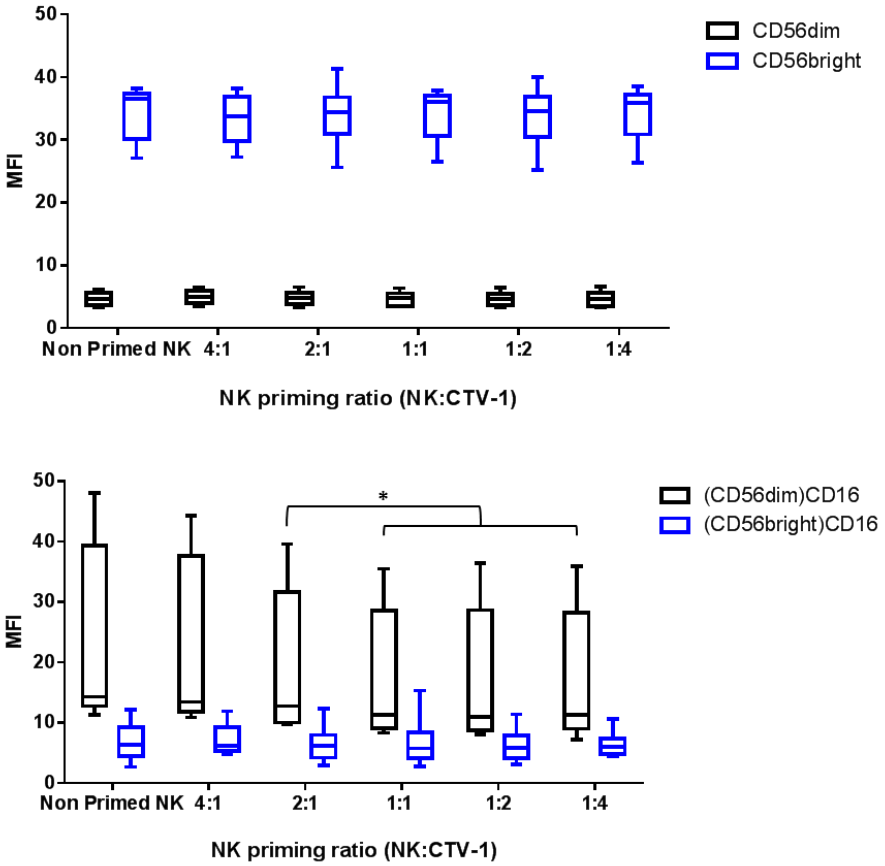

Figure 4.4: The influence of priming with CTV-1 on the expression of CD56 and CD16 on CD56^{dim} and CD56^{bright} NK cell subsets

NK cells were co-incubated with mitomycin C treated CTV-1 cells at NK:CTV ratios 4:1, 2:1, 1:1, 1:2, and 1:4 for 17 hrs. The expression of CD56 and CD16 on primed NK cells was compared to non-primed NK cells that were incubated in medium only for 17 hrs. Expression of CD56 and CD16 by the NK cells was measured by flow cytometry. The median fluorescence intensity (MFI) of CD56 (top graph) and CD16 (bottom graph) for the CD56^{dim} and CD56^{bright} NK subsets are shown. Each box plot has whiskers set to minimum and maximum with the line representing the median. Statistical analyses was done using a one way ANOVA in conjunction with a Tukey's multiple comparisons test. * $P \leq 0.05$.

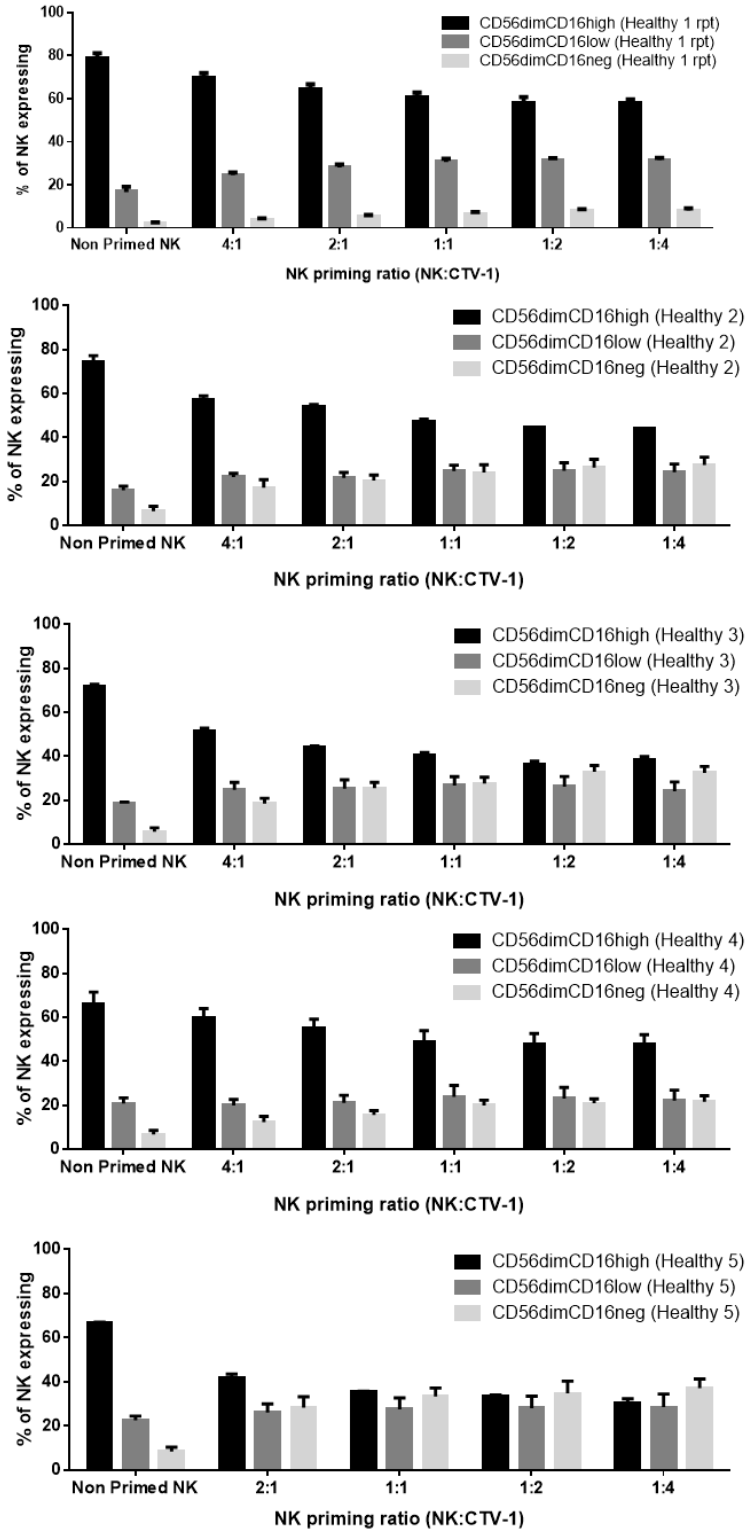

Figure 4.5: The identification of three $CD56^{dim}CD16^{+/-}$ NK cell subpopulations and the degree of which these subpopulations made up the NK population before and after priming.

NK cells were co-incubated with mitomycin C treated CTV-1 cells at NK:CTV ratios 4:1, 2:1, 1:1, 1:2, and 1:4 for 17 hrs. The expression of CD56 and CD16 on primed NK cells was compared to non-primed NK cells that were incubated in medium only for 17 hrs. Expression of CD56 and CD16 by the NK cells was measured by flow cytometry. For 5 healthy volunteers, the proportion of NK cells that were $CD56^{dim}CD16^{high}$, $CD56^{dim}CD16^{low}$ and $CD56^{dim}CD16^{neg}$ was measured for each priming ratio. Data are means ± SD of three measurements.

4.3.1.2.2 Influence of priming on the expression of CD56 and CD16 by CD56^{dim} NK cells

Although priming had no significant effect on the intensity of CD56 expression, it induced a decrease in CD16 expression on the CD56^{dim} NK cell subset only (Figure 4.4).

To accurately analyse CD16 expression, population were drawn on the basis of CD16 expression by non-primed NK cells and then applied to primed NK cells. Non-primed NK cells were divided into CD56^{dim} and CD56^{bright} subsets, with each subtype being further subdivided into CD16^{high}, CD16^{low} and CD16^{neg} subpopulations. The gates for the CD16^{high} and CD16^{low} subpopulations were positioned on the basis of the intensity of CD16 expression for each individual (which appeared to differ on a person to person basis), as indicated by the large box plot for non-primed NK cells (Figure 4.4). The cut off between the CD16^{high} gate and the CD16^{low} gate was set just below the highest density of CD56^{dim}CD16^{high} NK cells. The cut off between CD16^{low} and CD16^{neg} NK cells was gated at the same value between all volunteers. A representative example is shown in Figure 2.5. The analysis was focused on the CD56^{dim} subset, as the expression of CD16 was most notably altered on this subset (Figure 2.5).

As shown in Figure 4.5, for all five healthy volunteers, the CD56^{dim}CD16^{high} subset made up the majority of non-primed NK cells (range 66 to 79 %), followed by the CD56^{dim}CD16^{low} subset (range 16 to 23 %) and then the CD56^{dim}CD16^{neg} subset (2 to 9 %). NK cell priming at any priming ratio resulted in a decrease in the CD56^{dim}CD16^{high} subset and a subsequent increase in both the CD56^{dim}CD16^{low} and CD56^{dim}CD16^{neg} subsets, the extent of which was person-specific. Typically, the 1 : 4 NK : CTV-1 priming ratio resulted in the greatest decrease in the CD56^{dim}CD16^{high} population (percentage of CD56^{dim}CD16^{high} range 30 to 58) and the greatest increase in the CD56^{dim}CD16^{low} (percentage of CD56^{dim}CD16^{low} range 22 to 31) and CD56^{dim}CD16^{neg} subpopulations (percentage of CD56^{dim}CD16^{neg} range 8 to 37).

4.3.1.2.3 Influence of priming on the expression of the immunoglobulin superfamily receptors DNAM-1, TIGIT and CD96 by CD56^{dim} NK cells

NK cell priming had no effect on the expression of DNAM-1 (Figure 4.6). Priming also had no effect on the expression of the co-inhibitory receptor TIGIT, although a quantitatively small, but statistically significant difference in expression was observed at the 1 : 4 NK : CTV-1 ratio compared to the 2 : 1, 1 : 1 and 1 : 2 ratio. The expression of CD96 remained unaffected by NK cell priming until the NK : CTV-1 priming ratio 1 : 2 and 1 : 4, at which a significant decrease in the percentage of expression was observed compared to non-primed NK cells and NK cells primed at the 2:1, 1:1 and 1:2 ratios (Figure 4.6).

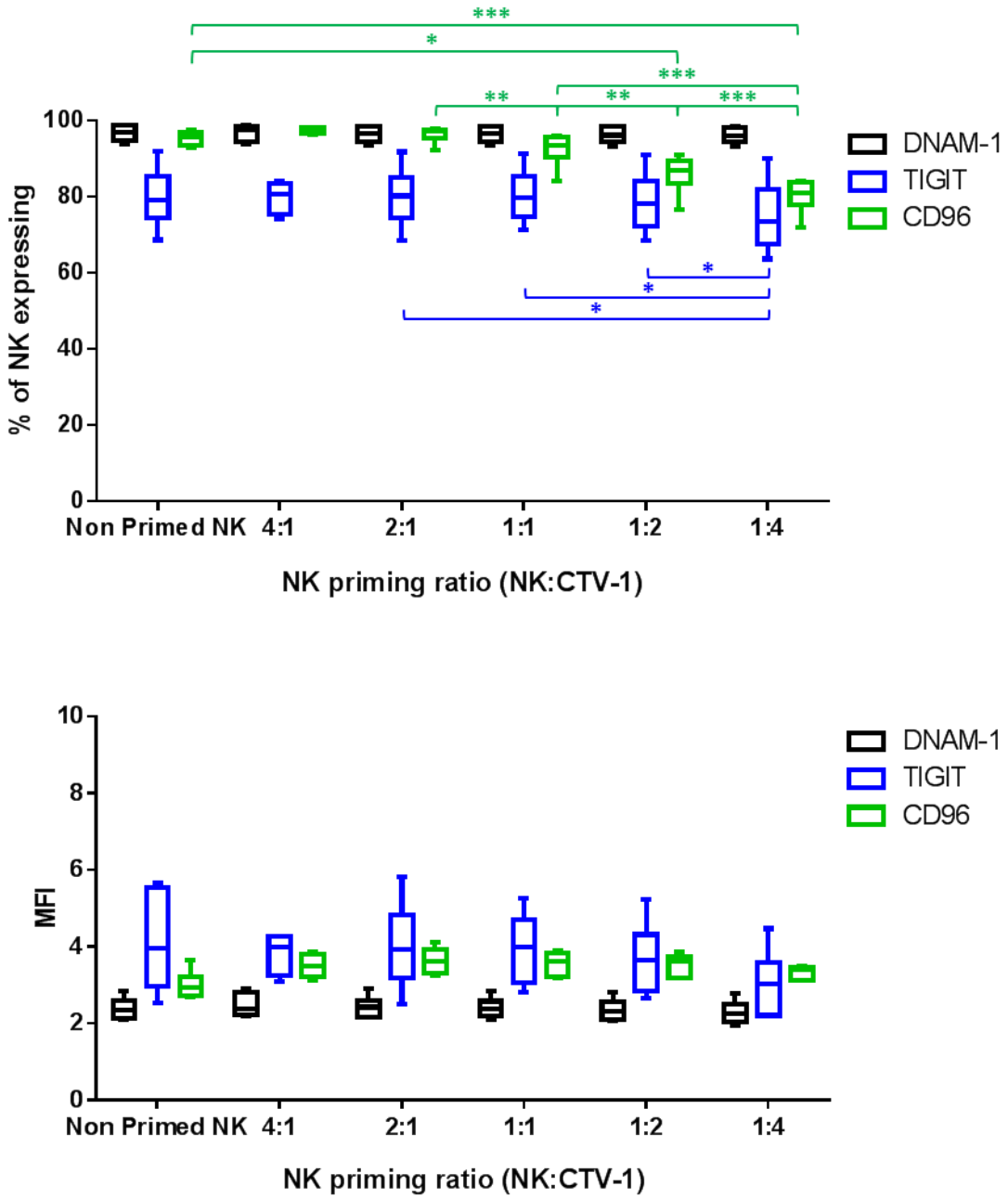

Figure 4.6: The influence of priming with CTV-1 on the expression of receptors DNAM-1, TIGIT and CD96 by NK cells

NK cells were co-incubated with mitomycin C treated CTV-1 cells at NK:CTV ratios 4:1, 2:1, 1:1, 1:2, and 1:4 for 17 hrs. The expression of DNAM-1, TIGIT and CD96 on primed NK cells was compared to non-primed NK cells that were incubated in medium only for 17 hrs. Expression of three receptors on NK cells was measured by flow cytometry. The percentage of NK cells expressing either DNAM-1, TIGIT or CD96 (top graph) and the median fluorescence intensity (MFI) of this expression (bottom graph) are shown. Each box plot has whiskers set to minimum and maximum with the line representing the median.

4.3.1.2.4 Influence of priming on the expression of the activating receptors NKp30, NKp44, NKp46, NKp80, NKG2D, 2B4 and the adhesion receptor CD2 by $CD56^+$ NK cells

Two of the three natural cytotoxicity receptors (NKp30 and NKp46) were each differentially expressed on non-primed and primed NK cells (Figure 4.7). The third natural cytotoxicity receptor, NKp44, was not expressed on either non-primed or primed NK cells (data not shown), whereas the expression of NKp30 and NKp46 ranged between 71 and 98 %. On non-primed NK cells, there was always a greater expression of NKp46, both in terms of percentage and intensity of expression than NKp30. Although NKp30 expression was unaffected by NK priming, there was a significant decrease in the percentage of primed NK cells expressing NKp46 when primed at the 1:2 and 1:4 NK : CTV-1 priming ratios compared to non-primed NK cells. There were also additional significant decreases in NKp46 expression between NK cells primed at the 2 : 1 compared to those that were primed at the 1 : 1, 1 : 2 and 1 : 4 (NK : CTV-1) ratios (Figure 4.7).

The expression of NKG2D on both non-primed and primed NK cells was like that of NKp46 expression (Figure 4.7). Both receptors appeared to be expressed at the same intensity (MFI), and this expression was unaffected by priming. Unlike NKp46 expression, NK cell priming at the 4 : 1 priming ratio appeared to initially increase the percentage of NK cells expressing NKG2D from 50 to 73 % of non-primed NK cells to 61 to 82% of primed (4 : 1) NK cells. Further increasing the proportion of CTV-1 cells in the priming ratios 2 : 1, 1 : 1, 1 : 2 and 1 : 4 progressively, and significantly, decreased the percentage of NK cells expressing NKG2D, with the 1 : 4 NK priming ratio resulting in the lowest percentage of NK cells expressing NKG2D (range of 29 to 59 %).

Similar to NKp30 expression, priming had no significant effect on the expression of activating receptors 2B4, NKp80 and the adhesion receptor CD2 (Figures 4.7 and 4.8). Both 2B4 and NKp80 were expressed on >98 % of non-primed and primed NK cells, whereas the expression of CD2 on non-primed and primed NK cells was slightly more variable and ranged between 60 to 82 %.

4.3.1.2.5 Priming up-regulates the expression of the co-stimulatory receptors CD69, CD137, CRTAM, OX40, GITR and the IL-2 alpha subunit CD25 by $CD56^+$ NK cells

Non-primed cells are essentially negative for the expression of CD25, the TNF (tumour necrosis factor) superfamily members; CD137, OX40 and the immunoglobulin family receptor CRTAM. They are positive for the early activation marker CD69 (range 34 to 94 %) and the other TNF superfamily member GITR (range 7 to 32 %). NK cell priming at any priming ratio significantly up-regulated the expression of these co-stimulatory molecules (Figures 4.8 and 4.9).

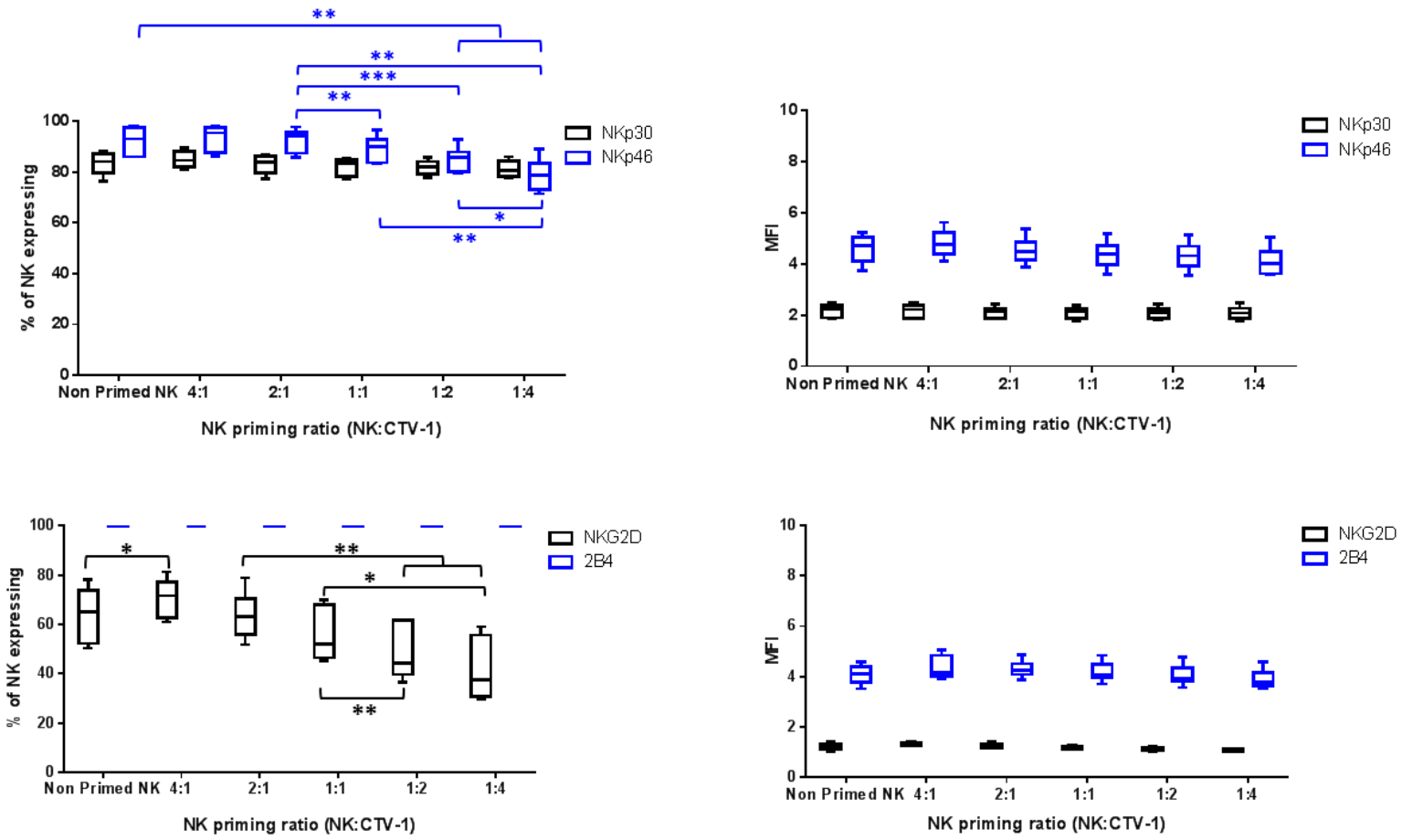

Figure 4.7: The influence of priming with CTV-1 on the expression of receptors NKp30, NKp46, NKG2D and 2B4 by NK cells

NK cells were co-incubated with mitomycin C treated CTV-1 cells at NK:CTV ratios 4:1, 2:1, 1:1, 1:2, and 1:4 for 17 hrs. The expression of NKp30, NKp46, NKG2D and 2B4 on primed NK cells was compared to non-primed NK cells that were incubated in medium only for 17 hrs. Expression of all four receptors on NK cells was measured by flow cytometry. The percentage of NK expressing either NKp30, NKp46, NKG2D and 2B4 (graphs on left top and bottom) and the median fluorescence intensity (MFI) of this expression (graphs on the right top and bottom) are shown. Each box plot has whiskers set to minimum and maximum with the line representing the median. Statistical analyses was done using a one way ANOVA in conjunction with a Tukey's multiple comparisons test. * $P \leq 0.05$, ** $P \leq 0.005$. *** $P \leq 0.0005$.

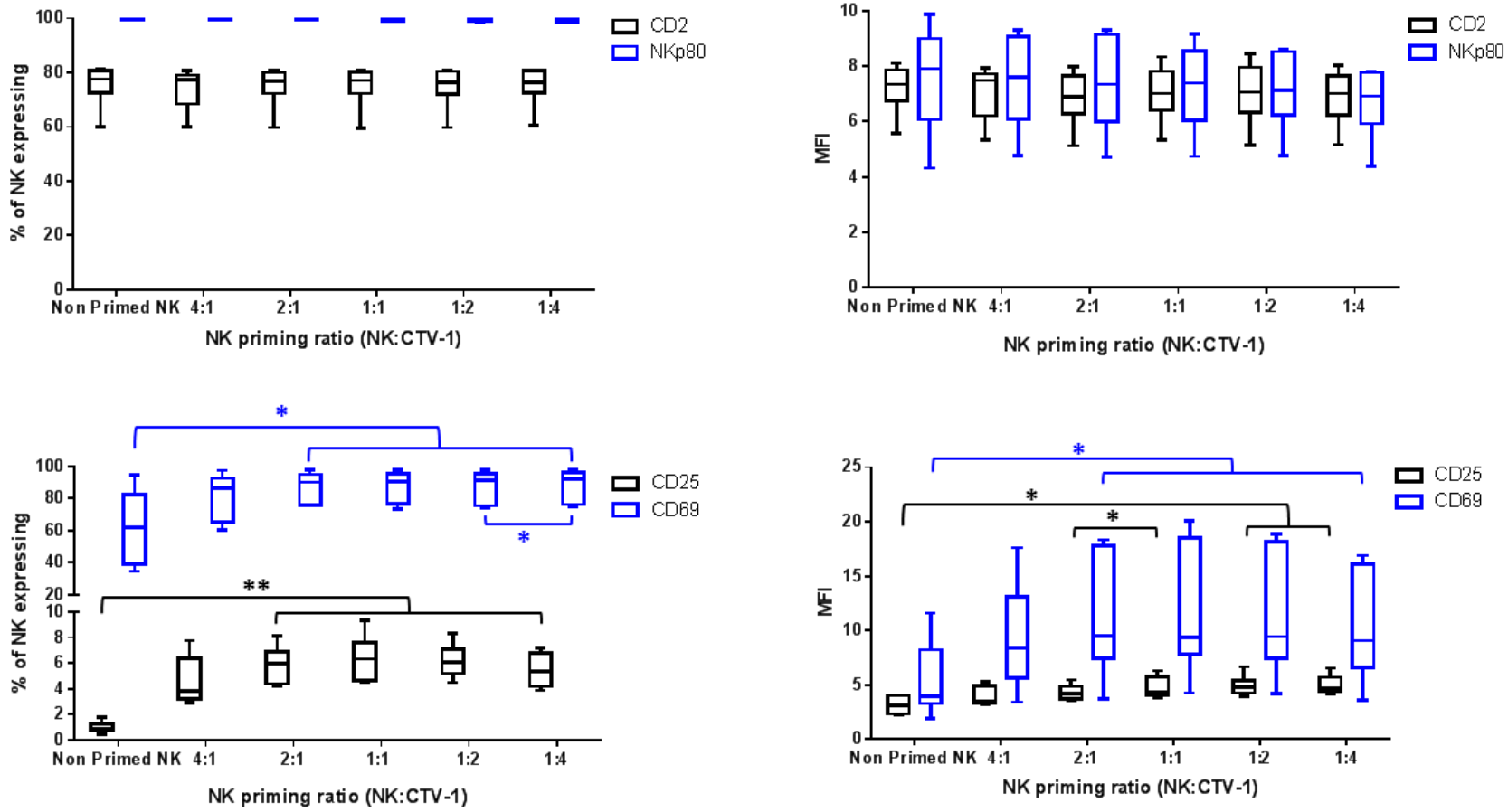

Figure 4.8: The influence of priming with CTV-1 on the expression of receptors NKp30, NKp46, NKG2D and 2B4 by NK cells

NK cells were co-incubated with mitomycin C treated CTV-1 cells at NK:CTV ratios 4:1, 2:1, 1:1, 1:2, and 1:4 for 17 hrs. The expression of NKp30, NKp46, NKG2D and 2B4 on primed NK cells was compared to non-primed NK cells that were incubated in medium only for 17 hrs. Expression of all four receptors on NK cells was measured by flow cytometry. The percentage of NK cells expressing either NKp30, NKp46, NKG2D and 2B4 (graphs on left top and bottom) and the median fluorescence intensity (MFI) of this expression (graphs on the right top and bottom) are shown. Each box plot has whiskers set to minimum and maximum with the line representing the median. Statistical analyses was done using a one way ANOVA in conjunction with a Tukey's multiple comparisons test. * $P \leq 0.05$.

Priming significantly up-regulated CD25 and CD69 expression, both in terms of percentage of NK cells expressing and the intensity of expression (Figure 4.8). Peak expression of both receptors was around the 2 : 1 to 1 : 2 ratio, although this was donor-dependent. Although the expression of CD25 was up-regulated, at peak expression only 4 to 9 % of primed NK cells expressed CD25 with only a slight up-regulation in MFI. In contrast, CD69 expression was highly up-regulated, with 77 to 98% of NK cells expressing this receptor at peak expression. The intensity level of CD69 expression differed greatly from person to person, ranging between 4 and 20 at peak expression on primed NK cells as compared to 2 and 12 on non-primed NK cells.

All three receptors belonging to the TNF superfamily (OX40, CD137, GITR) were significantly up-regulated by priming (Figure 4.9). Out of these receptors, priming had the least effect on OX40 expression, with between 5 and 11 % of NK cells expressing the receptor. The intensity of expression was extremely low (≤ 1 both for non-primed and primed NK cells) and was unaffected by priming. Primed NK cells expressed a higher level of CD137 (also known as 4-1ββ) than OX40, with a peak expression between 12 and 21 %. In contrast to OX40, there was also an increase in the intensity of CD137, which peaked with an MFI between 4 and 9. For both OX40 and CD137, the peak expression of these receptors occurred when priming NK cells at a NK : CTV-1 priming ratio of 1 : 1 or 1 : 2, although the response was again donor-dependent. In contrast, the expression of the GITR receptor peaked at the priming ratios 4 : 1 and 2 : 1 and was donor-dependent. There was no significant increase in the MFI of the receptor following priming, and its expression remained at a low intensity level (MFI range 1 to 2). Priming induced a significant increase in the percentage of NK cells expressing GITR. Out of all three TNF receptors expressed by the NK cells, the GITR receptor was the most up-regulated, with peak expression on primed NK cells between 24 and 59 % compared with 8 and 32 % on non-primed NK cells. Interestingly, the percentage of NK cells expressing GITR was significantly less when primed by the 1 : 4 NK : CTV-1 ratio than when the NK cells were primed at the 2:1, 1:1 and 1 : 2 ratios.

Expression of the CRTAM receptor increased following priming both in terms of the percentage of NK cells expressing the receptor and the intensity of that expression, peaking on NK cells primed with the 1 : 1 and 1 : 2 NK : CTV-1 ratios (Figure 4.9). The peak percentage of primed NK cells expressing CRTAM was seen to be between 20 and 38 %, with the MFI peaking between 5 and 16. Similar to the expression of GITR, the percentage of NK cells expressing CRTAM following priming with the 1 : 4 NK : CTV-1 ratio was significantly less compared to NK cells primed using the 1 : 2 ratio. As judged by the up-regulation of the above co-stimulatory receptors, the optimal NK : CTV-1 priming ratio appeared to be either 1 : 1 or 1 : 2, but was donor-dependent.

.

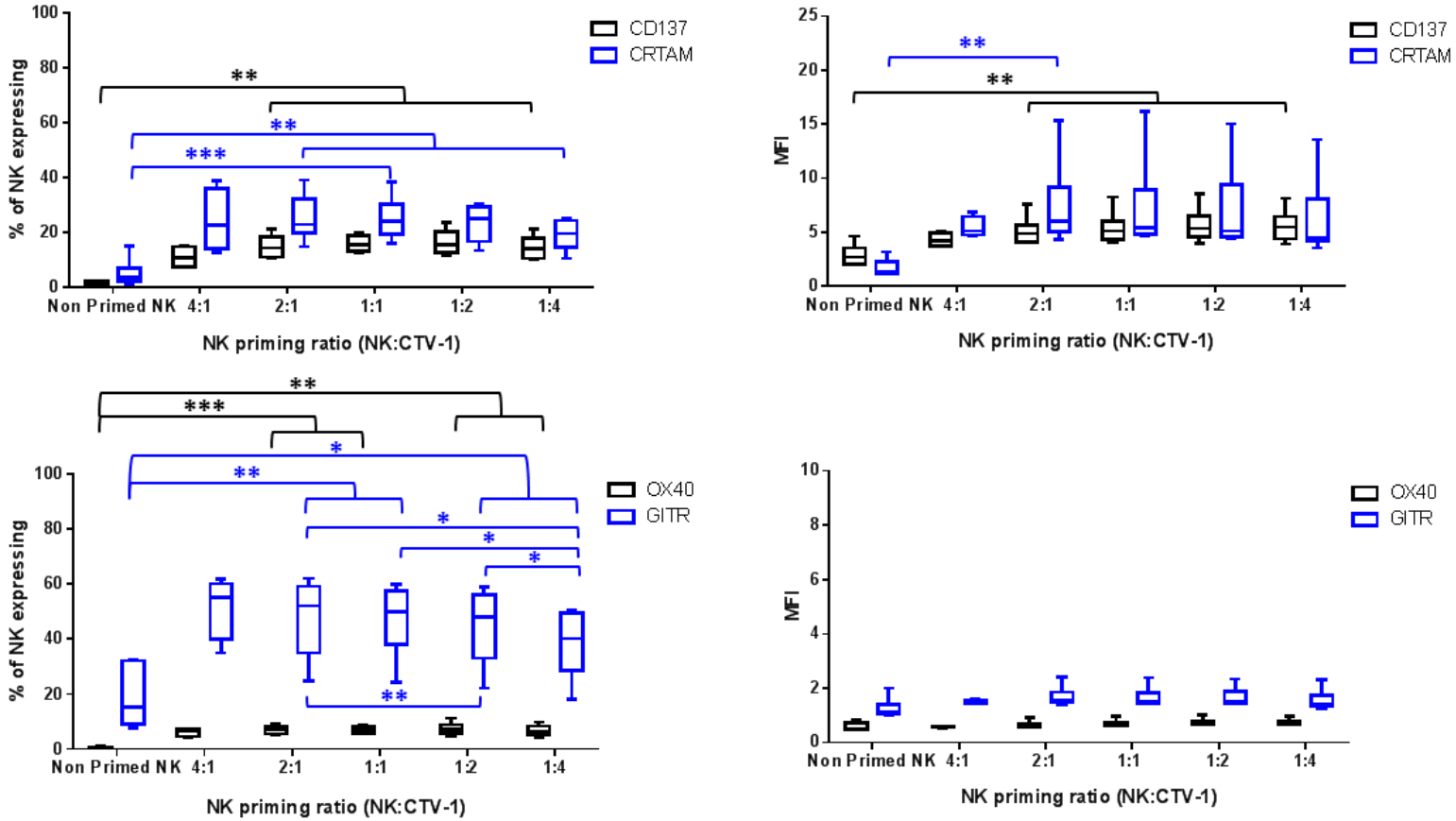

Figure 4.9: The influence of priming with CTV-1 on the expression of receptors CD137, CRTAM, OX40 and GITR by NK cells

NK cells were co-incubated with mitomycin C treated CTV-1 cells at NK:CTV ratios 4:1, 2:1, 1:1, 1:2, and 1:4 for 17 hrs. The expression of CD137, CRTAM, OX40 and GITR on primed NK cells was compared to non-primed NK cells that were incubated in medium only for 17 hrs. Expression of all four receptors on NK cells was measured by flow cytometry. The percentage of NK cells expressing either CD137, CRTAM, OX40 and GITR (graphs on left top and bottom) and the median fluorescence intensity (MFI) of this expression (graphs on the right top and bottom) are shown. Each box plot has whiskers set to minimum and maximum with the line representing the median. Statistical analyses was done using a one way ANOVA in conjunction with a Tukey's multiple comparisons test. * $P \leq 0.05$, ** $P \leq 0.005$. *** $P \leq 0.0005$.

4.3.1.3 Expression of activating, co-stimulatory and co-inhibitory receptors on $CD56^{dim}CD16^{high}$, $CD56^{dim}CD16^{low}$ and $CD56^{dim}CD16^{neg}$ NK cell subpopulations

As previously discussed in section 4.3.1.2.2, priming decreased the percentage of $CD56^{dim}CD16^{high}$ NK cells and increased the percentage of $CD56^{dim}CD16^{low}$ and $CD56^{dim}CD16^{neg}$ NK cell populations. These subpopulations, referred to from now on as $CD16^{high}$, $CD16^{low}$ and $CD16^{neg}$, were analysed separately for their expression of activating, co-stimulatory and co-inhibitory receptors. A representative gating strategy for this analysis is shown in Figure 2.5.

4.3.1.3.1 Expression of the immunoglobulin superfamily receptors DNAM-1, TIGIT and CD96 on $CD56^{dim}CD16^{high}$, $CD56^{dim}CD16^{low}$ and $CD56^{dim}CD16^{neg}$ NK cell subpopulations

Non-primed $CD16^{neg}$ NK cells expressed significantly less DNAM-1 (% of expression and MFI), and TIGIT (% of expression only) than $CD16^{high}$ NK cells. Significantly less TIGIT was expressed on $CD16^{neg}$ NK cells compared to $CD16^{low}$ NK cells. (Figure 4.10).

In terms of percentage of expression on primed NK cells, the expression of DNAM-1 and TIGIT did not significantly differ between the 3 subpopulations. For CD96, there was a trend towards primed $CD16^{neg}$ NK cells expressing less CD96 then both $CD16^{high}$ and $CD16^{low}$ NK cells, with the only significant difference being observed at 1 : 4 NK : CTV-1 priming ratio (Figure 4.11). The intensity of CD96 expression on primed NK cells was always significantly different between the 3 subpopulations, with the exception of the NK cells primed at the 1 : 4 NK : CTV-1 ratio for which there was no significant difference in the MFI between the $CD16^{low}$ and $CD16^{neg}$ subpopulations (Figure 4.11). For TIGIT, only the MFI of the $CD16^{high}$ and $CD16^{neg}$ subpopulations for NK cells primed at the 2 : 1 and 1 : 1 ratio was significantly different (Figure 4.10).

Priming had no significant effect on the percentage of $CD16^{high}$ and $CD16^{low}$ NK cells expressing DNAM-1 and TIGIT. An exception was that significantly less TIGIT was expressed on $CD16^{high}$ NK cells that were primed at the 1 : 4 primed than expressed on their non-primed counterparts. However, priming did significantly increase the percentage of $CD16^{neg}$ NK cells that expressed TIGIT. In contrast to the expression of TIGIT, the percentage of NK cells in all 3 subsets expressing CD96 significantly decreased after priming at NK : CTV-1 ratios 1 : 2 and 1 : 4 compared to equivalent non-primed NK cells. Furthermore, for all 3 subsets, the greater the proportion of CTV-1 cells in the priming ratio the greater the reduction of NK cells expressing CD96. Priming influenced the intensity of expression of TIGIT and CD96 on the $CD16^{high}$, $CD16^{low}$ and $CD16^{neg}$ subpopulations and the intensity of DNAM-1 on the $CD16^{neg}$ subpopulation only. The greatest change in expression of all 3 receptors was seen on $CD16^{neg}$

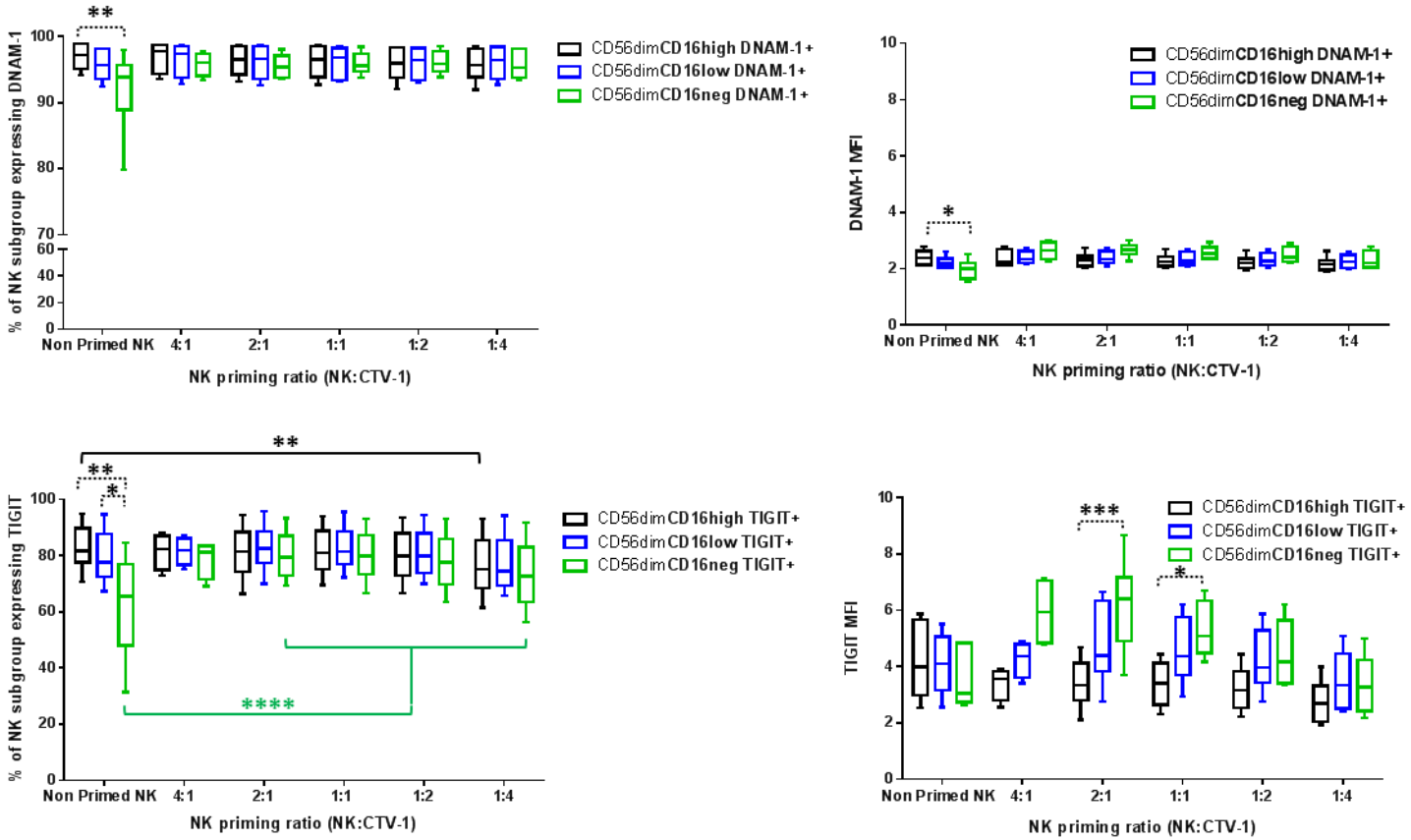

Figure 4.10: The influence of priming with CTV-1 on the expression of receptors DNAM-1 and TIGIT by $CD56^{dim}CD16^{high}$, $CD56^{dim}CD16^{low}$ and $CD56^{dim}CD16^{neg}$ NK cell subpopulations.

NK cells were co-incubated with mitomycin C treated CTV-1 cells at NK:CTV ratios 4:1, 2:1, 1:1, 1:2, and 1:4 for 17 hrs. The expression of receptors DNAM-1 and TIGIT on primed $CD56^{dim}CD16^{high}$, $CD56^{dim}CD16^{low}$ and $CD56^{dim}CD16^{neg}$ NK cell subpopulations was compared to the equivalent non-primed NK subpopulations that were incubated in medium only for 17 hrs. Expression of both receptors was measured by flow cytometry. The percentage of each NK cell subpopulation expressing DNAM-1 or TIGIT (graphs on the left, top and bottom) and the median fluorescence intensity (MFI) of this expression (graphs on the right, top and bottom) are shown. Each box plot has whiskers set to minimum and maximum with the line representing the median. Statistical analyses were done using a two way ANOVA in conjunction with a Tukey's multiple comparisons test. * $P \leq 0.05$, ** $P \leq 0.005$. *** $P \leq 0.0005$, **** $P \leq 0.00005$.

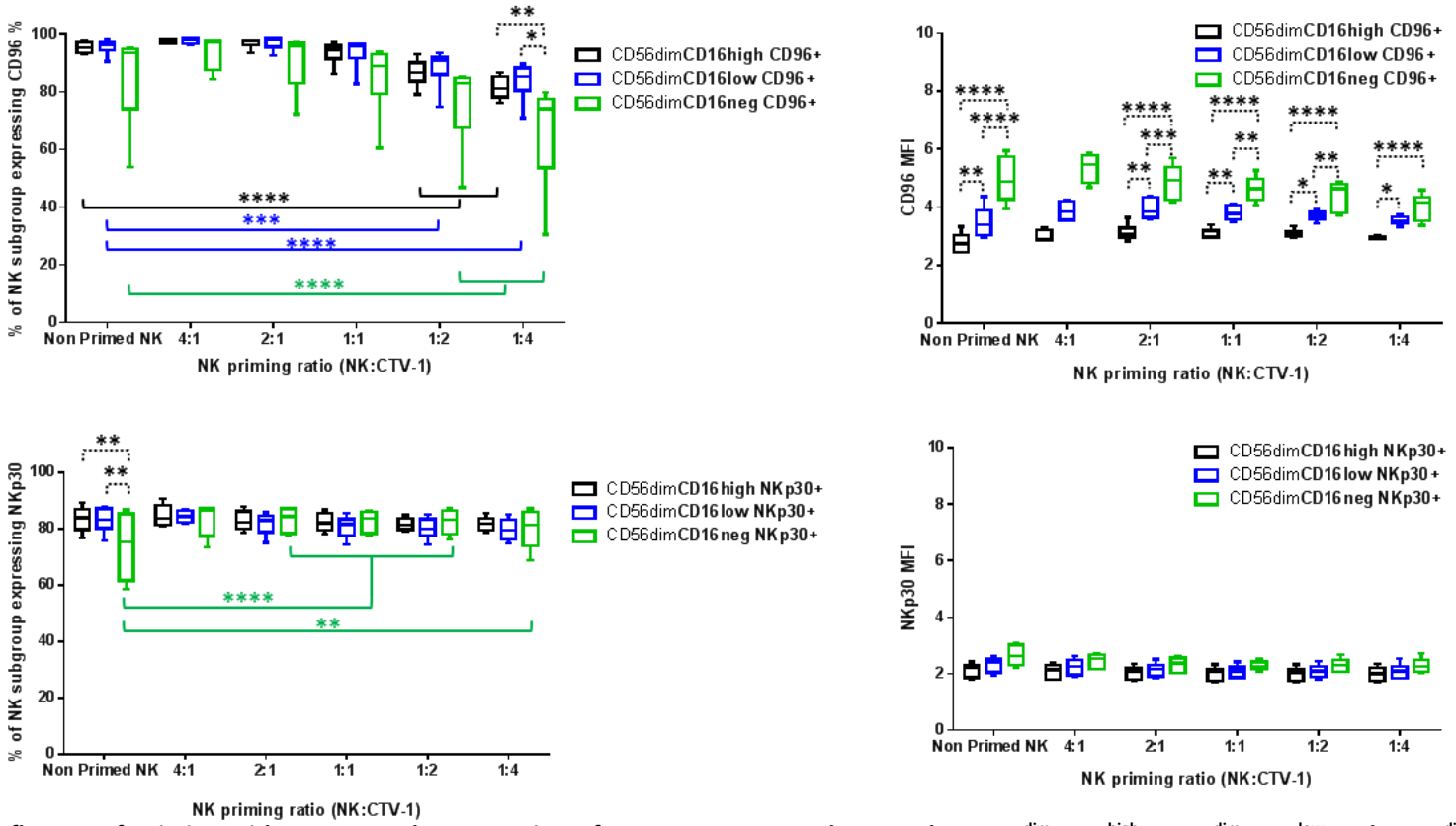

Figure 4.11: The influence of priming with CTV-1 on the expression of receptors CD96 and NKp30 by $CD56^{dim}CD16^{high}$, $CD56^{dim}CD16^{low}$ and $CD56^{dim}CD16^{neg}$ NK cell subpopulations.

NK cells were co-incubated with mitomycin C treated CTV-1 cells at NK:CTV ratios 4:1, 2:1, 1:1, 1:2, and 1:4 for 17 hrs. The expression of receptors CD96 and NKp30 on primed $CD56^{dim}CD16^{high}$, $CD56^{dim}CD16^{low}$ and $CD56^{dim}CD16^{neg}$ NK cell subpopulations was compared to the equivalent non-primed NK subpopulations that were incubated in medium only for 17 hrs. Expression of both receptors was measured by flow cytometry. The percentage of each NK cell subpopulation expressing CD96 or NKp30 (graphs on the left, top and bottom) and the median fluorescence intensity (MFI) of this expression (graphs on the right, top and bottom) are shown. Each box plot has whiskers set to minimum and maximum with the line representing the median. Statistical analyses were done using a one way ANOVA in conjunction with a Tukey's multiple comparisons test. * $P \leq 0.05$, ** $P \leq 0.005$. *** $P \leq 0.0005$, **** $P \leq 0.00005$.

subpopulation. Initially, the MFI for the 3 receptors increased as a result of priming, before decreasing as the proportion of CTV-1 cells in the priming ratio increased. The intensity of the expression of TIGIT and CD96 on the $CD16^{low}$ subpopulation also followed this trend (Figure 4.10).

4.3.1.3.2 Expression of the activating receptors NKp30, NKp46, NKG2D on $CD56^{dim}CD16^{high}$, $CD56^{dim}CD16^{low}$ and $CD56^{dim}CD16^{neg}$ NK cell subpopulations

Overall, the percentage of NK cells in the $CD16^{high}$ and $CD16^{low}$ subpopulations expressing NKG2D initially increased at the 4 : 1 NK : CTV-1 priming ratio before decreasing as the proportion of CTV-1 in the priming ratios increased, with significant differences seen between non-primed NK cells and the 1 : 2 and 1 : 4 (NK : CTV-1) primed NK cells (Figure 4.12). In contrast, priming decreased the percentage of $CD16^{neg}$ NK cells that expressed NKG2D. This decrease was significant between NK cells primed at the 1 : 1, 1 : 2 and 1 : 4 NK : CTV-1 priming ratios compared to non-primed NK cells.

The percentage of the non-primed $CD16^{neg}$ subpopulation expressing NKp30 was significantly less than the equivalent $CD16^{high}$ and $CD16^{low}$ subpopulations (Figure 4.11). However, there was no difference between the 3 subpopulations following priming, as the percentage of $CD16^{neg}$ subpopulation expressing NKp30 significantly increased and reached levels similar to the $CD16^{high}$ and $CD16^{low}$ subpopulations.

The non-primed $CD16^{neg}$ subpopulation expressed significantly less NKp46 as a percentage of expression on NK cells than the equivalent $CD16^{high}$ and $CD16^{low}$ subpopulations (Figure 4.12). This difference remained significant even when the NK cells were primed at any of the NK : CTV-1 ratios, with the exception of the 2 : 1 ratio. There was a trend towards the percentage of NK cells that were primed at the 1 : 2 and 1 : 4 ratios in the $CD16^{high}$ and $CD16^{low}$ subpopulations decreasing, with the only significant difference occurring between non-primed NK cells and the $CD16^{low}$ NK cells primed at the 1 : 4 ratio. In stark contrast, the percentage of $CD16^{neg}$ NK cells expressing NKp46 increased when primed at the 4 : 1 NK : CTV-1 ratio. As the proportion of CTV-1 cells increased in the subsequent priming ratios the percentage of NK in the $CD16^{neg}$ subpopulation expressing NKp46 significantly decreased with ratio.

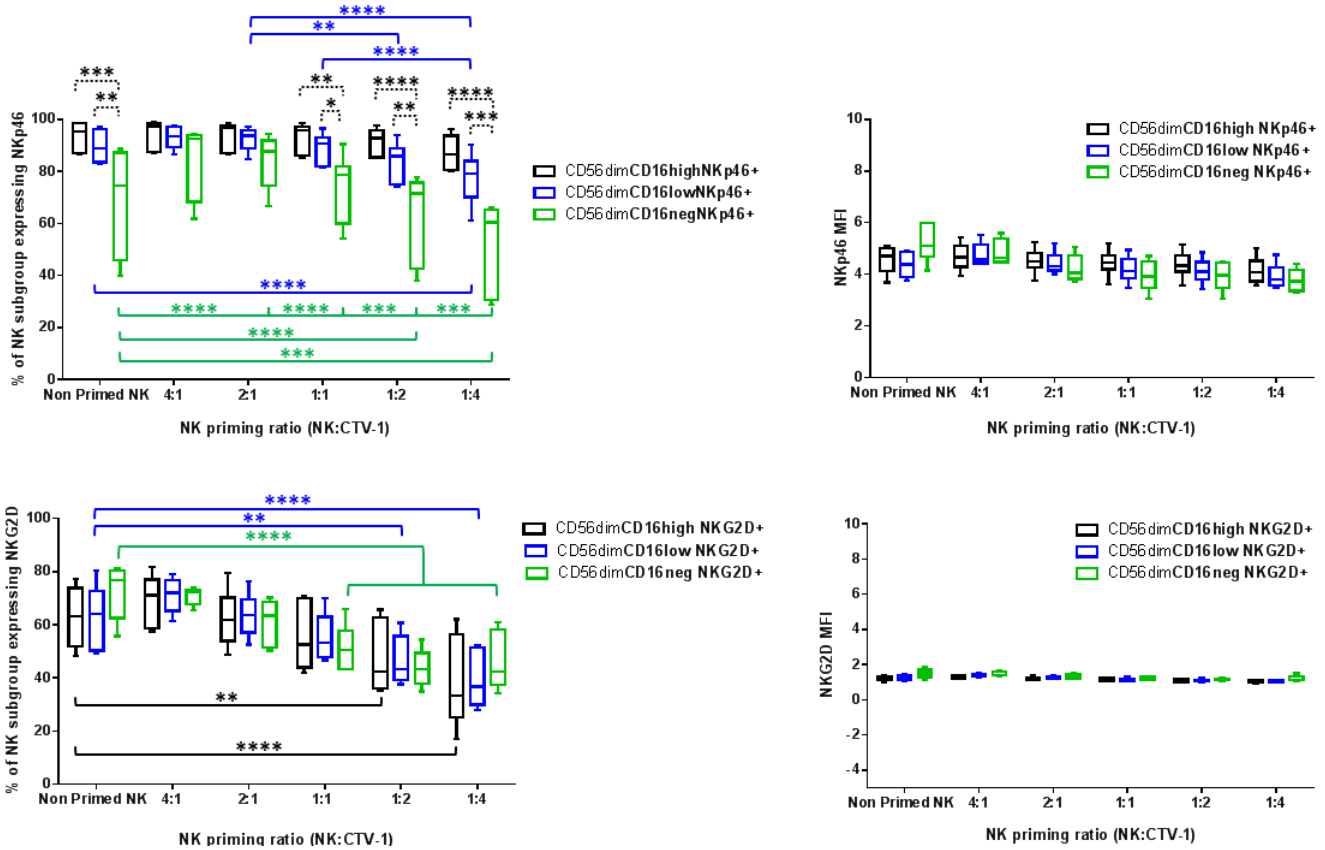

Figure 4.12: The influence of priming with CTV-1 on the expression of receptors NKp46 and NKG2D by $CD56^{dim}CD16^{high}$, $CD56^{dim}CD16^{low}$ and $CD56^{dim}CD16^{neg}$ NK cell subpopulations.

NK cells were co-incubated with mitomycin C treated CTV-1 cells at NK : CTV ratios 4 : 1, 2 : 1, 1:1, 1 : 2, and 1 : 4 for 17 hrs. The expression of receptors NKp46 and NKG2D on primed $CD56^{dim}CD16^{high}$, $CD56^{dim}CD16^{low}$ and $CD56^{dim}CD16^{neg}$ NK cell subpopulations was compared to the equivalent non-primed NK subpopulations that were incubated in medium only for 17 hrs. Expression of both receptors was measured by flow cytometry. The percentage of each NK cell subpopulation expressing NKp46 or NKG2D (graphs on the left, top and bottom) and the median fluorescence intensity (MFI) of this expression (graphs on the right, top and bottom) are shown. Each box plot has whiskers set to minimum and maximum with the line representing the median. Statistical analyses were done using a two way ANOVA in conjunction with a Tukey's multiple comparisons test. * $P \leq 0.05$, ** $P \leq 0.005$. *** $P \leq 0.0005$, **** $P \leq 0.00005$.

4.3.1.3.3 Expression of receptors CD2, CD25 and CD69 on $CD56^{dim}CD16^{high}$, $CD56^{dim}CD16^{low}$ and $CD56^{dim}CD16^{neg}$ NK cell subpopulations

The $CD16^{high}$, $CD16^{low}$ and $CD16^{neg}$ NK cell subpopulations expressed similar levels of CD2, with priming inducing a small, but significant up-regulation in the percentage of $CD16^{neg}$ NK cells expressing CD2 (Figure 4.13).

The $CD16^{high}$, $CD16^{low}$ and $CD16^{neg}$ NK cell subpopulations also expressed similar levels of CD69 (Figure 4.14). Priming at any of the priming ratios significantly increased the expression of CD69 on all 3 CD16 subpopulations in terms of both percentage of NK expressing CD69 and intensity of expression for that receptor. The only exception was that the increase in intensity of CD69 expression on the $CD16^{high}$ subpopulation which was induced by priming was not of statistical significance. Overall, the intensity of CD69 expression was lower on the primed $CD16^{high}$ and $CD16^{low}$ NK cell subpopulations at all priming ratios, as compared to the expression on the equivalent $CD16^{neg}$ subpopulation (Figure 4.14).

In contrast to the results for CD69, the level of up-regulation of CD25 following priming at any ratio was significantly different between the $CD16^{high}$, $CD16^{low}$ and $CD16^{neg}$ NK cell subpopulations (Figure 4.13). The primed $CD16^{high}$ subpopulation did not significantly up-regulate CD25, whereas the equivalent $CD16^{low}$ and $CD16^{neg}$ did. A significantly greater percentage of $CD16^{neg}$ NK cells expressed CD25 than their $CD16^{low}$ counterparts, and at higher intensity, although the difference in intensity was not found to be significant. The expression of CD25 was similar on all primed $CD16^{low}$ NK cells, irrespective of the ratio which was used to prime them. However, a significantly lower proportion of primed $CD16^{neg}$ NK cells expressed CD25 at 1 : 4 ratio, as compared to cells that had been primed at the 2 : 1, 1 : 1 and 1 : 2 ratios (Figure 4.13).

4.3.1.3.4 Up-regulation of TNF superfamily co-stimulatory receptors OX40, CD137 GITR and the immunoglobulin superfamily receptor CRTAM on $CD56^{dim}CD16^{high}$, $CD56^{dim}CD16^{low}$ and $CD56^{dim}CD16^{neg}$ NK cell subpopulations

As illustrated in Figures 4.14 and 4.15, the pattern of expression of the co-stimulatory receptors OX40, CD137 and CRTAM on the $CD16^{high}$, $CD16^{low}$ and $CD16^{neg}$ NK cell subpopulations is similar to the expression pattern for CD25. A significantly higher proportion of the primed $CD16^{neg}$ NK cells express OX40, CD137, CRTAM compared to the equivalent $CD16^{low}$ and $CD16^{high}$ subpopulations. Priming had no significant effect on the expression of OX40, CD137, CRTAM by

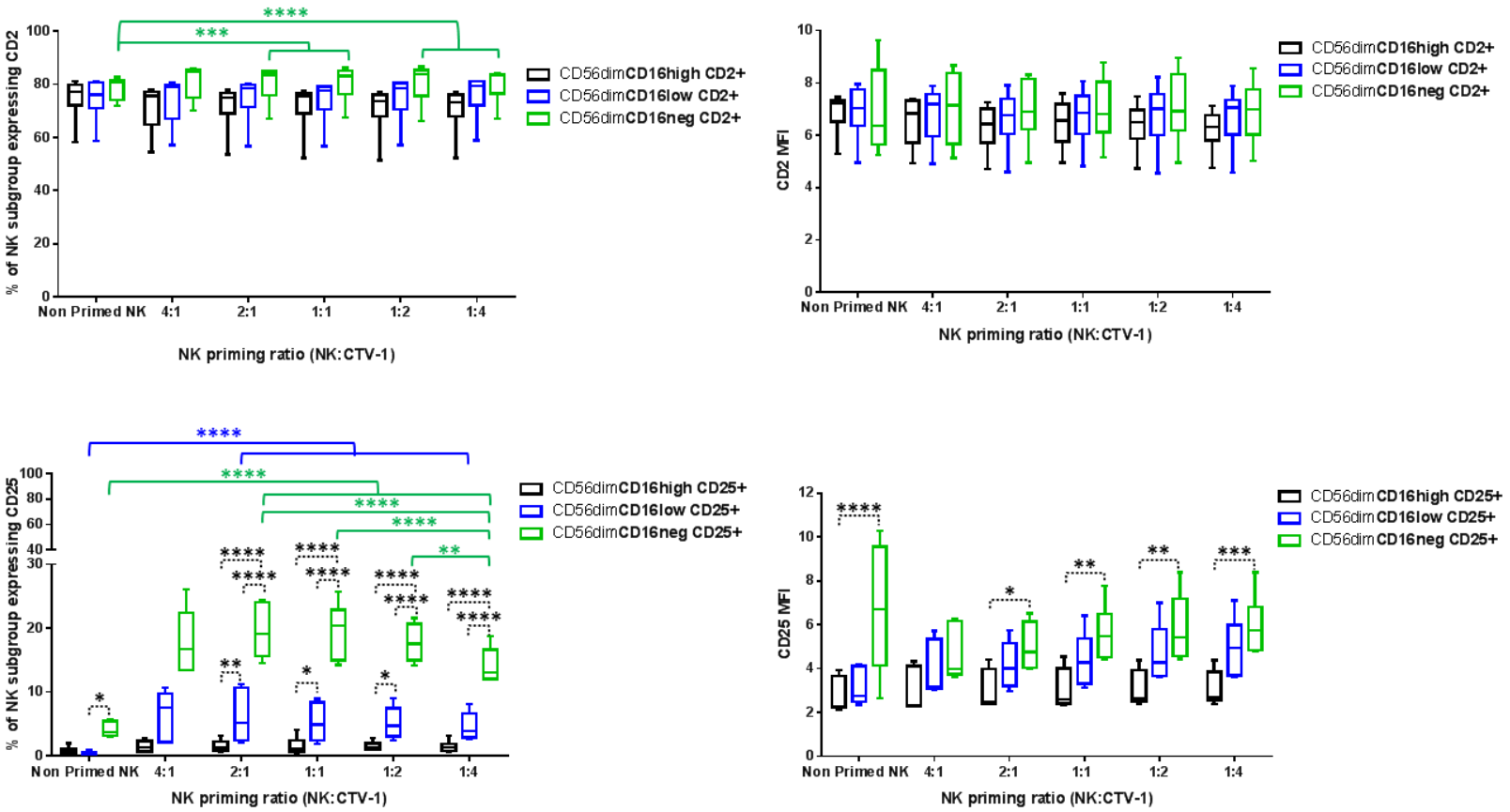

Figure 4.13: The influence of priming with CTV-1 on the expression of receptors CD2 and CD25 by CD56^{dim}CD16^{high}, CD56^{dim}CD16^{low} and CD56^{dim}CD16^{neg} NK cell subpopulations. NK cells were co-incubated with mitomycin C treated CTV-1 cells at NK:CTV ratios 4:1, 2:1, 1:1, 1:2, and 1:4 for 17 hrs. The expression of receptors CD2 and CD25 on primed CD56^{dim}CD16^{high}, CD56^{dim}CD16^{low} and CD56^{dim}CD16^{neg} NK cell subpopulations was compared to the equivalent non-primed NK cell subpopulations that were incubated in medium only for 17 hrs. Expression of both receptors was measured by flow cytometry. The percentage of each NK cell subpopulation expressing CD2 or CD25 (graphs on the left, top and bottom) and the median fluorescence intensity (MFI) of this expression (graphs on the right, top and bottom) are shown. Each box plot has whiskers set to minimum and maximum with the line representing the median. Statistical analyses were done using a two way ANOVA in conjunction with a Tukey's multiple comparisons test. * $P \leq 0.05$, ** $P \leq 0.005$. *** $P \leq 0.0005$, **** $P \leq 0.00005$.

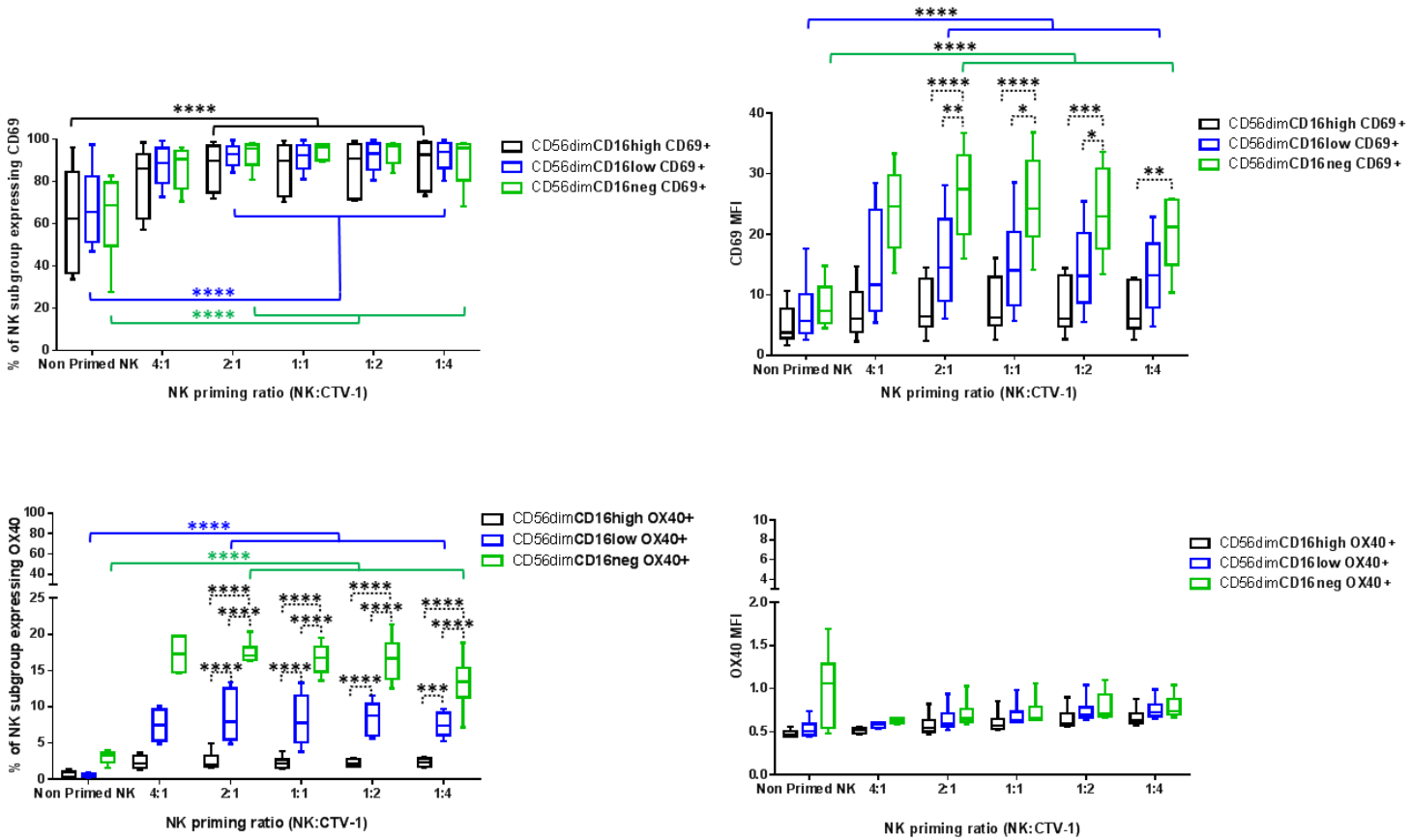

Figure 4.14: The influence of priming with CTV-1 on the expression of receptors CD69 and OX40 by $CD56^{dim}CD16^{high}$, $CD56^{dim}CD16^{low}$ and $CD56^{dim}CD16^{neg}$ NK cell subpopulations. NK cells were co-incubated with mitomycin C treated CTV-1 cells at NK:CTV ratios 4:1, 2:1, 1:1, 1:2, and 1:4 for 17 hrs. The expression of receptors CD69 and OX40 on primed $CD56^{dim}CD16^{high}$, $CD56^{dim}CD16^{low}$ and $CD56^{dim}CD16^{neg}$ NK cell subpopulations was compared to the equivalent non-primed NK cell subpopulations that were incubated in medium only for 17 hrs. Expression of both receptors was measured by flow cytometry. The percentage of each NK cell subpopulation expressing CD69 or OX40 (graphs on the left, top and bottom) and the median fluorescence intensity (MFI) of this expression (graphs on the right, top and bottom) are shown. Each box plot has whiskers set to minimum and maximum with the line representing the median. Statistical analyses were done using a two way ANOVA in conjunction with a Tukey's multiple comparisons test. * $P \leq 0.05$, ** $P \leq 0.005$. *** $P \leq 0.0005$, **** $P \leq 0.00005$.

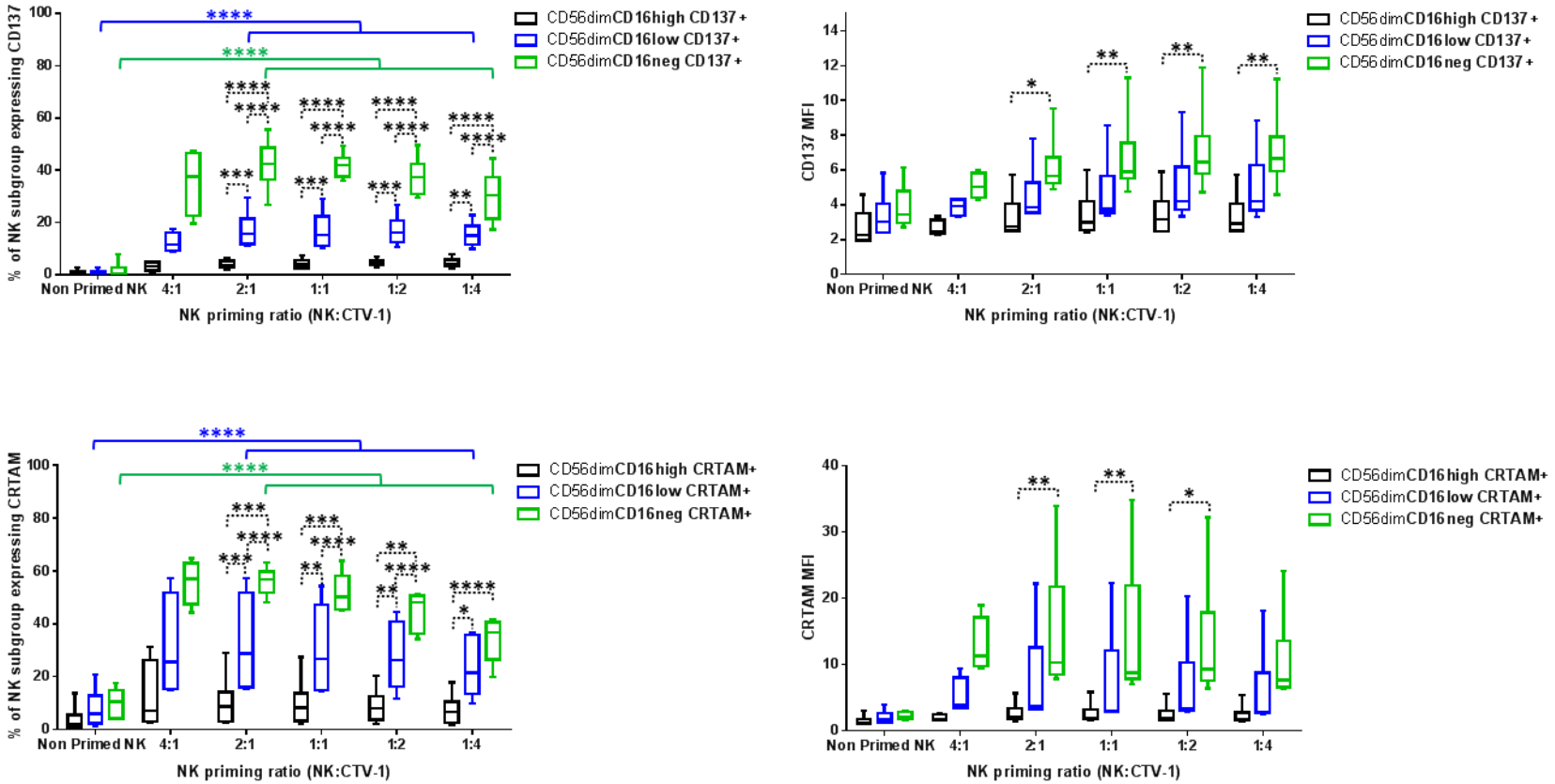

Figure 4.15: The influence of priming with CTV-1 on the expression of receptors CD137 and CRTAM by $CD56^{dim}CD16^{high}$, $CD56^{dim}CD16^{low}$ and $CD56^{dim}CD16^{neg}$ NK cell subpopulations.

NK cells were co-incubated with mitomycin C treated CTV-1 cells at NK:CTV ratios 4:1, 2:1, 1:1, 1:2, and 1:4 for 17 hrs. The expression of receptors CD137 and CRTAM on primed $CD56^{dim}CD16^{high}$, $CD56^{dim}CD16^{low}$ and $CD56^{dim}CD16^{neg}$ NK cell subpopulations was compared to the equivalent non-primed NK cell subpopulations that were incubated in medium only for 17 hrs. Expression of both receptors was measured by flow cytometry. The percentage of each NK cell subpopulation expressing CD137 or CRTAM (graphs on the left, top and bottom) and the median fluorescence intensity (MFI) of this expression (graphs on the right, top and bottom) are shown. Each box plot has whiskers set to minimum and maximum with the line representing the median. Statistical analyses were done using a two way ANOVA in conjunction with a Tukey's multiple comparisons test. * $P \leq 0.05$, ** $P \leq 0.005$. *** $P \leq 0.0005$, **** $P \leq 0.00005$.

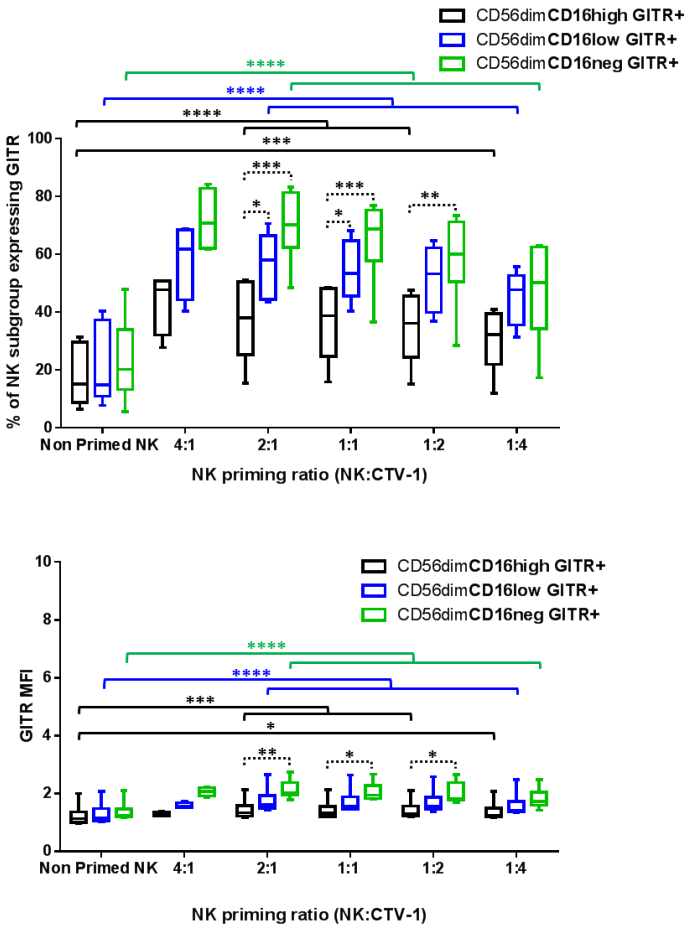

Figure 4.16: The influence of priming with CTV-1 on the expression of receptors CD2 and CD25 by CD56^{dim}CD16^{high}, CD56^{dim}CD16^{low} and CD56^{dim}CD16^{neg} NK cell subpopulations.
NK cells were co-incubated with mitomycin C treated CTV-1 cells at NK:CTV ratios 4:1, 2:1, 1:1, 1:2, and 1:4 for 17 hrs. The expression of receptors CD2 and CD25 on primed CD56^{dim}CD16^{high}, CD56^{dim}CD16^{low} and CD56^{dim}CD16^{neg} NK cell subpopulations was compared to the equivalent non-primed NK cell subpopulations that were incubated in medium only for 17 hrs. Expression of both receptors was measured by flow cytometry. The percentage of each NK cell subpopulation expressing CD2 or CD25 (graphs on the left, top and bottom) and the median fluorescence intensity (MFI) of this expression (graphs on the right, top and bottom) are shown. Each box plot has whiskers set to minimum and maximum with the line representing the median. Statistical analyses were done using a two way ANOVA in conjunction with a Tukey's multiple comparisons test. * P ≤ 0.05, ** P ≤ 0.005. *** P ≤ 0.0005, **** P ≤ 0.00005.

the CD16^{high} subpopulation at any ratio, as a consequence of which the proportion of CD16^{low} NK cells expressing the OX40, CD137, CRTAM was significantly higher than that for the equivalent CD16^{high} NK cells. Again, similar to the expression of CD25, primed CD16^{neg} NK cells express a higher intensity of OX40, CD137 and CRTAM than their CD16^{low} and CD16^{high} counterparts, although this difference was only found to be significant between the primed CD16^{high} and CD16^{neg} populations when expressing CD137 and CRTAM.

Similar percentages of the CD16^{high}, CD16^{low} and CD16^{neg} NK cell subpopulations expressed GITR before priming (Figure 4.16). Following priming at any ratio, a greater proportion of CD16^{neg} NK cells significantly up-regulated GITR compared to the equivalent CD16^{low} and CD16^{high}

subpopulations, and a greater proportion of CD16^{neg} NK cells expressed GITR compared to the CD16^{low} subpopulations. The peak expression of GITR for all 3 primed NK cell CD16 subpopulations was at the 4 : 1 priming ratio, with the proportion of NK cells expressing the receptor decreasing as the proportion of CTV-1 increased in the NK priming ratios. The most significant decreases in GITR expression was observed for the CD16^{neg} subpopulation. At all ratios, the CD16^{neg} subpopulation always expressed a higher intensity of GITR than both the CD16^{low} and CD16^{high} subpopulations (Figure 4.16).

4.3.2 Optimisation of a flow cytometry-based NK cell cytotoxic assay

Determining the functional consequence of priming requires the application of appropriate NK cell cytotoxicity assays, as a consequence of which a flow cytometry-based cytotoxic assay was developed. In the first instance, an adaptation of a previously-published assay was developed (Hopkinson et al, 2007). For this, target cells were stained with Mitotracker® Green FM and co-

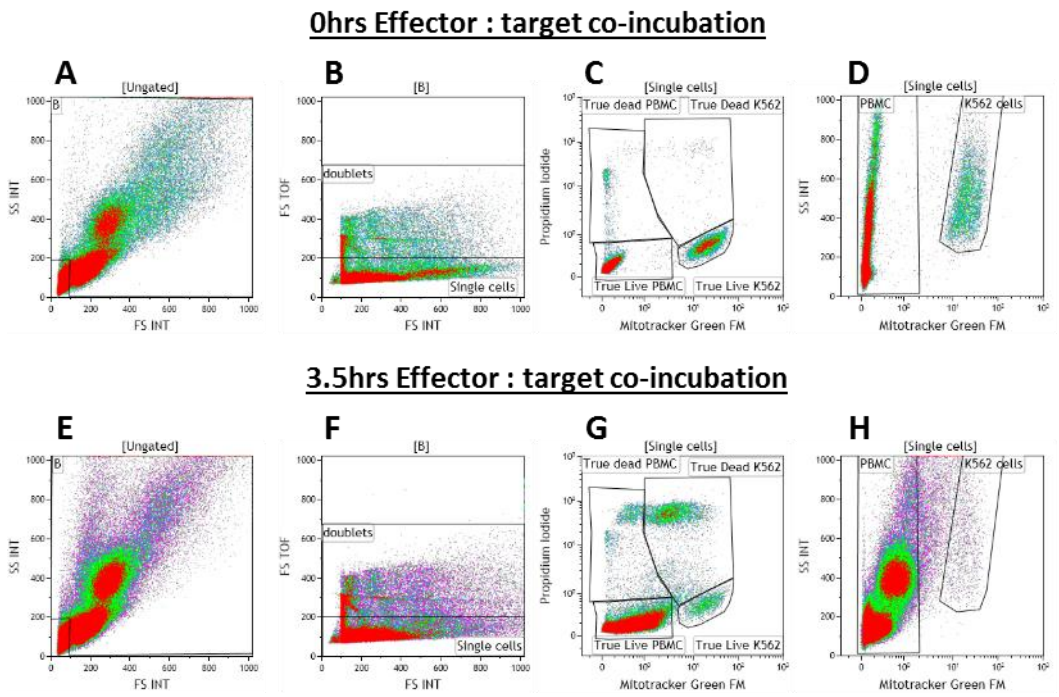

Figure 4.17: Gating strategy for the flow cytometry based NK cell cytotoxic assay when targeting non-primed NK cells against K562 target cells.
Isolated NK cells or PBMCs were targeted against K562 cells stained with Mitotracker® Green FM. Propidium Iodide was used to measure cell death. A to D) Represent the gating strategy for the 0 hr control whereby effector cells were added to the target cells just before acquisition on the flow cytometer. E to H) represent the gating strategy for the cytotoxic tube whereby effector cells were co-incubated with target cells for 3.5 hrs.

incubated with either PBMCs or isolated NK cells that were either primed or non-primed. The length of co-incubation was 3.5 hrs when K562 cells were used as targets, and 2.5 hrs when human PC3 prostate cancer cells were used as targets. The level of spontaneous cytotoxicity was determined by incubating effector cells and target cells separately under the same conditions and adding the cells together (5:1 effector to target cell ratio) immediately prior to analysis. To all tubes, 10 µl of propidium iodide (50 µg/ml stock concentration) was added immediately prior to being run on the flow cytometry. Data were acquired on a Beckman Coulter Gallios™ flow cytometer and analysed using Beckman Coulter Kaluza™ software using the gating strategy shown in Figure 4.17.

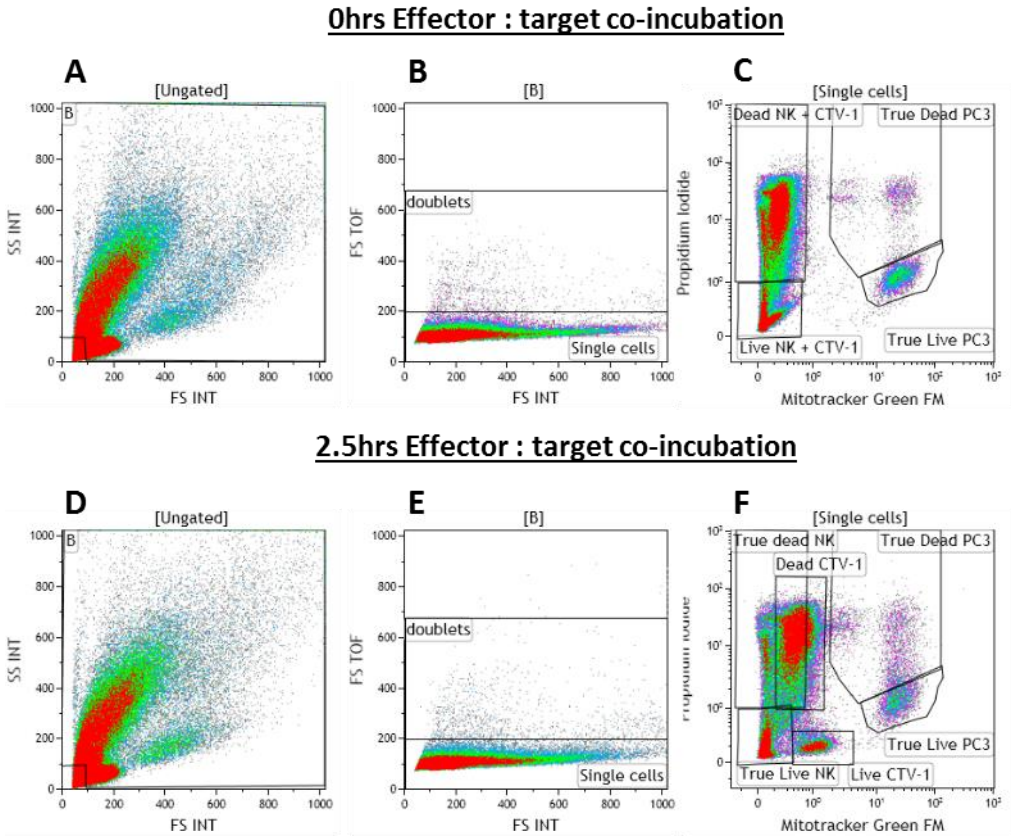

Figure 4.18: Gating strategy for the flow cytometry based NK cell cytotoxic assay when targeting primed NK cells against PC3 target cells.
Primed NK cells were targeted against PC3 cells stained with Mitotracker® Green FM. Propidium Iodide was used to measure cell death. A to D) Represent the gating strategy for the 0 hr control whereby primed NK cells were added to the PC3 cells just before acquisition on the flow cytometer. E to H) Represent the gating strategy for the cytotoxic tube whereby primed NK cells were co-incubated with PC3 cells for 2.5 hrs.

Cytotoxic killing was analysed on single cells following the removal of doublets. As shown in the control (Figure 4.17C), live PBMCs (effector cells) and live K562 cells (target cells) are gated in the bottom left and right gates respectively. Both populations were negative for propidium iodide staining, with only the K562 cells positive for Mitotracker® Green. The dead PBMCs and K562 cells are gated in the top left and right gates respectively. Both populations were positive

for propidium iodide, with the few dead K562 cells also being positive for Mitotracker® Green. As shown in Figure 4.14G, there was an increase in the percentage of dead K562 in the top right hand gate following co-incubation of PBMCs with K562 cells for 3.5 hrs. K562 cell death not only resulted in an increase in propidium iodide fluorescence, but also a decrease in the fluorescence of Mitotracker® Green. Interestingly there was a subsequent increase in PBMCs that were weakly fluorescent for Mitotracker® Green (Figures 4.17C, D, G and H). Although the

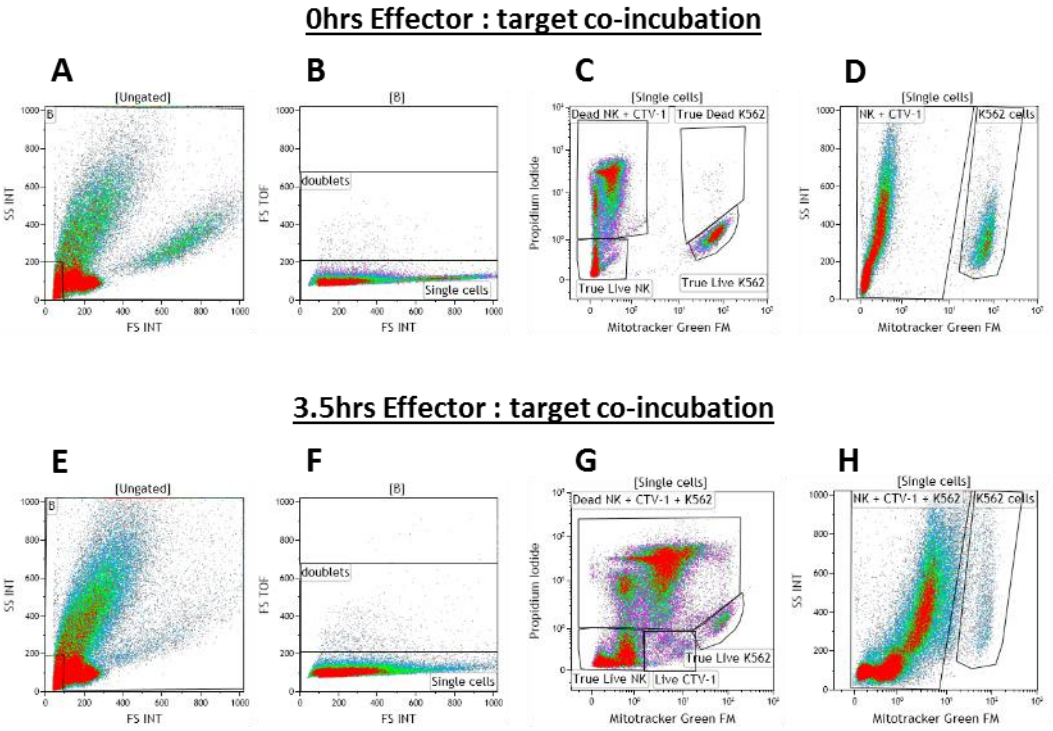

Figure 4.19: Gating strategy for the flow cytometry based NK cell cytotoxic assay when targeting primed NK cells against K562 target cells.
Primed NK cells were targeted against PC3 cells stained with Mitotracker® Green FM. Propidium Iodide was used to measure cell death. A to D) Represent the gating strategy for the 0 hr control whereby primed NK cells were added to the K562 cells just before acquisition on the flow cytometer. E to H) Represent the gating strategy for the cytotoxic tube whereby primed NK cells were co-incubated with K562 cells for 3.5 hrs.

cytotoxicity assay was set up in the same way when measuring the capacity of non-primed and primed NK cells to kill PC3 cells (Figure 4.18) and K562 cells (Figure 4.19), live and dead CTV-1 cells were also present when using primed NK cells as effectors cells. The effector : target cell ratio was kept at 5:1, with the proportion of effector cells being based on the number of live NK cells. The CTV-1 cells, whether live or dead, increased their Mitotracker® Green fluorescence following co-incubation with either PC3 or K562 targets cells in the cytotoxic tubes (Figure 4.18F and Figure 4.19G respectively) compared to control tubes (Figure 4.18C, Figure 4.19C). The magnitude of the increase in Mitotracker® Green fluorescence was dependent on the extent of target cell death. When targeting primed NK cells against K562 cells, a proportion of dead CTV-1 cells and a proportion of dead K562 cells exhibited similar propidium iodide and Mitotracker®

Green fluorescence, as a consequence of which the two populations overlapped on the density plot (Figure 4.19G).

Calculating the capacity of primed NK cells to kill PC3 cells and K562 cells required adjustments to the method of calculating percentage of target cell lysis. When initially optimising the flow cytometry cytotoxic method for resting PBMCs or isolated NK cells against K562 cells, calculation method 1 was used and compared to calculation method 2 (calculation method described in section 2.5.4.2). Due to the presence of CTV-1 cells complicating the analysis when using primed NK cells, calculation method 3 (section 2.5.4.2) was used. In order to ensure that all three calculation methods were accurately calculating K562 lysis, all 3 approaches were used to calculate the percentage of K562 cell lysis when PBMCs isolated from 3 healthy volunteers were used as effector cells for optimisation and validation of the flow cytometry cytotoxic method. The K562 cell lysis values for all 3 calculation methods are compared in Figure 4.20, the calculated values for which were comparable.

4.3.2.1 Comparison of the flow cytometry and ^{51}chromium Release cytotoxicity assays.

The cytotoxicity of PBMCs isolated from the peripheral blood of 3 healthy volunteers (healthy 1, healthy 2 and healthy 5) against K562 cells was determined using both the flow cytometry and ^{51}chromium release assays, and the results compared. The results between the assays using PBMCs from healthy volunteers 1 and healthy 5 were comparable and the percentage of total lysed K562 cells did not differ by greater than 10 %. However, for healthy volunteer 2, the percentage of total lysed K562 cells from the flow cytometry based cytotoxic assay was greater than 10 % compared to the results from the ^{51}chromium release assay at both 50 : 1 and 25 : 1 effector : target ratio (Figure 4.21).

4.3.2.2 Optimising the co-incubation period of primed NK effector cells and PC3 target cells for the flow cytometry-based cytotoxicity assay.

NK cells were primed at the 1 : 2 (NK : CTV-1) ratio and incubated with PC3 cells at an effector : target ratio of 5 : 1 for different lengths of time (i.e. 1 hr, 2 hrs, 3 hrs and 4 hrs). The aim was to identify optimal co-incubation time for measuring target cell lysis. Previous studies had utilised a co-incubation time of 3.5 hrs. As shown in Figure 4.22, the highest percentage of PC3 lysis recorded for primed NK cells using samples obtained from healthy volunteers 1 and 2 were 39 % and 42 % measured following 3 hrs and 2 hrs co-incubation respectively. The assay was repeated for volunteer healthy 2 and the optimal length of time of co-incubation was 4 hrs, with the

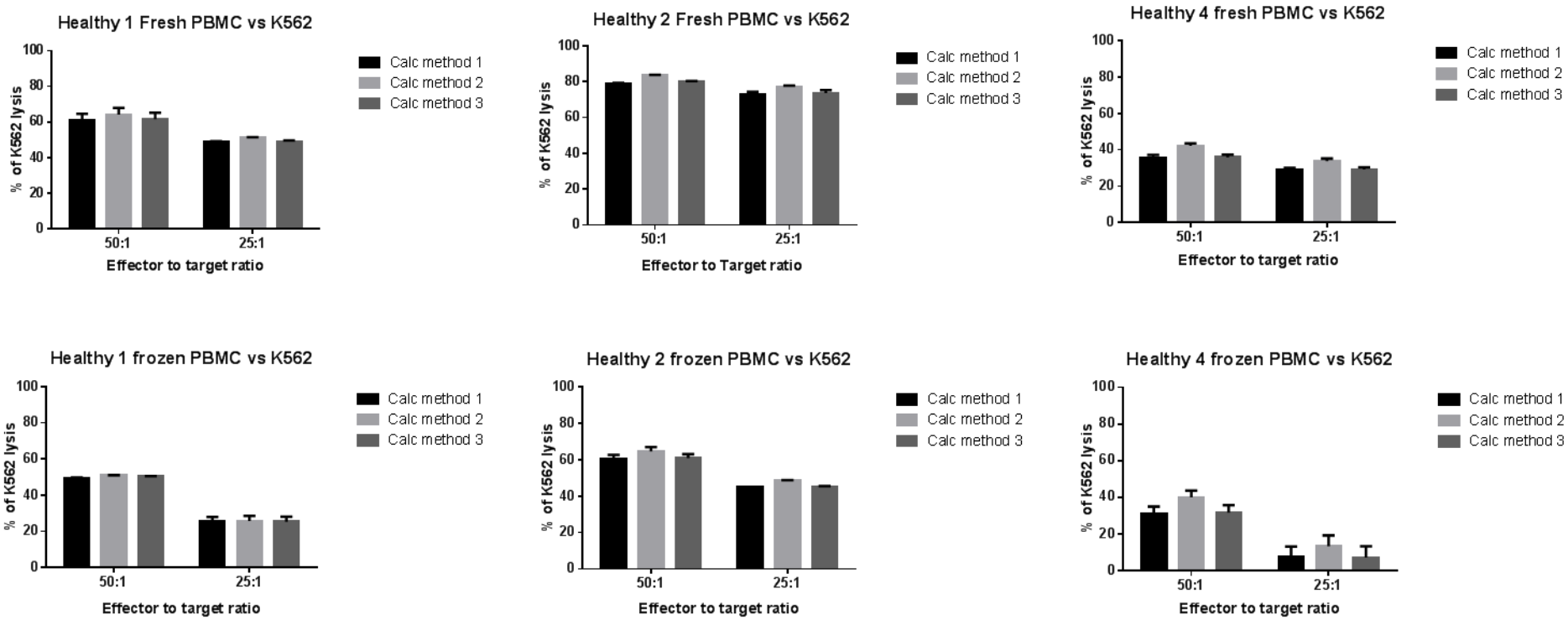

Figure 4.20: Comparison of the cytotoxicity results using the three different calculation methods when targeting fresh and frozen PBMC against K562 using the flow cytometry based cytotoxic assay.

The cytotoxic ability of PBMCs isolated from three healthy volunteers to lyse K562 targets was measured by the flow cytometry based cytotoxicity assay. The cytotoxic killing by fresh PBMCs (top row of graphs) was compared to the cytotoxic killing by thawed PBMCs (bottom row of graphs) in order to observe whether the freeze-thaw process compromises the cytotoxic capacity of the NK cells within the PBMCs. For each experiment, the percentage of lysed K562 was calculated using the three different calculation methods developed in order to consistency between the three methods. Data are presented as the means ± SD from two experiments.

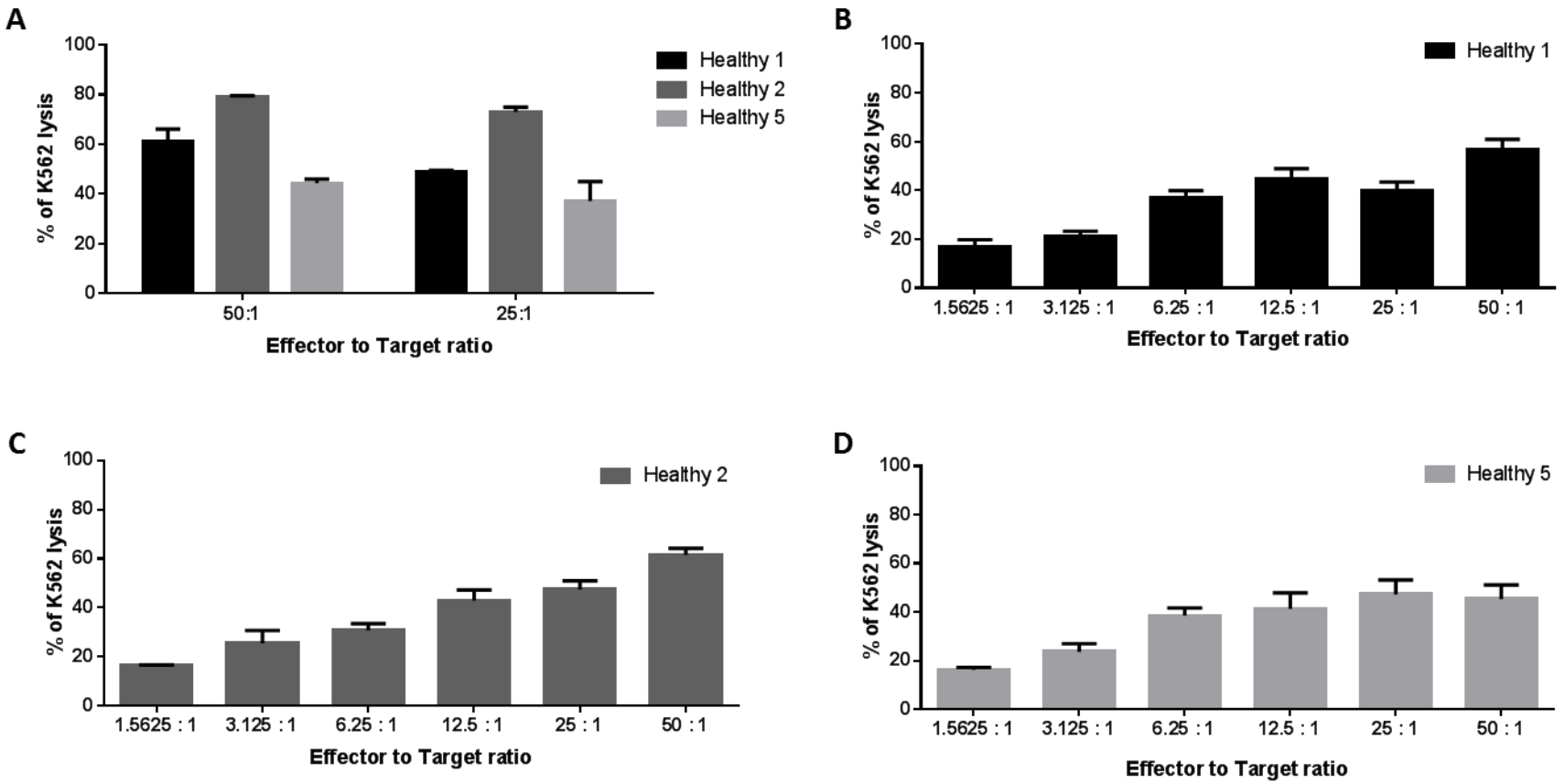

Figure 4.21: Comparing the cytotoxic killing results of the flow cytometry based cytotoxic assay with the standard ^{51}chromium release assay.
PBMCs were isolated from three healthy volunteers and targeted against K562 using both the flow cytometry based cytotoxic assay and the ^{51}chromium release assay in order to establish how comparable the cytotoxic killing results are between the two assays. A) The cytotoxic killing results for all three healthy volunteers, as measured by the flow cytometry based cytotoxic assay. B to D) The cytotoxic killing results for each healthy volunteer, as measured by the ^{51}chromium release assay.

maximum percentage of target cell lysis being 44 %. In all of the assays, the total percentage of target cell lysis measured at 2 hrs, 3 hrs and 4 hrs ranged within 10 % and a near maximal level of target cell lysis had been achieved between 2 hrs and 3 hrs co-incubation. For volunteer healthy 1, when the effector cells and target cells were co-incubated for 4 hrs (optimal length of time was 3 hrs) there was 10 % less target cell lysis recorded. It was concluded that the optimal length of time for co-incubation of effector cells with target cells was potentially specific to each person, or even assay, but appeared to be between 2 hrs and 3 hrs, and beyond which there was an increased chance of measuring decreased levels of target cell lysis. The co-incubation time for primed NK cells with PC3 cells was therefore set at 2.5 hrs for the remainder of the assays.

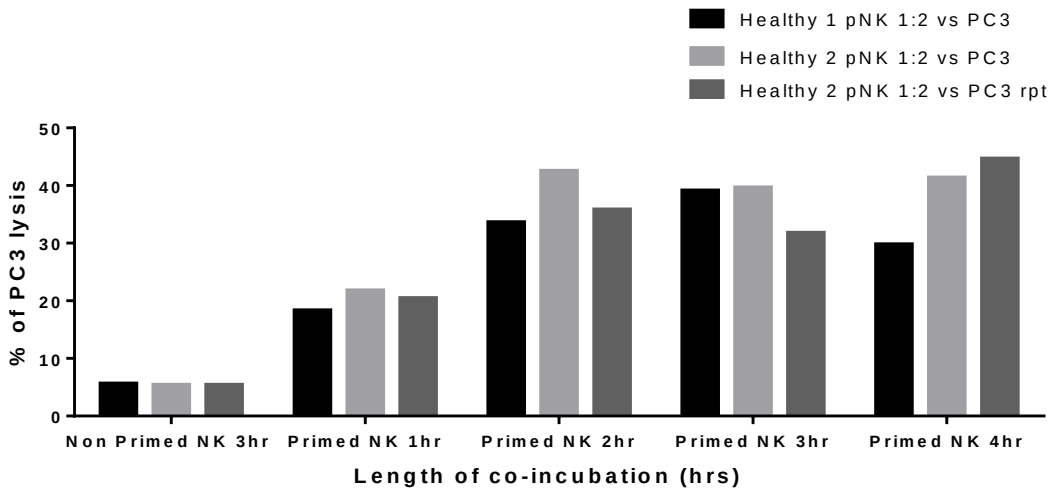

Figure 4.22: Measuring the percentage of PC3 lysis by primed NK cells over the course of 4 hrs using the flow cytometry based cytotoxic assay.
NK cells were isolated from two healthy individuals and primed with CTV-1 cells for 17 hrs. Using the flow cytometry based cytotoxic assay, the ability of primed NK cells to lyse PC3 targets was measured every hour over the course of 4 hours. The percentage of non-primed NK cells to lyse PC3 cells after 3 hours was used as a control.

4.3.2.3 Determining the optimal NK : CTV-1 priming ratio for measuring PC3 cell killing by primed NK cells.

Having established the optimised conditions for the flow cytometry-based cytotoxic assay, this assay was used to assess the optimal conditions for priming the NK cells that were to be used in the cytotoxicity assays. Additional cytotoxic assays using K562 cells as targets were set up in order to measure the ability of primed NK cells to kill K562 cells. The optimised length of time for co-incubation was 2.5 hrs. The percentage of target cell lysis measured at each ratio is an average of cytotoxic killing performed in duplicate.

As shown in Figure 4.23, the percentage of lysed PC3 cells killed by non-primed NK cells averaged between 3 and 10 %. Priming, even at the lowest NK : CTV- 1 ratio, increased the ability of

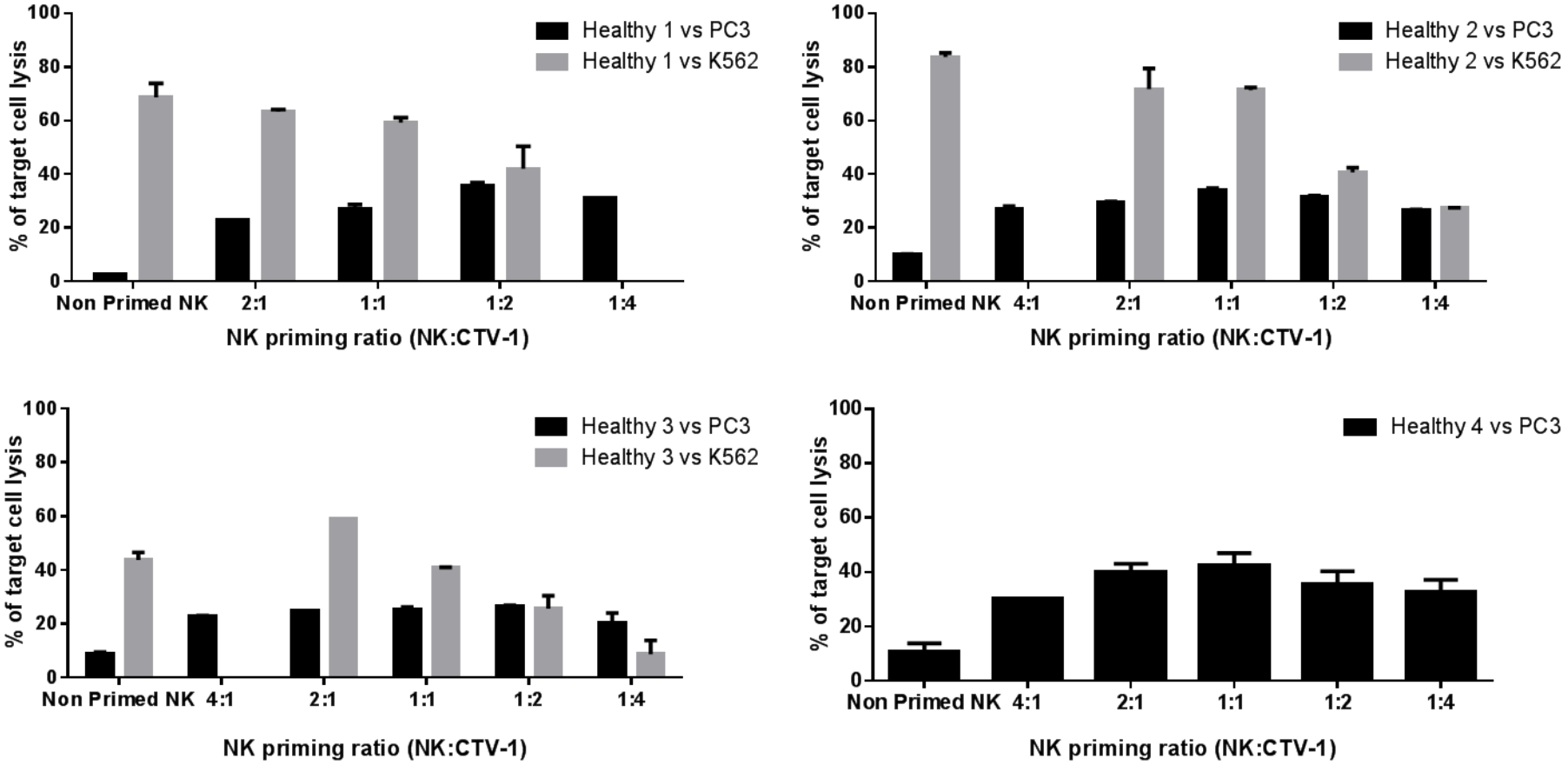

Figure 4.23: Comparing the ability of healthy non-primed and primed NK cells to kill PC3 cells at different effector : target ratios.
The ability of non-primed and primed NK cells (following co-incubation with CTV-1 cells at different NK :CTV-1 ratios) to kill PC3 and K562 cells was measured using the flow cytometry based cytotoxic assay. Cytotoxic tubes were set up whereby non-primed or primed NK cells were co-incubated with target cells for 2.5 hrs at a 5 : 1 effector : target ratio. For each priming ratio (including the non-primed control) control tubes were set up that co-incubated effector and target cells immediately prior to acquisition on the flow cytometer in order to measure spontaneous target cell death. Each cytotoxic tube and control tube was measured in duplicate. The above results displaying the mean percentage of target cell lysis with the bars representing the SD.

NK cells to kill PC3 cells, and the percentage of lysed PC3 cells ranged between 23 and 30 % across the individuals that were examined. The maximum average percentage of PC3 lysis by primed NK cells for the 4 volunteers ranged between 27 and 42 %. This peak level of PC3 killing was achieved at the 1 : 1 and 1 : 2 (NK : CTV-1) priming ratios and was person-specific. Interestingly, the cytotoxic activity of primed NK cells progressively decreased at NK cell priming ratios greater than the optimal ratio.

For 3 of the healthy volunteers i.e. healthy 1, 2 and 3, the ability of the primed NK cells to lyse K562 cells was also measured. The average percentage of K562 lysis by non-primed NK cells for the healthy volunteers 1, 2 and 3 were 69, 84 and 44 % respectively. For healthy volunteers 1 and 2, priming decreased the ability of the NK cells to kill K562 cells. At the 2 : 1 (NK : CTV-1) ratio, the percentage of K563 lysis decreased to 63 % and 72 % respectively. At the lowest NK cell priming ratio measured, the percentage of K562 lysis for healthy volunteers 1 and 2 was 42% and 27%. Healthy volunteer 3 followed a similar pattern, with the exception that at the 2 : 1 (NK : CTV-1) priming ratio, where the percentage of K562 lysis had risen from 44 % to 59 % and then decreased to 9 % at the lowest NK priming ratio. However, it should be noted that the K562 lysis result for the 2 : 1 (NK : CTV-1) NK priming was calculated from a single measurement due to an insufficient number of primed NK cells being available for use in experimental replicates (Figure 4.23).

4.3.2.4 Correlation between K562 cell lysis and the expression of NKG2D and NKp46

In an attempt to explain why priming NK cells decreased their ability to lyse K562, the cytotoxic capacity of primed NK cells against K562 cells was correlated with their expression of NKG2D and NKp46. As shown in Figure 4.24, cytotoxic potential significantly correlated with the expression of these receptors. NKG2D correlated with the percentage of K562 lysis (P=0.0015) with a Spearman rank correlation coefficient of 0.7802. NKp46 also significantly correlated with the percentage of K562 lysis (P=0.0153), but had a slightly lower Spearman rank correlation coefficient of 0.6425.

4.3.3. Optimisation of the CD107a degranulation assay

4.3.3.1 Optimising the amount of GolgiStop (containing monensin) needed.

The published literature reports that monensin is required to prevent re-internalisation of CD107a following expression on the T cell and NK cell surface at the point of degranulation (Alter et al., 2004, Betts et al., 2003). In order to determine how much GolgiStop (containing monensin) to add when co-incubating non-primed and primed effector cells and target cells at a 5 : 1 effector to target cell ratio, non-primed NK cells were co-incubated with K562 plus CD107a antibody in the presence of 1 µl, 2 µl, 3 µl or 4 µl of GolgiStop (buffer alone as control) following

an initial 1 hr effector : target co-incubation. Effector and target cells were then co-incubated for a further 3 hrs. Following co-incubation, NK cells were washed and stained for their expression of CD3, CD19, CD56 and CD16 in conjunction with Live / Dead viability stain. The cells were then analysed by flow cytometry.

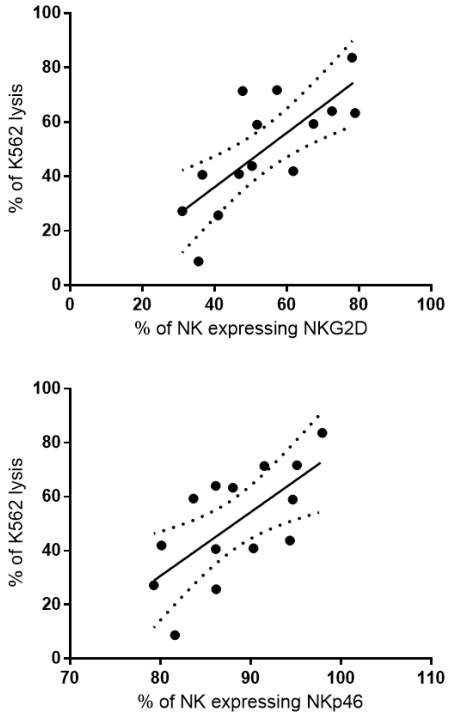

Figure 4.24: Correlation between the percentage of K562 lysis and percentage of NK cells expressing NKG2D and NKp46.
For each healthy volunteer, the percentage of K562 that were lysed by non-primed and primed NK cells was measured by the flow cytometry based cytotoxic assay. In a separate experiment the phenotype of each healthy volunteers non-primed and primed NK cells were measured. For both sets of experiments NK cells were primed in the same experimental conditions for 17 hrs. Significant positive correlations between the percentage of K562 lysis and the percentage of NK cells expressing NKG2D (top graph, spearman rank coefficient = 0.780, P = 0.0015) or NKp46 (bottom graph, Spearman rank coefficient = 0.643, P = 0.0153) on the primed and non-primed NK cells were found.

As shown in Figure 4.25A and Figure 4.26, the highest up-regulation of CD107a, both in terms of the percentage of NK cells expressing CD107a (17 %) and its intensity of expression (MFI, 120) was observed in the absence of GolgiStop. This expression profile reduced to 8 % of positive cells with an MFI of 102 in the presence of 1 µl of GolgiStop. The level of CD107a expression progressively decreased as the concentration of GolgiStop increased. Cytotoxic tubes measuring the effect of the GolgiStop on the percentage of K562 lysis were setup in parallel with CD107a degranulation tubes (Figure 4.25 B). The highest percentage of K562 lysis was 47 % when no GolgiStop was added to the tubes. Upon the addition of 1 µl of GolgiStop the percentage of K562 lysis decreased to 21 %. However, further addition of GolgiStop increased the percentage of

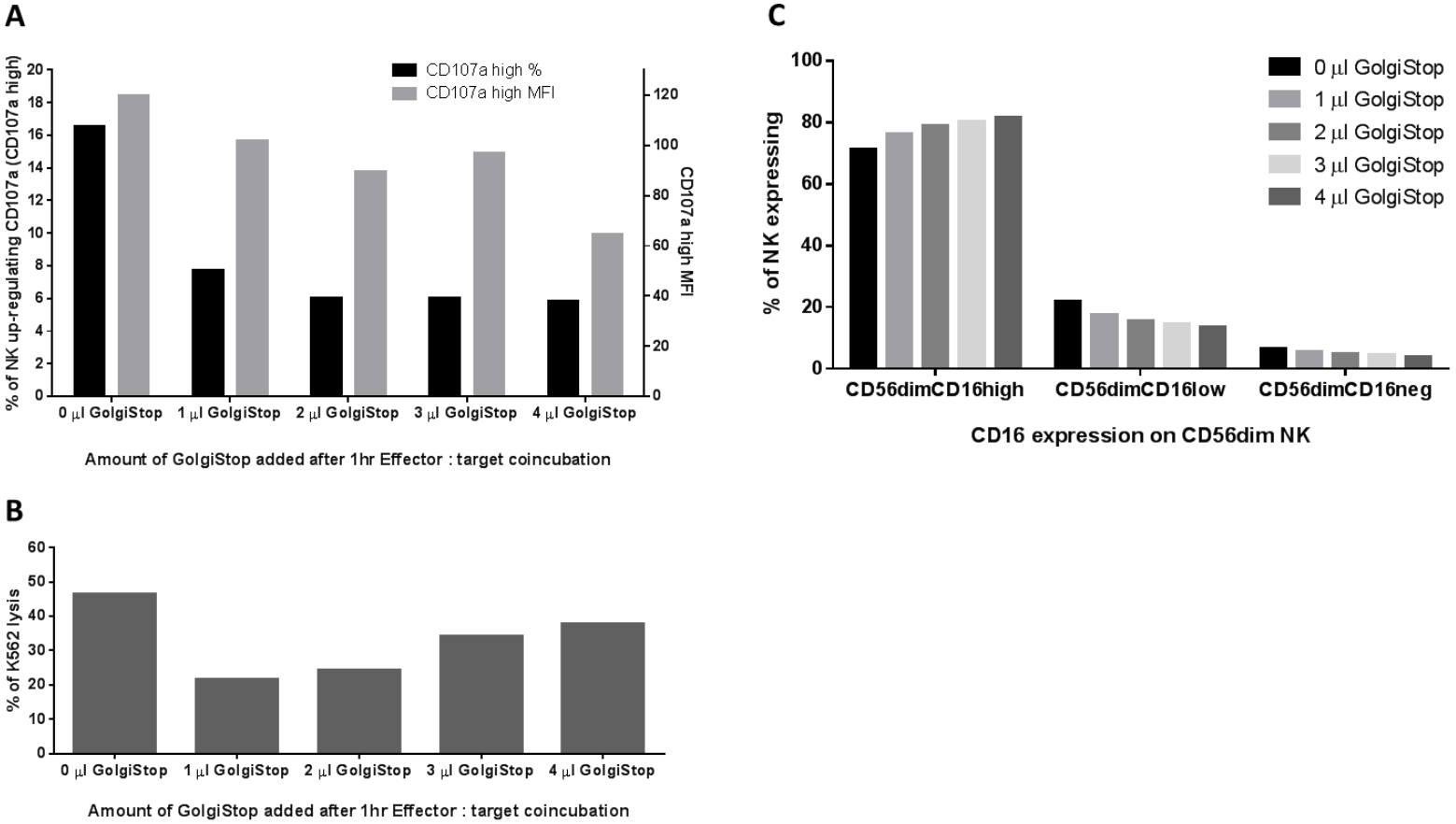

Figure 4.25: Determining the effects of GolgiStop on CD107a expression, the percentage of K562 lysis and proportion of NK cell subpopulations when used in a CD107a degranulation assay.

The amount of GolgiStop to be added to the co-incubation of effector and target cells in a CD107a degranulation assay was assessed. Resting NK cells were co-incubated with K562 cells at a 5 : 1 effector : target ratio. Following a 1 hr co-incubation, 1 to 4 µl of GolgiStop was added to the tubes as appropriate and the cells co-incubated for a further 3 hrs. No addition of GolgiStop was used as the negative control. The effect of GolgiStop on the expression of CD107a on NK cells (A), the percentage of K562 lysis by NK cells (B) and the percentage of NK cells that were $CD56^{dim}CD16^{high}$, $CD56^{dim}CD^{low}$ and $CD56^{dim}CD16^{neg}$ as a result of shedding CD16 (C) was determined.

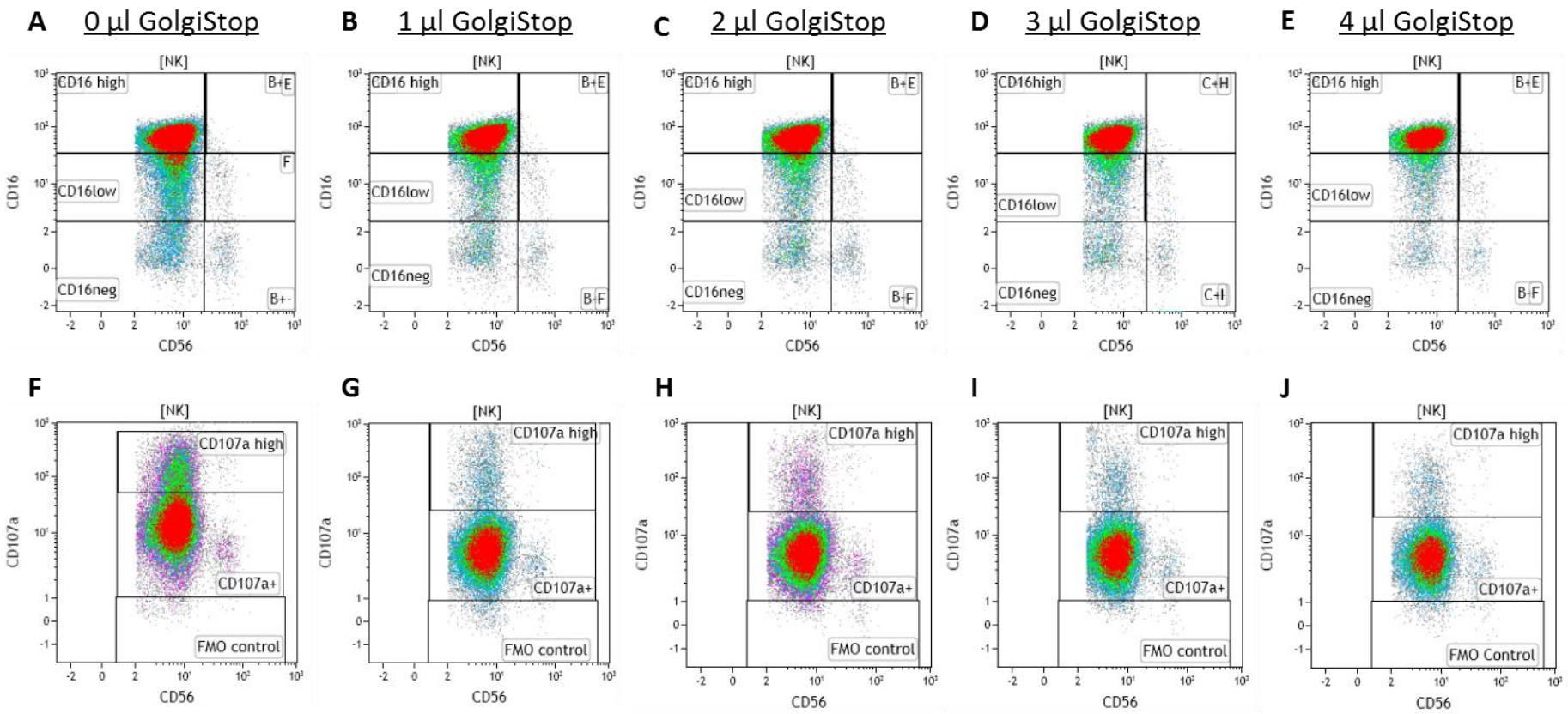

Figure 4.26: A graphical representation of the proportion of NK cells expressing CD56, CD16 and CD107a following exposure to different amounts of GolgiStop during a CD107a degranulation assay.

The amount of GolgiStop to be added to the co-incubation of effector and target cells in a CD107a degranulation assay was assessed. Resting NK cells were co-incubated with K562 cells at a 5 : 1 effector : target ratio. Following a 1 hr co-incubation, GolgiStop was added to the tubes the cells co-incubated for a further 3 hrs. No addition of GolgiStop was used as the negative control. The top row of density plots display a graphical representation of the proportions of the $CD56^{dim}CD16^{high}$, $CD56^{dim}CD^{low}$ and $CD56^{dim}CD16^{neg}$ NK subpopulations. The bottom row of density plots display a graphical representation of the expression of CD107a expressed on the NK cells. The proportion of NK cell subpopulations and the expression of CD107a are shown for NK cells treated with 0 µl (plots A and F), 1 µl (plots B and G), 2 µl (plots C and H), 3 µl (plots D and I) and 4 µl (plots E and J) of GolgiStop.

K562 lysis to a value of 38 % when 4 µl of GolgiStop was added.

The influence of GolgiStop on the expression of CD16 on $CD56^{dim}$ NK cells was also measured. GolgiStop increased the percentage of NK cells that were $CD56^{dim}CD16^{high}$, whilst decreasing the percentage of NK that were $CD56^{dim}CD16^{low}$ and $CD56^{dim}CD16^{neg}$ (Figure 4.25 C and Figure 4.26). These findings indicate that GolgiStop should not be used when performing CD107a degranulation assays.

4.3.3.2 Optimising CD107a expression analysis.

Two different methods for performing a CD107a degranulation assay have been described in the literature. One method involves adding monoclonal antibodies against CD107a at the point of effector : target cell co-incubation, followed by the addition of GolgiStop 1 hr later and an additional 3 hr incubation (Alter 2004). The second method involves co-incubating effector : target cells for 2 hrs in the absence of GolgiStop or monensin, with NK cells being stained for CD107a after the co-incubation. To determine when best to add CD107a, parallel tubes were set up:

- CD107a antibody was added at the point of co-incubation
- CD107a antibody was added after the co-incubation

No GolgiStop was added to either tube.

Following co-incubation, the NK cells were washed and stained with NK cell defining antibodies (i.e. CD3, CD19, CD56 and CD16) and Live / Dead viability dye and were then analysed by flow cytometry. Additionally, in order to determine the optimal length of time of effector to target co-incubation, 5 sets of tubes were setup and left to co-incubate for either 0 hr, 1 hr, 2 hrs, 3 hrs or 4 hrs. An FMO tube was also set up, in which NK cells were not stained with CD107a antibody in order to determine where the CD107a negative NK population would be on the density plot. As shown in Figure 4.27, the staining for the CD107a negative NK cells was just above the 10^0 log, with the expression of CD107a on NK cells being above that of the CD107a negative NK cells. Co-incubation of K562 target cells with the NK cells, even for just 1 hr, increased the proportion of NK cells expressing CD107a (termed $CD107a^{high}$). Increasing the co-incubation period progressively increased the proportion of CD107a cells. Interestingly, if the CD107a antibody was added at the start of the effector : target co-incubation, then the entire NK cell population expressed CD107a, with a sub-population expressing $CD107a^{high}$. In the equivalent tubes where the NK cells were stained with CD107a after co-incubation, the main NK population did not increase their expression of CD107a. In this instance, the NK cells that had up-regulated CD107a expressed the receptor at a higher intensity. The proportion of NK cells that had up-regulated

CD107a peaked at 3 hrs co-incubation at 20 %. It should be noted that at 2 hrs co-incubation, 19 % of NK cells had up-regulated CD107a expression, but after 4 hrs only 14 % of NK cells had upregulated their expression of CD107a.

4.3.3.3 Optimising the co-incubation period between primed NK cells and PC3 target cells

Non-primed NK cells or primed NK cells were co-incubated with PC3 cells for different lengths of time i.e. 0 hr, 1 hr, 2 hrs, 3 hrs or 4 hrs, after which the NK cells were stained for CD107a, as described in section 4.3.1.5.2. Surprisingly, 13 % of primed NK cells already had up-regulated CD107a before encountering PC3 target cells (MFI value of 9). In comparison, CD107a was not upregulated on non-primed NK cells prior to contact with PC3 cells. Although only 11 % of primed NK cells expressed CD107a following co-incubation with PC3 cells for 1 hr, they had increased their intensity of expression to an MFI value of 20. The percentage of NK cells with up-regulated CD107a had decreased to 10 % and their intensity of expression had reduced to an MFI of 10 after 2 hrs. After 4 hrs, only 7 % of primed NK cells had up-regulation of CD107a with an MFI value 8 (Figure 4.28).

4.3.3.4 Analysis of CD107a up-regulation on $CD56^{dim}CD16$ subpopulations

The analysis of up-regulated CD107a expression on $CD56^{dim}CD16^{high}$, $CD56^{dim}CD16^{low}$ and $CD56^{dim}CD16^{neg}$ NK cell subpopulations revealed that the $CD56^{dim}CD16^{neg}$ subpopulation contained the greatest proportion of NK cells that had up-regulated CD107a (29%), followed by the $CD56^{dim}CD16^{low}$ subpopulation (22%), whereas the proportion of $CD56^{dim}CD16^{high}$ NK cells expressing CD107a was 6 %. However, considering the number of NK cells in the analysis, numerically the $CD56^{dim}CD16^{low}$ NK cells made up the majority of NK cells that up-regulated CD107a (Figure 4.29).

4.3.3.5 Analysis of primed NK cells up-regulating CD107a, CRTAM and CD137

The antibody panels for the CD107a degranulation assay had been designed so that additional NK cell-specific antibodies could be added to the antibody staining panel in order to allow the co-expression of CD137 and CRTAM on CD107a positive NK cell subpopulations to be determined. As shown in Figure 4.30 (a single experiment), only 3% of the 20% of primed NK cells that had up-regulated CRTAM expressed CD107a. The majority of primed NK cells that had up-regulated CD107a were therefore negative for CRTAM. A similar pattern was seen for the co-expression of CD107a and CD137. Out of the 10 % of NK cells that up-regulated CD137, only 2 % had up-regulated CD107a. Again the majority of primed NK cells that had up-regulated CD107a were CD137 negative (Figure 4.30). The majority of primed NK cells that up-regulated CD107a were therefore negative for CRTAM and CD137 (Figure 4.31)

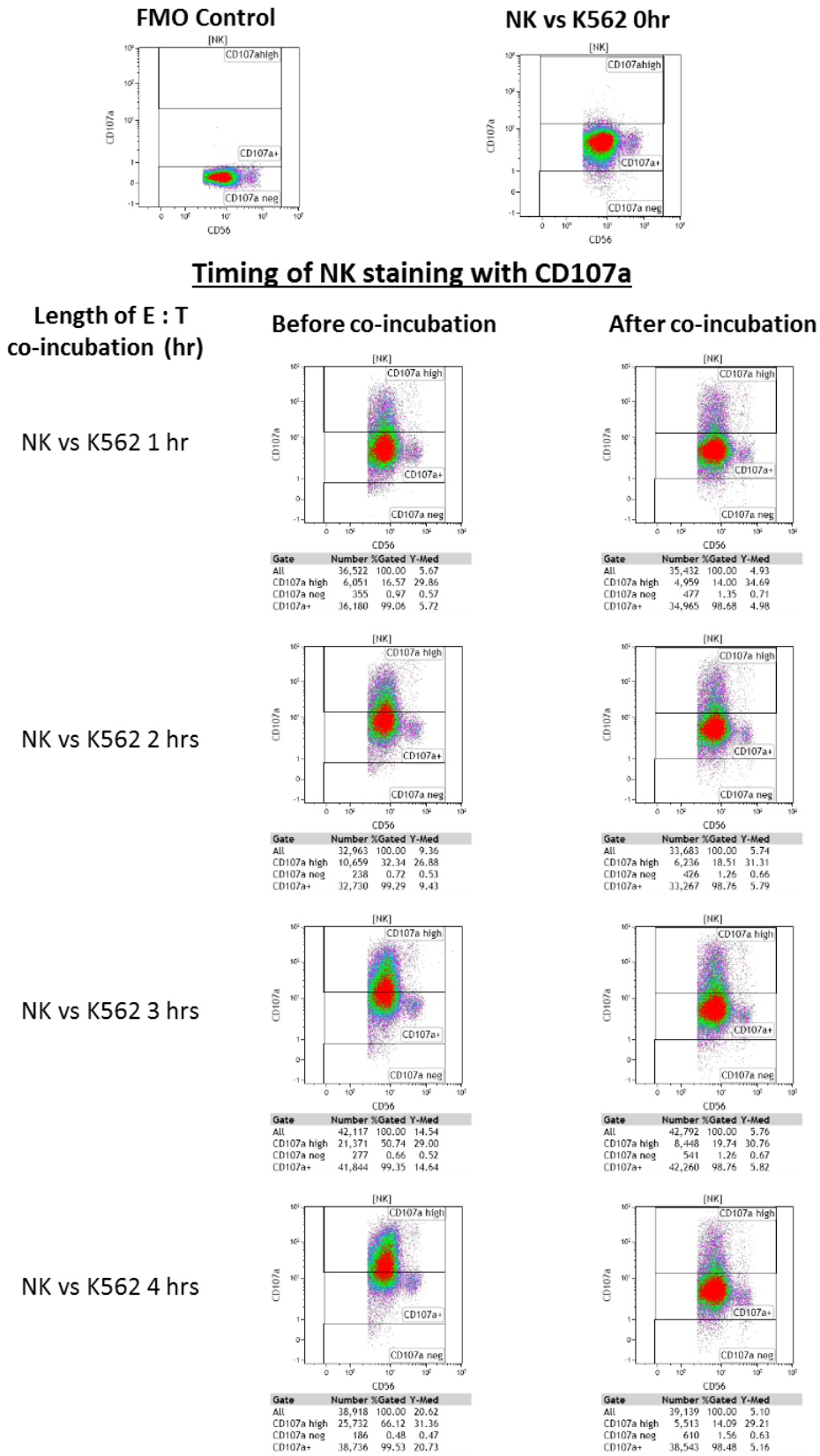

Figure 4.27: Graphical representation of the difference in expression of CD107a when staining NK cells with the CD107a antibody at the start of the effector : target co-incubation or following co-incubation in a CD107a degranulation assay.

Resting NK cells were co-incubated with K562 cells at a 5 : 1 effector : target ratio and the expression of CD107a on NK cells measured over the course of 4 hrs by flow cytometry. The density plots above compares CD107a staining on NK cells when the antibody was added at the start or after effector : target co-incubation. CD107a expression on NK cells prior to exposure to target cells (0 hr) and in absence of the CD107a antibody (FMO) were used as negative controls.

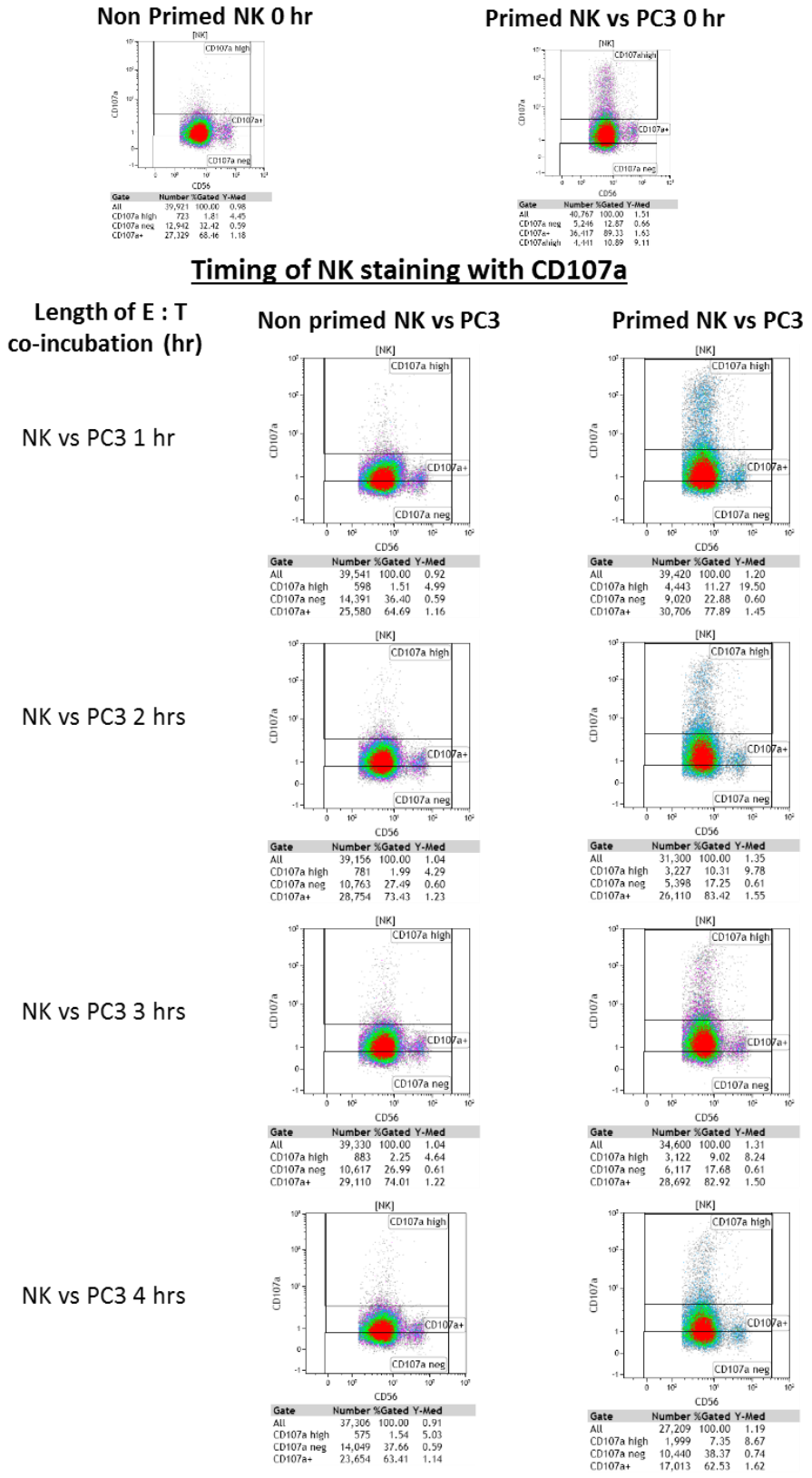

Figure 4.28: Graphical representation of expression of CD107a expressed on non-primed NK cells and primed NK cells targeted against PC3 cells over the course of 4 hrs in a CD107a degranulation assay.

Non-primed or primed NK cells were co-incubated with PC3 target cells for up to 4 hrs at a 5 : 1 effector : target cell ratio. No mitomycin C was added. Following co-incubation NK cells were then stained for their CD107a expression using a CD107a antibody and measured by flow cytometry. Non-primed and primed NK cells that were not co-incubated with PC3 targets were used as controls.

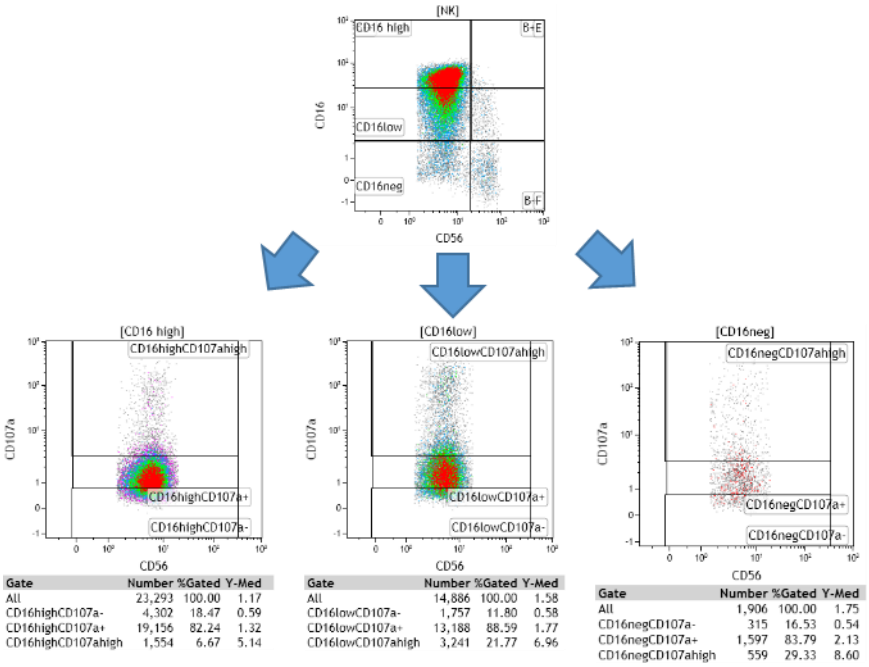

Figure 4.29: Graphical representation of the analysis of CD107a expression on primed CD56^{dim}CD16^{high}, CD56^{dim}CD16^{low}, CD56^{dim}CD16^{neg} NK subpopulations following exposure to PC3 cells.

Primed NK cells were targeted against PC3 cells at a 5 : 1 effector : target cell ratio in a CD107a degranulation assay. The primed NK cells were then analysed as a live, single cell NK cell population which was then gated into CD56^{dim}CD16^{high}, CD56^{dim}CD16^{low} and CD56^{dim}CD16^{neg} subpopulations. The NK cell subpopulations were then analysed for their CD107a expression.

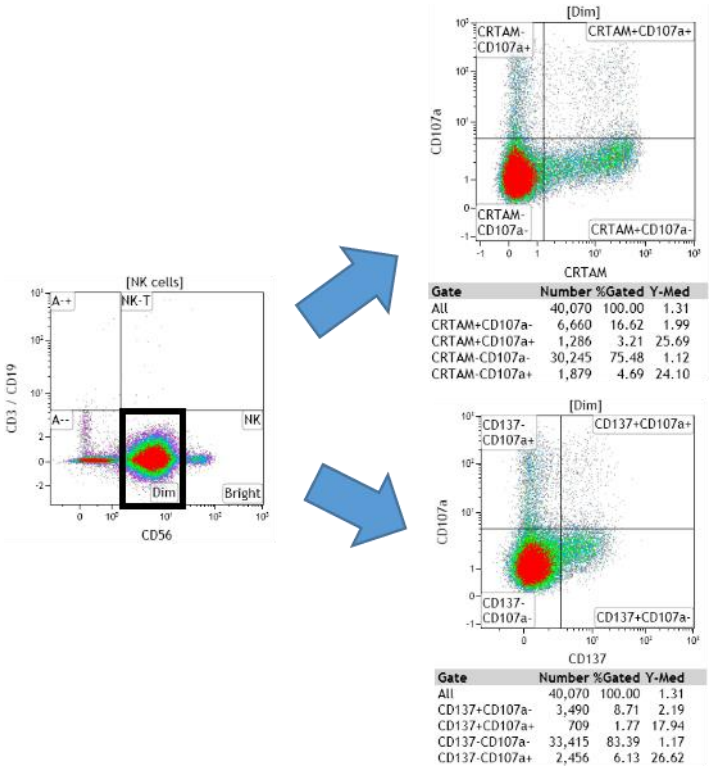

Figure 4.30: Graphical representation of the analysis of CD107a, CRTAM co-expression and CD107a, CD137 co-expression on primed NK cells following exposure to PC3 cells.

Primed NK cells were targeted against PC3 cells at a 5 : 1 effector : target cell ratio in a CD107a degranulation assay. The primed NK cells were analysed as a live, single NK cell population which was subsequently gated into four subpopulations based on either their level of CD107a and CRTAM co-expression (top right density plot) or their level of CD107a and CD137 co-expression (bottom right density plot).

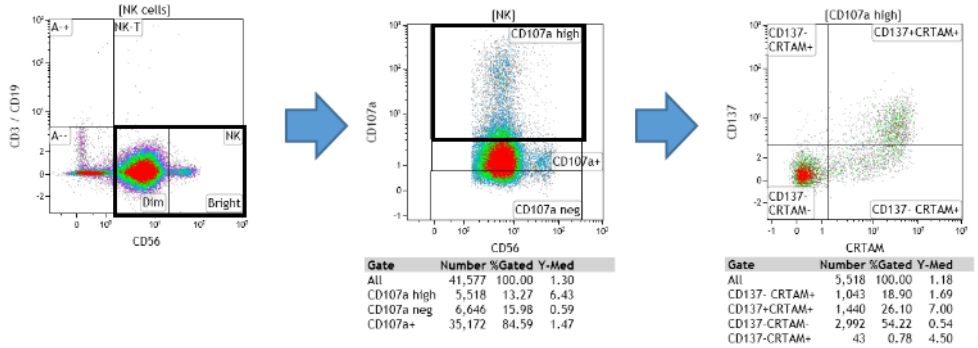

Figure 4.31: Graphical representation of the co-expression of CRTAM and CD137 on CD107a^{high} positive primed NK cells following exposure to PC3 cells.
Primed NK cells were targeted against PC3 cells at a 5 : 1 effector : target cell ratio in a CD107a degranulation assay. The primed NK cells were analysed as live, single cell NK cells. Cells that were CD107a^{high} were further sub-gated to analyse the co-expression of CD137 and CRTAM on primed NK cells following exposure to PC3 cells.

.

4.4 Discussion

The aim of this part of the study was to develop and optimise assays which could be used to accurately measure the function of NK cells from patients with prostate cancer in order to observe whether there are differences in NK function between patients with different grades of prostate cancer and also between patients with prostate cancer compared to benign patients.

Relatively recently, Mark Lowdell's group at University College London identified a new mechanism for the activation (termed 'priming') of NK cells. They reported that the co-incubation of fresh resting NK cells with irradiated CTV-1 cells (a T cell leukaemic cell line) induced an upregulation of CD25 and CD69 expression on the NK cells, and significantly increased their cytotoxic capacity against NK cell-resistant cell lines such as DU145 cells (metastatic prostate cancer cell line) (North et al., 2007, Sabry et al., 2011). Interestingly, despite CTV-1 cells being able to prime NK cells, they were resistant to NK cell killing themselves. This led to the hypothesis that the mechanism of cytotoxic killing could be split into two stages; 'priming' and 'triggering'. 'Priming' involves transduction of activating signals via cytokines or a combination of signals. 'Triggering' involves the engagement of at least one additional activating receptor that specifically recognises stressed cells and therefore only cancerous or virally infected cells are killed, leaving healthy cells alive (Sabry and Lowdell, 2013). The early activation receptor CD69 was postulated to serve as one of the triggering receptors, as blocking this receptor significantly decreased the lysis of Raji cells by primed NK cells. However, experiments targeting acute myeloid leukaemia (AML) cells using primed NK cells suggested that CD69 was not the only triggering signal, and that additional triggering signals that are delivered via

interactions with additional receptors was required in order to induce killing of some primary AML samples (North et al., 2007).

Given the importance of NK cell-mediated immunosurveillance in the protection against cancer, it might be that the ability of NK cells in patients with cancer to be primed, and therefore their ability to kill solid tumours is compromised. In order to test this hypothesis, it was essential to better characterise the 'priming' process in the context of the phenotypic changes that are induced, and establish its influence on NK cell functional capacity by optimising and developing NK cell cytotoxicity assays.

Mitomycin C treated CTV-1 cells were able to prime thawed NK cells in a similar way to that which has been reported. The optimal NK : CTV-1 priming ratio, judged by both phenotype and function of the primed NK cells, appeared to be 1 : 1 or 1 : 2, although this was dependent on the donor. Priming up-regulated the expression of CD25 and CD69, although the expression of CD25 was about around 10 fold less then reported by Sabry et al (Sabry et al., 2011), whereas CD69 expression was greater than 2 fold higher. These differences could reflect that frozen-thawed PBMCs were used as the source of NK cells in the current study, whereas Sabry et al used freshly isolated NK cells (Sabry et al., 2011).

In addition to the up-regulation of CD25 and CD69, the expression of other co-stimulating receptors such as members of the TNF superfamily OX40, CD137, and GITR which are more commonly associated with expression on T cells was up-regulated by priming (Melero et al., 2013). Expression of the receptor CRTAM, a member of the same immunoglobulin receptor family as DNAM-1, was also up-regulated and is known to bind to NECL2 (nectin-like family member 2). The expression of OX40, CD137 and CRTAM peaked around the 1 : 1 and 1 : 2 NK : CTV-1 priming ratios, but was then reduced following priming using a 1 : 4 ratio. The extent of cytotoxic killing of PC3 cells by healthy primed NK cells was largely similar, ranging between 27 and 42 %. Peak cytotoxic killing of PC3 cells occurred following priming at NK : CTV-1 ratios 1 : 1 and 1 : 2 before decreasing at the 1 : 4 ratio. The reduced expression of co-stimulatory receptors and the reduction in cytotoxic function against PC3 cells at the 1 : 4 ratio compared to ratios 1 : 1 and 1 : 2 suggests that at the 1 : 4 ratio NK cells may have been stimulated beyond optimum and may have started to become 'exhausted'.

The up-regulation of the co-stimulatory receptors OX40, CD137, CRTAM and GITR following priming prompts the question – 'are these receptors triggering receptors?' Further investigation needs to be undertaken in order to answer this question. However, in a single experiment using the CD107a degranulation assay, the relationship between CRTAM and CD137 expression with up-regulated CD107a expression was investigated. Even though primed NK cells co-expressing

all three receptors were identified, the majority of NK cells on which CD107a expression had been upregulated did not express CRTAM and CD137, whereas a small percentage of NK cells up-regulating CD107a expressed CRTAM only. These results suggest that CRTAM and CD137 may not receive signals that ultimately trigger the cytotoxic response, but that they may receive signals that influence the NK functional response.

Although the analysis of cell phenotype can characterise the priming process, it is important to generate insight into the functional capacity (i.e. cytotoxic potential) of these cells. Cytotoxic killing is a primary readout for NK cell function and can be as measured on the basis of the direct lysis of target cells or indirectly via the expression of CD107a on the NK cell surface as an indicator of degranulation (Fregni et al., 2013, Mamessier et al., 2011b, Platonova et al., 2011, Tallerico et al., 2013). Historically, the ^{51}chromium release assay which directly measures the lysis of target cells has been used to measure NK cell cytotoxic function (Betts et al., 2003, Brunner et al., 1968), and derivatives of the assay now exist (Liu et al., 2002, Sheehy et al., 2001). However, a number of flow cytometry-based cytotoxicity assays have now been described as a cheaper, potentially more informative way of measuring NK cell cytotoxicity. They avoid complications of using and disposing of radioactive materials, and have the advantage that fluorescent dyes used to label target cells do not spontaneously leak out of the cell and contribute to a false positive signal, unlike the ^{51}chromium release assay (Hopkinson et al., 2007). Furthermore, these assays allow a more detailed interrogation of the cytotoxic process and insight into the phenotypes involved and the consequence of the cytotoxic process on the effector and target cell populations.

The standard target to use in cytotoxic assays is the K562 cell line, since it is deficient in MHC class I expression and therefore resistant to being killed by T cells. However, as shown by the experiments targeting non-primed NK cells against K562, NK cells isolated from different people are differentially capable of killing K562 cells. Although NK cells from healthy volunteer 2 killed 80 % of K562 in 3.5 hrs, NK cells from healthy volunteer 3 only killed ~ 40% of K562 cells under the same conditions. If using K562 cells as a targets for measuring the cytotoxic killing of NK cells from cancer patients, it would be difficult to determine whether a potentially low NK cell cytotoxic killing response is due to immunosuppression by the patients cancer or due to the patients naturally reduced ability to kill the K562 cell line compared to other individuals with a naturally high cytotoxic response against the same cell line.

The measurement of NK cell cytotoxicity against a cancer cell line that is NK cell-resistant requires NK cells to be stimulated with recombinant IL-2 prior to the cytotoxic assay (Nagler et al., 1989). This method has been commonly used to measure patient NK cell responses against different cancer cell lines (Fregni et al., 2013, Mamessier et al., 2011a, Platonova et al., 2011).

However, the addition of IL-2 to NK cells *in vitro* expands the $CD56^{bright}$ population to a much greater extent than the $CD56^{dim}$ population and therefore changes the ratio of the two NK subsets (Nagler et al., 1989). Furthermore, IL-2 stimulation increases the expression of activating receptors e.g. NKG2D, NKp46, NKp30, NKp44 on the NK cells (Hromadnikova et al., 2013, Markel et al., 2009). In the context of measuring patient NK cell cytotoxic responses against relevant NK-resistant cancer lines, IL-2 stimulation will dramatically alter the phenotype and ratio of the $CD56^{dim}$ and $CD56^{bright}$ subsets and the results obtained are unlikely to reflect their *in vivo* phenotype and function.

In the present study, the measurement of cytotoxic killing through direct lysis of target cells was performed using a modified version of a previously published method (Hopkinson et al., 2007). For this, target cells were labelled with Mitotracker® Green and cell death was measured by the uptake of propidium iodide. An additional tube was added per functional test to measure spontaneous death of target cells over the 3.5 hrs effector target co-incubation. For this, effector and target cells were kept apart for the 3.5 hr co-incubation and only added together, with propidium iodide, prior to running on the flow cytometer. Any cell death in this tube would represent background death of target cells and could be taken off the percentage of target cell death measured in the cytotoxic tube in which effector and target cells were co-incubated together. Interestingly, effector cells in the cytotoxic tube, despite not being stained with Mitotracker® Green, positively fluoresced for the dye after contact with the Mitotracker® Green stained target cells, whereas effector cells in the control tube remained negative for Mitotracker® Green. This suggests that Mitotracker® Green only leaks out of the target cell if the cell membrane becomes compromised.

Upon cytotoxic killing of target cells, NK cells are known to release granzyme B and perforin from lytic granules (Peters et al., 1991). Perforin has been shown to create tubular lesions in the plasma membrane of target cells (Liu et al., 1986). The tubular lesions could allow a small amount of Mitotracker® Green dye to leak out of the target cells and then absorbed by the NK cells. This would account for why NK cells / PBMC effector cells started to fluoresce slightly for the dye and why dying target cells began to lose fluorescence in our experiments.

Measuring the up-regulation of CD107a on the cell surface of NK cells is an alternative, indirect way of measuring NK cell cytotoxic killing, as the expression of CD107a on the cell surface indicates degranulation and release of granzyme B and perforin (Alter et al., 2004, Betts et al., 2003, Peters et al., 1991). Monensin has been reported to prevent the re-internalisation of CD107a from the cell surface after release of lytic granule contents (Alter et al., 2004, Betts et al., 2003). Experiments undertaken in the current study revealed that monensin did not improve cell surface expression of CD107a on the NK cell surface, rather it inhibited detectable levels of

expression. GolgiStop has been described by the manufacturer (BD Biosciences) as a protein transport inhibitor that blocks intracellular protein transport processes and, in doing so, results in the accumulation of cytokines and/or proteins in the Golgi complex. Lytic granules containing granzymes and perforin have been reported to bud off the trans Golgi reticulum in T cells, and a similar process is thought to occur in NK cells (Burkhardt et al., 1989, Peters et al., 1991). Following the CD107a degranulation method published by Alter et al (Alter et al., 2004), GolgiStop is not added to the effector target co-incubation until after 1 hr, thereby allowing early release of some lytic granules and expression of a small amount of CD107a on the cell surface. However, GolgiStop is likely to inhibit the transport and release of lytic granules, therefore preventing CD107a expression from being up-regulated on the cell surface and preventing NK cell killing of targets. Although GolgiStop increased target cell death, it did not induce CD107a expression. Given that monensin is known to be toxic to erythrocytes and since K562 cells are thought to be a erythroleukaemic cell line, it might be that monensin is toxic to K562 and caused the increase in K562 cell death (Bhavsar et al., 2010).

Experiments optimising the length of effector target co-incubation without GolgiStop revealed that CD107a can be optimally measured between 2 and 3 hrs co-incubation. Experiments showed that at 4 hrs co-incubation less CD107a is up-regulated on the NK cell surface when compared to 2 hrs and 3 hrs, thereby suggesting that up-regulated CD107a re-internalises, as has previously been suggested (Betts et al., 2003). The point at which CD107a antibody is added during the CD107a degranulation assay also appears to be important. Staining of CD107a at the start of effector target co-incubation, as described by Alter G et al, appeared to increase the intensity of background levels of CD107a expression on NK cells that had appeared not to up-regulate additional CD107a (as indicated by a higher MFI value) (Alter et al., 2004). Staining NK cells for CD107a expression after completion of the 2 to 3 hr effector target co-incubation, similar to a method published by Brysceson YT et al (Bryceson et al., 2005), prevents the increase in intensity of background CD107a staining on NK cells that have not further up-regulated CD107a. Therefore, only the NK cells that have upregulated CD107a display an increase in CD107a expression. Overall, these findings suggest that monensin should not be used in the CD107a degranulation assay and that the staining for CD107a should take place after co-incubation.

Surprisingly, although priming increased the ability of NK cells to kill PC3 cells, it reduced their ability to kill K562 cells. Significant positive correlations between the expression of activating receptors NKG2D and NKp46 with the percentage of K562 lysis were observed. These data suggest that NKG2D and NKp46 are important for transducing the activating signals that promote the capacity of NK cells to kill K562 cells. In contrast, North et al reported no change in

K562 lysis following NK cell priming (North et al., 2007). It is known that there are at least 3 sublines of K562 and there is evidence that the cellular characteristics of cell lines may change as a result of passaging (Dimery et al., 1983). Therefore, the reason for different abilities of primed NK cells to kill K562 between the two laboratories could be due to different ligands being expressed on the K562 cells following passaging. This conclusion highlights the need to know / monitor the expression of NK cell ligands on targets cells, as they could influence conclusions which may contribute to discrepancies between similar studies from different laboratories.

The aim of the work described in this chapter was to develop and optimise assays that can be used to accurately measure the cytotoxic function of NK cells isolated from prostate cancer patients. This has been achieved through development and optimisation of flow cytometry based assays capable of measuring either direct target cell lysis or NK cell degranulation (indirect measurement). Crucially, it is not just the development of functional assays that are important, but also how they are used. Through literature research I questioned how accurately current studies measure the cytotoxic function of NK cells when using either the MHC class I deficient K562 cells as targets, or when stimulating NK cells with cytokines to promote their ability to kill more relevant NK cell-resistant cancer lines. I believe that the NK cell priming method described by Lowdell et al (North et al., 2007, Sabry et al., 2011) not only offers a potential immunotherapeutic, but also offers a method that may better measure NK cell function. Using Lowdell et al's method two measurements of NK cell function can be measured: 1) the ability of the NK cell to become 'primed' (i.e. activated) through the measurement of its phenotype. 2) the ability of the primed NK cell to kill a relevant NK cell-resistant cancer cell line. In theory, any deficiencies in the phenotype of the NK cell prior to priming may affect the ability of the NK cell to become primed when in contact with the CTV-1 cells. Any reduction in activation of the primed NK cells may then in theory directly affect the ability of the primed NK cell to kill the relevant NK cell-resistant target cell. Lowdell et al's method thereby allows for the measurement of the NK cells cytotoxic function that is more relevant to the way NK cells would target cancer cells *in vivo*. Interestingly, Lowdell et al described downregulation of the NKG2D and NKp46 receptors following NK cell priming (Sabry et al., 2011). The data in this chapter support this observation and challenges the commonly held view that down-regulation of NK cell activating receptors represents suppression of NK cell responses reviewed by (Sabry and Lowdell, 2013). The next chapter describes the results of experiments designed to measure the function of NK cells in patients with prostate cancer using the experimental approaches and functional assays described in this chapter.

Chapter 5 - RESULTS

Assessing the ability of NK cells from patients with prostate cancer to become primed, as measured by changes in their phenotype

5.1 Introduction

The term immunological synapse was first defined in the late 1990s as being the crucial junction for enabling receptor-ligand interactions between T cells and antigen presenting cells (Grakoui et al., 1999, Monks et al., 1998). Subsequent studies described the formation of immunological synapses between different immune cells, and between immune cells and non-immune cells (Orange, 2008). This resulted in the immunological synapse being defined as the 'intentional arrangement of molecules in an immune cell at the interface with another cell' (Orange, 2008).

NK cells rely on cell-to-cell contact to mediate their effector functions, using activating and inhibitory receptors to sense the presence of stress ligand and MHC class I molecules respectively, and to ultimately determine whether or not to engage the target cell of interest. To this end, NK cells exhibit different types of immunological synapses; lytic synapses, inhibitory synapses and regulatory synapses (Eissmann and Davis, 2010, Mace and Orange, 2011).

As reviewed by Orange (Orange, 2008), the immunological synapse has been proposed to have multiple functions in NK cells:

- Ligand Recognition – The formation of a critical zone in which ligands on a target cell are recognised by receptors with precision.
- Co-stimulation – NK cells have been reported to form dual synapses with other innate immune cells and T cells. The innate immune cell induces the expression of co-stimulatory ligands on the NK cell surface (e.g. OX40L) which can be recognised by the T cell.
- Cytotoxicity – Precise targeting of target cells by NK cells, thereby protecting neighbouring cells from damage.
- Directed secretion – The creation of a conduit which enables the focused secretion of lytic granules, cytokines and other cellular components.
- Multi-directional secretion – Activating signals can induce the secretion of cytokines and chemokines from other sites on the NK cell.
- Protein transfer – Cell-surface proteins can be transferred between NK cells and their targets
- Inhibition of activation – Formation of an inhibitory synapse that prevents activation.

- Signal termination – molecular patterns facilitate NK cell receptor internalisation and / or the end of productive signalling

Using confocal microscopy the supramolecular organisation of NK cell receptors at inhibitory synapses have been analysed (Davis et al., 1999, Orange et al., 2002). At the inhibitory synapse where an NK cell and its target meet, clusters of killer inhibitory receptor (KIR) – MHC class 1 interactions were shown to form. The KIR – MHC class I interactions created a ring around the interactions between LFA-1 and ICAM. Unlike with lytic synapses, actin-mediated cytoskeletal movement is not required for the formation of the inhibitory synapse and this might explain why NK cells remain 'rounder' when engaging inhibitory synapses as compared to lytic synapses (Davis et al., 1999, Orange et al., 2002). Interestingly, it was shown that one NK cell can simultaneously form inhibitory synapses with multiple targets, and also that one target can simultaneously form inhibitory synapses with multiple NK cells (Davis et al., 1999).

The formation and function of lytic synapses require the coordinated regulation of cytoskeletal elements, signalling molecules, cellular organelles and lytic granules. Mace and colleagues proposed that the formation of a lytic synapse can grouped into 3 stages; recognition, effector and termination, and that these comprise 48 steps and potential checkpoints (Mace et al., 2014).

During the initial contact between an NK cell and a potential target, a brief initial interaction is potentially made via tethering receptors such as CD62L or PSGL-1 or adhesion receptors such as CD2, LFA-1, DNAM-1, NKG2D (Grégoire et al., 2007). A firmer adhesion is then formed via the binding of LFA-1 to ICAM-1. In order for this binding to occur, the structure of LFA-1 needs to assume an open conformation, a form of which only ~10 % of peripheral blood NK cells have been found to express. Stimulation via DNAM-1, NKG2D, 2B4 or CD2 promotes the formation of the LFA-1 open conformation, with this type of signalling being known as 'inside-out' signalling (Bryceson et al., 2009). LFA-1 engagement initialises the initial stages of synapse formation by inducing the reorganisation of the actin cytoskeleton and promoting polarisation (Barber et al., 2004, Mace et al., 2009). Lytic granules, which are already formed, move along microtubules and converge on the microtubule organising centre (MTOC). At this point, the NK cell is not yet committed to cytotoxicity, as this lytic granule convergence occurs in both lytic and inhibitory synapse formation. However, the NK cell is thought to be preparing for cytotoxic commitment (Mentlik et al., 2010). Inhibitory signalling, which is controlled via the spatial presence of SHP-1, Lck and talin at the area of cell-to-cell contact, can quickly disrupt multiple points of activation including conjugate formation, actin accumulation, activating receptor clustering and calcium influx (Burshtyn et al., 2000, Kaufman et al., 1995, Liu et al., 2012, Vyas et al., 2002). Firm adhesion to the target cells is achieved and sustained and the NK cell is committed to cytotoxicity once F-actin polymerisation and reorganisation occurs.

In comparison with NK cells forming an inhibitory synapse, those NK cells forming a lytic synapse appear flattened and the diameter of the immunological synapse increases (Orange et al., 2002). Dynamic micro-clustering of activating receptors (e.g. NKG2D) and inhibitory receptors then occurs, and it has been suggested that there is some sort of interplay between the two types of receptors, the significance of which is still being investigated (Abeyweera et al., 2011, Mace et al., 2014, Pageon et al., 2013). Activation signalling and the cytoskeleton are dependent on each other, with the disruption of one affecting the other and preventing functional cytotoxicity (Mace et al., 2014). Transduction of activating signals results in the mobilisation of ions, particularly Ca^{2+} from stores in the endoplasmic reticulum (Bryceson et al., 2005, Feske et al., 2012). At some point during the adhesion of the NK cell to its target via the cytoskeleton and the micro-clustering of activating and inhibitory receptors at the immunological synapse, a lytic cleft forms. The cleft represents the gap between the NK cell and the target cell, into which the contents of lytic granules are secreted (Orange, 2008). However, it now seems that there is more to the function of cleft, as membrane proteins such as receptors and their ligands transfer between the NK cell and its target via membrane protrusions in a process known as trogocytosis (Nakamura et al., 2013, Roda-Navarro et al., 2006, Williams et al., 2007). Acquisition of NKG2D ligands from target cells has been shown to render the NK cells susceptible to fratricide by neighbouring NK cells, thereby suggesting a form of negative regulation of activated NK cells (Nakamura et al., 2013). Following the formation of the lytic cleft and more rearrangement of the actin cytoskeleton, the microtubule organising centre (MTOC) and associated lytic granules polarise towards the synapse (Krzewski et al., 2008, Orange et al., 2003, Orange et al., 2002). Golgi and mitochondria have also been shown to move toward the synapse (Abarca-Rojano et al., 2009, Kupfer et al., 1983). The lytic granules then fuse with the plasma membrane and the granule contents cross the lytic left to the target cell and induce apoptosis (Liu et al., 2011). This marks the end of the effector stage. During the termination stage, there is a period of inactivity followed by detachment. The mechanisms surrounding this stage are still being investigated (Mace et al., 2014).

5.2 Aims and hypothesis

The aim of this part of the study was to assess the ability of NK cells from patients with prostate cancer to become primed following co-incubation with mitomycin C treated CTV-1 cells, as measured by changes in their phenotype. This is important, as it will provide insight into the potential therapeutic value of NK cell priming for the treatment of patients with prostate cancer. For the purposes of this element of the study, only NK cells from patients having benign, Gleason 6 and Gleason 9 disease were studied, as these encompass key stages of the disease. The priming

capability of the NK cells from the patient groups was also compared to that of NK cells from healthy volunteers.

It was hypothesised that NK cells isolated from patients with a higher grade cancer (Gleason 9) would have a reduced capacity to become primed, as would be evident by the extent of up-regulation of co-stimulatory receptors, compared to NK cells isolated from benign patients, patients with low grade cancer (Gleason 6) and NK cells from healthy volunteers.

5.3 Results

5.3.1 Comparing the phenotype of primed NK cells from healthy volunteers with that of primed NK cells from patients with benign disease and prostate cancer

PBMCs isolated from the peripheral blood of both healthy volunteers and patients with prostate cancer and benign disease were thawed, from which NK cells were isolated by negative selection using magnetic beads. For each subject, half the isolated NK cells were primed using mitomycin C treated CTV-1, whereas the others were cultured in the absence of CTV-1 cells under the same conditions (non-primed controls). Following 17 hrs incubation, both non-primed and primed NK cells were stained using antibody panels 1, 4, 5, 6 (thereby measuring receptors; CD56, CD16, CD3, CD19, CD8, DNAM-1, NKG2D, NKp46, NKp30, CD2, CD96, CD25, CD69, OX40, NKp80, CD137, CRTAM, 2B4, TIGIT, GITR and CD107a) and their phenotype determined using flow cytometry. The phenotypes of non-primed and primed NK cells from healthy volunteers were compared to that of equivalent NK cells from patients with prostate cancer and benign disease using Beckman Coulter Kaluza™ software and GraphPad Prism.

5.3.1.1 Influence of priming on the phenotypes of $CD56^{dim}CD16^{high}$, $CD56^{dim}CD16^{low}$ and $CD56^{dim}CD16^{neg}$ NK cell subpopulations

Similar to NK cells from healthy volunteers, priming led to a downregulation / shedding of CD16 from NK cells for patients with prostate cancer and benign disease. In all subject groups, there was a significant decrease in the percentage of $CD56^{dim}CD16^{high}$ NK cells, whereas there was a significant increase in the percentage of $CD56^{dim}CD16^{low}$ and $CD56^{dim}CD16^{neg}$ NK cells. There were no significant differences in the magnitude of these responses across the subject groups that were analysed (Figure 5.1).

No significant changes in the intensity of CD56 expression (MFI) on $CD56^{dim}$ and $CD56^{bright}$ NK cell subsets was observed as a result of NK cell priming for any of the subject groups. However, there was a significant difference in the MFI of CD56 expression on primed $CD56^{bright}$ NK cells between healthy volunteers and patients with benign disease, and also Gleason 9 prostate cancer

patients. Furthermore, there was also a significant difference between non-primed NK cells from healthy volunteers and Gleason 9 patients. In contrast, within each subject group there was a

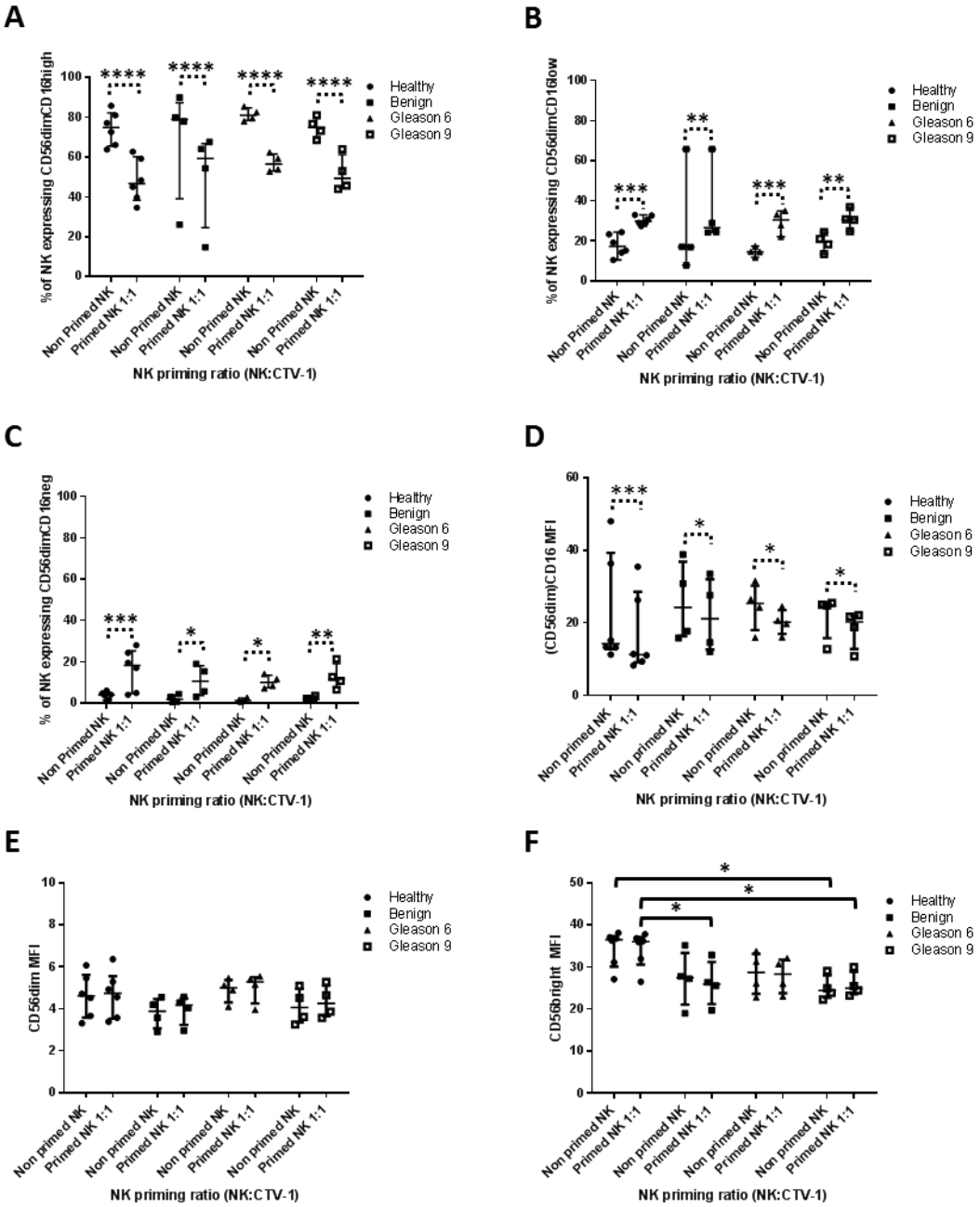

Figure 5.1: The influence of priming on the expression of CD56 and CD16 on healthy volunteers compared to patients with prostate cancer or benign disease

NK cells from healthy volunteers and patients with prostate cancer or benign disease were primed with mitomycin C treated CTV-1 at a 1 : 1, NK : CTV-1 ratio for 17 hrs. Both primed NK cells and non-primed control NK cells were stained with NK cell defining antibodies CD56, CD16, CD3 and CD19. The expression of these receptors was measured by flow cytometry. NK cells were defined as $CD3^{-}$ $CD19^{-}$ $CD56^{+}$ cells. A to C) The proportion of NK cells with the phenotype $CD56^{dim}CD16^{high}$, $CD56^{dim}CD16^{low}$ and $CD56^{dim}CD16^{neg}$ respectively, D) Median intensity fluorescence (MFI) of CD16 on $CD56^{dim}$ NK cells, E) MFI of CD56 on the $CD56^{dim}$ subset, F) MFI of CD56 on the $CD56^{bright}$ subset. Statistical analysis was done using parametric ANOVA and associated comparison tests; Tukeys multiple comparisons test (solid black line), uncorrected Fishers least significant difference test (dotted black line). * P<0.05, ** P<0.005, ***P<0.0005, **** P<0.00005.

significant decrease in the intensity of expression of CD16 on the $CD56^{dim}$ subset between non-primed NK cells and NK cells primed at the 1 : 1 NK : CTV-1 ratio. However, despite an apparent trend indicating that patient NK cells shed less CD16, no significant difference in the intensity of CD16 expression between healthy volunteer $CD56^{dim}$ NK cells and patient $CD56^{dim}$ NK cells (irrespective of disease) was observed. The down-regulation / shedding of CD16 appeared to be confined to the $CD56^{dim}$ subset only (Figure 5.1).

5.3.1.2 Influence of priming on expression of activating receptors NKp30, NKp46 and NKG2D.

NK cell priming did not significantly alter the intensity of expression or percentage of NK cells expressing NKp30 for any of the subject groups that were analysed. The percentage of NK cells expressing NKp30 in patients with Gleason 6 disease was more variable than that in the other sample groups. However, there was no significant difference (Figure 5.2)

In contrast to NKp30, the percentage of NK cells from the patient groups (irrespective of disease status) expressing NKp46 was lower on the primed NK cells compared to the non-primed NK cells. This result was highly significant for all three patient groups. Interestingly, the percentage of primed NK cells expressing NKp46 in the healthy volunteer group was not significantly lower than the equivalent non-primed NK cells. The patterns of expression for NKG2D and NKp46 were similar. Despite NK cells from healthy volunteers appearing to down-regulate NKG2D expression following priming, the difference was not found to be of statistical significance (Figure 5.2)

The percentage of NK cells expressing NKp46 and NKG2D on primed NK cells from the patient groups appeared to be lower than that observed for NK cells from health volunteers. For NKp46, the proportion of primed NK cells from patients with benign disease and patients with Gleason 9 disease expressing NKp46 was significantly lower than that observed for primed NK cells from healthy volunteers. For NKG2D, a significant difference was only observed between healthy volunteer primed NK cells and primed NK cells from patients with benign disease.

5.3.1.3 Influence of priming on the expression of CD2, CD25 and CD69

Although priming had no effect on the expression of the adhesion receptor CD2, differences in the level of CD2 expression by NK cells from healthy volunteers and the patient groups were apparent but not significant. Sixty to 82 % of NK cells from healthy individuals expressed CD2, with NK cells from 4 individuals comprising between 76 and 82 % $CD2^+$ cells, and in one individual 60 % the NK cell population was $CD2^+$. In comparison, the NK cell population in individuals with benign disease was between 53 and 89 % $CD2^+$ and ranged between 26 and 72 % $CD2^+$ in patients with Gleason 6 disease. For both groups, approximately 60% of the NK cells in the majority of individuals were $CD2^+$. For patients with Gleason 9 disease, between 66 and 91 % of their NK

cells expressed CD2. Interestingly, the profile of CD2 expression intensities aligned with that for the proportion of $CD2^+$ NK cells. NK cells from individuals with benign disease and patients with

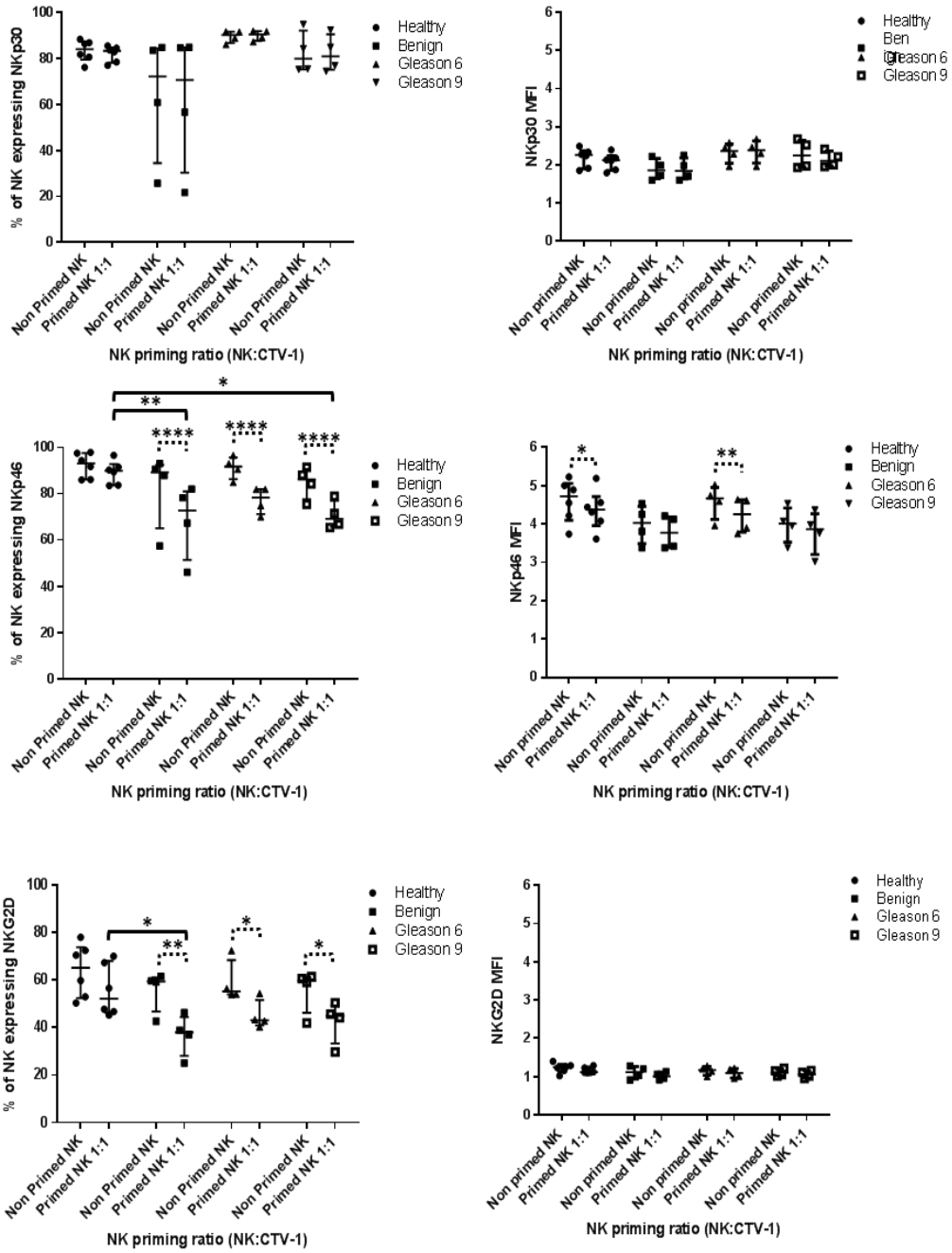

Figure 5.2: The influence of priming on the expression of NKp30, NKp46 and NKG2D on healthy volunteers compared to patients with prostate cancer or benign disease.

NK cells from healthy volunteers and patients with prostate cancer or benign disease were primed with mitomycin C treated CTV-1 at a 1 : 1, NK : CTV-1 ratio for 17 hrs. Both primed NK cells and non-primed control NK cells were stained for NK cell defining antibodies and antibodies for NKp30, NKp46, NKG2D. The expression of these receptors was measured by flow cytometry. The percentage of NK cells expressing and the median fluorescence intensity (MFI) of that expression for each receptor are shown; NKp30 (top graphs), NKp46 (middle graphs), NKG2D (bottom graphs). Statistical analysis was done using parametric ANOVA and associated comparison tests; Tukeys multiple comparisons test (solid black line), uncorrected Fishers least significant difference test (dotted black line). * P<0.05, ** P<0.005, ***P<0.0005, ****

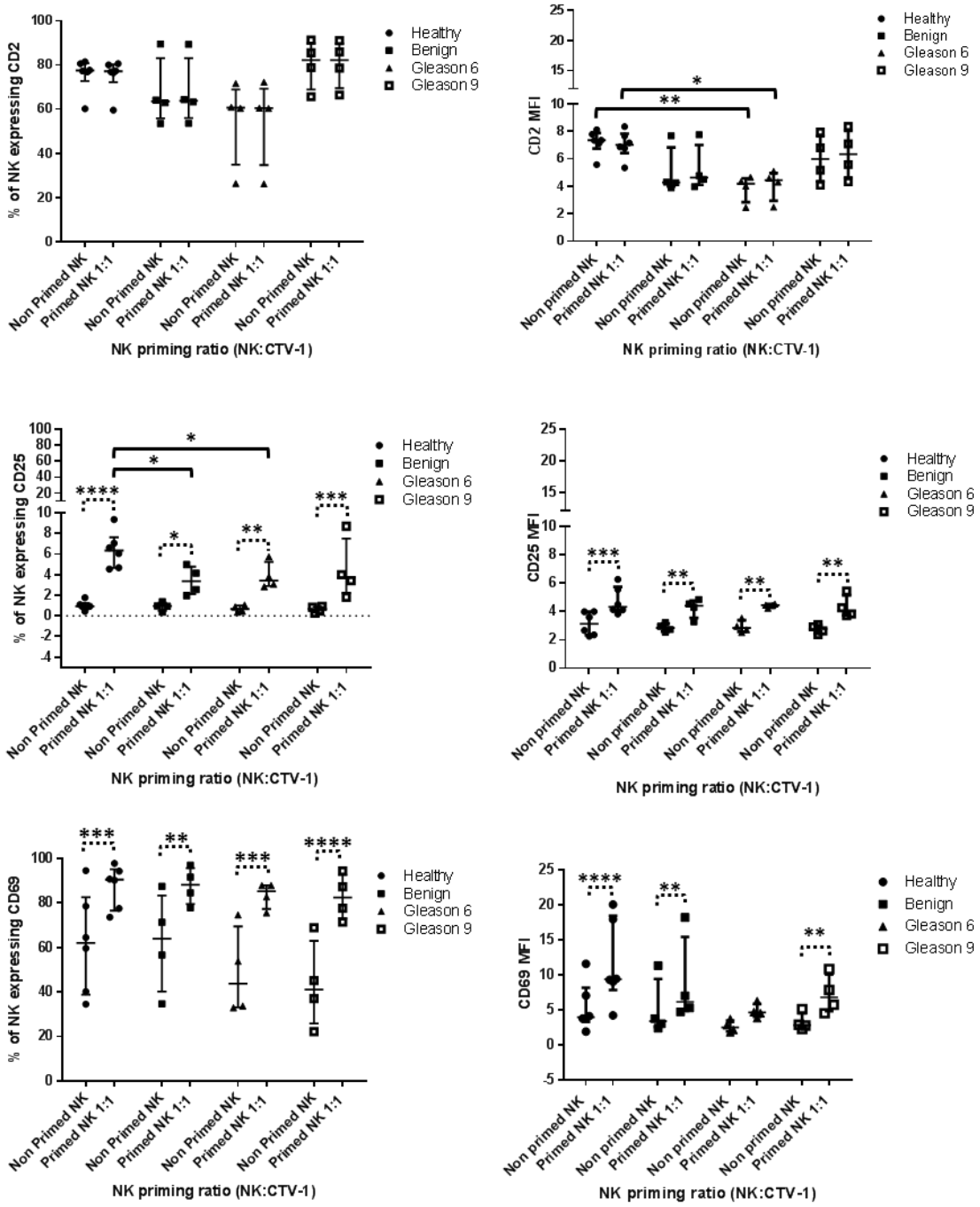

Figure 5.3: The influence of priming on the expression of CD2, CD25 and CD69 on healthy volunteers compared to patients with prostate cancer or benign disease

NK cells from healthy volunteers and patients with prostate cancer or benign disease were primed with mitomycin C treated CTV-1 at a 1 : 1, NK : CTV-1 ratio for 17 hrs. Both primed NK cells and non-primed control NK cells were stained with NK cell defining antibodies and antibodies for CD2, CD25, CD69. The expression of these receptors was measured by flow cytometry. The percentage of NK cells expressing and the median fluorescence intensity (MFI) of that expression for each receptor are shown; CD2 (top graphs), CD25 (middle graphs), CD69 (bottom graphs). Statistical analysis was done using parametric ANOVA and associated comparison tests; Tukeys multiple comparisons test (solid black line), uncorrected Fishers least significant difference test (dotted black line). * P<0.05, ** P<0.005, ***P<0.0005, **** P<0.00005.

Gleason 6 prostate cancer appeared to express CD2 at a lower intensity than that expressed by NK cells from healthy volunteers and Gleason 9 disease. The intensity of CD2 expression on NK cells from patients with Gleason 6 disease was significantly lower than expressed by NK cells from healthy volunteers (Figure 5.3).

NK cells from healthy volunteers and the three patient groups did not express CD25 prior to being primed. Following priming, the NK cells from individuals in all 4 subject groups significantly up-regulated CD25 expression, both in terms of the percentage of NK cells expressing the receptor and the intensity of that expression. However, the increase in CD25 expression was quantitatively small.

Interestingly, a lower proportion of NK cells from the patient groups up-regulated CD25 than for healthy volunteer NK cells, and this difference was significant when comparing the responses of primed NK cells from healthy volunteers with that of primed NK cells from individuals with benign disease and Gleason 6 prostate cancer. The proportion of NK cells expressing CD25 in patients with Gleason 9 disease was similar to that in individuals with benign disease and patients with Gleason 6 disease, with 1 patient in the Gleason 9 group exhibiting a similar proportion of NK cells expressing CD25 as the healthy volunteer group (Figure 5.3).

In contrast to the expression of CD25, CD69 was expressed on non-primed NK cells from each healthy volunteer, individual with benign disease and patients with prostate cancer. For each subject group, there was a large variation in the proportion of NK cells expressing CD69. This may be due to both the activation level of the NK cells prior to blood donation and possibly the effects of freeze-thawing on the NK cells. Irrespective of CD69 expression on the NK cells prior to priming, both healthy volunteers and patients significantly up-regulated CD69 expression both in terms of receptor intensity and the percentage of NK expressing CD69 following priming, with no significant differences being observed between subject groups. The only exception was that priming did not increase the intensity of CD69 expression on NK cells from patients with Gleason 6 disease. For each individual, for all subject groups, greater than 70 % of their NK cells had up-regulated CD69.

5.3.1.4 Influence of priming on the expression of the immunoglobulin superfamily receptor members; DNAM-1, TIGIT and CD96

Priming had no effect on the level of DNAM-1 expression on NK cells from any of the individuals tested. The proportion of NK cells expressing DNAM-1 remained very high regardless of whether the NK cells were primed or not and regardless of whether the individual was healthy or not. In contrast, within each subject group the intensity of expression and the proportion of NK cells

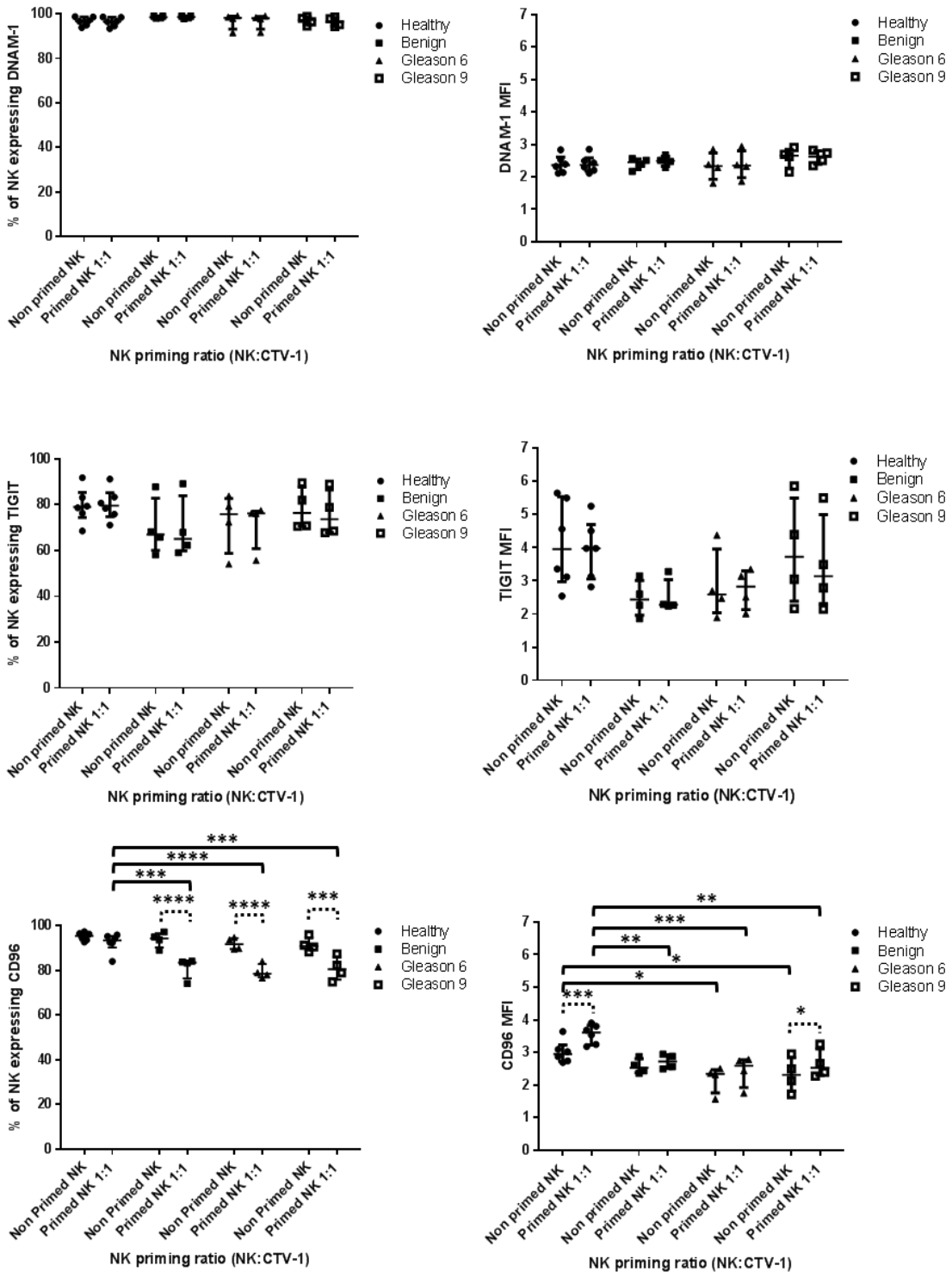

Figure 5.4: The influence of priming on the expression of DNAM-1, TIGIT and CD96 on healthy volunteers compared to patients with prostate cancer or benign disease

NK cells from healthy volunteers and patients with prostate cancer or benign disease were primed with mitomycin C treated CTV-1 at a 1 : 1, NK : CTV-1 ratio for 17 hrs. Both primed NK cells and non-primed control NK cells were stained with NK cell defining antibodies and antibodies for DNAM-1, TIGIT, CD96. The expression of these receptors was measured by flow cytometry. The percentage of NK cells expressing and the median fluorescence intensity (MFI) of that expression for each receptor are shown; DNAM-1 (top graphs), TIGIT (middle graphs), CD96 (bottom graphs). Statistical analysis was done using parametric ANOVA and associated comparison tests; Tukeys multiple comparisons test (solid black line), uncorrected Fishers least significant difference test (dotted black line). * P<0.05, ** P<0.005, ***P<0.0005, **** P<0.00005.

expressing TIGIT was more variable. NK cell priming did not significantly affect the expression of TIGIT, and no significant differences in the expression of TIGIT on NK cells between subject groups were observed (Figure 5.4).

In contrast to the above, priming induced a significant decrease in the percentage of NK cells expressing CD96 in all 3 patient groups. Although the proportion of NK cells from healthy volunteers expressing CD96 also decreased after priming, the change was quantitatively smaller and not statistically significantly different to non-primed NK cells. Conversely, the intensity of CD96 expression on NK cells from healthy volunteers increased after priming. A highly significant difference between the expression of CD96 on primed NK cells from healthy volunteers compared to that on primed NK cells from all 3 patient groups, both in terms of percentage and intensity of expression, demonstrates that priming has a greater effect on the expression of CD96 expression on NK cells from individuals with benign disease and prostate cancer (Figure 5.4).

5.3.1.5 Influence of priming on the expression of the TNF co-stimulatory receptors OX40, CD137 and the immunoglobulin superfamily co-stimulatory receptor CRTAM

Although non-primed NK cells from healthy volunteers and patients did not express OX40, CD137 or CRTAM, priming significantly induced the expression of all three receptors, both in terms of the percentage of cells expressing and the intensity of expression (Figure 5.5). In general, for both healthy volunteers and patients, a smaller proportion of NK cells up-regulated OX40 compared to those that up-regulated CD137 and CRTAM. Furthermore, for each individual irrespective of their health, less than 40 % their total NK cell population up-regulated the receptor CRTAM, whereas for CD137 and OX40 less than 20 % of their total NK population had up-regulated these receptors (Figure 5.5).

A greater proportion of primed NK cells from healthy volunteers expressed CD137 and CRTAM than did primed NK cells from individuals with benign disease and patients with prostate cancer. This difference in expression was of statistical significance for NK cells from healthy volunteers *versus* NK cells from individuals with benign disease and Gleason 6 prostate cancer. Furthermore, a significantly greater proportion of primed NK cells from healthy volunteers expressed CRTAM compared to primed NK cells from patients with Gleason 9 prostate cancer. Once primed, the intensity of CD137 and CRTAM expression on NK cells from healthy volunteers and the patient groups was comparable.

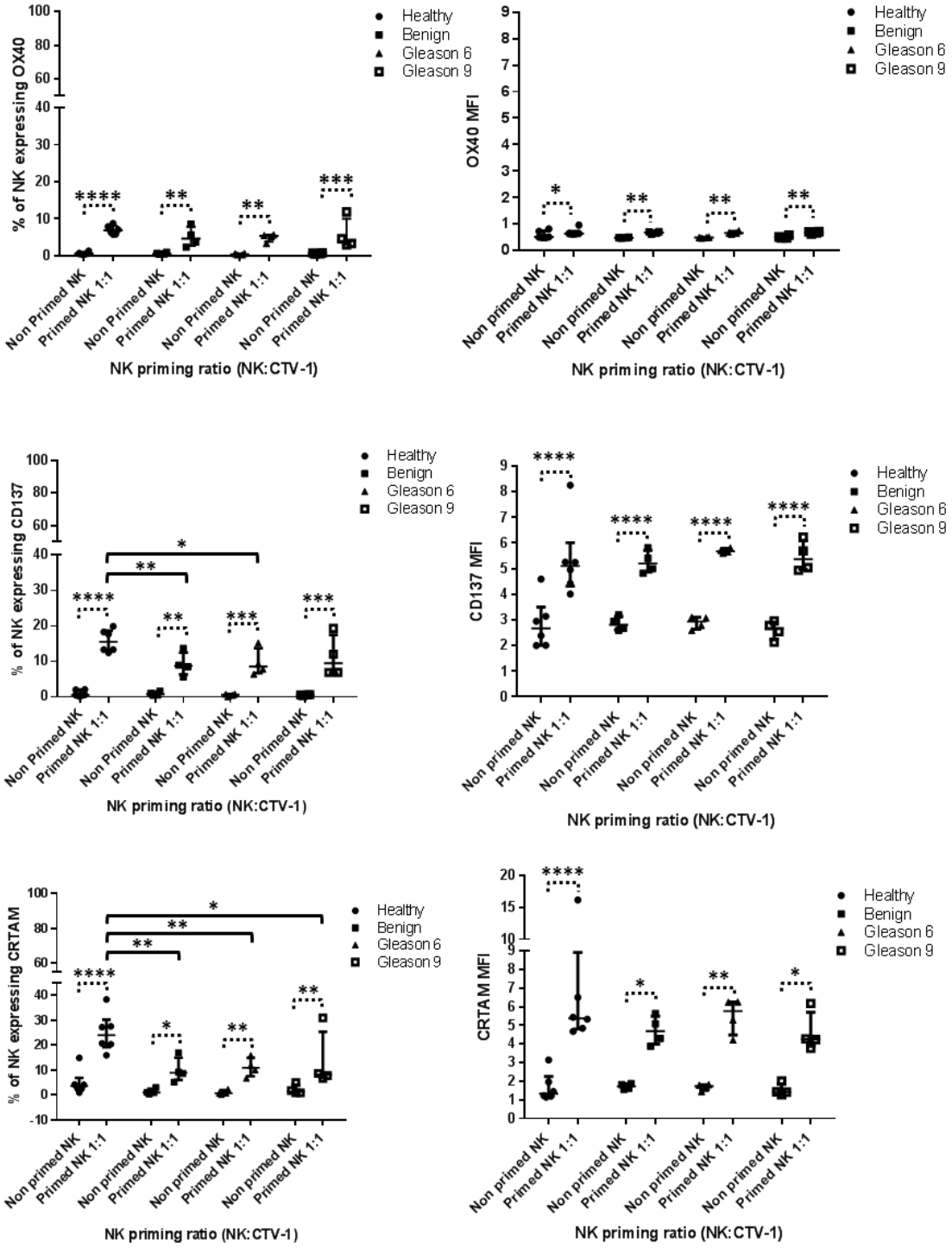

Figure 5.5: The influence of priming on the expression of OX40, CD137 and CRTAM on healthy volunteers compared to patients with prostate cancer or benign disease

NK cells from healthy volunteers and patients with prostate cancer or benign disease were primed with mitomycin C treated CTV-1 at a 1 : 1, NK : CTV-1 ratio for 17 hrs. Both primed NK cells and non-primed control NK cells were stained with antibodies for OX40, CD137, CRTAM and their expression measured by flow cytometry. The percentage of NK cells expressing and the median fluorescence intensity (MFI) of that expression for each receptor are shown; OX40 (top graphs), CD137 (middle graphs), CRTAM (bottom graphs). Statistical analysis was done using parametric ANOVA and associated comparison tests; Tukeys multiple comparisons test (solid black line), uncorrected Fishers least significant difference test (dotted black line). * P<0.05, ** P<0.005, ***P<0.0005, **** P<0.00005.

Although priming induced an increase in the proportion of NK cells from healthy volunteers, individuals with benign disease and patients with prostate cancer expressing OX40, the increase in intensity of that expression was minimal and overall remained extremely low at <1 MFI.

5.3.1.6 Influence of priming on the expression of the TNF receptor GITR and the CD107a receptor

On average, a similar proportion of non-primed NK cells in each subject group expressed GITR, with the proportion of NK cells expressing GITR mainly ranging between 7 and 32 %. Following priming, all subject groups significantly up-regulated both the intensity of expression and the proportion of NK cells expressing GITR. The increase in intensity was relatively minor. There was

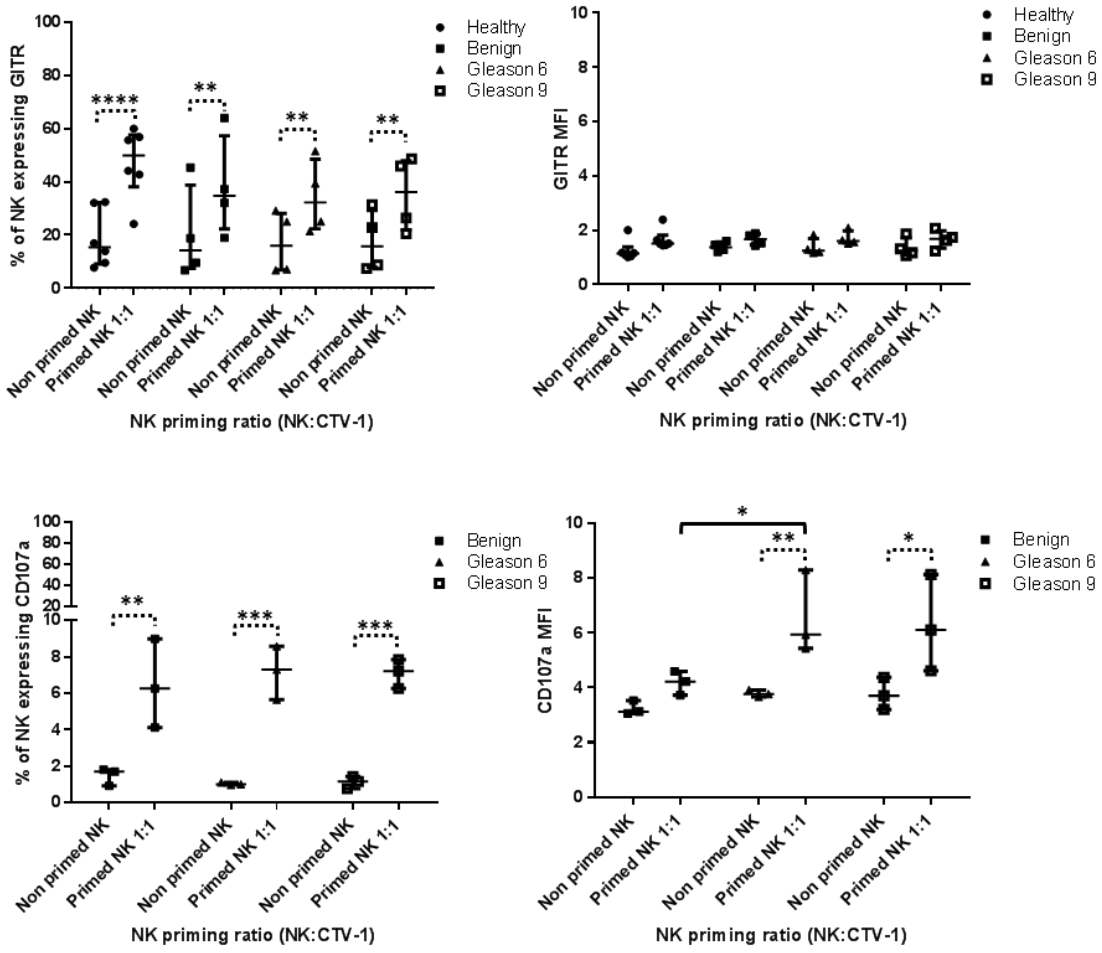

Figure 5.6: The influence of priming on the expression of GITR and CD107a on healthy volunteers compared to patients with prostate cancer or benign disease

Isolated thawed NK cells from healthy volunteers and patients with prostate cancer or benign disease were primed with mitomycin C treated CTV-1 at a 1 : 1, NK : CTV-1 ratio for 17 hrs. Both primed NK cells and non-primed control NK cells were stained NK cell defining with antibodies and antibodies for GITR, CD107a. The expression of these receptors was measured by flow cytometry. The percentage of NK cells expressing and the median fluorescence intensity (MFI) of that expression for each receptor are shown; GITR (top graphs), CD107a (bottom graphs). Statistical analysis was done using parametric ANOVA and associated comparison tests; Tukeys multiple comparisons test (solid black line), uncorrected Fishers least significant difference test (dotted black line). * P<0.05, ** P<0.005, ***P<0.0005, **** P<0.00005.

no statistical difference between the proportion of primed NK cells expressing GITR between each subject group. The proportion of primed NK cells expressing GITR from healthy volunteers (range 43 – 60 %) was generally greater than individuals from the patient groups (range 20 – 39%). However, the proportion of primed NK cells from 4 out of the 12 patients tested that expressed GITR was similar to that observed for NK cells in the majority of the healthy volunteers (Figure 5.6).

CD107a expression was only measured on patient NK cells before and after priming as a result of a change in protocol. No CD107a was expressed on non-primed NK cells. Following priming the NK cells from all three patient groups up-regulated CD107a. The proportion of primed NK cells up-regulating CD107a ranged between 4 and 9 %. Although the intensity of expression was also up-regulated, this up-regulation was only significant for the Gleason 6 and Gleason 9 patient groups. Furthermore, the intensity of CD107a expression on Gleason 6 primed NK cells was significantly greater than on primed NK cells from patients with benign disease (Figure 5.6).

5.3.2 Comparison of the $CD56^{dim}CD16^{high}$, $CD56^{dim}CD16^{low}$ and $CD56^{dim}CD16^{neg}$ subpopulation phenotypes of healthy volunteer and patient NK cells

For each healthy volunteer and patient, the total NK cell population was subdivided into 3 subpopulations; $CD56^{dim}CD16^{high}$ ($CD16^{high}$), $CD56^{dim}CD16^{low}$ ($CD16^{low}$) and $CD56^{dim}CD16^{neg}$ ($CD16^{neg}$). The phenotype of each subpopulation was then further analysed in order to observe any differences in the expression of activating receptors, co-stimulatory receptors and co-inhibitory receptors before and after priming.

5.3.2.1 The influence of NK cell priming on the expression of NKp46 and NKG2D on $CD56^{dim}CD16^{high}$, $CD56^{dim}CD16^{low}$ and $CD56^{dim}CD16^{neg}$ subpopulations

For each patient group, the expression of NKp46 was significantly decreased on all 3 NK cell subpopulations following priming (Figure 5.7). The proportion of $CD16^{neg}$ NK cells down-regulating NKp46 was greater than both the $CD16^{low}$ and $CD16^{high}$ NK cells. Interestingly, there was no significant difference in the proportion of NK cells down-regulating NKp46 in individuals with benign disease and patients with prostate cancer. This was true for all 3 subpopulations. In contrast, the proportion of each NK cell subpopulation in the healthy volunteer group only marginally increased, with the proportion of the $CD56^{dim}CD16^{neg}$ NK cell subpopulation increasing the greatest. For both healthy volunteers and patients, the intensity of NKp46 expression was also down-regulated on all 3 NK cell subpopulations following NK cell priming. The magnitude of this down-regulation was similar for both healthy volunteer and patient NK cells, with the exception of the $CD56^{dim}CD16^{neg}$ in individuals with benign disease (Figure 5.8).

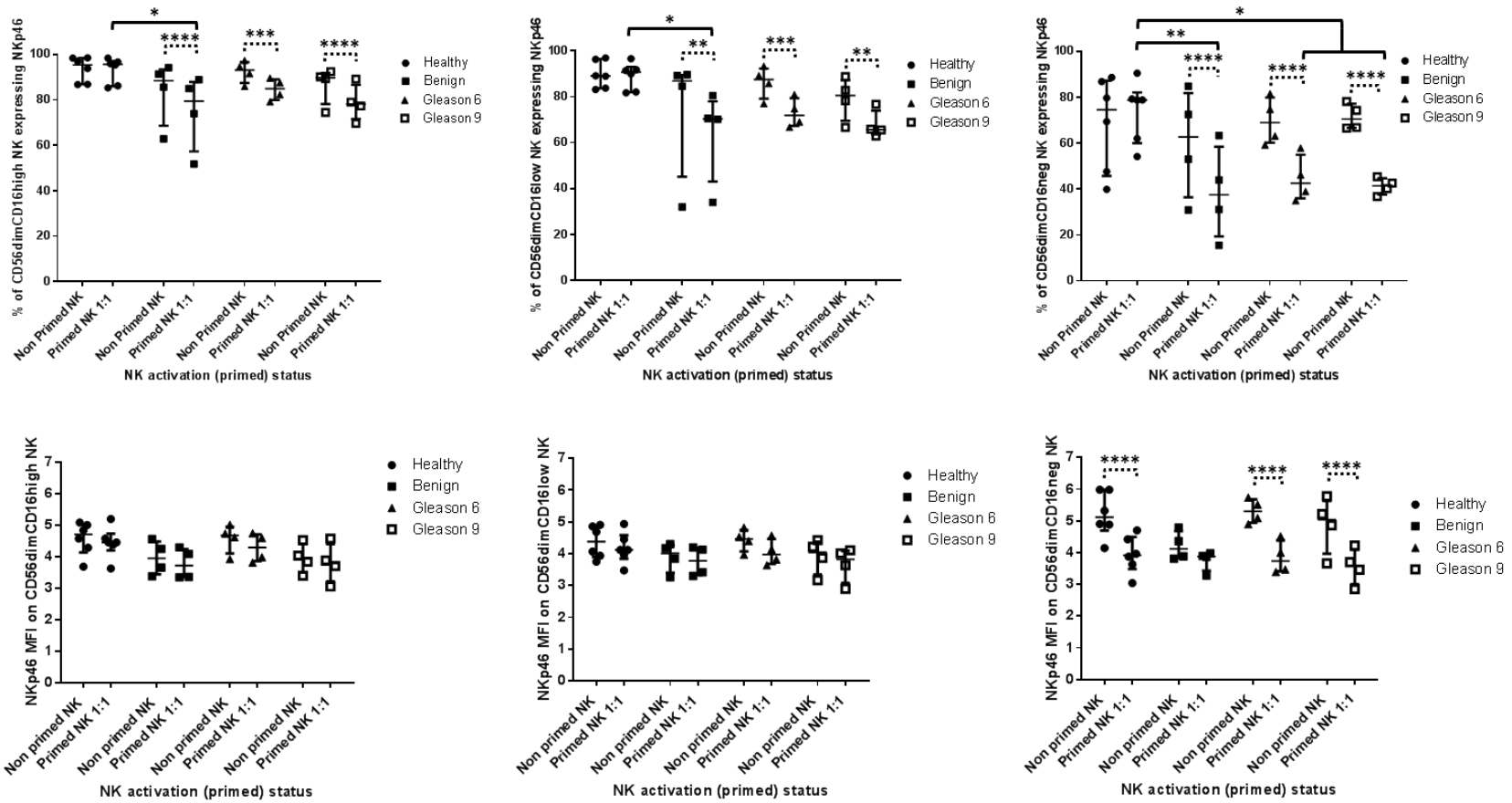

Figure 5.7: The influence of NK cell priming on the expression of NKp46 on the three NK cell subpopulations; $CD56^{dim}CD16^{high}$, $CD56^{dim}CD16^{low}$ and $CD56^{dim}CD16^{neg}$.
NK cells from healthy volunteers and patients with prostate cancer or benign disease were primed with mitomycin C treated CTV-1 at a 1 : 1, NK : CTV-1 ratio for 17 hrs. Both primed NK cells and non-primed control NK cells were stained with NK cell defining antibodies and the NKp46 antibody. The expression of these receptors was measured by flow cytometry. The expression of NKp46 by the three NK cell subpopulations; $CD56^{dim}CD16^{high}$, $CD56^{dim}CD16^{low}$ and $CD56^{dim}CD16^{neg}$, was analysed. The percentage of each NK subpopulation expressing NKp46 (top row of graphs) and the intensity of that expression (bottom for of graphs) was measured. Statistical analysis was done using parametric ANOVA and associated comparison tests; Tukeys multiple comparisons test (solid black line), uncorrected Fishers least significant difference test (dotted black line). * P<0.05, ** P<0.005, ***P<0.0005, **** P<0.00005.

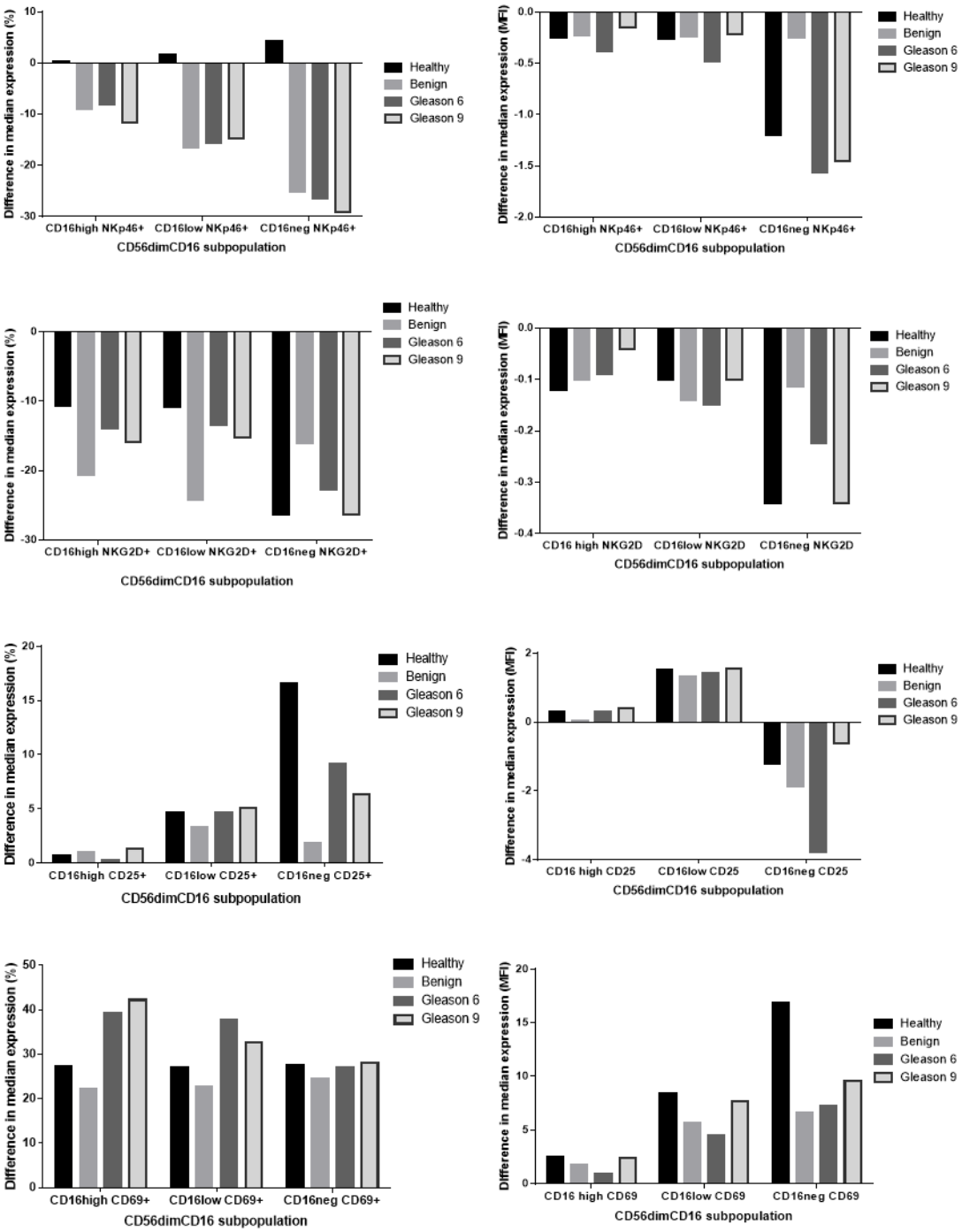

Figure 5.8: The difference in median expression of non-primed and primed NK cells expressing the receptors NKp46, NKG2D, CD25 and CD69 within each NK subpopulation for both healthy volunteers and patients.

For healthy volunteers and each patient group (i.e. Benign, Gleason 6 cancer, Gleason 9 cancer) flow cytometry was used to measure the median fluorescence intensity (MFI) and the percentage of each NK subpopulation expressing the receptors NKp46, NKG2D, CD25 and CD69 before and after priming. For each measurement, the bar graphs above show the difference in the median expression of each receptor between non-primed and primed NK cells from both healthy volunteers and patients.

However, the down-regulation in NKp46 intensity was found to be significant for the healthy volunteer Gleason 6 and Gleason 9 patient groups on the $CD56^{dim}CD16^{neg}$ NK subpopulation only (Figure 5.7).

Similarly to the pattern of expression for NKp46, the proportion of NKG2D was also down-regulated on all 3 NK cell subpopulations following priming for both healthy volunteers and patients. A significant difference within the $CD16^{high}$ and $CD16^{low}$ subpopulations between the primed NK cells of healthy volunteers and the primed NK of patients with benign disease was observed (Figure 5.9). The intensity of NKG2D expression was also decreased on all 3 NK cell subpopulations for both healthy volunteers and patients following priming. However, there was no significant difference in the magnitude of this down-regulation between the three subject groups (Figure 5.8).

5.3.2.2 The influence of NK cell priming on the expression of CD25 and CD69 on $CD56^{dim}CD16^{high}$, $CD56^{dim}CD16^{low}$ and $CD56^{dim}CD16^{neg}$ subpopulations

Although NK cell priming resulted in the up-regulation of CD25, the significance of this increase in expression was limited to the $CD16^{low}$ and $CD16^{neg}$ NK cell subpopulations (with the exception of the benign patient group) for healthy volunteers, Gleason 6 and Gleason 9 patients (Figure 5.10). The proportion of the $CD16^{high}$ NK cell subpopulation up-regulating CD25 averaged between 0.87 and 1.89 % for all subject groups. For the $CD16^{low}$ subpopulation, the average proportion of NK cells expressing CD25 ranged between 3.4 and 5.2 % for all subject groups. The greatest up-regulation of CD25 was observed in the $CD16^{neg}$ subpopulation, with an average proportion of NK cells expressing CD25 ranging between 10.3 and 20.4 %. For all subject groups, the $CD16^{high}$ and $CD16^{low}$ subpopulations marginally up-regulated the intensity of CD25 expression, whereas the $CD16^{neg}$ subpopulations from all subject groups down-regulated the intensity of CD25 expression (Figures 5.8 and 5.10). This disparity is likely due to the low numbers of non-primed NK cells measured in the $CD16^{neg}$ gate during data analysis. Any outliers with a high CD25 MFI may have had a greater effect on the overall MFI value of the non-primed $CD16^{neg}$ subpopulation obtained for each individual regardless of their health status.

For both healthy volunteer and patient NK cells, CD69 was expressed by all 3 subpopulations prior to priming. Furthermore, a large range in the proportion of NK cells expressing CD69 was observed for each subpopulation. CD69 expression (proportion of positive cells and intensity of expression) was significantly, and similarly, upregulated on all 3 NK cell subpopulations from healthy volunteers and patients following priming. However, there was a difference in the magnitude of the intensity of CD69 expression between all 3 NK cell subpopulations (Figure 5.11). In general, for both healthy volunteers and patients, the up-regulation in the intensity of CD69 expression was greater on the $CD16^{neg}$ subpopulation compared to the $CD16^{low}$ and $CD16^{high}$ subpopulations (Figure 5.8). The $CD16^{high}$ subpopulation up-regulated CD69 the least, whereas the $CD16^{neg}$ subpopulation upregulated CD69 the most (Figure 5.8). Noticeably, the $CD16^{neg}$ population from healthy volunteers on average up-regulated a greater intensity of CD69

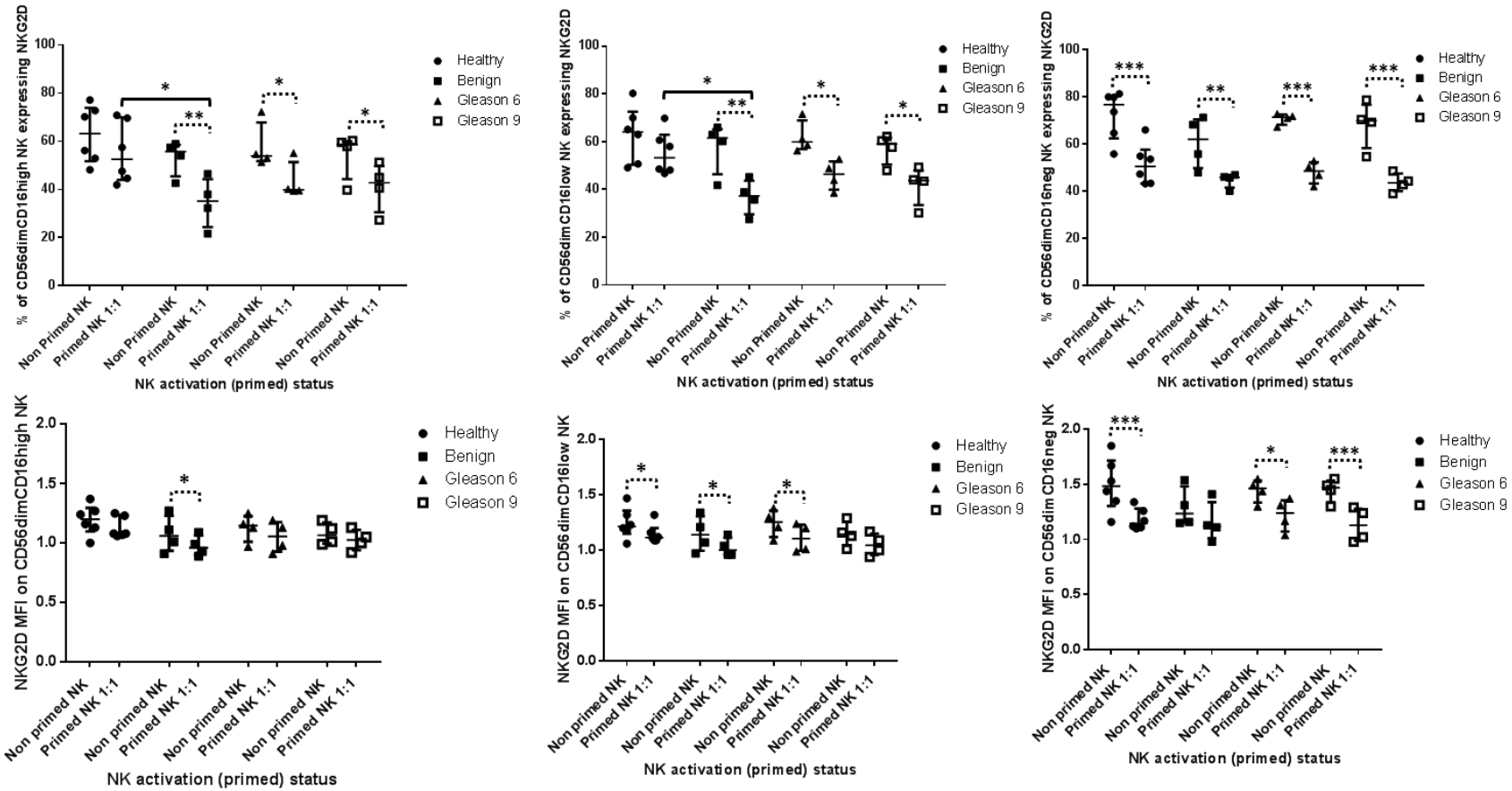

Figure 5.9: The influence of NK cell priming on the expression of NKG2D on the three NK cell subpopulations; $CD56^{dim}CD16^{high}$, $CD56^{dim}CD16^{low}$ and $CD56^{dim}CD16^{neg}$.

NK cells from healthy volunteers and patients with prostate cancer or benign disease were primed with mitomycin C treated CTV-1 at a 1 : 1, NK : CTV-1 ratio for 17 hrs. Both primed NK cells and non-primed control NK cells were stained with NK cell defining antibodies and the NKG2D antibody. The expression of these receptors was measured by flow cytometry. The expression of NKG2D by the three NK cell subpopulations; $CD56^{dim}CD16^{high}$, $CD56^{dim}CD16^{low}$ and $CD56^{dim}CD16^{neg}$, was analysed. The percentage of each NK subpopulation expressing NKG2D (top row of graphs) and the intensity of that expression (bottom for of graphs) was measured. Statistical analysis was done using parametric ANOVA and associated comparison tests; Tukeys multiple comparisons test (solid black line), uncorrected Fishers least significant difference test (dotted black line). * P<0.05, ** P<0.005, ***P<0.0005, **** P<0.00005.

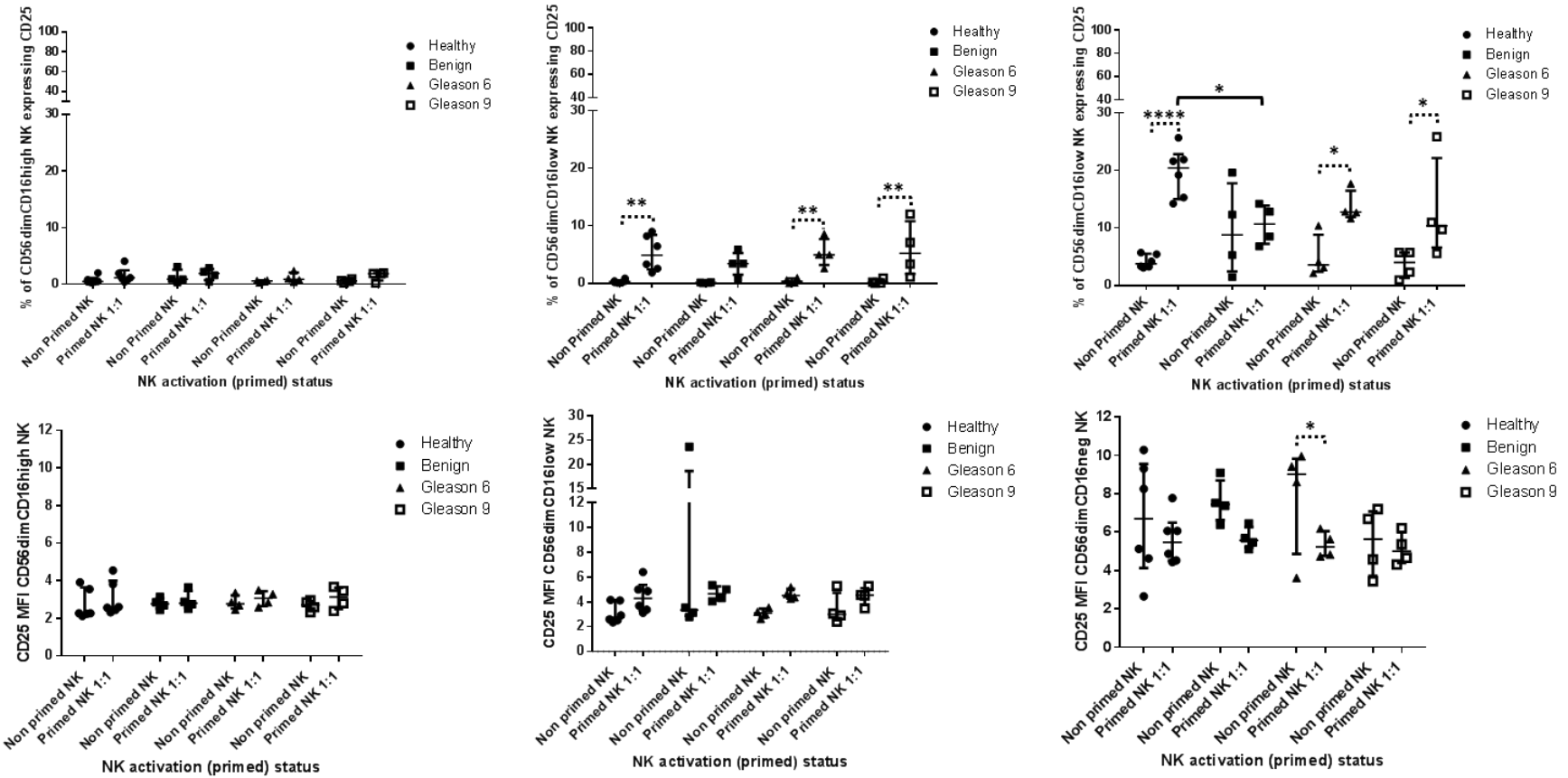

Figure 5.10: The influence of NK cell priming on the expression of CD25 on the three NK cell subpopulations; $CD56^{dim}CD16^{high}$, $CD56^{dim}CD16^{low}$ and $CD56^{dim}CD16^{neg}$.
NK cells from healthy volunteers and patients with prostate cancer or benign disease were primed with mitomycin C treated CTV-1 at a 1 : 1, NK : CTV-1 ratio for 17 hrs. Both primed NK cells and non-primed control NK cells were stained with NK cell defining antibodies and the CD25 antibody. The expression of these receptors was measured by flow cytometry. The expression of CD25 by the three NK cell subpopulations; $CD56^{dim}CD16^{high}$, $CD56^{dim}CD16^{low}$ and $CD56^{dim}CD16^{neg}$, was analysed. The percentage of each NK cell subpopulation expressing CD25 (top row of graphs) and the intensity of that expression (bottom for of graphs) was measured. Statistical analysis was done using parametric ANOVA and associated comparison tests; Tukeys multiple comparisons test (solid black line), uncorrected Fishers least significant difference test (dotted black line). * P<0.05, ** P<0.005, ***P<0.0005, **** P<0.00005.

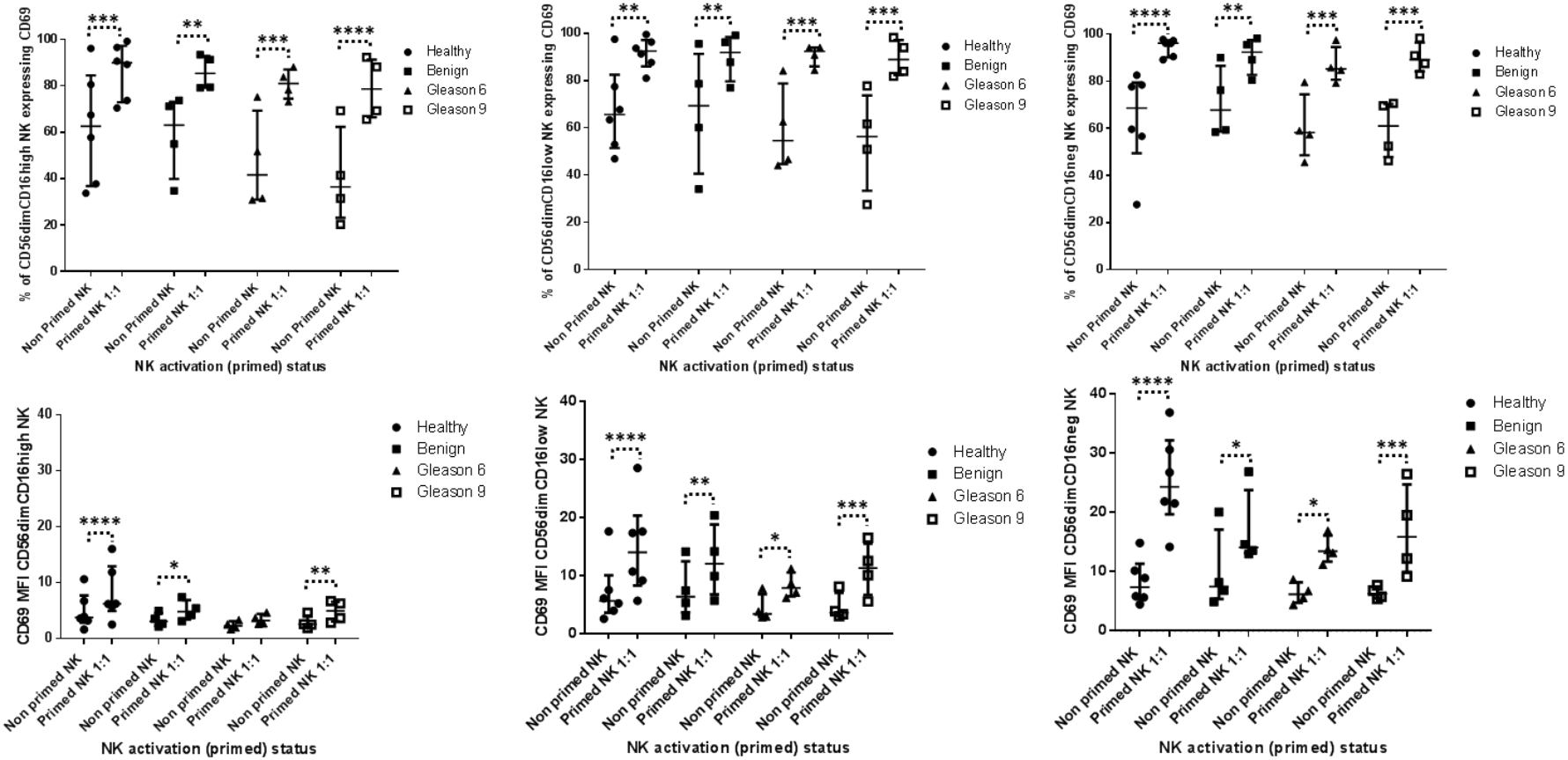

Figure 5.11: The influence of NK cell priming on the expression of CD69 on the three NK cell subpopulations; $CD56^{dim}CD16^{hig}$h, $CD56^{dim}CD16^{low}$ and $CD56^{dim}CD16^{neg}$.
NK cells from healthy volunteers and patients with prostate cancer or benign disease were primed with mitomycin C treated CTV-1 at a 1 : 1, NK : CTV-1 ratio for 17 hrs. Both primed NK cells and non-primed control NK cells were stained with NK cell defining antibodies and the CD69 antibody. The expression of these receptors was measured by flow cytometry. The expression of CD69 by the three NK cell subpopulations; $CD56^{dim}CD16^{high}$, $CD56^{dim}CD16^{low}$ and $CD56^{dim}CD16^{neg}$, was analysed. The percentage of each NK cell subpopulation expressing CD69 (top row of graphs) and the intensity of that expression (bottom for of graphs) was measured. Statistical analysis was done using parametric ANOVA and associated comparison tests; Tukeys multiple comparisons test (solid black line), uncorrected Fishers least significant difference test (dotted black line). * P<0.05, ** P<0.005, ***P<0.0005, **** P<0.00005.

compared to the NK cells from patients which generally up-regulated the expression of CD69 to a similar degree.

5.3.2.3 Influence of NK cell priming on the expression of OX40, CD137, GITR and CRTAM on $CD56^{dim}CD16^{high}$, $CD56^{dim}CD16^{low}$ and $CD56^{dim}CD16^{neg}$ subpopulations

Analysis of the expression of OX40, CD137 and CRTAM on the 3 NK cell subpopulations revealed a similar pattern of up-regulation of all 3 receptors for both healthy volunteers and patients following priming. In regards to the proportion of NK cells expressing OX40, CD137 and CRTAM following priming, in general there was little to no up-regulation on the $CD16^{high}$ subpopulation. A greater proportion of the $CD16^{low}$ NK cell subpopulation up-regulated OX40, CD137 and CRTAM. However, this was less than the $CD16^{neg}$ subpopulation in which the highest proportion of primed NK cells up-regulated OX40, CD137 and CRTAM (Figures 5.12 to 5.15). Focusing on the $CD16^{low}$ subpopulation, a similar proportion of primed NK cells from healthy volunteers and patients expressed OX40 (median expression ranged 5 to 8 %) and CD137 (median expression ranged 14 to 15). In contrast, there was a greater difference in the median proportion of NK cells expressing CRTAM; NK cells from healthy volunteers 26.7 %, NK cells from individuals with benign disease and Gleason 6 disease 17 and 20.4 % respectively, NK cells from patients with Gleason 9 disease 12.6 %. Regarding the $CD16^{neg}$ subpopulation, in general a greater proportion of NK cells from healthy volunteers expressed CD137 and CRTAM compared to NK cells from patients, whereas a similar proportions of NK cells from healthy volunteers and patients expressed the OX40 receptor. The median proportion of $CD16^{neg}$ NK cells from healthy volunteers expressing CD137 and CRTAM was 42 and 50 % respectively, whereas the median proportion of $CD16^{neg}$ NK cells from patients expressing CD137 and CRTAM ranged between 22.7 and 28.9 % and 21 and 28 % respectively (Figures 5.13 and 5.14).

For all subject groups, the intensity of OX40 expression on each NK cell subpopulation only marginally changed after priming. In contrast, a greater increase in MFI for CD137 and CRTAM was observed following NK cell priming, with the magnitude of this increase being different for the 3 NK cell subpopulations. However, when comparing the MFI of OX40, CD137 and CRTAM expression on primed NK cells from healthy volunteers and patients, no significant differences was observed. In general, priming induced only a minor increase in the expression (MFI) of CD137 and CRTAM on the $CD16^{high}$ NK cell subpopulation. In comparison, the $CD16^{low}$ subpopulation exhibited a slightly greater increase in the intensity of expression of both receptors following priming. The $CD16^{neg}$ subpopulation exhibited the greatest increase in the intensity of expression for CD137 and CRTAM of the 3 NK cell subpopulations.

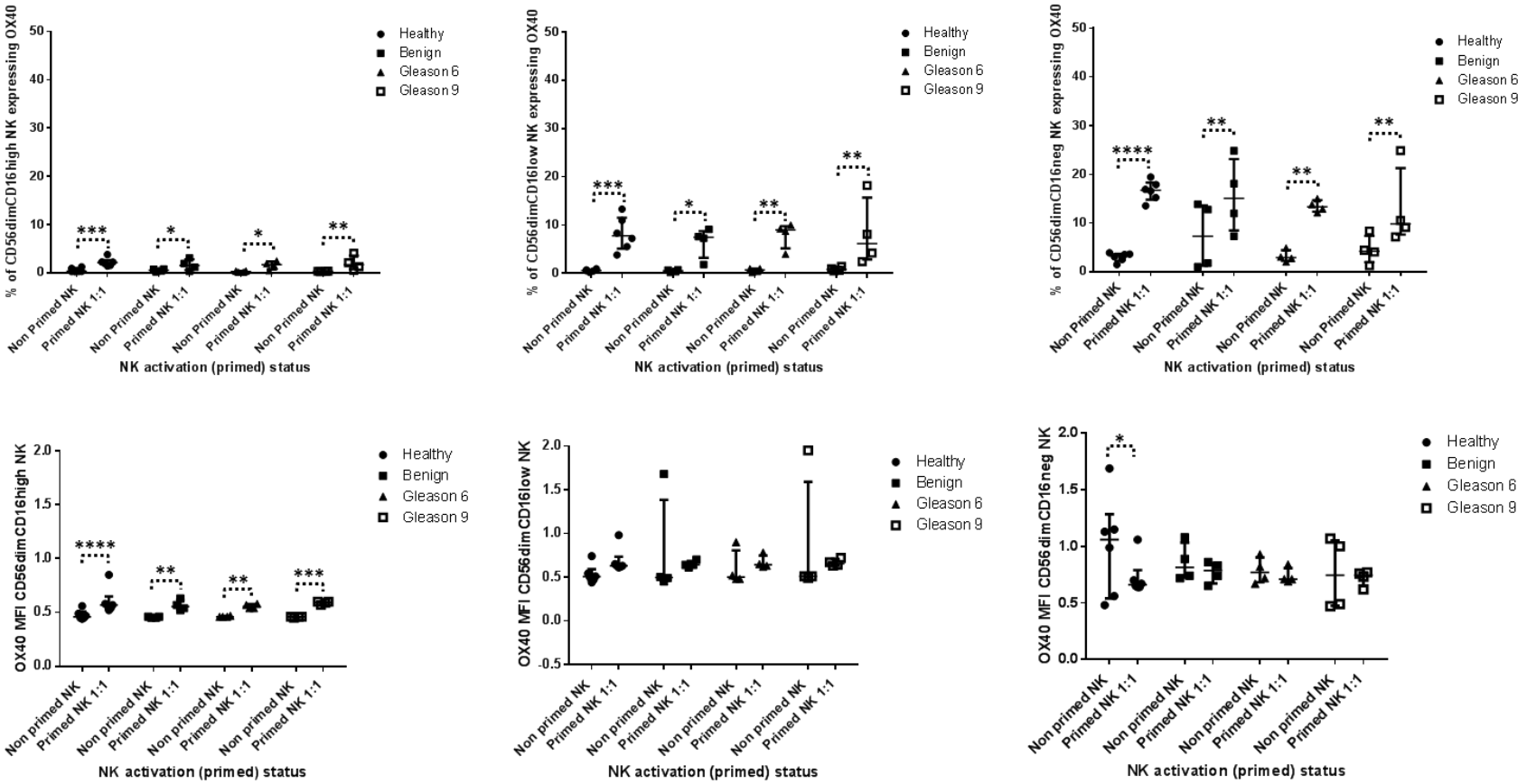

Figure 5.12: The influence of NK cell priming on the expression of OX40 on the three NK cell subpopulations; $CD56^{dim}CD16^{high}$, $CD56^{dim}CD16^{low}$ and $CD56^{dim}CD16^{neg}$.
NK cells from healthy volunteers and patients with prostate cancer or benign disease were primed with mitomycin C treated CTV-1 at a 1 : 1, NK : CTV-1 ratio for 17 hrs. Both primed NK cells and non-primed control NK cells were stained with NK cell defining antibodies and the OX40 antibody. The expression of these receptors was measured by flow cytometry. The expression of OX40 by the three NK cell subpopulations; $CD56^{dim}CD16^{high}$, $CD56^{dim}CD16^{low}$ and $CD56^{dim}CD16^{neg}$, was analysed. The percentage of each NK cell subpopulation expressing OX40 (top row of graphs) and the intensity of that expression (bottom for of graphs) was measured. Statistical analysis was done using parametric ANOVA and associated comparison tests; Tukeys multiple comparisons test (solid black line), uncorrected Fishers least significant difference test (dotted black line). * P<0.05, ** P<0.005, ***P<0.0005, **** P<0.00005.

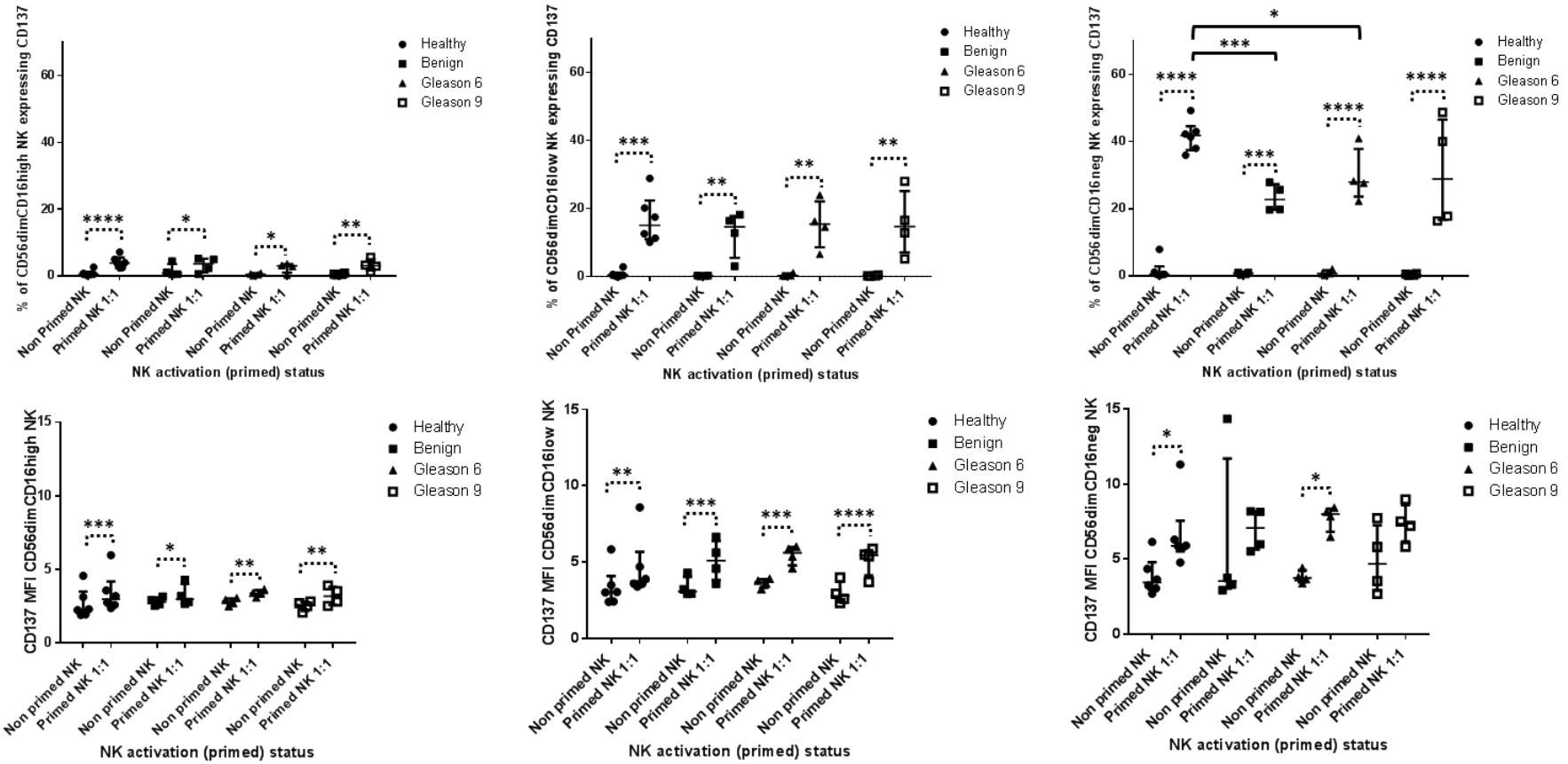

Figure 5.13: The influence of NK cell priming on the expression of CD137 on the three NK cell subpopulations; $CD56^{dim}CD16^{high}$, $CD56^{dim}CD16^{low}$ and $CD56^{dim}CD16^{neg}$.
NK cells from healthy volunteers and patients with prostate cancer or benign disease were primed with mitomycin C treated CTV-1 at a 1 : 1, NK : CTV-1 ratio for 17 hrs. Both primed NK cells and non-primed control NK cells were stained with NK cell defining antibodies and the CD137 antibody. The expression of these receptors was measured by flow cytometry. The expression of CD137 by the three NK cell subpopulations; $CD56^{dim}CD16^{high}$, $CD56^{dim}CD16^{low}$ and $CD56^{dim}CD16^{neg}$, was analysed. The percentage of each NK cell subpopulation expressing CD137 (top row of graphs) and the intensity of that expression (bottom for of graphs) was measured. Statistical analysis was done using parametric ANOVA and associated comparison tests; Tukeys multiple comparisons test (solid black line), uncorrected Fishers least significant difference test (dotted black line). * P<0.05, ** P<0.005, ***P<0.0005, **** P<0.00005.

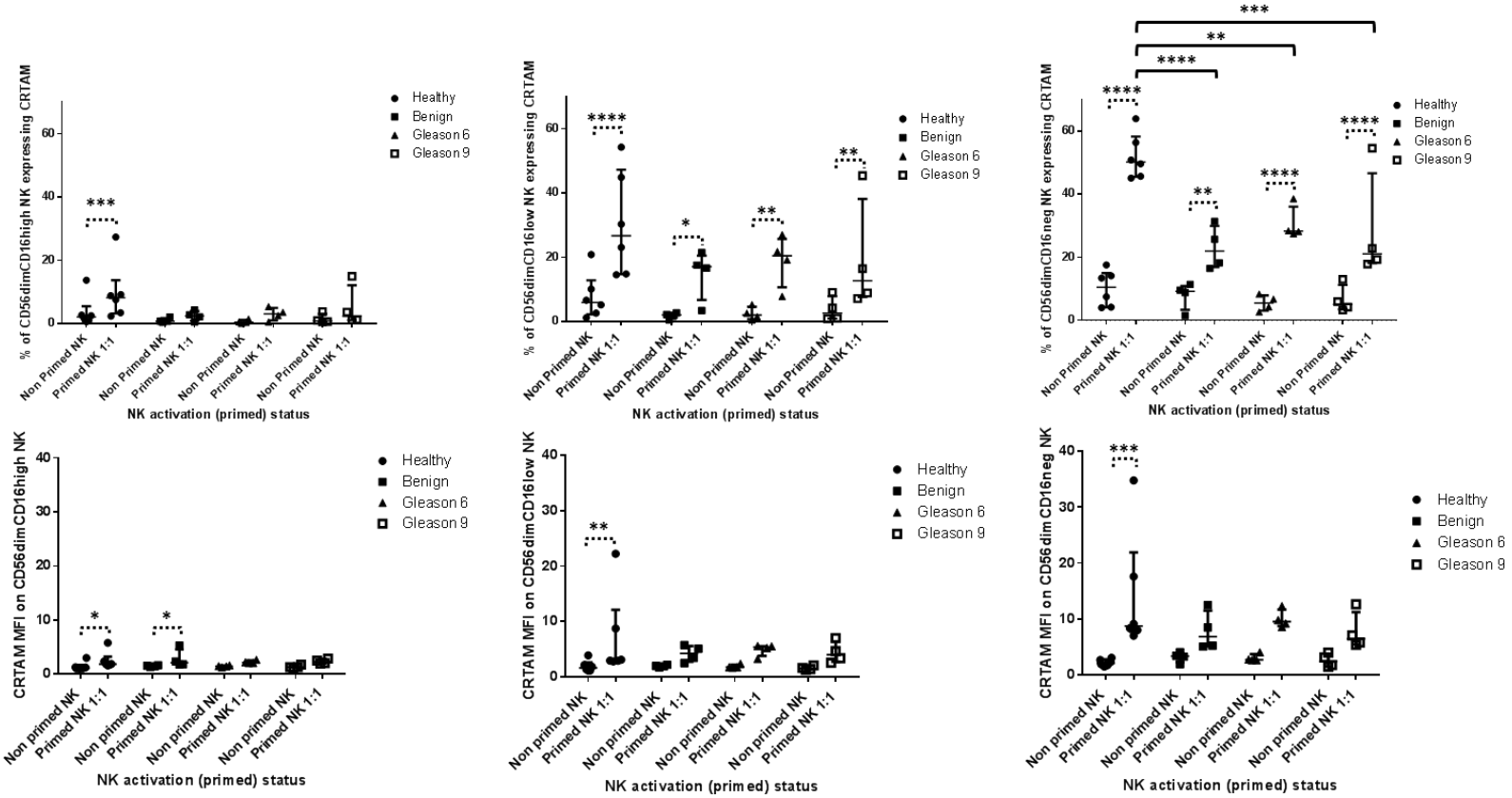

Figure 5.14: The influence of NK cell priming on the expression of CRTAM on the three NK cell subpopulations; CD56^{dim}CD16^{high}, CD56^{dim}CD16^{low} and CD56^{dim}CD16^{neg}.
NK cells from healthy volunteers and patients with prostate cancer or benign disease were primed with mitomycin C treated CTV-1 at a 1 : 1, NK : CTV-1 ratio for 17 hrs. Both primed NK cells and non-primed control NK cells were stained with NK cell defining antibodies and the CRTAM antibody. The expression of these receptors was measured by flow cytometry. The expression of CRTAM by the three NK cell subpopulations; CD56^{dim}CD16^{high}, CD56^{dim}CD16^{low} and CD56^{dim}CD16^{neg}, was analysed. The percentage of each NK cell subpopulation expressing CRTAM (top row of graphs) and the intensity of that expression (bottom for of graphs) was measured. Statistical analysis was done using parametric ANOVA and associated comparison tests; Tukeys multiple comparisons test (solid black line), uncorrected Fishers least significant difference test (dotted black line). * P<0.05, ** P<0.005, ***P<0.0005, **** P<0.00005.

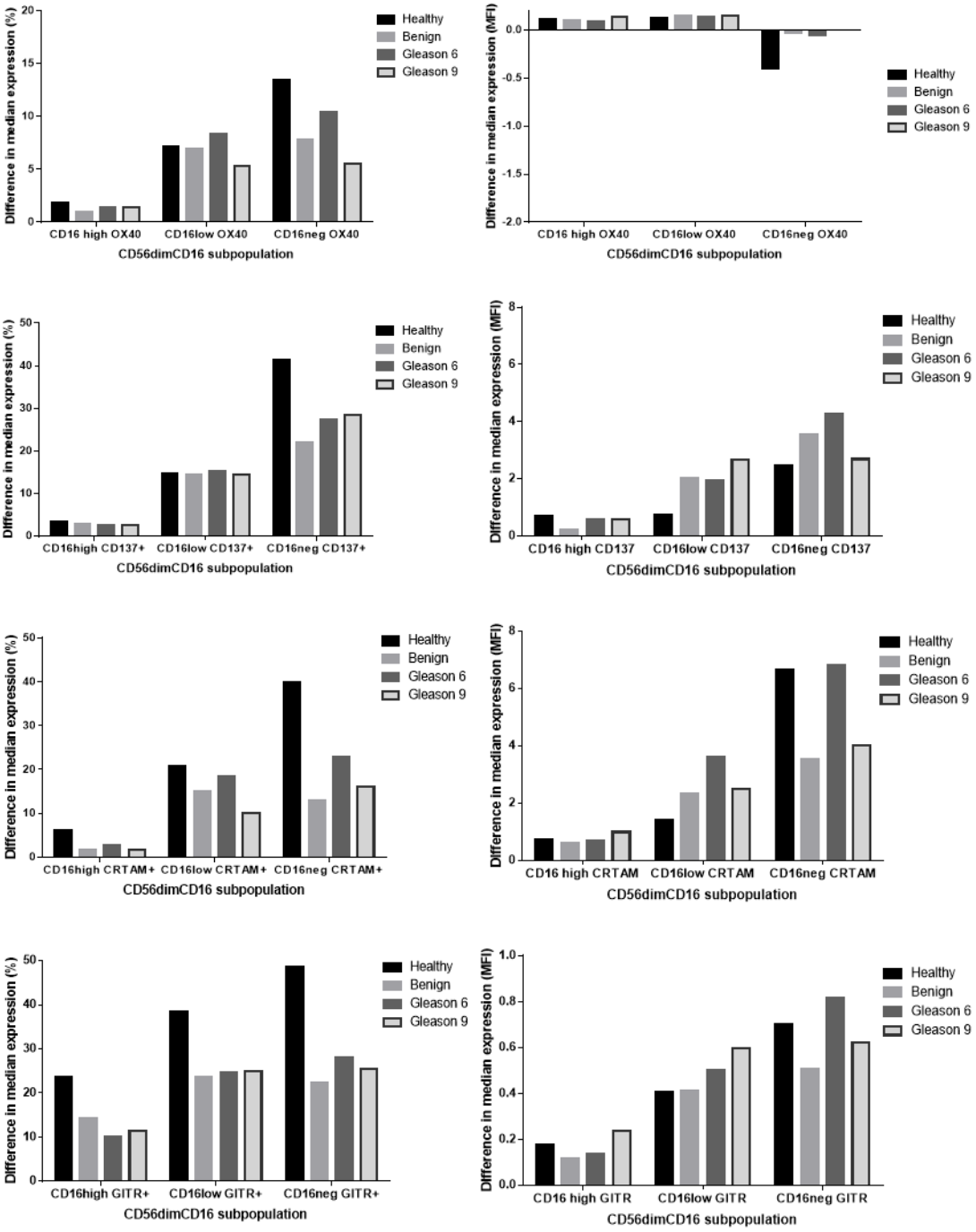

Figure 5.15: The difference in median expression of the receptors OX40, CD137, CRTAM and GITR by non-primed and primed NK cells within each NK cell subpopulation for both healthy volunteers and patients.

For healthy volunteers and each patient group (i.e. benign disease, Gleason 6 cancer, Gleason 9 cancer), flow cytometry was used to measure the median fluorescence intensity (MFI) and the percentage of each NK cell subpopulation expressing the receptors OX40, CD137, CRTAM and GITR before and after priming. For each measurement, the bar graphs above show the difference in the median expression of each receptor between non-primed and primed NK cells.

Although non-primed NK cells from healthy volunteers and patients expressed no OX40, CD137 or CRTAM (only background levels) they did express GITR, but with no significant difference between them. Nor was a difference observed between NK cell subpopulations of non-primed NK cells. Following NK priming, the proportion of NK cells from healthy volunteers and patients

expressing GITR increased for all 3 NK cell subpopulations (Figure 5.16). In general, for both healthy volunteers and patients, a similar proportion of primed $CD16^{neg}$ NK cells expressed GITR compared to primed $CD16^{low}$ NK cells, whereas less $CD56^{dim}CD16^{high}$ NK cells expressed GITR. On average, a greater proportion of NK cells from healthy individuals expressed GITR than NK cells from patients, which in turn all expressed GITR to a similar degree. This was true for all 3 NK subpopulations.

Similar to CD137 and CRTAM, the median intensity of GITR significantly increased following NK cell priming, with the exception of the $CD16^{neg}$ NK cell subpopulation for the Benign and Gleason 9 patients for which the increase in GITR expression was not found to be significant. As with the expression of CD137 and CRTAM, the intensity of GITR expression was higher on the $CD16^{neg}$ subpopulation compared to the $CD16^{low}$ and $CD16^{high}$ subpopulations. The $CD16^{neg}$ NK cells expressed the lowest intensity of GITR. In general, there was no noticeable difference in the intensity of GITR expression on non-primed and primed NK cells between healthy volunteers and patients.

5.3.2.4 Expression of DNAM-1, TIGIT and CD96 on CD16 subpopulations.

For both healthy volunteers and patients, there was no increase in the proportion of $CD16^{high}$ and $CD16^{low}$ NK cells expressing DNAM-1 following NK cell priming. The proportion of $CD16^{high}$ and $CD16^{low}$ NK cells expressing DNAM-1 ranged between 93 and 99 % for both primed and non-primed NK cells. However, a small increase in the proportion of the $CD16^{neg}$ NK cell subpopulation from healthy volunteers and patients expressing DNAM-1 was observed following priming. Only the increase seen on NK cells from patients with Gleason 9 disease was found to be significant (Figure 5.17).

For both healthy volunteers and patients, the intensity of DNAM-1 expression on $CD16^{neg}$ NK cells was also significantly up-regulated following NK cell priming - from an MFI of ~2 expressed by non-primed NK cells to an MFI level of ~2.5 expressed by primed NK cells. Changes in the intensity of DNAM-1 on the $CD16^{high}$ and $CD16^{low}$ NK subpopulations were not significant and appeared to be a combination of minor up-regulation and down-regulation (Figure 5.17).

Similar to DNAM-1, NK cell priming did not significantly alter the proportion of $CD16^{high}$ and $CD16^{low}$ NK cells from healthy volunteers and patients expressing TIGIT. However, the proportion of $CD16^{neg}$ NK cells from all subject groups expressing TIGIT significantly increased following NK cell priming. The median proportion of non-primed $CD16^{neg}$ NK cells expressing TIGIT for healthy volunteers (66%) was higher than the median for the patient NK cell groups; individuals with

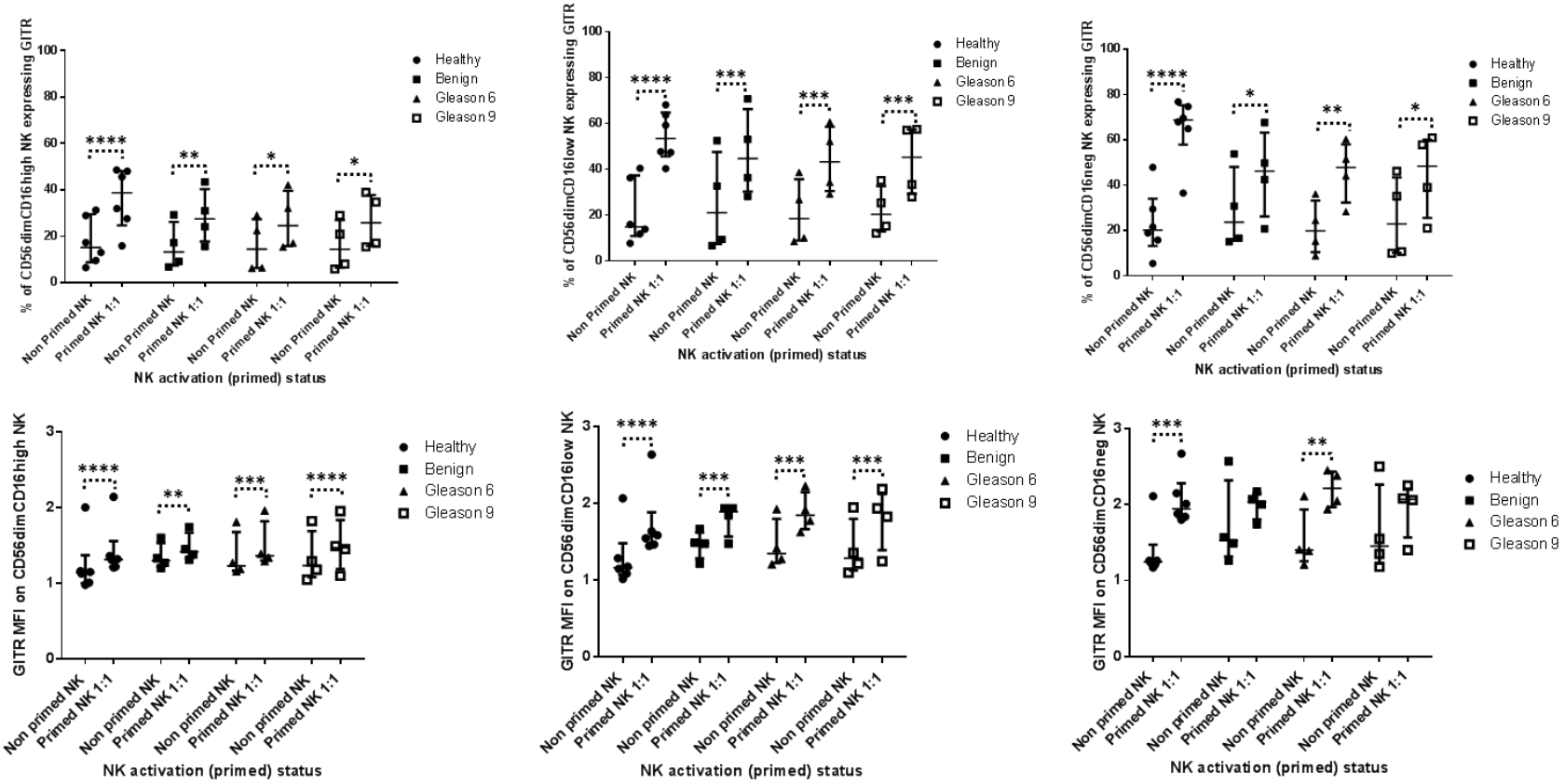

Figure 5.16: The influence of NK cell priming on the expression of GITR on the three NK cell subpopulations; $CD56^{dim}CD16^{high}$, $CD56^{dim}CD16^{low}$ and $CD56^{dim}CD16^{neg}$.
NK cells from healthy volunteers and patients with prostate cancer or benign disease were primed with mitomycin C treated CTV-1 at a 1 : 1, NK : CTV-1 ratio for 17 hrs. Both primed NK cells and non-primed control NK cells were stained with NK cell defining antibodies and the GITR antibody. The expression of these receptors was measured by flow cytometry. The expression of GITR by the three NK cell subpopulations; $CD56^{dim}CD16^{high}$, $CD56^{dim}CD16^{low}$ and $CD56^{dim}CD16^{neg}$, was analysed. The percentage of each NK cell subpopulation expressing GITR (top row of graphs) and the intensity of that expression (bottom for of graphs) was measured. Statistical analysis was done using parametric ANOVA and associated comparison tests; Tukeys multiple comparisons test (solid black line), uncorrected Fishers least significant difference test (dotted black line). * P<0.05, ** P<0.005, ***P<0.0005, **** P<0.00005.

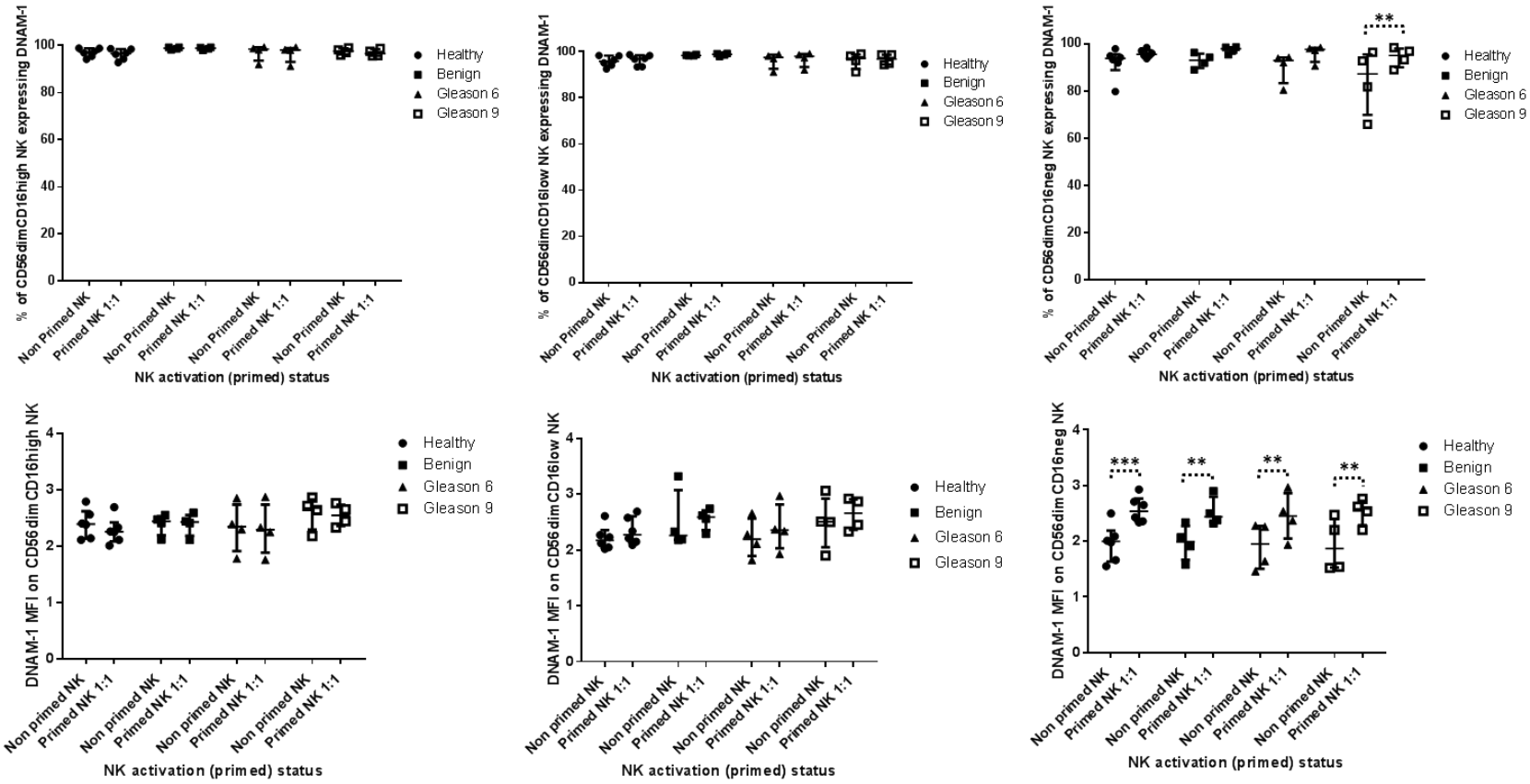

Figure 5.17: The influence of NK cell priming on the expression of DNAM-1 on the three NK cell subpopulations; $CD56^{dim}CD16^{high}$, $CD56^{dim}CD16^{low}$ and $CD56^{dim}CD16^{neg}$.
NK cells from healthy volunteers and patients with prostate cancer or benign disease were primed with mitomycin C treated CTV-1 at a 1 : 1, NK : CTV-1 ratio for 17 hrs. Both primed NK cells and non-primed control NK cells were stained with NK cell defining antibodies and the DNAM-1 antibody. The expression of these receptors was measured by flow cytometry. The expression of DNAM-1 by the three NK cell subpopulations; $CD56^{dim}CD16^{high}$, $CD56^{dim}CD16^{low}$ and $CD56^{dim}CD16^{neg}$, was analysed. The percentage of each NK cell subpopulation expressing DNAM-1 (top row of graphs) and the intensity of that expression (bottom for of graphs) was measured. Statistical analysis was done using parametric ANOVA and associated comparison tests; Tukeys multiple comparisons test (solid black line), uncorrected Fishers least significant difference test (dotted black line). * P<0.05, ** P<0.005, ***P<0.0005, **** P<0.00005.

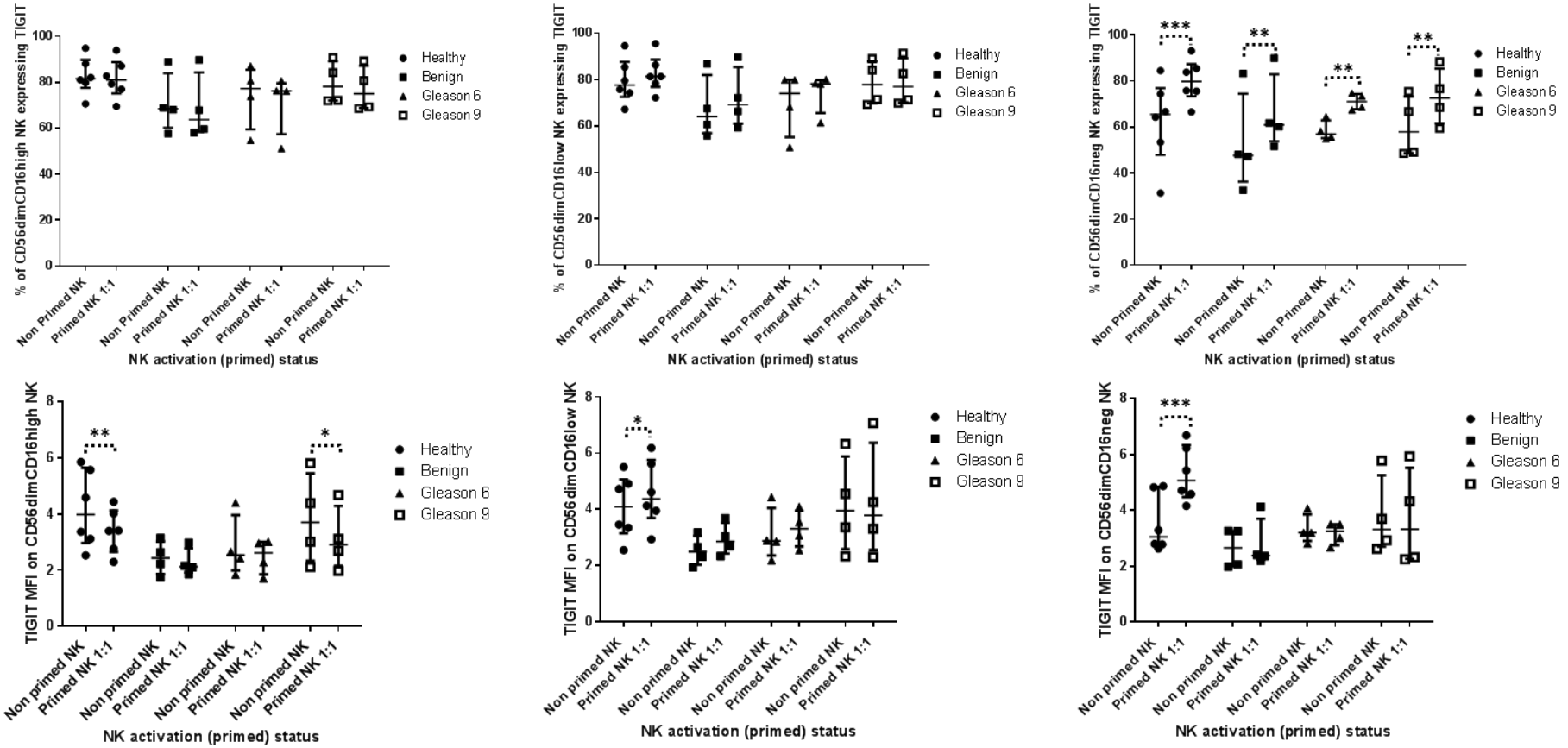

Figure 5.18: The influence of NK cell priming on the expression of TIGIT on the three NK cell subpopulations; CD56^{dim}CD16^{high}, CD56^{dim}CD16^{low} and CD56^{dim}CD16^{neg}.
NK cells from healthy volunteers and patients with prostate cancer or benign disease were primed with mitomycin C treated CTV-1 at a 1 : 1, NK : CTV-1 ratio for 17 hrs. Both primed NK cells and non-primed control NK cells were stained with NK cell defining antibodies and the TIGIT antibody. The expression of these receptors was measured by flow cytometry. The expression of TIGIT by the three NK cell subpopulations; CD56^{dim}CD16^{high}, CD56^{dim}CD16^{low} and CD56^{dim}CD16^{neg}, was analysed. The percentage of each NK cell subpopulation expressing TIGIT (top row of graphs) and the intensity of that expression (bottom for of graphs) was measured. Statistical analysis was done using parametric ANOVA and associated comparison tests; Tukeys multiple comparisons test (solid black line), uncorrected Fishers least significant difference test (dotted black line). * P<0.05, ** P<0.005. ***P<0.0005. **** P<0.00005.

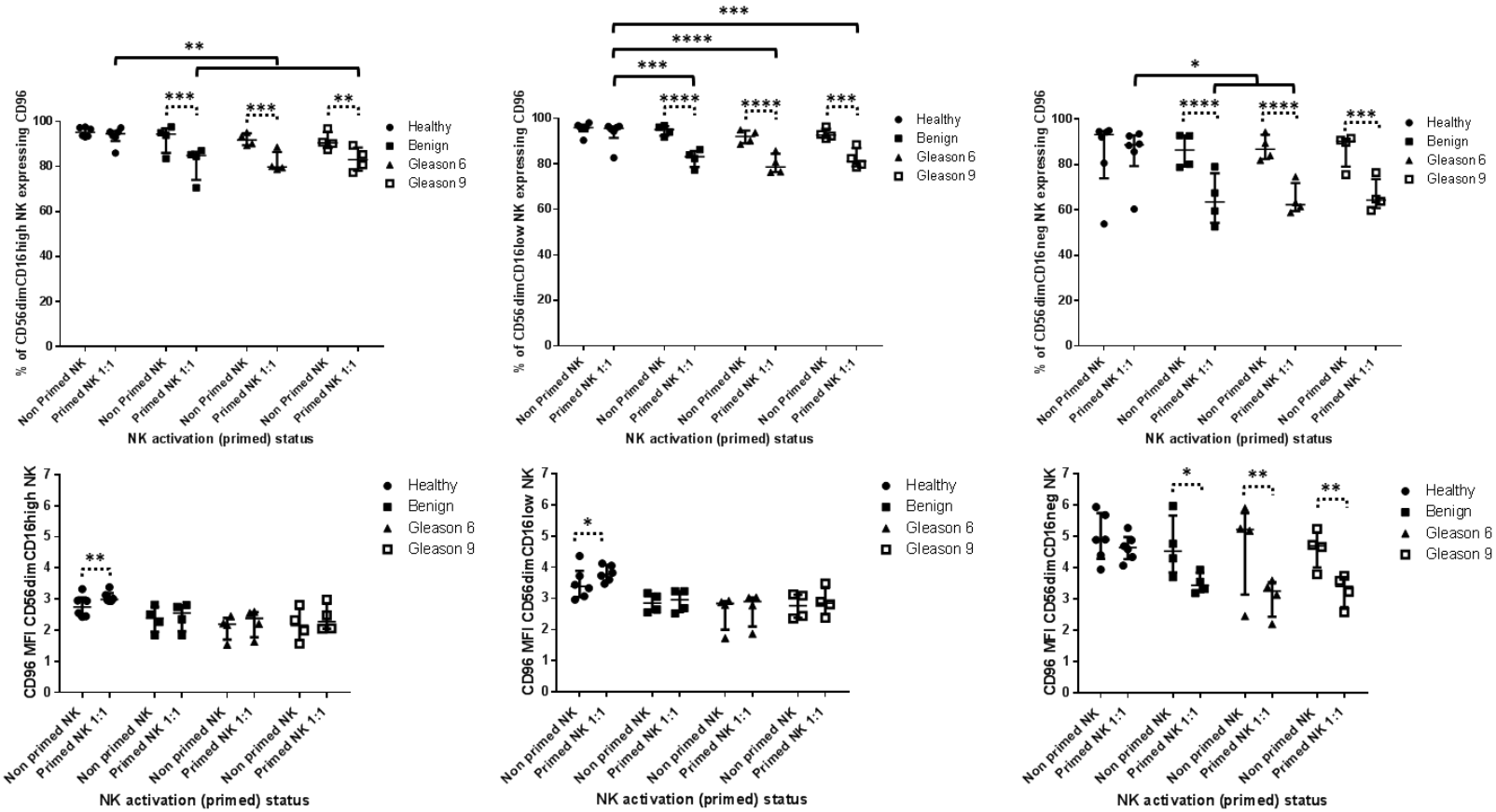

Figure 5.19: The influence of NK cell priming on the expression of CD96 on the three NK cell subpopulations; $CD56^{dim}CD16^{high}$, $CD56^{dim}CD16^{low}$ and $CD56^{dim}CD16^{neg}$.
NK cells from healthy volunteers and patients with prostate cancer or benign disease were primed with mitomycin C treated CTV-1 at a 1 : 1, NK : CTV-1 ratio for 17 hrs. Both primed NK cells and non-primed control NK cells were stained with NK cell defining antibodies and the CD96 antibody. The expression of these receptors was measured by flow cytometry. The expression of CD96 by the three NK subpopulations; $CD56^{dim}CD16^{high}$, $CD56^{dim}CD16^{low}$ and $CD56^{dim}CD16^{neg}$, was analysed. The percentage of each NK subpopulation expressing CD96 (top row of graphs) and the intensity of that expression (bottom for of graphs) was measured. Statistical analysis was done using parametric ANOVA and associated comparison tests; Tukeys multiple comparisons test (solid black line), uncorrected Fishers least significant difference test (dotted black line). * P<0.05, ** P<0.005, ***P<0.0005, **** P<0.00005.

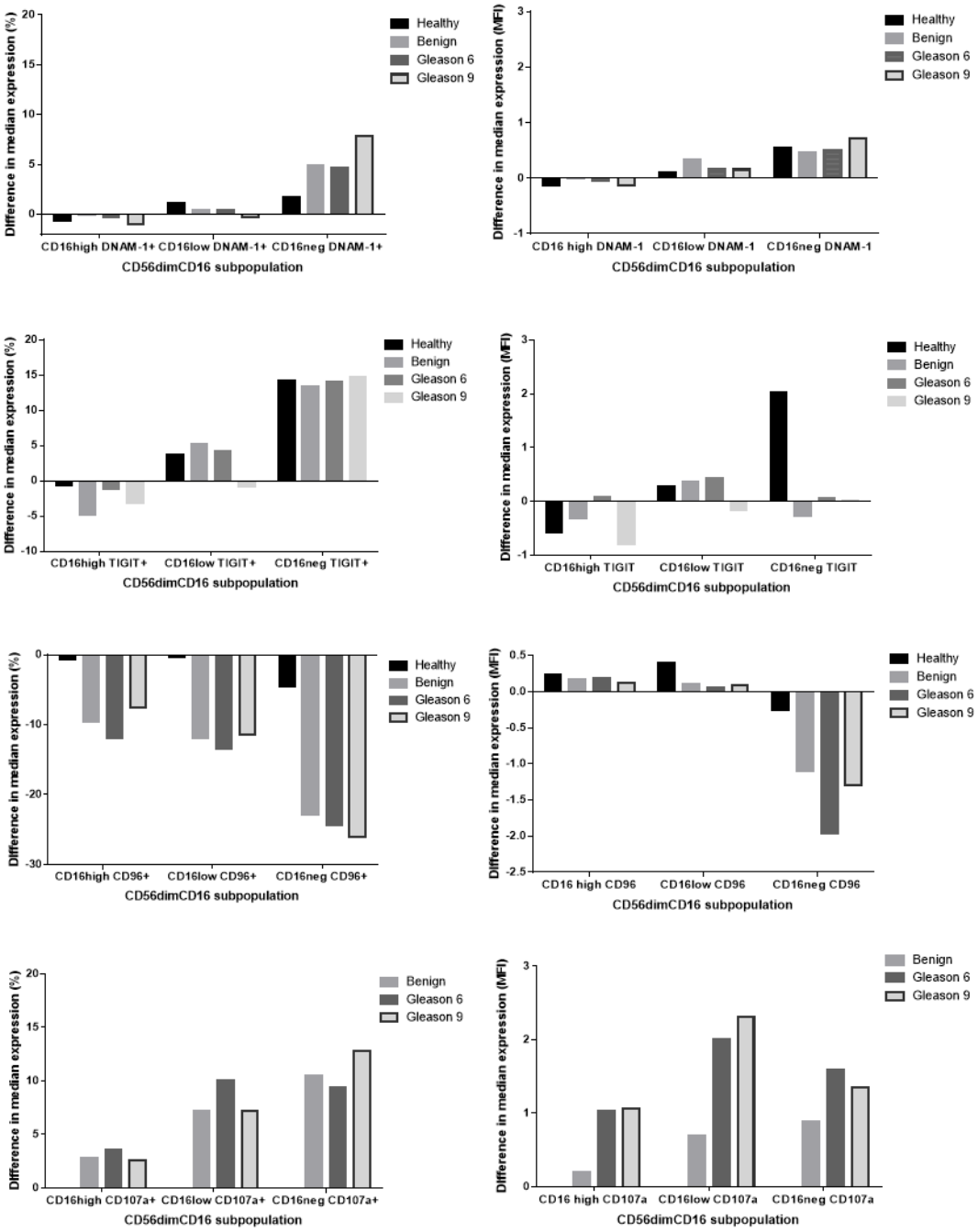

Figure 5.20: The difference in median expression of the receptors DNAM-1, TIGIT, CD96 and CD107a by non-primed and primed NK cells within each NK subpopulation for both healthy volunteers and patients.

For healthy volunteers and each patient group (i.e. benign disease, Gleason 6 cancer, Gleason 9 cancer), flow cytometry was used to measure the median fluorescence intensity (MFI) and the percentage of each NK cell subpopulation expressing the receptors DNAM-1, TIGIT, CD96 and CD107a before and after priming. For each measurement, the bar graphs above show the difference in the median expression of each receptor between non-primed and primed NK cells.

benign disease 48 %, patients with Gleason 6 disease 57 %, patients with Gleason 9 disease 58%. Upon priming, the median proportion of NK cells from healthy volunteers expressing TIGIT increased to 80 % which again was higher than the median values for NK cells from the patient groups; individuals with benign disease 61 %, patients with Gleason 6 disease 71 %, patients

with Gleason 9 disease 73 %. In contrast, only the $CD16^{neg}$ NK cell subpopulation from the healthy volunteers significantly up-regulated their TIGIT expression following priming (MFI 3 vs 5, non-primed vs primed respectively, Figure 5.18).

The pattern of expression of CD96 on the 3 NK cell subpopulations following priming was different compared to TIGIT and DNAM-1. Priming resulted in the proportion of all 3 NK subpopulations from the 3 patient groups significantly down-regulating the expression of CD96. In contrast, priming had no significant effect on the expression of CD96 by the 3 NK cell subpopulations from healthy volunteers (Figure 5.19). Furthermore, priming down-regulated the intensity of CD96 expression on the $CD16^{neg}$ NK cell subpopulation from the 3 patient groups. This down-regulation was not observed on the $CD16^{low}$ and $CD16^{high}$ subpopulations. In contrast to the patient groups, the intensity of CD96 expression on the $CD16^{neg}$ NK cell subpopulation from healthy volunteers was significantly down-regulated by priming, whereas the $CD16^{high}$ and $CD16^{low}$ subpopulations significantly up-regulated their expression of CD96. The intensity of CD96 expression on the $CD16^{high}$ and $CD16^{low}$ NK cell subpopulations from patients did not significantly change following priming.

5.3.2.5 Expression of CD107a and its correlation with other receptors

Due to time constraints, the influence of priming on CD107a expression was only determined using NK cells obtained from patients. Although non-primed NK cells did not express CD107a, expression, in terms of the intensity of expression and the proportion of NK cells expressing, was upregulated on all 3 NK cell subpopulations following priming (Figure 5.20). Similar to the expression of CD25, CD137 and CRTAM, a greater proportion of the $CD16^{neg}$ NK cell subpopulation up-regulated CD107a following priming compared to both the $CD16^{low}$ and $CD16^{high}$ NK cell subpopulations. The $CD16^{high}$ NK cell subpopulation exhibited the smallest increase in the proportion of cells expressing CD107a (Figures 5.21). In terms of the proportion of NK cells, there were no significant differences between the ability of the 3 patient groups to up-regulate CD107a. Although the intensity of CD107a expression on all 3 NK cell subpopulations increased as result of priming, the increase was not significant for any of the 3 patient groups in regards to the $CD16^{neg}$ NK cell subpopulation. In contrast, the increase in CD107a intensity was significant on the $CD16^{high}$ and $CD16^{low}$ NK cell subpopulations, but only for the Gleason 6 and Gleason 9 patients. The increase in CD107a intensity of the $CD16^{high}$ population for both Gleason 6 and Gleason 9 patients was significantly higher than the individuals with benign disease.

Next, using data from all 3 patient groups I wanted to test whether the up-regulation in the proportion of NK cells expressing CD107a correlated with the proportion of NK cells expressing other receptors such as OX40, CD137, CRTAM, GITR, CD25, CD96, NKp46 and NKG2D that were

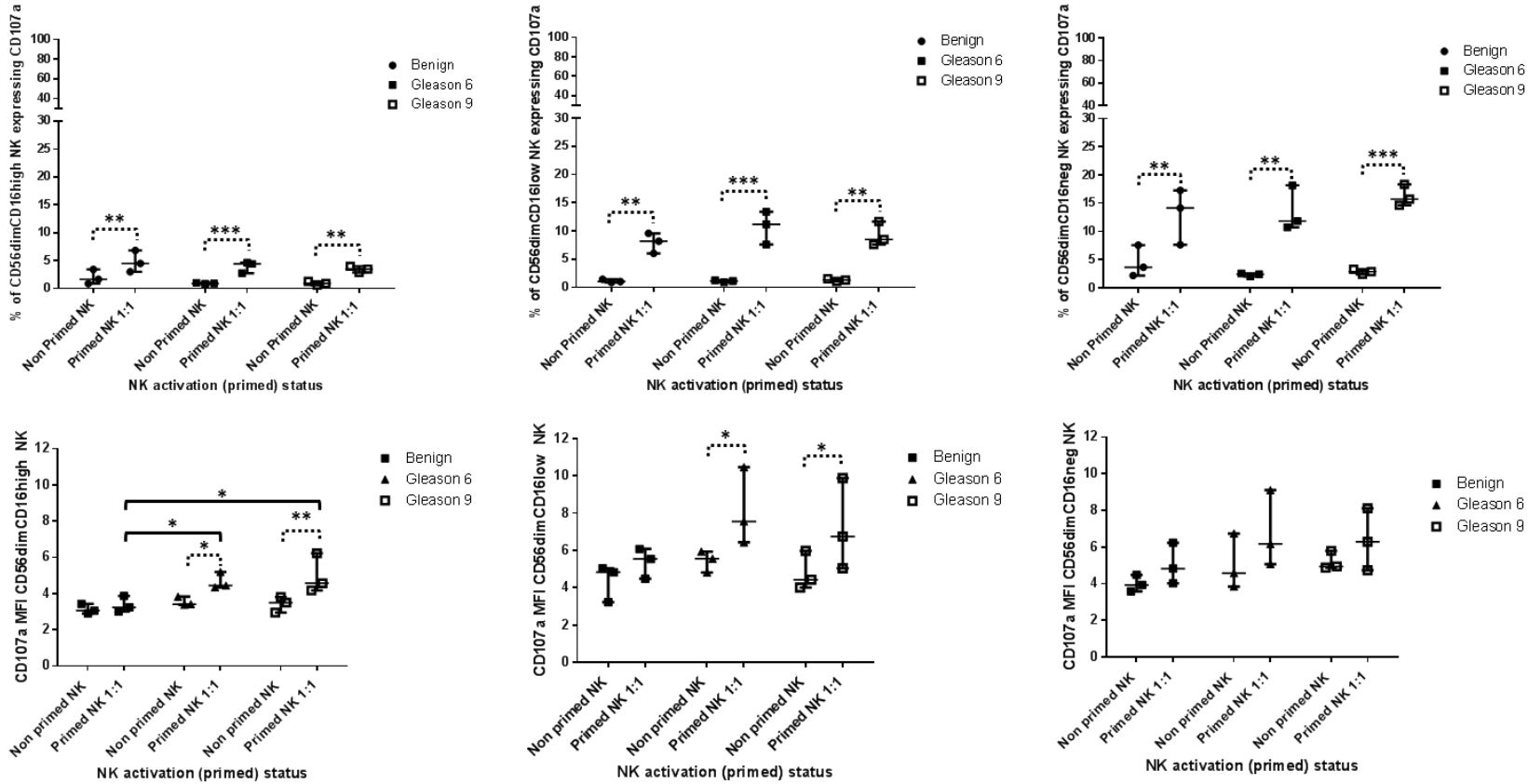

Figure 5.21: The influence of NK cell priming on the expression of CD107a on the three NK cell subpopulations; $CD56^{dim}CD16^{high}$, $CD56^{dim}CD16^{low}$ and $CD56^{dim}CD16^{neg}$.
NK cells from healthy volunteers and patients with prostate cancer or benign disease were primed with mitomycin C treated CTV-1 at a 1 : 1, NK : CTV-1 ratio for 17 hrs. Both primed NK cells and non-primed control NK cells were stained with NK cell defining antibodies and the CD107a antibody. The expression of these receptors was measured by flow cytometry. The expression of CD107a by the three NK cell subpopulations; $CD56^{dim}CD16^{high}$, $CD56^{dim}CD16^{low}$ and $CD56^{dim}CD16^{neg}$, was analysed. The percentage of each NK cell subpopulation expressing CD107a (top row of graphs) and the intensity of that expression (bottom for of graphs) was measured. Statistical analysis was done using parametric ANOVA and associated comparison tests; Tukeys multiple comparisons test (solid black line), uncorrected Fishers least significant difference test (dotted black line). * P<0.05, ** P<0.005, ***P<0.0005, **** P<0.00005.

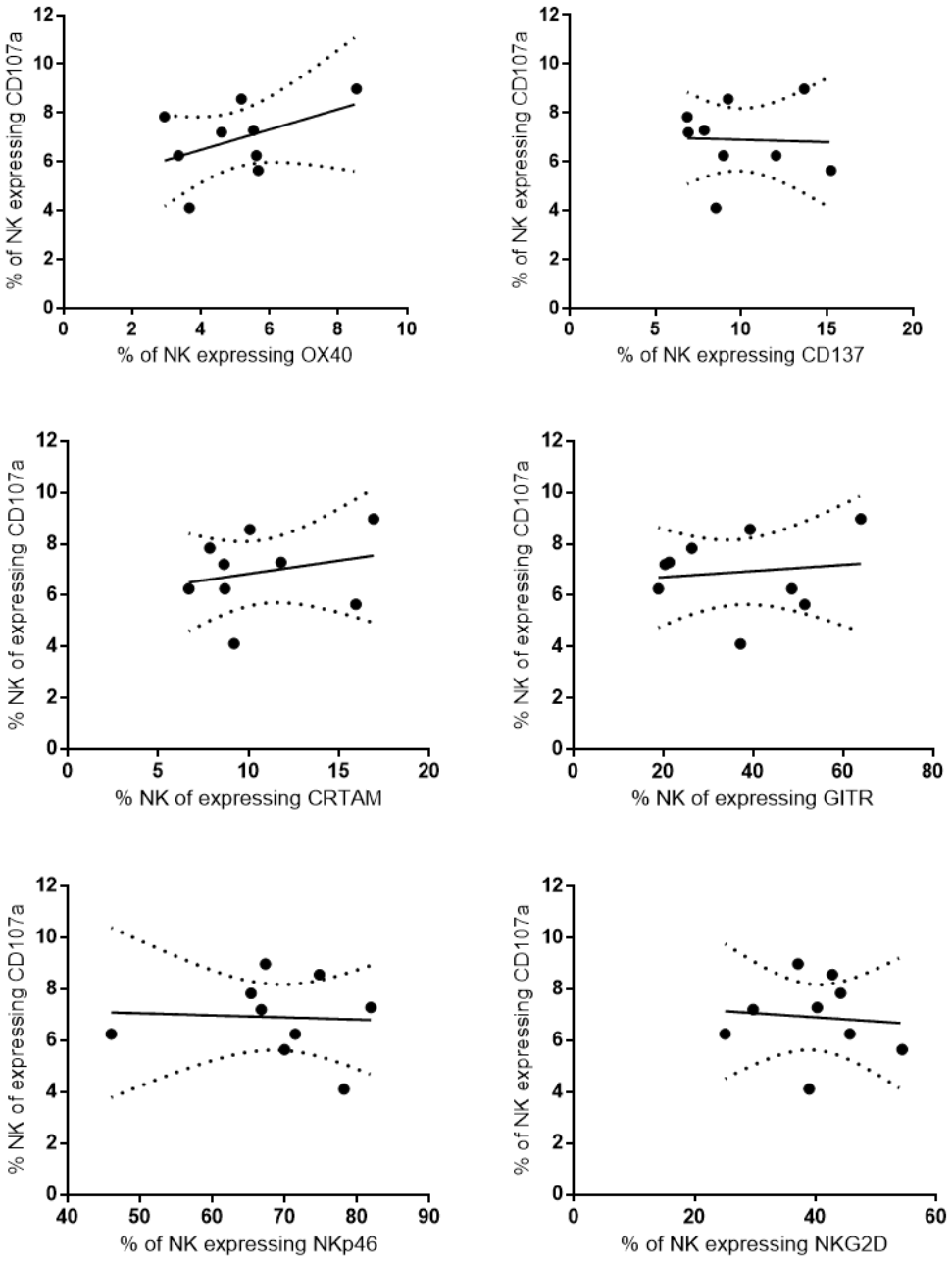

Figure 5.22: Correlation between CD107a expression and the expression of receptors OX40, CD137, CRTAM, GITR, NKp46 and NKG2D on primed NK cells.
NK cells from patients with Gleason 6 prostate cancer, Gleason 9 prostate cancer and individuals with benign disease were primed with mitomycin C treated CTV-1 at a 1 : 1, NK : CTV-1 ratio for 17 hrs. Primed NK cells were stained with NK cell defining antibodies, CD107a, OX40, CD137, CRTAM, GITR, NKp46 and NKG2D antibodies. For each individual, the expression of CD107a on primed NK cells was correlated with their expression of the receptors OX40, CD137, CRTAM, GITR, NKp46 and NKG2D.

also modified as a result of priming (Figure 5.22). Surprisingly, only the proportion of NK cells expressing CD96 correlated (negatively) with the proportion of NK cells up-regulating CD107a (Figure 5.23). The negative correlation had a Spearman rank coefficient of -0.96 and was highly significant $P < 0.0001$ (Figure 5.23A). Further analysis correlating the proportion of NK cells

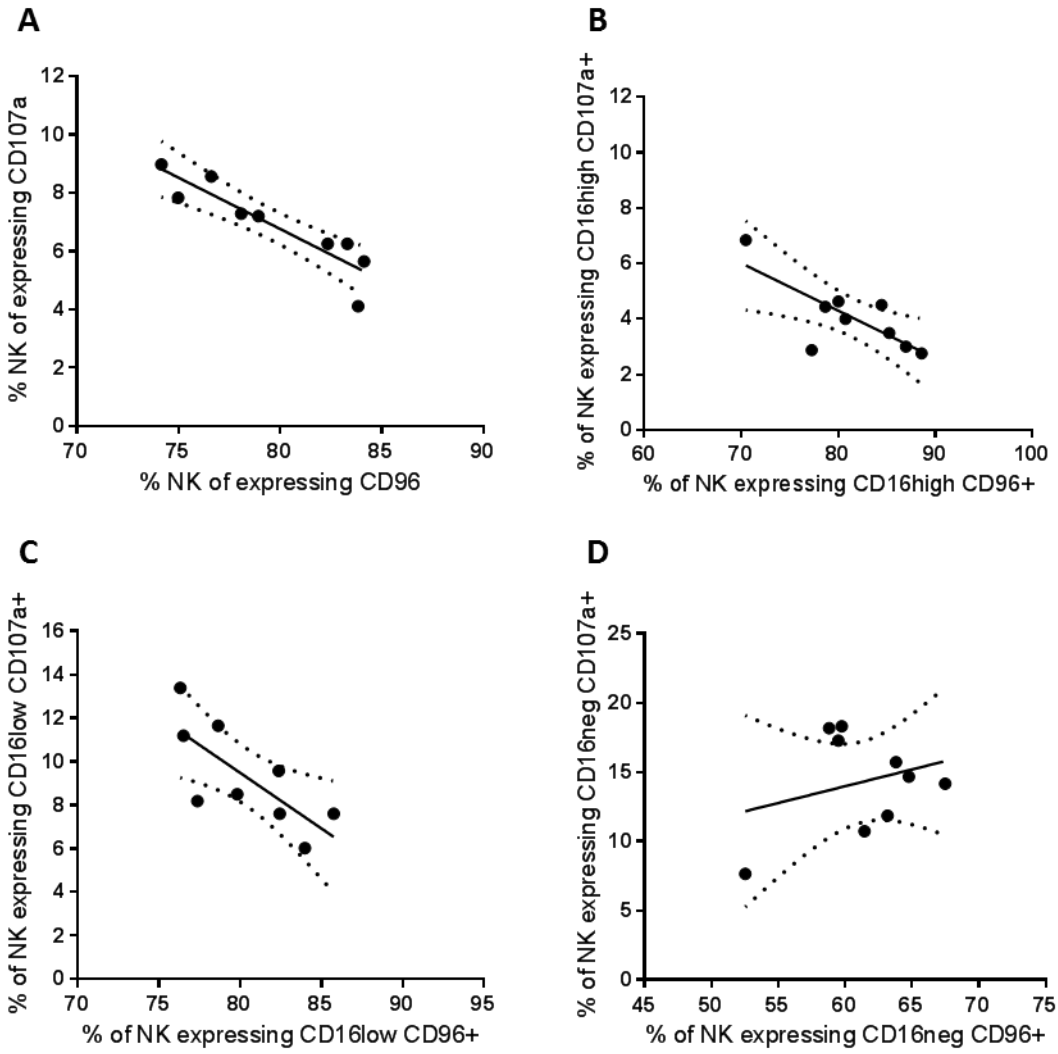

Figure 5.23: Correlation between CD107a expression and the expression of the receptor CD96 on patient primed NK cells as a total population and broken down into the $CD56^{dim}CD16^{high}$, $CD56^{dim}CD16^{low}$ and $CD56^{dim}CD16^{neg}$ subpopulations.

NK cells from patients with prostate cancer or individuals with benign disease were primed with mitomycin C treated CTV-1 at a 1 : 1, NK : CTV-1 ratio for 17 hrs. Primed NK cells were stained with NK cell defining antibodies and the CD107a, CD96 antibodies. The expression of CD107a and CD96 was measured on the total NK cell population and on the individual NK cells subpopulations and then correlated: A) On total NK cells a significant negative correlation, Spearman Rank -0.9624, P<0.0001, B) On the $CD56^{dim}CD16^{high}$ a non-significant negative correlation, Spearman Rank -0.5667 P<0.1206, C) On $CD56^{dim}CD16^{low}$ a significant negative correlation, Spearman Rank -0.8201, P=0.0086, D) On $CD56^{dim}CD16^{neg}$ no correlation.

expressing CD96 and CD107a on the 3 NK cell subpopulations revealed only a significant negative correlation on the $CD16^{low}$ subpopulation (Spearman rank coefficient of -0.82, significance P=0.0086). Although there was a degree of negative correlation in the $CD16^{high}$ subpopulation, it was not of statistical significance. Surprisingly, there was no correlation between CD96 and CD107a expression in the $CD16^{neg}$ subpopulation which, on average, exhibited the greatest proportion of NK cells up-regulating CD107a.

5.4. Discussion

The aim of this part of the study was to use the NK cell priming method to provide insight into the functional ability/potential of NK cells from patient groups and examine any differences in that may correlate with the Gleason grade of the patients. The findings will also provide insight into the capacity of NK cells from patients with prostate cancer to be primed, and hence the suitability of these patients for therapeutic strategies that are based on NK cell priming.

Due to time constraints, the number of priming experiments which could be performed was limited and additional studies need to be performed in order to increase confidence in the findings and their interpretation. However, the spread of expression data for some of the NK cell receptors measured e.g. CD137 and CRTAM, was narrow and statistically the results may be accurate. For other receptors e.g. CD69, GITR, CD107a, the range of data is greater and therefore these results are likely less statistically accurate. Due to the low numbers of subjects within each group I was forced to use parametric statistical tests despite the data often being non-Gaussian in nature. Normally, non-Gaussian data would require the use of non-parametric statistical tests, but due to the low sample numbers these tests were simply not powerful enough to provide accurate statistical analysis. For accurate statistical analysis using the non-parametric statistical tests a minimum of 7 subjects per group is required.

In addition, sample availability restricted the analysis of patient samples to priming, and it was not possible to undertake functional tests to measure the ability of the primed NK cells to kill PC3 target cells. These studies could have provided additional important information regarding the function of patient-derived NK cells. It is unknown how well phenotypic changes reflect the ability of the NK cell to kill its target. Measurement of the NK cell phenotype following priming was enough to suggest that the proportion of NK cells capable of becoming primed is reduced in patients suspected of prostate cancer compared to healthy volunteers. This was highlighted by a lower proportion of NK cells from patients, irrespective of the presence of cancer and its Gleason grade, being able to up-regulate CD25, CD137, CRTAM and GITR following priming. However, NK cells from some patients from each patient group could up-regulate these markers to a degree that was comparable to the healthy volunteers.

Surprisingly, the decrease in the proportion of NK cells from patients expressing CD96 following priming, negatively and significantly correlated with the increase in the proportion of NK cells up-regulating CD107a. Since CD107a is an indirect marker of degranulation, these results contradict those derived from the analysis of NK cells from healthy volunteers that are reported in Chapter 4 which suggested that the loss of CD96 was associated with decreased lysis of PC3 cells. It is known from studies conducted by other groups which have analysed the structure of

the CD96 receptor that in humans the receptor has the potential to be both co-stimulatory and co-inhibitory (Meyer et al., 2009). Further studies are needed to define the role of CD96 in NK cell priming and determine whether down-regulation means a loss of stimulation or inhibition.

Although the NK cell priming method was able to distinguish NK cell functional differences between healthy volunteers and patients, there was little overall difference between the ability of NK cells from patients with different Gleason grades of cancer to respond to priming. Regardless of whether individuals had benign disease, low grade prostate cancer (Gleason 6) or even high grade cancer (Gleason 9), the ability of the patient NK cells to become primed and to up-regulate CD107a appeared to be comparable. It should be noted that the range age of the healthy volunteers was 31 to 51 yrs, with a median age of 41 yrs, whereas the age range of the patients was 54 to 81 yrs, with a median of 63.5 yrs. As a consequence, the healthy volunteers were significantly younger than the patients, and the difference in the ability of the NK cells to become primed between the two groups could simply be due to age. Studies have shown that NK cell cytotoxicity decreases with age and consequently is a high risk factor for the appearance of infections in old age. Preservation of NK cell cytotoxicity in middle age may be crucial to avoid some age-related diseases (Mariani et al., 1990, Mocchegiani and Malavolta, 2004, Mocchegiani et al., 2003, Ogata et al., 1997). A Japanese study further supports this conclusion (Imai et al., 2000). In that study, the cytotoxic function of NK cells from 3625 residents was measured by targeting NK cells against K562 and, over the course of an 11-year follow up, their NK cell function was correlated with the incidence of cancer and death from all causes. They found that medium and high cytotoxic function was associated with reduced cancer risk, whereas low cytotoxic activity was associated with increased cancer risk (Imai et al., 2000). Therefore, in the present study the reason why NK cells from patients appeared to be significantly less able to become primed compared to NK cells from healthy volunteers could simply be due to age. This would account for why there was no statistical difference between the priming ability of NK cells from all 3 patient groups; benign, Gleason 6 and Gleason 9. Consequently, this calls into question whether the phenotype and function of peripheral NK cells reflects that of intratumoural NK cells.

Unfortunately, the ability of NK cells from healthy volunteers to up-regulate CD107a was not measured, nor was the ability of NK cells from patients to lyse PC3 cells. A lack of correlation between the expression of co-stimulatory receptors CD137, CRTAM, OX40, GITR and the up-regulation of CD107a on primed NK cells from patients suggest that these receptors do not serve as triggering receptors. Therefore, it is still unknown how well the phenotype of primed NK cells reflects their cytotoxic function. However, signalling through receptors such as OX40, CD137 and GITR may still yet effect NK cell functions by influencing or promoting the predominance of

specific NK cell responses such as cytokine release, degranulation, proliferation or even down-regulation of NK cell function in general. Therefore. further experiments should study what impact these receptors have on NK cell function.

One important finding regarding the phenotype of NK cells following priming are the differences in the phenotype of the 3 NK cell subpopulations within the $CD56^{dim}CD16^{high}$ NK, $CD56^{dim}CD16^{low}$ NK and $CD56^{dim}CD16^{neg}$ NK cell subpopulations. Generally, as seen for both healthy volunteers and patients, the primed $CD56^{dim}CD16^{neg}$ NK cell subpopulation contained a higher proportion of NK cells expressing CD137, CRTAM, OX40, CD107a and CD25 compared to both primed $CD56^{dim}CD16^{low}$ NK and primed $CD56^{dim}CD16^{high}$ NK cells. A greater intensity of expression for the receptors CD137, CRTAM and CD107a on the primed $CD56^{dim}CD16^{neg}$ NK cells was also observed. There was an upregulation in the proportion of $CD56^{dim}CD16^{low}$ NK cells expressing CD137, CRTAM, OX40, CD107a and CD25 following priming, but this was always less than the $CD56^{dim}CD16^{neg}$ population, yet greater than the $CD56^{dim}CD16^{high}$ population which up-regulated very little. These results suggest that the NK cells that remain $CD56^{dim}CD16^{high}$ following priming may have a different function within the total NK cell population than the $CD56^{dim}CD16^{low}$ and $CD56^{dim}CD16^{neg}$ populations. The extent to which the NK cells from an individual down-regulates CD16 appears to be vary from person to person for both healthy and cancer patients, including those in the same Gleason group. Therefore, the extent CD16 down-regulation and the resulting ratio of $CD56^{dim}CD16^{high}$, $CD56^{dim}CD16^{low}$ and $CD56^{dim}CD16^{neg}$ NK cell subpopulations may have important consequences on the overall function of that individual's NK cell population and their ability to fight different types of diseases. Whether there is a functional or even multifunctional difference between $CD56^{dim}CD16^{low}$ and $CD56^{dim}CD16^{neg}$ subpopulations requires further investigation. The greater extent of up-regulation of CD107a seen in the $CD56^{dim}CD16^{neg}$ subpopulations suggests that they will be the more cytotoxic subpopulation. However, the $CD56^{dim}CD16^{low}$ subpopulation were greater in proportion and in number than the $CD56^{dim}CD16^{neg}$ subpopulation. Therefore, whether it is more beneficial to have more $CD56^{dim}CD16^{low}$ NK cells or $CD56^{dim}CD16^{neg}$ NK cells following NK cell activation remains an unanswered question that requires further investigation.

Despite the small number of healthy volunteers, patients with benign disease and patients with cancer tested using the NK priming method, it has been shown that the NK cells from all these individuals can be primed. They therefore had the potential to kill PC3 cells and this means NK priming has the potential to be a immunotherapy for prostate cancer patients. Interestingly, although the NK cells from all three groups can be primed, the degree of the phenotypic changes in response to this priming varies within a group. Therefore, even though patients can be grouped according to the Gleason grade of the cancer the responsiveness of these patient's

immune systems (in this case NK cell immune response) may differ and therefore their ability to respond to different immunotherapeutic treatments may differ. It is therefore entirely possible that in the future, in order to determine the patient's prognosis and treatment plan both the grade of cancer and the ability of the patient's immune response to stimulus may need to be taken into account.

It is unlikely that we have sampled the full range in the variation of phenotypic changes in response to NK cell priming and more people need to be tested using this method. Overall, we saw some differences in the phenotype of primed NK cells between healthy volunteers and patients, particularly regarding the expression of receptors NKp46, CD25, CD96, CD137, CRTAM and GITR. Unfortunately, there was not time to measure the cytotoxic function of the primed patient NK cells. As a consequence, we do not know if the phenotypic differences between healthy volunteers and patients or even the phenotypic similarities between patients translate into similarities or differences in cytotoxic function. Future work needs to focus on completing these experiments. Only then can conclusions be made regarding how well the NK cell priming method measures NK cell cytotoxic function and whether this measurement can be used to improve patient diagnosis, improve determination of a patients prognosis and better inform what treatment plan to out the patient on.

Chapter 6 - DISCUSSION

6. Discussion

According to the Prostate Cancer UK website, over 44,000 men in the UK are diagnosed with prostate cancer every year. Currently, over 330,000 men are either living with and/or have had prostate cancer, and over 10,500 men die from the disease each year. Prostate cancer mainly effects men over the age of 50 yrs, with the average age of diagnosis being between 65 and 69 yrs. It is estimated that 1 in 8 men will develop prostate cancer at some point in their life time. The figure is 1 in 4 men if they are of African heritage, with twice as many men is this group dying of the disease each year compared to their Caucasian counterparts.

The aim of this PhD programme was to characterise the phenotype and function of NK cells in the periphery in patients suspected of having prostate cancer in order to detect phenotypic profiles that may potentially improve patient diagnosis and / or prognosis. This aim was based on the concept that immunological dialogue between cancer and the immune system is reflected by changes in immunological profiles in the periphery. The study was undertaken in parallel with other studies that examined the influence of prostate cancer on the prevalence and phenotype of T cells and T cell subsets in the periphery. Although beyond the scope of the current study, additional studies will integrate these datasets and use computational intelligence and other bioinformatics-based approaches to more deeply interrogate and interpret the influence of prostate cancer on phenotypic profiles in the periphery. The overall goal of these studies is to improve the accuracy of prostate cancer diagnosis in men, and thereby provide clinicians with information which will assist the management and treatment of these patients. This is particularly important in the context of prostate cancer for which it is essential to distinguish indolent from aggressive forms of the disease. Inappropriate treatment can have dramatic effects on the quality of life.

Until recently, with the development of the transperineal (TP) biopsy, there had been limited improvements in the detection and diagnosis of prostate cancer since the 1980s. Although the TRUS biopsy was developed by Watanabe et al in 1971 (Watanabe et al., 1971), it was not until the mid-1980s, when high resolution scanners were developed, that the technique was generally used in the clinic (Lee et al., 1989). The technique improved the accuracy of prostate cancer diagnosis and aided earlier detection of prostate cancer. The prostate specific antigen (PSA) ELISA test was developed by Kuriyama et al in 1980 and was implemented as a biomarker test for prostate cancer in 1986. The introduction of the PSA test increased the earlier detection of prostate cancer (Nafie et al., 2014a). However, studies have shown that the PSA test is not a

specific test for prostate cancer, as patients with benign disease can have elevated PSA levels and the fact that PSA levels in patients with early and advanced cancer overlap means that the PSA test cannot be used to predict the stage of prostate cancer (Hudson et al., 1989, Stamey et al., 1987). The PSA levels measured in the prostate cancer patient cohort analysed in this PhD study also reflect the challenges in using PSA levels as a diagnostic test. When grouping the TP and TRUS patients on the basis of Gleason grade, it was clearly seen that levels varied greatly and that the range of PSA levels within the individuals with benign disease and patients with prostate cancer overlapped. It is also important to note that a 'normal' PSA test cannot exclude the possibility of cancer. As a consequence, the PSA test can deliver false positive and false negative results, and a definitive diagnosis therefore requires additional, typically invasive, procedures. Notwithstanding these problems, the introduction of the PSA test into the clinic and its use in combination with the DRE test improved the accuracy of prostate cancer detection (Catalona et al., 1991). Using historical data, the introduction of the PSA test has been associated with an increase in the incidence of prostate cancer detection and the number of organ-confined cancers diagnosed, and a decrease in patient mortality (Hankey et al., 1999, Lee et al., 1989).

Despite the improvements in prostate cancer diagnosis which have been enabled by the introduction of the PSA test, the application of the TRUS biopsy and the DRE test, patients continue to be misdiagnosed. As stated above, the PSA test is not specific and, at best, tells a clinician that something is wrong with the prostate, but does not necessarily reflect the presence of cancer. Studies focusing on the accuracy of the TRUS biopsy have shown that the detection rate of prostate cancer at initial TRUS biopsy is low, and ranges between 26 and 33 % (Aganovic et al., 2011, Naughton et al., 2000, Welch et al., 2007, Yuasa et al., 2008). Upon repeat biopsy following an initial negative TRUS biopsy, the detection rate of cancer has been reported to range between 18 and 35.7 % (Aganovic et al., 2011, Yuasa et al., 2008). Of the 18 % of patients with cancer positive biopsies that were detected in the latter study, 73 % were organ confined with an average Gleason grade of 6 upon repeat biopsy, compared to 44 % of the cancers being organ confined upon initial biopsy (Yuasa T 2008). These results suggest that the TRUS biopsy tends to pick up the more obvious, perhaps larger prostate cancers, yet struggles to detect some early stage cancers that are still organ confined. Studies using saturation biopsy techniques on both initial and repeat biopsy in order to improve prostate cancer detection and reduce the need for repeat biopsies did not greatly increase the rate of detection. Using the saturation biopsy technique, the detection rate on initial biopsy was 43 % and between 24 and 34 % upon repeat biopsy (Lane et al., 2008, Stewart et al., 2001). Early studies showed that the majority of prostate cancer (74 %) can be found in the peripheral zone of the prostate and therefore can be

biopsied using the TRUS biopsy (Chen et al., 2000). However, it has been reported that there is a subgroup of patients who develop tumours in the anterior region of the prostate and that, despite having abnormal PSA levels, appear negative for prostate cancer by TRUS biopsy (Tiguert et al., 1998). The possibility of patients having rising PSA levels despite having a set of two negative TRUS biopsies has been described as a major concern for clinicians (Nafie et al., 2014b). It was recommended that patients with abnormal PSA values and a negative TRUS biopsy undergo biopsies in the anterior region (Tiguert et al., 1998).

More recently, a biopsy technique known as the Transperineal template prostate biopsy (TP biopsy) has been developed. The technique was established by adapting the template grid used to assist transrectal ultrasound guided brachytherapy (Demura et al., 2005). Currently, there is no standard method for performing the TP biopsy and consequently there is variation in the technique and equipment used between studies. In a study analysing the distribution of carcinoma cores within the prostate using the TP biopsy, it was concluded that the majority of positive carcinoma cores in DRE positive patients was found in the posterior region (77 %) compared to the anterior region. In patients that were DRE negative, the carcinoma positive cores were equally distributed throughout the entire prostate (Demura et al., 2005). Studies have shown that in patients having elevated PSA levels who had a set of negative TRUS biopsies, between 26 % and 68 % of the men had prostate cancer (Dimmen et al., 2012, Mabjeesh et al., 2012, Nafie et al., 2014b, Pal et al., 2012). In two of the studies, it was shown that between 44 % and 83 % of the patients with prostate cancer, had cancer in the anterior zone (Mabjeesh et al., 2012, Pal et al., 2012). In one study analysing a cohort of 122 men, 58 % of men who had previously had two negative TRUS biopsies were found to have prostate cancer with 49 % of the cancer positive cores being found in the anterior zone, 31 % found in the middle zone and 20 % found in the posterior zone (Nafie et al., 2014b). The results from these studies show that a significant proportion of patients with rising PSA levels, despite being negative by TRUS biopsy, often have prostate cancer in the regions of the prostate that the TRUS biopsy cannot sample. The TP biopsy offers improved detection of prostate cancer in all regions of the prostate, including in the peripheral zone where 20 % of positive cores were found despite these patients undergoing two TRUS biopsies (Nafie et al., 2014b). This was further emphasised by a study comparing the prostate cancer detection level of the TRUS biopsy to the TP biopsy in a cohort of men who were biopsy naïve, benign by DRE with a PSA <20 ng/ml (Nafie et al., 2014a). Out of 50 participants, 60 % were positive for prostate cancer, as detected by the TP biopsy, with a median Gleason score of ≥ 7 (indicating clinically significant disease). The fact that the TRUS biopsy only identified 32 % of the participants as being positive for prostate cancer highlights that the TRUS biopsy is likely to miss 28 % of prostate cancer cases in patients with elevated PSA

and a benign feeling DRE. The authors concluded the TP biopsy appeared not to increase the risk of prostate cancer over-diagnosis and advised that patients with elevated PSA levels and a benign feeling DRE should undergo TP biopsy. Patients with an abnormal DRE should still be considered for TRUS biopsy as it is unlikely that this biopsy technique will miss-diagnose the prostate cancer in this group of men.

Despite the improved detection rate of the TP biopsy, there are advantages and disadvantages to the technique. As reviewed by Chang et al (Chang et al., 2013) the TP biopsy is more expensive to perform as it often requires operating theatre time and an intravenous or general anaesthetic. The equipment used for the technique is generally less readily available, and requires better probes, disposable grids and with some methods an MRI. However, the advantage of the TP biopsy is not just the improved detection rate of prostate cancer, but also fewer complications, despite the increased number of biopsy cores. Due to the nonsterile transfaecal method of the TRUS biopsy, patients are at risk of developing life threatening sepsis and urinary tract infections (UTIs). Although the routine prescription of perioperative antibiotics significantly lowers the risk of infection, it consequently increases the incidence of microbial antibiotic resistance. The TP biopsy can be performed aseptically and has the potential to reduce the incidence of sepsis. Providing the patient's urine is sterile, antibiotics are not required. No significant difference in the development of erectile dysfunction, urinary retention or the presence of blood in the urine or semen between the two biopsy techniques has been observed (Chang et al., 2013, Pal et al., 2012). The downside to using both the TRUS and TP biopsy techniques to diagnose prostate cancer is that both techniques are invasive.

The John van Geest Cancer Research Centre is dedicated to the identification of biomarkers that may improve cancer diagnosis and / or represent targets for immunotherapy that can be used to treat cancer patients. This PhD is part of a larger investigation into measuring the phenotype of peripheral immune cells in patients with and without cancer in order to identify biomarkers that may help improve diagnosis and provide clinicians with accurate information regarding patient prognosis and potentially help identify the best treatment plan for these patients. A review of studies analysing the immune infiltrate entering the prostate in prostate cancer patients found a surprising lack of information regarding the precise phenotypic profiles of leukocytes infiltrating prostate tumours. Such information would aid the identification of ideal immune populations to target for immunotherapy and provide biomarkers to assess therapeutic efficacy (Strasner and Karin, 2015). The aim of this PhD was to measure the phenotype and function of patient peripheral NK cells and observe whether this measurement could improve prostate cancer diagnosis and / or patient prognosis, and thereby provide more accurate

information to clinicians and assist them in their decision-making process regarding the best treatment plan for the patient.

The idea for measuring the phenotype and function of peripheral prostate cancer patient NK cells as a tool for patient diagnosis and prognosis is based on a link between the presence of inflammation, the development of cancer and their effects on the immune system of the patient. It is now thought that there are two pathways whereby the presence of inflammation promotes the development of cancer: an intrinsic pathway and an extrinsic pathway. Prostate cancer is thought to be an the extrinsic pathway, in that inflammatory conditions increase the risk of cancer development (Mantovani et al., 2008).

The ability of cancer to avoid immune destruction has been described as an emerging hallmark of cancer (Hanahan and Weinberg, 2011). The concept that cells of both the innate and adaptive immune system (e.g. T cells and NK cells) continually survey the host tissues for the presence of transformed cells has been termed 'cancer immunosurveillance', and this concept is now widely accepted (Dunn et al., 2004a). Dunn et al proposed the 'cancer immunoediting' process, whereby the host protective cancer immunosurveillance activities of the immune system actually shapes the development of tumours (Dunn et al., 2002, Dunn et al., 2004a, Dunn et al., 2004b). Cancer immunoediting can be divided into three phases: elimination, equilibrium and escape. During the equilibrium phase, the immune system is initially able to constrain the growth of heterogeneous tumours that are composed of cells that are genetically unstable and rapidly mutating. Although the immune system destroys the original tumours, new variants with more mutations emerge. The immune response destroys the more immunogenic phenotypes, but remains unable to destroy the less immunogenic phenotypes. The outcome of this process re-shapes the development of the tumour enabling it to survive in its local environment. The tumour cells that survive the equilibrium phase enter the escape phase, during which they are able to grow without restraint from the immune system (Dunn et al., 2004a).

The inflammatory tumour microenvironment plays an important role within both the equilibrium and escape phases by promoting a pro-tumour environment using various mechanisms which are the subject of intense study. There have been many reviews in this area, and so herein I will be provide a brief overview of tumour microenvironment, how it promotes tumourogenesis and how it affects the phenotype and function of NK cells, which in turn may be measured by sampling peripheral blood.

Studies have shown that the inflammatory milieu within the tumour microenvironment can destabilise the genome of cells undergoing transformation. This can occur either directly by inducing DNA damage or indirectly by influencing DNA repair mechanisms or dysregulating cell

cycle checkpoints (reviewed by (Colotta et al., 2009, Vitale et al., 2014)). Inflammatory mediators are induced following abnormal activation of transcription factors e.g. NF-κβ, STAT3 and HIF-1α, in both tumour and inflammatory cells (reviewed by (Harris, 2002, Karin, 2006, Vitale et al., 2014, Yu et al., 2007)). Tumour derived factors such as fibroblast growth factor (FGF), TGF-β, and platelet-derived growth factor (PDGF) induce tumour associated fibroblasts (TAFs) to produce factors that are involved in tumour cell transformation – these include TGF-β, insulin growth factor (IGF), and hepatocyte growth factor (HGF). TAFs also secrete extracellular matrix remodelling enzymes that promote tumour evasion – these include matrix metalloproteinases (MMPs) and vascular endothelial growth factor (VEGF), and also chemokines which promote inflammation – these include CCL2, CXCL12, CXCL8 (reviewed by (Servais and Erez, 2013, Vitale et al., 2014)). Studies in melanoma have shown that TAFs can reduce NK cell function by down-regulating their expression of NKp44 and NKp30 via the release of PGE2, and down-regulating the expression of DNAM-1 via cell-to-cell contact (Balsamo et al., 2009).

Cell transformation can also be influenced by immune cells from the innate immune system that are recruited and / or activated by the tumour microenvironment. Tumour associated macrophages (TAMs) are particularly abundant at tumour sites. TAMs play a role in the cytotoxicity against tumours, but also appear to undergo polarisation to an immunoregulating, tumour favourable M2-like phenotype during tumour progression (Biswas and Mantovani, 2010). In prostate cancer, studies have associated higher numbers of $CD68^{+}$ TAMs with higher stage of cancer, higher Gleason scores (> Gleason 8) and disease progression (Gannon et al., 2009, Lanciotti et al., 2014, Nonomura et al., 2011). Like TAFs, TAMs are also capable of reducing NK cell function. However, the mechanisms involved in this inhibitory capacity remain unknown (Biswas and Mantovani, 2010, Vitale et al., 2014). Myeloid derived suppressor cells (MDSCs) and regulatory T (Treg) cells can also be found in the tumour microenvironment and these cells are known to secrete suppressive cytokines such as TGF-β and IL-10 (Gabrilovich et al., 2012, Vitale et al., 2014). The secretion of TGF-β by MDSCs and Treg cells have been reported to down-regulate NK cell expression of NKp30 and NKG2D respectively (Ghiringhelli et al., 2005, Hoechst et al., 2009). Although increased numbers of Treg cells and MDSCs have been identified in the prostate of patients with prostate cancer, as compared to individuals with benign disease and healthy volunteers, no correlation with the Gleason score was observed (Ebelt et al., 2009, Idorn et al., 2014, Strasner and Karin, 2015). Therefore, overall there are a number of cells types within the microenvironment of cancers that are capable of suppressing the function of NK cells by down-regulating their expression of activating receptors. Although the number of TAMs, Tregs and MDSCs have been found to be increased in patients with prostate cancer compared to

individuals with benign disease and healthy donors, no studies have yet measured the effect of these cells on the phenotype and function of NK cells in patients with prostate cancer.

In theory, the suppressive effects of TAMs, TAFs, Tregs and MDSC on the phenotype and function of intratumoural NK cells could be reflected in the phenotype and function of NK cell populations in the peripheral blood following recirculation of the intratumoural cells. This concept forms the basis of this PhD, the aim of which was to measure the phenotype and function of peripheral blood NK cells in patients with prostate cancer and observe whether they can provide a 'window' on the disease and inform the diagnosis and prognosis of the disease.

A study comparing the phenotype and function of peripheral and intratumoural NK cells in patients with breast cancer found significant decreases in the intensity of expression of the activating receptors NKp30, NKG2D, DNAM-1 and 2B4 on peripheral blood NK cells from patients with invasive breast cancer compared to healthy controls and patients with non-invasive breast cancer. The down-regulation of activating receptor expression was associated with significant down-regulation in the capacity of NK cells to degranulate, their ability to kill K562 cells and also their capacity to synthesise IFN-γ and TNF-α. Furthermore, a comparison of the phenotype and function of peripheral blood NK cells with intratumoral NK cells from the same patients with invasive breast cancer revealed that features of intratumoural NK cells were reflected by NK cells in the periphery, albeit to a less pronounced level. It therefore appears that alterations detected in the peripheral blood may derive from recirculating intratumoural NK cells and / or be induced by soluble factors that are secreted by the tumour (Mamessier et al., 2011b). These results suggest that it is possible to gauge the level of immunosuppression exerted by the presence of cancer on the immune system by measuring the phenotype of immune populations in the periphery. This potentially means that measurement of peripheral immune populations could help diagnosis and / or provide information on patient prognosis and perhaps inform which treatment plan is best for the patient. However, in another study Platonova et al showed that the phenotype of peripheral blood NK cells from patients with lung carcinoma did not reflect the phenotype of intratumoural NK cells. The down-regulation of NKp30, NKp80, NKG2D and DNAM-1 expression was only observed on intratumoural NK cells and was significantly different compared to the peripheral blood NK cells (Platonova et al., 2011). Similar results have been observed in a study of patients with ovarian cancer, in which tumour associated NK cells displayed a significantly different phenotype to that of peripheral NK cells which, in turn, were not significantly different to the phenotype of peripheral NK cells from healthy donors (Carlsten et al., 2009). The studies by Platonova et al and Carlsten et al highlight that peripheral blood NK cells may only reflect the phenotype of intratumoural NK cells in some forms of cancer. Furthermore, in some cancers the phenotype of patient peripheral NK cells may not be

significantly different to that of healthy people and therefore cannot be used to inform diagnosis or patient prognosis.

A limitation of this PhD study was that it was not possible to measure the phenotype of intratumoural NK cells, either by flow cytometry of isolated cells or by immunohistochemical staining for infiltrating NK cell populations. The needle biopsies that were routinely obtained from patients as part of the diagnostic process are not of sufficient size to enable the isolation of sufficient numbers of NK cells for flow cytometric analysis, or be used for immunohistochemical staining of the immune populations to identify the extent and phenotype of the immune infiltrate entering the prostate. The availability of sufficient clinical material to undertake these studies would require the patient to undergo a radical prostatectomy, a treatment option which was not necessary for the majority of the patients that were included in the study.

However, this study was able to compare the phenotypes of peripheral blood NK cells in patients with different grades of prostate cancer with those in individuals having elevated PSA levels, but benign disease. The study has revealed that the proportion of NK cells expressing NKp30 and NKp46 in patients with low grade prostate cancer (i.e. the Gleason 6 and Gleason 7 patient groups) was higher than that in individuals with benign disease, and that this was then decreased in patients with advanced disease (i.e. the Gleason 8+9 patient group). The increase and decrease in expression of NKp30 and NKp46 suggests that these receptors could be involved in the recognition of prostate cancer. In a very recent study measuring NK cell phenotype in patients with metastatic prostate cancer, Pasero et al found that patients whose NK cells expressed a higher intensity of NKp30 and NKp46 on their NK cells exhibited an increased overall survival compared to patients with NK cells exhibiting low MFI expression of the two receptors. Furthermore, functional studies involving blocking antibodies revealed that the NK cell receptors NKp46, DNAM-1, NKG2D and, to a lesser extent, NKp30 regulated the recognition of prostate cancer cell lines by healthy NK cells (Pasero et al., 2015). Although in this PhD study a significant change in the MFI expression of NKp30 and NKp46 was not observed in our patient cohort, the connection between the proportion of NK cells expressing NKp30 and NKp46 with the grade of cancer supports the conclusions from Pasero et al's study that NKp30 and NKp46 are involved in prostate cancer recognition. In contrast to the study of Pasero et al, changes in the expression of NKG2D and DNAM-1 on peripheral blood NK cells in patients with prostate cancer were not observed. As I was unable to analyse the intratumoural NK cell phenotype in my patient cohort, it was not possible to determine whether the expression of NKG2D and DNAM-1 are altered on intratumoural NK cells, but not reflected by the phenotype of NK cells in the peripheral blood, as has been reported by Platonova et al in lung cancer (Platonova et al., 2011). Pasero et al

concluded that the measurement of peripheral blood NK cell phenotypes has prognostic value and suggested that NK cell markers could be screened on blood samples for routine diagnosis, given that peripheral blood NK cells may reflect intratumoural NK phenotypes (Pasero et al., 2015).

The results from this PhD study suggest that, despite significant changes in the expression of some of the NK receptors i.e. NKp30, NKp46 and 2B4, the differences were not sufficient to distinguish patients with prostate cancer from those with benign disease. The conclusion from my studies is that it is not possible to use the measurement of the peripheral blood NK cell phenotype as a diagnostic tool in the context of prostate cancer. However, in agreement with Pasero et al, the evidence supports that in light of the decrease in the median percentage of NK cells expressing NKp30 and NKp46 between Gleason 7 and Gleason 8+9 patient groups, continuous measurement of these two NK cell markers has the potential to indicate cancer progression. Furthermore, we also observed that the intensity of 2B4 expression was also significantly lower in Gleason 8+9 patients, as compared to those with Gleason 7 disease, as a consequence of which the measurement of this receptor could also potentially be used to assess prostate cancer progression. However, further studies will be needed in order to assess whether the progression of prostate cancer is associated with down-regulation in the expression of NKp30, NKp46 and 2B4 on peripheral blood NK cells. Due to the slow growing nature of prostate cancer and the absence of taking repeated blood samples, I was unable to confirm the association of cancer progression with the down-regulation of NKp30, NKp46 and 2B4 expression.

The analysis of NKp30 expression on peripheral blood NK cells revealed that there was a large range in the percentage of NK cells expressing NKp30 in individuals with benign disease. It appeared that, on the basis of NKp30 expression, individuals in this cohort could be segregated into two groups: one group with a high percentage of NK cells expressing NKp30 (similar to that of Gleason 6 patients) and a second group with a more variable range in percentage of NK cells expressing NKp30. The greater variation in the second group could be attributed to natural differences in NKp30 expression which are dictated by genetics, as described by Markel et al (Markel et al., 2009). Markel and colleagues showed that the expression of NK cell activating receptors such as NKp30 naturally varies between healthy individuals, both in terms of the percentage of NK cells expressing the receptor and the intensity of that expression (Markel et al., 2009). The cohort of individuals with benign disease in our study was further subdivided according to the presence of tissue abnormalities such as high grade prostatic intraepithelial neoplasia (HGPIN) and atypical small acrinar proliferation (ASAP). HGPIN essentially describes a state in which the epithelial cells lining the acini and ducts become abnormal, but crucially

remain intact. This is in contrast to prostate cancer in which the epithelial lining is ruptured and malignant cells penetrate the tissue of the prostate gland itself. ASAP is proliferation of usually small acini with features highly suggestive but not diagnostic for carcinoma (www.harvardprostateknowledge.org). It is currently unclear whether the presence of HGPIN and or ASAP leads to the development of prostate cancer (El-Hakim and Moussa, 2010, Vral et al., 2012).

In a study looking at the presence of prostate cancer upon repeat biopsy following an initial diagnosis of HGPIN or ASAP, only 21.9 % of patients who were initially diagnosed with HGPIN were diagnosed with cancer upon repeat biopsy. This detection rate was further reduced to 15 % when further broken down into each biopsy session. In contrast, 51.9 % of patients initially diagnosed with ASAP were diagnosed with prostate cancer upon repeat biopsy (Amin et al., 2007). As a consequence, it has been recommended that patients with HGPIN only be re-biopsied on an individual basis indicated by PSA density, the number of initial biopsy cores taken and DRE results. For patients initially diagnosed with ASAP, it is recommended that the patients be re-biopsied (Amin et al., 2007, El-Hakim and Moussa, 2010). In this PhD study, the allocation of individuals with benign disease to benign, HGPIN, ASAP and HGPIN + ASAP subgroups revealed a trend towards evidence that individuals with ASAP exhibited a higher percentage of NK cells expressing NKp30 (similar to the Gleason 6 patients) compared to individuals with HGPIN and benign disease that showed no evidence of ASAP. Although the result was not significant, it is plausible that, with larger group sizes that it may become significant. This concept warrants further investigation.

The biology of NK cells require the analysis of multiple parameters simultaneously. Using a CyTof™ mass cytometer, Horowitz et al found up to 30,000 phenotypic NK cell populations in a given individual, and concluded that the expression of inhibitory receptors was strongly influenced by genetics whereas the expression of activating and co-receptors was influenced by environmental factors (Horowitz et al., 2013). The results from the phenotype analysis of NK cells in patients suspected of prostate cancer in this PhD study reflect the findings of Horowitz et al. The expression of inhibitory receptors appeared unaltered by the presence of prostate cancer, whereas expression of the activating receptors NKp30, NKp46 and 2B4 appeared altered in association with the presence and grade of prostate cancer. Although changes in the expression of NKp30, NKp46 and 2B4 appeared to be associated with an increase in the Gleason grade, the mechanism is unclear and warrant further investigation. It is also unclear whether the increase in the percentage of NK cells expressing NKp30 and NKp46 in patients with Gleason 6 and Gleason disease, as compared to individuals with benign disease, is a result of up-regulation of NKp30 and NKp46 by these NK cells or the expansion of specific NK cell phenotypic subgroups.

The fact that the intensity of NKp30 and NKp46 expression was not significantly altered is suggestive of alterations in the proportion of particular NK cell phenotypic subgroups rather than an up-regulation of NKp30 and NKp46 expression on the NK cell surface. It is also not clear whether the lower percentage of NK cells expressing NKp30 and NKp46 in patients with Gleason 8+9 disease as compared to patients with Gleason 7 disease was the result of increased immunosuppression by the prostate cancer in the Gleason 8+9 patients.

The presence of immunosuppressive cytokines and factors in the plasma / serum of the patients were not measured, nor was it possible to examine prostate tissue biopsies by immunohistochemistry. As far as I am aware, there are no reports measuring the presence of immunosuppressive cytokines and factors in the prostate of prostate cancer patients. It is therefore unclear to what degree prostate cancer secretes immunosuppressive cytokines and factors, or to what extent these factors might influence the phenotype of immune cells within the prostate and the periphery. Clinical data for both TRUS and TP patients revealed that individuals diagnosed with Gleason 6 and Gleason 7 disease were generally benign, T1 or T2 stage cancers, thereby indicating organ-confined cancer. Patients diagnosed with Gleason 9 disease were more likely to have stage 4 cancers, meaning the cancer had broken through the prostate capsule and was starting to spread to nearby organs (www.prostatecanceruk.org). It is therefore unknown whether the decrease in the percentage of NK cells expressing NKp30 and NKp46 in patients with Gleason 8+9 disease compared to the those in patients with Gleason 7 disease was the result of an increased dispersal of immunosuppressive cytokines and factors outside of the prostate due to the spread of cancer beyond the prostate. Alternatively, it is plausible that the decrease in the expression of NKp30 and NKp46 was an age-related phenomenon. The Gleason 8+9 patient group was shown to be significantly older than all of the other patient groups, and other studies have shown that the percentage of NK cells expressing NKp30 and NKp46 decreases with age (Almeida-Oliveira et al., 2011, Hazeldine et al., 2012).

A third possibility to explain the lower expression of NKp30 and NKp46 could relate to the recently proposed ‘discontinuity theory’ which states ‘that effector immune responses are induced by an antigenic discontinuity; that is, by the appearance of molecular motifs that are qualitatively or quantitatively different from those with which the immune system has regularly interacted with so far’ (Pradeu et al., 2013). The authors go on to state that the duration of antigenic exposure is crucial, as cells that have been chronically exposed to stimulation become desensitised over time due to the activation of either intrinsic or extrinsic regulatory pathways. In the case of NK cells, it is thought that they detect and respond to sudden modifications in their environment, but that they adapt to the modifications and cease to respond when these modifications are prolonged (Pradeu et al., 2013). In the case of this PhD study, the NK cells in

the Gleason 8+9 patients could simply have been exposed to a greater volume of cancer and / or for longer considering that prostate cancer tends to be asymptomatic until metastatic spread to areas of the body like the bones. This long-term exposure may decrease the expression of NKp30 and NKp46 on the NK cells (the decrease in the MFI expression of NKp46 on Gleason 8+9 patient NK cells compared to the other patient groups did not quite reach significance) or reduce the proliferation of specific NK cell phenotypic subsets expressing NKp30 and NKp46. As a consequence, NK cells in the Gleason 8+9 patients may simply be adapting to the presence of prostate cancer and consequently reducing their effector functions against the cancer.

As discussed above, measuring the changes in the phenotype of the patient NK cells did not distinguish patients with prostate cancer from those with benign tissue. Nor could it distinguish patients with different grades of prostate cancer. This was because the heterogeneity of data within the patient groups for the expression of any given receptor overlapped. Only the median expression of some of the receptors i.e. NKp46, NKp30 and 2B4 increased or decreased in association with the presence of increasingly advanced cancer. It was therefore decided to measure the function of the NK cells to see if NK cell function could better distinguish patients with prostate cancer from those with benign disease or 'no disease'.

This approach required the development of a suitable assay to measure NK cell function in patients with prostate cancer. Typically, the standard approach is to determine the function of patient NK cells by measuring their cytotoxic activity against target cells, typically K562 cells (Carlsten et al., 2009, Mamessier et al., 2011b, Platonova et al., 2011). The cytotoxic function can be measured using either a ^{51}chromium release assay (Brunner et al., 1968), a flow cytometry-based cytotoxic assay (Hopkinson et al., 2007) or on the basis of a CD107a degranulation assay (Alter et al., 2004). The K562 leukaemic cell line is deficient in the expression of MHC class I (Nishimura et al., 1994) and is therefore inherently sensitive to NK cell killing, but insensitive to killing by $CD8^+$ T cells. K562 cells are therefore a suitable target for measuring the cytotoxic function of purified NK cells and NK cells in PBMC preparations. However, the relevance of K562 cells as targets for measuring the cytotoxic function of NK cells isolated from prostate cancer patients is questionable given that prostate cancer cells can express MHC class I. Indeed, prostate cancer cell lines such as DU145, PC3 and LNCaps are known to be NK cell-resistant and all three cell lines express MHC class I molecules (Seliger et al., 2010). It is likely that prostate cancers are MHC class I positive and so will demonstrate an inherent resistance to the cytotoxic effects of NK cells. Since MHC class I molecules induce inhibitory signals upon contact with NK inhibitory receptors, it is likely that the ability of patient NK cells to kill the MHC class I deficient K562 cells does not reflect the ability of patient NK cells to kill an MHC class I positive prostate cancer target. Interestingly, it has been shown that healthy individuals kill K562

cells with varying degrees (Almeida-Oliveira et al., 2011). Even with the limited experiments which used previously frozen isolated NK cells as effector cells against K562 in this PhD study, the percentage of K562 cells lysed ranged between 44 % and 84 %. Thus, when measuring the cytotoxic killing ability of NK cells from patients against K562 it is unclear whether the potentially poor cytotoxic killing ability is due to immunosuppression by the cancer or whether the patient's NK cells are inherently poor at killing K562.

NK cells can be induced to kill NK cell-resistant cell lines by stimulation with cytokines such as IL-2 and IL-15 (Carlsten et al., 2009, El-Sherbiny et al., 2007, Mamessier et al., 2011a). The stimulation of $CD56^{dim}CD16^{+}$ NK cells to kill NK cell-resistant cell lines has been shown to require around 100 U/ml IL-2 and incubation periods between 18 hrs and 7 days (El-Sherbiny et al., 2007, Mamessier et al., 2011a, Nagler et al., 1989). Stimulation of NK cells with IL-2 (500 U/ml) has been reported to significantly increase the expression of NK receptors such as NKG2D, NKp30 and NKp44 within 24 hrs (Markel et al., 2009). It is therefore likely that, in these studies, the NK cells are being stimulated with IL-2 beyond physiological levels and consequently altering their phenotype and the ratio of the $CD56^{dim}$ and $CD56^{bright}$ NK cell subsets (Nagler et al., 1989). This will result in an NK cell population that no longer represents the original phenotype which was present in patients. As a consequence, the ability of IL-2 stimulated NK cells to kill relevant NK cell-resistant cell lines is no longer a reflection of NK cell function in patients.

Overall, it was not felt that using K562 cells as target cells, or IL-2 stimulated NK cells as effector cells would accurately reflect the NK cell function of the prostate cancer patients. As a consequence, I based my NK cell functional assays on the methods published by Mark Lowdell's group from University College London. They discovered that co-incubating NK cells with the CD15 positive CTV-1 cell line generated 'primed' NK cells that were then subsequently able to kill NK cell-resistant cell lines such as DU145 prostate cancer cells and Raji cells (North et al., 2007, Sabry et al., 2011). NK cell priming required cell-to-cell contact with the MHC class I positive CTV-1 cell line. Although the NK cells were primed by the CTV-1 cells, they could not kill the CTV-1 cell line, but could subsequently kill other NK cell-resistant cell lines (North et al., 2007). The authors concluded that stimulation of NK cells to kill its target can be split into two stages: priming and triggering. Priming is postulated to involve the transduction of activating signals by the NK cells through either the binding of cytokines (via cytokine receptors) or through the binding of the correct combination and intensity of stress ligands expressed on tumour cells (via NK activating receptors). Triggering of the cytotoxic immune response requires the binding of one more activating receptors to its stress ligand expressed on the tumour cell, thereby avoiding autoreactivity with healthy cells (North et al., 2007, Sabry and Lowdell, 2013). The priming of NK cells was shown to be associated with a change in NK cell phenotype, as

characterised by decreases in the expression of CD16 expression and the NKG2D, NKp46 and NKp80 activating receptors, and an increase in the expression of CD69 and CD25 (North et al., 2007, Sabry et al., 2011). This work highlights that the down-regulation of activating receptors on NK cells from patients is not necessarily a sign of cancer immunosuppression, but could represent activation of a NK response that has ultimately failed to eradicate the cancer.

Publications from Lowdell's group suggested and used primed NK cells as an immunotherapy to treat patients with acute myelogenous leukaemia (AML) (Kottaridis et al., 2015, Sabry et al., 2011). On the basis of these studies, I proposed that the NK : CTV-1 priming method has the potential to be used as a method for accurately measuring NK cell potential and function. Two functions of the patient NK cells could be measured using the NK priming method; 1) how well the patient NK cells are primed following contact with CTV-1 cells, as measured on the basis of the up-regulation and down-regulation of NK cell receptors and 2) the subsequent ability of the primed NK cells to kill a relevant cancer cell line, as measured using relevant cytotoxicity assays. The measurement of these two functions *in vitro* will mimic the ability of NK cells to become activated and exert their cytotoxic function following contact with cancer cells *in vivo*. If the patient's cancer has suppressed NK cell function via the down-regulation of activating receptors such as NKp30 or NKp46 (as potentially observed through patient NK cell phenotypic analysis), or through other unknown mechanisms, then the ability of the NK cells to become primed will be reduced. This will then affect the up-regulation of triggering receptors and the down-regulation of activating receptors such as NKG2D on the NK cell surface, and thus subsequently influence the ability of the primed NK cells to kill the NK resistant cancer lines, as measured using cytotoxic assays.

In the original study published by North et al (North et al., 2007), fresh NK cells were primed by co-incubating them with irradiated CTV-1 cells for up to 20 hrs. The experiments in this PhD study have shown that NK cells that have been previously frozen can also be primed using mitomycin C treated CTV-1 cells, and that these primed NK cells can subsequently kill up to 42 % of PC3 prostate cancer cells. Furthermore, similar to the published literature, it was shown that the NK cells primed by mitomycin C treated CTV-1 cells also down-regulated or shed CD16, down-regulated their expression of NKG2D and NKp46, but up-regulated their expression of CD69 and CD25. Through blocking experiments with a recombinant CD69 protein, North et al showed that CD69 is one of the receptors involved in the triggering of the cytotoxic response, but hypothesised that there may be other triggering receptors since 3 out of 10 AML samples were resistant to being killed by primed NK cells despite expressing CD69L (North et al., 2007).

The work in this PhD study has shown that in addition to primed NK cells up-regulating CD69 and to some extent CD25, they also up-regulate the co-stimulatory receptors; CD137 (4-1ββ),

GITR, OX40, CRTAM and CD107a. Based on one CD107a degranulation experiment, it appears that the co-receptors CD137 and CRTAM are not triggering receptors, as the majority of NK cells that up-regulated CD107a did not also up-regulate CD137 and CRTAM. The remainder of the NK cells either co-expressed CD107a and CRTAM or co-expressed CD107a, CRTAM and CD137. No NK cells co-expressed CD107a and CD137 only. More experiments will be needed to confirm if CD137, GITR, OX40 and CRTAM are triggering receptors. However, even if these receptors are not triggering receptors, based on studies in the literature it is likely that these receptors will influence NK cell function.

Although CRTAM is known to bind NECL2 expressed on tumour cells and is believed to play a role in cell-to-cell adhesion, there are conflicting reports regarding whether it promotes cytotoxicity (Arase et al., 2005, Boles et al., 2005). The co-receptors CD137, GITR and OX40 are currently the targets of monoclonal antibodies designed to stimulate the immune response against different forms of cancer which are now undergoing clinical trials. All three receptors are members of the TNFR superfamily and can be found on a range of cell types. Although the expression of CD137 and OX40 is absent on resting T cells and NK cells, expression is up-regulated upon activation. OX40 can also be expressed by NKT cells and neutrophils, while CD137 expression can also be found on activated B cells, dendritic cells, myeloid precursors and mast cells. The pattern of expression for the GITR receptor is slightly different, as there is a basal expression on resting T cells and NK cells which is then up-regulated upon activation. Eosinophils, basophils, macrophages and B cells also express GITR (reviewed by (Melero et al., 2013)).

The study of OX40 has been mostly confined to its expression on T cells (Croft, 2010) and even the primed NK cells in this PhD study express very low levels of OX40. Out of the three co-receptors, CD137 and GITR are the two receptors that have been studied the most on NK cells. It appears that both receptors play a role in the crosstalk between NK cells and other cells. Depending on the cell type and / or interaction with the two co-receptors, the outcome of this interaction can inhibit NK cell function or activate NK cells and even promote a type I immune response. Studies have reported that CD137L is expressed on a percentage of acute myeloid leukaemia (AML) cells (35 %) and on B chronic lymphocytic leukaemia (B-CLL) cells. For both sets of leukaemia patients, CD137 was found to be significantly up-regulated compared to healthy controls (Baessler et al., 2010, Buechele et al., 2012). Both studies stimulated the primary leukaemic cells using immobilised CD137-Ig and found that immunomodulating cytokines were released. The AML cells were stimulated to produce TNF and IL-10 whilst the B-CLL cell were stimulated to produce TNF and IL-8. Both studies co-cultured allogenic NK cells with their respective leukaemic cells in the presence of an anti-CD137 monoclonal antibody and in both

studies the NK cells increased their ability to both lyse the leukaemic cells and produce IFN-γ (Baessler et al., 2010, Buechele et al., 2012). Furthermore, Bueschele et al also reported that sera from patients with B-CLL was able to weakly induce CD137 expression on NK cells from healthy donors, whereas sera from healthy donors did not induce CD137 expression. These studies suggest that the leukaemic cells not only up-regulate CD137L, but also promote the expression of CD137 on NK cells via cytokines. The ligation of CD137 and CD137L on leukaemic cells promotes two immunosuppressive effects: 1) CD137:CD137L ligation directly inhibits NK cell cytotoxicity and IFN-γ production 2) CD137:CD137L ligation promotes the leukaemic cell to release immunosuppressive cytokines into the microenvironment, both of which can have immunosuppressive effects on T cells and dendritic cells. In contrast, Kohrt et al found that adding an anti-CD137 agonist monoclonal antibody could significantly enhance rituximab (anti CD20 monoclonal antibody) induced ADCC against Raji, Ramos, and DH-4 cell lines (Kohrt et al., 2011). Therefore, depending on the type of interaction, CD137L may be activating or inhibitory. It should be noted though that there is some speculation in the literature regarding whether or not the enhancement of cytotoxic function by the anti-CD137 monoclonal antibody in Kohrt et al's study was due to blocking CD137L from binding to the CD137 receptor (Buechele et al., 2012). Similar to CD137L on leukaemic cell lines, ligation of immobilised GITR-Ig fusion protein with GITRL positive tumour cells (e.g. MCF7 and HCT116 cell lines) resulted in the secretion of TGF-β by those tumour cells. In co-cultures of unstimulated and IL-15 stimulated NK cells with GITRL positive tumour cells in the presence and absence of an anti-GITR monoclonal antibody, the presence of the antibody increased NK cell cytotoxicity and IFN-γ release in comparison to its absence (Baltz et al., 2007). Overall, it seems that tumour cells seem to be able to use the bidirectional signalling abilities of the TNF superfamily to their advantage by down-regulating NK cell function whilst promoting their own secretion of immunosuppressive cytokines. Therefore, the use of anti-CD137 and anti-GITR monoclonal antibodies to block CD137:CD137L and GITR:GITRL interactions appears to be an attractive immunotherapeutic approach for boosting anti-tumour immunity by blocking inhibitory signals. These monoclonal antibodies are currently being used alongside other immunotherapeutic treatments that induce ADCC and also treatments that block inhibitory immune receptors such as CTLA-4 and PD-1 (Mentlik James et al., 2013).

The published literature suggests that the expression of CD137 and GITR on activated NK cells is associated with the transduction of inhibitory signals that suppress NK cell responses. However, this is not the complete picture. In stark contrast, in the limited studies that have been undertaken in humans, CD137:CD137L and GITR:GITRL interactions can enhance cytotoxicity (and in some cases IFN-γ release) when involved in NK cell cross talking with healthy immune

cells such as γδ T lymphocytes (γδ T cells) and plasmacytoid pre-dendritic cells (pDCs). In a study by Maniar et al (Maniar et al., 2010), activated γδ T cells were co-incubated with immobilised human immunoglobulin G1 (hIgG1) primed NK cells. CD69 expression was upregulated on 25 % of NK cells that had been primed with hIgG1. The addition of γδ T cells increased the proportion of activated NK cells to 45.9 %. This increase in CD69 expression was associated with cell-to-cell contact. They observed that OX40L and CD137L were only expressed on activated γδ T cells. HIgG1 primed NK cells expressed OX40 and CD137, and this expression was further enhanced following contact with the activated γδ T cells. Crucially, hIgG1 primed NK cells could not kill squamous cell carcinoma head and neck tumour cell lines (SCCHN), melanoma, breast cancer or B and T lymphoma cells lines. However, following contact with activated γδ T cells, the NK cells significantly increased their ability to lyse these cell lines. Blocking of the CD137:CD137L interactions using a CD137Ig fusion protein decreased the cytolytic activity of the NK cells against SCCHN by 40%, thereby indicating that signalling through CD137 is at least partially involved in the regulation of NK cell cytolytic activity (Maniar et al., 2010). In a study by Hanabuchi et al (Hanabuchi et al., 2006), activated pDCs have been shown to express high levels of GITRL, whereas NK cells were shown to up-regulate GITR expression following exposure to IL-2, IL-12 and IL-15, but not IFN-α. pDCs activated through exposure to a B-type CpG ligand (known to induce GITRL expression and only a small amount of type I IFN production) induced strong NK cytotoxic activity and IFN-γ release against both K562 and the NK-resistant Daudi cell line. The cytotoxic activity against Daudi cells was higher than when the NK cells were stimulated with IFN-α alone. Furthermore, they showed that blocking GITRL with monoclonal antibodies inhibited the increase in cytotoxic function and IFN-γ release. Interestingly, blocking the initial IFN-α release by activated pDCs completely prevents the NK cells from killing Daudi cells and from secreting IFN-γ. Overall, studies in the literature and the results from this PhD study have shown that the expression of TNF receptors OX40, CD137 and GITR are up-regulated following activation of NK cells (via cytokine stimulation, hIgG1 or CTV-1 tumour cells). Ligation of these receptors with their respective ligands following cross talk with other immune cells e.g. dendritic cells and γδ T lymphocytes, may not trigger cytotoxic activity and IFN-γ release, but instead enhance these NK functions, thereby increasing the ability of the NK cells to kill NK-resistant tumour cell lines. However, it seems that tumours have developed mechanisms that can counter these effects by taking advantage of the TNF receptor bidirectional signalling and promoting the up-regulation of CD137 and GITR expression and in turn inhibiting NK function following ligation with these receptors.

The results from this PhD study and from publications by Lowdell's group (North et al., 2007, Sabry et al., 2011) show that resting NK cells can be primed following co-incubation with the

CTV-1 cell line, and that this enables them to kill solid tumour cells lines (DU145 and PC3), a lymphoma cell line (Raji), a multiple myeloma cell line (RPMI8226), leukaemic cell lines (ARH77) and 7 out of 10 primary AML samples. This led to the hypothesis that the primed NK cells appear to be insensitive to inhibitory signals from the target cells (North et al., 2007). Further work will be needed to determine whether these CTV-1 primed NK cells are sensitive to signalling via CD137, GITR and OX40 and if so whether they are receiving activating or inhibitory signals from their targets. Its plausible that the 3 primary AML samples that could not be killed by primed NK cells in the study by North et al managed to suppress the cytotoxic function of the primed NK cells via signalling through the three TNF receptors. This is assuming that the three TNF receptors were up-regulated on the primed NK cells in North et al's study, similar to the primed NK cells in this PhD study.

Interestingly, the analysis of the CTV-1 primed NK cells generated in this PhD study revealed that NK cell priming primarily involves the $CD56^{dim}$ subset. Since NK cells require cell-to-cell contact with CTV-1 cells in order to be primed, the observation that it is mainly the $CD56^{dim}$ subset that is primed is in line with studies by Fauriat et al (Fauriat et al., 2010). Studies by this group concluded that $CD56^{dim}$ subsets are activated by cell-to-cell contact rather than by cytokine stimulation, whereas $CD56^{bright}$ cells are strongly activated by cytokines, but not by cell-to cell contact (Fauriat et al., 2010). Thus, the NK : CTV-1 priming method can be used to activate $CD56^{dim}$ subsets without altering the $CD56^{dim}$: $CD56^{bright}$ ratio which is altered through cytokine stimulation (e.g. IL-2) of NK cells. Furthermore, it was observed in this PhD study that the down-regulation / shedding of CD16 which was observed to be associated with NK cell priming by CTV-1 cells allowed the $CD56^{dim}$ subset to be divided into three further subpopulations: $CD56^{dim}CD16^{high}$, $CD56^{dim}CD16^{low}$ and $CD56^{dim}CD16^{neg}$. Following priming, the proportion of NK cells within each of the three subpopulations expressing OX40, CD137, GITR and CD107a generally differed. Few $CD56^{dim}CD16^{high}$ NK cells expressed each of the 4 receptors, whereas a greater proportion of $CD56^{dim}CD16^{low}$ and $CD56^{dim}CD16^{neg}$ NK cells expressed them. Often, the $CD56^{dim}CD16^{neg}$ population contained the highest proportion of NK cells expressing each of the 4 receptors. The MFI for CD137, GITR and CRTAM expression also followed the same pattern of expression. All NK cells from healthy volunteers and patients with prostate cancer (irrespective of whether they had cancer and the grade of cancer) were primed and their phenotypes followed the same pattern of expression described above. This suggests that the priming method appears to affect different NK cell phenotypic subpopulations in different ways. The primed NK cells that continue to express high levels of CD16, with very few NK cells up-regulating the three TNF receptors and the CD107a receptor suggests that this population is not the

population which is responsible for the increased cytotoxic killing of NK cell-resistant tumour cells such as PC3 cells.

The enhanced loss of CD16 expression by $CD56^{dim}CD16^{low}$ and $CD56^{dim}CD16^{neg}$ NK cells, combined with the greater proportion of these NK cell subpopulations expressing the three TNF receptors plus the CD107a receptor suggest that primed NK cells from these two subpopulations are responsible for the cytotoxic killing of PC3 cells. This observation aligns with reports describing the phenotype of NK cells that kill K562 target cells. Using a CD107a degranulation assay, resting NK cells responsible for killing K562 targets cells have been shown to be from the $CD56^{dim}$ subset and associated with reduced or negative expression for CD16 (Grzywacz et al., 2007). The down-regulation of CD16 was found to be due to CD16 shedding which could be inhibited using a broad spectrum matrix metalloproteinase inhibitor (GM6001). Interestingly, the shedding of CD16 was not a requirement for the NK cells to kill the K562 cells (Grzywacz et al., 2007). The differences in the phenotypes of the three $CD56^{dim}$CD16 subpopulations following NK priming suggests that the different NK phenotypic subpopulations may be differentially activated, and involves the selection of NK cell subpopulations having particular phenotypes and stimulating them to become activated. Due to the large number of different NK cell phenotypes within the NK cell population of just one person which has been described by Horowitz et al (Horowitz et al., 2013), it is likely the NK cells are stimulated to different degrees depending on the number of activating and inhibitory receptor ligand pairings that are made. In line with reports by Fauriat et al (Fauriat et al., 2010), the different degree of stimulation received by the NK cells could in theory influence the type of NK cell effector response i.e. a cytotoxic response or an IFN-γ response or both, and whether or not it is associated with additional cytokine and chemokine release. The up-regulation in expression of CD25 (IL-2 alpha subunit) on the 3 primed $CD56^{dim}$ CD16 subpopulations followed a similar expression pattern to the three TNF receptors and the CD107a receptor. These results suggest that the NK cell priming method initiates and or mimics a potential *in vivo* selection mechanism, whereby NK cells with the correct phenotype to respond to the target cell are selected and could potentially be expanded via stimulation of small amounts of *in vivo* IL-2 to form an NK cell immune response that is both specific to the threat, but also capable of initiating and or recruiting a wider immune response. Currently, this model is just theoretical. Measurement of the proliferation and cytotoxic killing capacity of the 3 primed $CD56^{dim}$ CD16 NK cell subpopulations following cell sorting and IL-2 stimulation could be used to test the validity of the proposed *in vivo* NK immune response selection model.

The detection of CD107a at the surface of primed NK cells that had not encountered a target cell was unexpected. During NK cell and T cell degranulation it is widely accepted that CD107a in the lysosomal membrane of lytic granules is exposed to the cell surface following fusion of lytic

granules with the cell surface membrane, resulting in the release of their contents into the cleft of the immunological synapse (Mace et al., 2014, Peters et al., 1991). This mechanism forms the basis of the CD107a degranulation assay used for indirectly measuring NK cell and T cell cytotoxic responses which can be further adapted to provide information about the phenotype of the NK cells and T cells that are responsible for target cell killing (Alter et al., 2004, Betts et al., 2003, Grzywacz et al., 2007). Although I never tested it myself (this is the subject of future experiments), it is known that NK cells primed by CTV-1 cells cannot actually kill CTV-1 cells despite being able to kill other NK cell-resistant tumour cell lines (North et al., 2007). This suggests that primed NK cells do not degranulate following contact with CTV-1 cells. Yet for some reason the data from this PhD study has shown that they up-regulate CD107a on their cell surface.

There could be two explanations for this: 1) the CTV-1 cells somehow prevent granzyme B from passing through the cell membrane (which I think is unlikely) or 2) the lytic granules incompletely fuse with the NK cell membrane, as has recently been described by Liu et al (Liu et al., 2011). The incomplete fusion of lytic granules has been suggested to explain why stable clusters of exocytosed LAMP-1 had been detected on cell surface of live degranulating NK cells in the absence of granule polarisation in earlier studies by the same group (Liu et al., 2009). Therefore, it is possible that the up-regulation of CD107a on the primed NK cells following contact with CTV-1, but prior to contact with susceptible target cells, represents incomplete fusion of lytic granules and no release of granzyme B and perforin. Assuming that this is correct, the next question would be is the incomplete fusion of lytic granules the result of missing triggering signals? This is a question I hope to answer in future experiments.

There were two ways in which the CTV-1 : NK priming model could be used to measure the functional potential of patients with prostate cancer: 1) how well patient NK cells are primed following contact with CTV-1 cells, as determined on the basis of the up-regulation and down-regulation of NK cell receptors and 2) the ability of the primed NK cells to kill a relevant cancer cell line, as measured using cytotoxicity assays. Unfortunately, due to limited time, I was only able to measure the phenotypic changes induced by priming using NK cells from healthy volunteers, individuals with benign disease, and patients with Gleason 6 and Gleason 9 prostate cancer. Although I was able to determine the cytotoxic function of non-primed and primed NK cells from healthy volunteers against K562 and PC3 targets, it was not possible to undertake the same functional assays for NK cells from patients with prostate cancer and benign disease. Despite the limited amount of NK cell functional data, patterns in the data started to emerge. The most surprising pattern was that NK cells from all three prostate cancer patient groups i.e. benign, Gleason 6 and Gleason 9, could be primed, and to a similar degree. However, there were

differences in the priming of NK cells from healthy volunteers and individuals with prostate cancer. Generally, there was no difference in the ability of both primed NK cells from healthy individuals and patients with prostate cancer to down-regulate CD16 / shed CD16. As a consequence, there were no significant difference in the proportion of $CD56^{dim}CD16^{high}$, $CD56^{dim}CD16^{low}$ and $CD56^{dim}CD16^{neg}$ NK cell subpopulations in samples from healthy volunteers and patients with prostate cancer. Likewise, the down-regulation of NKG2D and up-regulation of CD69 by NK cells from healthy individuals and patients with prostate cancer was generally comparable. The proportion of NK cells that upregulated the expression of OX40 in healthy individuals and patients with prostate cancer were generally comparable, with the exception of the $CD56^{dim}CD16^{neg}$ subpopulation. In this subpopulation of NK cells, a greater up-regulation of OX40 was observed on NK cells from healthy individuals as compared to NK cells from patients with Gleason 6 and Gleason 9 prostate cancer.

Overall, the upregulation of CD137 expression on NK cells was greater following the priming of NK cells from healthy individuals. Although the proportion of $CD56^{dim}CD16^{high}$ and $CD56^{dim}CD16^{low}$ NK cells up-regulating CD137 was generally similar following NK priming, the up-regulation of CD137 on $CD56^{dim}CD16^{neg}$ NK cells from healthy individuals was generally greater than that by $CD56^{dim}CD16^{neg}$ NK cells from patients with prostate cancer. Regarding the expression of CRTAM, this was induced to a greater extent on NK cells from healthy individuals, as compared to patients with prostate cancer, with the greatest effect being seen for $CD56^{dim}CD16^{neg}$ cells from healthy individuals. There was a greater variation in the proportion of NK cells from patients with prostate cancer up-regulating GITR expression as compared to NK cells from healthy individuals. On average, the upregulation of GITR was more marked for NK cells from healthy individuals, and this was particularly apparent for the $CD56^{dim}CD16^{neg}$ population.

To my surprise, the proportion of NK cells expressing CD96 and NKp46 was lower for patients with prostate cancer, as compared to NK cells from healthy individuals, and this was true for all three $CD56^{dim}$CD16 subpopulations. When determining the optimal NK : CTV-1 priming ratio. the down-regulation of CD96 was associated with a decrease in the ability of the NK cells to kill PC3 target cells. In contrast, for the prostate cancer patients, there was a significant negative correlation between the proportion of NK cells down-regulating CD96 and the proportion of NK cells up-regulating CD107a. Although the reasons for these findings are unclear, the discovery by Liu et al (Liu et al., 2009) that CD107a can be expressed on the NK cell surface in the absence of lytic granule polarisation, which has been suggested to be due to incomplete fusion of lytic granules, could provide some explanation. Despite the differences in the phenotypes of primed NK cells from healthy individuals and patients with prostate cancer, there is no definitive way to

tell if these phenotypic differences will lead to differences in cytotoxic function or IFN-γ release without direct measurement of these two NK cell functions following NK priming. Overall, more patient samples will be needed to determine if the CTV-1 : NK priming method and the direct measurement of cytotoxic function is a superior approach for assessing NK cell function in patients with cancer than the standard methods that are currently in use.

It is important to point out that there were limitations to using the CTV-1 : NK cell method, particularly when using previously-frozen PBMCs. Inevitably, NK cells will be lost following thawing and the priming process was associated with a loss in NK cell viability (up to roughly 50 % in some cases). It is therefore unknown if there is a loss of some important NK cell subpopulations as a result of freeze thawing. The results in this PhD study also highlight the effects of freeze thawing on the loss of NK cytotoxic function, even against the easily killed K562 cell line. Therefore, ideally NK cell priming and subsequent functional assays should be undertaken using fresh NK cells in order to best retain NK cell numbers and phenotypic sub-populations, as well for maintaining NK cell function.

Although the NK cell functional assays in this PhD study had their limitations, there was no significant difference in the function of NK cells from patients with benign disease and Gleason 6 and Gleason 9 prostate cancer, despite differences in NK cell function being observed between the NK cells from these patients and NK cells of healthy patients. Furthermore, the results show no correlation in changes in patient NK cell phenotype with changes in their NK cell function as the grade of prostate cancer increases.

Overall, the phenotype and functional results for the prostate patient cohort suggest:

1) Changes in NK cell phenotype do not necessarily or accurately reflect changes in NK cell function. Measurement of NK cell phenotype must always be used in association with direct functional assays to draw accurate conclusions on patient NK cell function.
2) There is no apparent prostate cancer driven immunosuppression on peripheral blood NK cells.
3) If there is immunosuppression of intratumoural NK cell function associated with some grades of prostate cancer, then it is not reflected in the function of peripheral NK cell populations and therefore questions the meaning of the observed NK cell phenotypic changes.
4) Highlights that the phenotype and function of both peripheral and intratumoural NK cells ideally need to be measured in order to draw accurate conclusions regarding the effects of prostate cancer on NK cell populations.

In addition to the measurement of NK cell function in patients with cancer, I believe that the CTV-1 : NK priming method can be used to investigate the molecular processes involved in the function of different immunological synapses. It is now recognised that there are three types of immunological synapses: lytic synapses, inhibitory synapses and regulatory synapses (Mace and Orange, 2011). As briefly reviewed by Mace and Orange, determination of the function of the immunological synapse seems to be dictated by the type and health of the cell targeted (i.e. the expression level of MHC class I molecules and stress ligands), the clustering of activating and inhibitory receptors on NK cells, actin accumulation by NK cells, polarisation of the NK cell microtubule organising centre (MTOC) and lytic granules towards the synapse and, lastly, the length of interaction between the NK cell and its target. Lytic synapses are formed with MHC class I deficient stressed cells, whereby activating signals predominate, reorganisation of the actin cytoskeleton at the synapse occurs, the MTOC and lytic granules polarise towards the synapse and the target is killed.

In the case of inhibitory synapses, inhibitory signals predominate, the actin cytoskeleton is blocked from reorganising, polarisation of the MTOC and lytic granules towards the synapse does not occur and the target cell survives. Regulatory synapses have been described mostly in association with dendritic cells and appear to be a mixture of the process of the lytic and inhibitory processes. Although dendritic cells present cytokines (IL-12, IL-15 and IL-18) at the synapse to moderately activate NK cells, in order to prevent the formation of a lytic synapse they instead reorganise their actin cytoskeleton to allow for clustering of MHC class I at the inhibitory synapse and the provision of inhibitory signals to the NK cell (Mace and Orange, 2011). It has been suggested that the regulatory synapse described between NK cells and dendritic cells can promote NK cell survival, NK cell proliferation and priming for further responsiveness (Brilot et al., 2007). The CTV-1 : NK priming model may be useful in further investigating the molecular mechanisms involved in the formation of activating, inhibitory and regulatory immune synapses. It is currently unknown whether the formation of the immunological synapse between the NK cell and the CTV-1 is an example of a regulatory synapse or a failed lytic synapse. Further investigation using immunofluorescence can be used to determine what type of synapse it is and what molecular processes are involved in its formation.

The differential priming of NK cells by CTV-1 cells which leads to the generation of what appears to be three $CD56^{dim}$ subsets having different levels of CD16 expression and potentially different functions, has the potential to aid the investigation regarding the formation of different immunological synapses. The CD107a receptor was up-regulated on a proportion of $CD56^{dim}CD16^{neg}$ cells (but not all) and hardly at all on $CD56^{dim}CD16^{high}$ NK cells, thereby suggesting the presence of different immunological functions which in turn suggests the

formation of different immunological synapses with the targets cells. Furthermore, this PhD study highlighted significant correlations between the proportion of NK cells down-regulating NKG2D and NKp46 following NK cell priming and the decreased ability of the primed NK cells to kill K562 cells, thereby suggesting that both activating receptors play a significant role in the cytotoxic function of NK cells against K562 cells. However, these same primed NK cells exhibited an enhanced ability to kill PC3 cells. Further investigation will be needed in order to decipher the reason for these discrepancies, especially with regard to the suggestion that the down-regulation of NKG2D at the immunological synapse is thought to occur at the termination of the immunological synapse following the release of lytic granules (Mace et al., 2014). The NK cell priming model could also be used to further elucidate the mechanisms regarding the release of lytic granules contents at the lytic synapse. It is plausible that primed NK cells, before making contact with their target cells, are experiencing incomplete fusion of lytic granules at their cell surface which is why CD107a can be detected in the absence of CTV-1 cell death. Upon contact with susceptible targets, complete fusion of lytic granules occurs. Therefore, this CTV-1:NK priming method has the potential to be used to determine the molecular mechanisms involved with complete and incomplete fusion of lytic granules with the plasma membrane. Potential triggering receptors could also be identified. So far, there is no information regarding the roles of co-stimulatory receptors such as OX40, GITR and CD137 in the regulation of immunological synapses, as a consequence, the NK cell priming method could also provide further information regarding roles of these receptors.

The *in vitro* demonstration that CTV-1 primed NK cells have the ability to kill both leukaemic and solid tumours cells lines suggests that there is potential in the use of primed NK cells as an immunotherapy (Sabry et al., 2011). Their mechanism of action is different to other immunotherapeutic strategies such as bispecific and trispecific killer cell engagers (BiKEs and TriKEs) and monoclonal antibody therapies targeting either cancer antigens (e.g. HER2, CD20, EGRF), co-stimulatory TNF receptors (OX40, CD137, GITR) or immune checkpoint inhibitors (e.g. PD-1, CTLA-4), which kill tumour targets through ADCC (Ferris et al., 2010, Gleason et al., 2014, Mentlik James et al., 2013, Scott et al., 2012).

BiKEs and TriKEs are yet to have been tested in clinical trials, while a number of monoclonal antibody treatments have been approved for clinical use by the FDA (e.g. Cetuximab targeting EGRF, Ipilimumab targeting CTLA-4, Herceptin targeting ERBB2 positive breast cancer) (Scott et al., 2012). However, monoclonal antibody therapy response rates are about 8-10 % when used on their own and up to 30 % when used in conjunction with other treatments. They are also associated with adverse side-effects, particularly when targeting cancer antigens due to off-target responses resulting from the low expression of the cancer antigens on healthy cells (Ferris

et al., 2010). In comparison to *in vitro* studies of Cetuximab-activated NK cells, CTV-1 primed NK cells appear to be more potent at killing NK cell-resistant tumours (Roda et al., 2007, Sabry et al., 2011). This PhD study showed that CTV-1 primed NK cells can up-regulate TNF receptors for potential crosstalk with other immune cells such as dendritic cells and γδ T lymphocytes. Cetuximab has been shown to promote activated NK cell crosstalk with dendritic cells which in turn promotes the expansion of EGRF-specific T cells (Srivastava et al., 2013). Even BikES targeting CD19 Raji cells were thought to crosstalk with the Raji cells, presumably via TNF receptors and an enhancement of the release of NK cell-derived cytokines and chemokines which have the potential to attract other immune cells into the microenvironment (Gleason et al., 2014). It is reasonable to conclude that the use of CTV-1 primed NK cells as an immunotherapeutic has the potential to be as effective, if not better, than other current and up and coming immunotherapeutic treatments.

Completion of a recent Phase I clinical trial using donor NK cells that have been primed using a CTV-1 lysate as an immunotherapeutic strategy in high risk AML patients who were not eligible for curative standard allogenic stem cell procedures or other conventional treatments has confirmed the immunotherapeutic potential of primed NK cells to kill primary AML tumours (Kottaridis et al., 2015). No toxicities were reported from the infusion of *ex vivo* primed NK cells, and none of the patients developed any evidence of graft *versus* host disease (GVHD) in any organs. Although patients did suffer from cytopenias (low immune cell counts which included neutropenia and thrombocytopenia), it was likely that this was due to the lymphodepleting conditioning regime comprising of flurdarabine treatment for 3 days followed by a single dose of total body radiation (Kottaridis et al., 2015). Other studies have shown that patients receiving high intensity conditioning regimes using cyclophosphamide and fludarabine have also developed neutropenia (Miller et al., 2005). Six months following infusion of primed NK cells, out of 6 people three patients achieved complete remission and remained in remission, two patients relapsed and one had died. A further patient achieved complete remission 50 days after infusion. He remained in complete remission for 10 months before relapsing. A protocol amendment allowed him to receive a second dose without lymphodepleting conditioning. He never regained complete remission, but remained stable for a further 203 days while in relapse. After one year post-infusion, only one patient remained in complete remission while three had relapsed. During the two year follow up, six out of seven trial patients died (5 patients due to AML relapse, one due to intracranial haemorrhage due to thrombocytopenia and the other due to septic shock). Three of seven patients had detectable donor NK cells in their peripheral blood and / or bone marrow at more than one time-point post infusion, indicating donor chimerism. Six of seven patients showed an increase in activated NK cells in their circulation, whereas five

of six evaluable patients exhibited the presence of circulating primed NK cells, as measured by their ability to lyse the NK cell-resistant Raji cell line. Overall, the results were positive and indicated that donor primed NK cells are tolerated by patients and their use as a treatment is associated with promising clinical outcomes (Kottaridis et al., 2015).

In summary, the work in this PhD study contributes to what is known about the changes in phenotype of NK cells in the periphery of patients with prostate cancer. At present, it is not possible to use changes in peripheral NK cell phenotype to inform patient diagnosis, but there is a suggestion it could potentially be used to determine patient prognosis. However, further investigation is needed. The NK cell priming results in this PhD study and in studies by Lowdell's group bring into question how accurately changes in peripheral NK cell phenotype reflect changes in NK cell function in the periphery. Down-regulation in the expression of receptors does not necessarily mean a loss in NK cell function, but instead could mean activation of the NK cells. Furthermore, it is unclear how well the phenotype and function of NK cells in the peripheral circulation reflects intratumoural phenotype and function due to the small size of the prostate and the lack of access to intratumoural NK cells. No studies have looked at the phenotype and function of intratumoural NK cells and no studies to my knowledge have looked at immunosuppressive cytokines and factors secreted within in the prostate. It is therefore impossible to tell whether the changes in the peripheral phenotype of NK cells from prostate cancer patients is even due to the presence of their prostate cancer. Further investigation is needed regarding this. There is evidence to suggest that these phenotypic changes could be due to old age which is plausible given that prostate cancer is more likely to develop in older men.

It is in my opinion that the current methods of measuring NK cell function involving either targeting resting NK cells against K562 cells or targeting cytokine stimulated NK cells against NK cell-resistant tumour cells lines are not adequate to accurately measure the NK cell function in patients with cancer. The development of the CTV-1 induced NK cell priming method and its further characterisation in this PhD suggests it has the potential to more accurately measure the NK cell function of cancer patients. However, further work is needed to confirm this. There is therapeutic potential regarding the use of primed NK cells to treat patient tumours due to their increased capability to kill NK cell-resistant tumour cell lines and primary AML cells from patients. There are plans to further investigate the therapeutic potential of primed NK cells for the treatment of a variety of cancers. Furthermore, there is potential for the CTV-1 based NK cell priming method to be used to further investigate the formation of immunological synapses using immunofluorescent imaging techniques.

Further Work

This PhD study used an adapted version of the NK cell priming method originally developed by Lowdell at UCL to measure the cytotoxic function of NK cells. Unfortunately, I could only draw comparisons on the function of NK cells from healthy individuals and patients with prostate cancer on the basis of phenotypic changes on the NK cell surface following priming with CTV-1. Further work should focus on extending these observations and in addition measure the actual cytotoxic ability of the patient NK cells to kill PC3 and other prostate cancer cells following NK cell priming. This would not only allow the determination of whether there is a difference in cytotoxic killing between healthy volunteers, patients with benign disease and patients with prostate cancer, but also whether the phenotype of the primed NK cells truly reflects their cytotoxic function. These results will have implications regarding whether priming NK cells with CTV-1 and targeting them against a relevant cancer cell line is a suitable method for measuring NK cell function.

Currently, prostate cancer is the only form of solid tumour that is known to be susceptible to being killed by CTV-1 primed NK cells *in vitro*. It would be interesting to know if solid tumours from other organs e.g. ovarian, breast, colon, are also susceptible to being killed by primed NK cells *in vitro*, but crucially also *in vivo* in pre-clinical immunocompromised murine models such as NOD SCID mice. It is important that future studies focus on the efficacy of the primed NK cells to kill tumours in pre-clinical animal models as this will ultimately determine the future of primed NK cells as an immunotherapeutic strategy to treat cancer. To this end the John van Geest Cancer Research Centre has recently started a body of work in collaboration with UCL and INmune Bio International Ltd to study the ability of primed fresh NK cells to kill ovarian cancer cell lines (e.g. SKOV3) both *in vitro* and *in vivo* in NOD SCID murine models.

One important aspect of future work would be to define what a primed NK cell is and how they compare to NK cells exposed to cytokines and / or K562 cells. It is important to know whether NK cells respond differently to the three activation methods. Do the three methods activate the same or different signalling cascades producing phenotypically and functionally similar or different NK cell populations? This work can be easily achieved by using nanoString gene expression profiling technology to measure gene expression and flow cytometry assays to measure NK cell phenotype and function. Both primed NK cells and NK cells that have killed K562 have been shown to shed CD16 from their cell surface (Grzywacz et al., 2007, North et al., 2007). It has been shown in this study that following priming with CTV-1 cells the shedding of CD16 creates NK cell subpopulations that are phenotypically different and potentially have different functions. To my knowledge this has not been investigated in NK cells that have been exposed

to K562 cells. It would be interesting to compare if similar NK subpopulations are created using the two different activation methods.

Although we have observed the creation of NK subpopulations following priming, analysis has so far been limited to the number of antibodies that can be accommodated into a single 9 colour antibody panel, of which 6 panels have been created in this study. Flow cytometry analysis programs such as Infinicyt™ have been created that allows phenotypic analysis of NK cells using antibodies from two or more separate panels. Whilst such analysis would require validation, the software allows the potential identification of NK cell subpopulations using 2 or more 9 colour antibody panels.

Further investigation regarding the functions of the NK cell subpopulations would also be needed. This study has shown that following priming the receptors CD107a and CD137 are mainly up-regulated on separate NK cell populations, potentially suggesting that these two NK cell subpopulations may be functionally different. Future studies should investigate the extent and range of primed NK cell functions, as this information may have important implications on the success of the NK cell priming as a suitable immunotherapy.

As published by Lowdell and colleagues (North et al., 2007), NK cells cannot kill CTV-1 cells. It was therefore surprising that primed NK cells could up-regulate CD107a following priming with CTV-1, but prior to exposure to PC3 target cells. The ability of primed NK cells to kill fresh CTV-1 targets was not measured in this study. It will be important to do these experiments in order to confirm the observations by Lowdell and colleagues. If an upregulation of CD107a expression on NK cells in the absence of killing is confirmed, then both flow cytometry and immunofluorescence could be used to determine the architecture and molecular mechanisms involved in the formation of immunological synapses between primed NK cells and CTV-1 cells and between primed NK cells and target cells. This work would improve our knowledge of how NK cells function and determine exactly what signals need to be provided to trigger the primed NK cell immune response. Future studies should also focus on whether the primed NK cell responses can be enhanced or inhibited via stimulation with different cytokines. It would be important to know whether the function and / or survival of primed NK cells could be enhanced through exposure to cytokines such as IL-15 and IL-2. Equally, it would be important to know whether primed NK cells are susceptible or not to immunosuppression by cytokines such as TGF-β and IL-10, which may limit their potential as an immunotherapy.

References

ABARCA-ROJANO, E., MUNIZ-HERNANDEZ, S., MORENO-ALTAMIRANO, M. M., MONDRAGON-FLORES, R., ENRIQUEZ-RINCON, F. & SANCHEZ-GARCIA, F. J. 2009. Re-organization of mitochondria at the NK cell immune synapse. *Immunol Lett,* 122**,** 18-25.

ABEYWEERA, T. P., MERINO, E. & HUSE, M. 2011. Inhibitory signaling blocks activating receptor clustering and induces cytoskeletal retraction in natural killer cells. *J Cell Biol,* 192**,** 675-90.

AGANOVIC, D., PRCIC, A., KULOVAC, B. & HADZIOSMANOVIC, O. 2011. Prostate Cancer Detection Rate and the Importance of Premalignant Lesion in Rebiopsy. *Med Arh,* 65**,** 109-112.

AJCC. 2009. American Joint Commitee on Cancer. Available: https://cancerstaging.org/references-tools/quickreferences/Documents/ProstateSmall.pdf.

ALMEIDA-OLIVEIRA, A., SMITH-CARVALHO, M., PORTO, L. C., CARDOSO-OLIVEIRA, J., RIBEIRO, A. D. S., FALCÃO, R. R., ABDELHAY, E., BOUZAS, L. F., THULER, L. C. S., ORNELLAS, M. H. & DIAMOND, H. R. 2011. Age-related changes in natural killer cell receptors from childhood through old age. *Human Immunology,* 72**,** 319-329.

ALTER, G., MALENFANT, J. M. & ALTFELD, M. 2004. CD107a as a functional marker for the identification of natural killer cell activity. *J Immunol Methods,* 294**,** 15-22.

AMIN, M. M., JEYAGANTH, S., FAHMY, N., BEGIN, L., ARONSON, S., JACOBSON, S., TANGUAY, S. & APRIKIAN, A. G. 2007. Subsequent prostate cancer detection in patients with prostatic intraepithelial neoplasis or atypical small acinar proliferation. *Canadian Urological Association Journal,* 1**,** 245-9.

ANDERSSON, L. C., NILSSON, K. & GAHMBERG, C. G. 1979. K562—A human erythroleukemic cell line. *International Journal of Cancer,* 23**,** 143-147.

ANEGON, I., CUTURI, M. C., TRINCHIERI, G. & PERUSSIA, B. 1988. Interaction of Fc receptor (CD16) ligands induces transcription of interleukin 2 receptor (CD25) and lymphokine genes and expression of their products in human natural killer cells. *J Exp Med,* 167**,** 452-72.

ARASE, N., TAKEUCHI, A., UNNO, M., HIRANO, S., YOKOSUKA, T., ARASE, H. & SAITO, T. 2005. Heterotypic interaction of CRTAM with Necl2 induces cell adhesion on activated NK cells and CD8+ T cells. *Int Immunol,* 17**,** 1227-37.

ARNON, T. I., LEV, M., KATZ, G., CHERNOBROV, Y., PORGADOR, A. & MANDELBOIM, O. 2001. Recognition of viral hemagglutinins by NKp44 but not by NKp30. *European Journal of Immunology,* 31**,** 2680-2689.

ASH, D., FLYNN, A., BATTERMANN, J., DE REIJKE, T., LAVAGNINI, P. & BLANK, L. 2000. ESTRO/EAU/EORTC recommendations on permanent seed implantation for localized prostate cancer. *Radiother Oncol,* 57**,** 315-21.

ASHIRU, O., BOUTET, P., FERNÁNDEZ-MESSINA, L., AGÜERA-GONZÁLEZ, S., SKEPPER, J. N., VALÉS-GÓMEZ, M. & REYBURN, H. T. 2010. Natural Killer Cell Cytotoxicity Is Suppressed by Exposure to the Human NKG2D Ligand MICA*008 That Is Shed by Tumor Cells in Exosomes. *Cancer Research,* 70**,** 481-489.

BAESSLER, T., CHARTON, J. E., SCHMIEDEL, B. J., GRUNEBACH, F., KRUSCH, M., WACKER, A., RAMMENSEE, H. G. & SALIH, H. R. 2010. CD137 ligand mediates opposite effects in human and mouse NK cells and impairs NK-cell reactivity against human acute myeloid leukemia cells. *Blood,* 115**,** 3058-69.

BALSAMO, M., SCORDAMAGLIA, F., PIETRA, G., MANZINI, C., CANTONI, C., BOITANO, M., QUEIROLO, P., VERMI, W., FACCHETTI, F., MORETTA, A., MORETTA, L., MINGARI, M. C. & VITALE, M. 2009. Melanoma-associated fibroblasts modulate NK cell phenotype and antitumor cytotoxicity. *Proceedings of the National Academy of Sciences,* 106**,** 20847-20852.

BALTZ, K. M., KRUSCH, M., BRINGMANN, A., BROSSART, P., MAYER, F., KLOSS, M., BAESSLER, T., KUMBIER, I., PETERFI, A., KUPKA, S., KROEBER, S., MENZEL, D., RADSAK, M. P., RAMMENSEE, H. G. & SALIH, H. R. 2007. Cancer immunoediting by GITR (glucocorticoid-induced TNF-related protein) ligand in humans: NK cell/tumor cell interactions. *FASEB J,* 21**,** 2442-54.

BARBER, D. F., FAURE, M. & LONG, E. O. 2004. LFA-1 Contributes an Early Signal for NK Cell Cytotoxicity. *The Journal of Immunology,* 173**,** 3653-3659.

BARREIRA DA SILVA, R., GRAF, C. & MUNZ, C. 2011. Cytoskeletal stabilization of inhibitory interactions in immunologic synapses of mature human dendritic cells with natural killer cells. *Blood,* 118**,** 6487-98.

BAUER, S., GROH, V., WU, J., STEINLE, A., PHILLIPS, J. H., LANIER, L. L. & SPIES, T. 1999. Activation of NK cells and T cells by NKG2D, a receptor for stress-inducible MICA. *Science,* 285**,** 727-9.

BAUMAN, G., RUMBLE, R. B., CHEN, J., LOBLAW, A. & WARDE, P. 2012. Intensity-modulated radiotherapy in the treatment of prostate cancer. *Clin Oncol (R Coll Radiol),* 24**,** 461-73.

BETTS, M. R., BRENCHLEY, J. M., PRICE, D. A., DE ROSA, S. C., DOUEK, D. C., ROEDERER, M. & KOUP, R. A. 2003. Sensitive and viable identification of antigen-specific CD8+ T cells by a flow cytometric assay for degranulation. *Journal of Immunological Methods,* 281**,** 65-78.

BHAVSAR, S. K., EBERHARD, M., BOBBALA, D. & LANG, F. 2010. Monensin induced suicidal erythrocyte death. *Cell Physiol Biochem,* 25**,** 745-52.

BINICI, J., HARTMANN, J., HERRMANN, J., SCHREIBER, C., BEYER, S., GULER, G., VOGEL, V., TUMULKA, F., ABELE, R., MANTELE, W. & KOCH, J. 2013. A soluble fragment of the tumor antigen BCL2-associated athanogene 6 (BAG-6) is essential and sufficient for inhibition of NKp30 receptor-dependent cytotoxicity of natural killer cells. *J Biol Chem,* 288**,** 34295-303.

BISWAS, S. K. & MANTOVANI, A. 2010. Macrophage plasticity and interaction with lymphocyte subsets: cancer as a paradigm. *Nat Immunol,* 11**,** 889-896.

BOLES, K. S., BARCHET, W., DIACOVO, T., CELLA, M. & COLONNA, M. 2005. The tumor suppressor TSLC1/NECL-2 triggers NK-cell and CD8+ T-cell responses through the cell-surface receptor CRTAM. *Blood,* 106**,** 779-86.

BORG, C., JALIL, A., LADERACH, D., MARUYAMA, K., WAKASUGI, H., CHARRIER, S., RYFFEL, B., CAMBI, A., FIGDOR, C., VAINCHENKER, W., GALY, A., CAIGNARD, A. & ZITVOGEL, L. 2004. NK cell activation by dendritic cells (DCs) requires the formation of a synapse leading to IL-12 polarization in DCs. *Blood,* 104**,** 3267-75.

BORRELLO, M. G., ALBERTI, L., FISCHER, A., DEGL'INNOCENTI, D., FERRARIO, C., GARIBOLDI, M., MARCHESI, F., ALLAVENA, P., GRECO, A., COLLINI, P., PILOTTI, S., CASSINELLI, G., BRESSAN, P., FUGAZZOLA, L., MANTOVANI, A. & PIEROTTI, M. A. 2005. Induction of a proinflammatory program in normal human thyrocytes by the RET/PTC1 oncogene. *Proceedings of the National Academy of Sciences of the United States of America,* 102**,** 14825-14830.

BRANDT, C. S., BARATIN, M., YI, E. C., KENNEDY, J., GAO, Z., FOX, B., HALDEMAN, B., OSTRANDER, C. D., KAIFU, T., CHABANNON, C., MORETTA, A., WEST, R., XU, W., VIVIER, E. & LEVIN, S. D. 2009. The B7 family member B7-H6 is a tumor cell ligand for the activating natural killer cell receptor NKp30 in humans. *J Exp Med,* 206**,** 1495-503.

BRAUD, V. M., ALLAN, D. S. J., O'CALLAGHAN, C. A., SODERSTROM, K., D'ANDREA, A., OGG, G. S., LAZETIC, S., YOUNG, N. T., BELL, J. I., PHILLIPS, J. H., LANIER, L. L. & MCMICHAEL, A. J. 1998. HLA-E binds to natural killer cell receptors CD94/NKG2A, B and C. *Nature,* 391**,** 795-799.

BRILOT, F., STROWIG, T., ROBERTS, S. M., ARREY, F. & MUNZ, C. 2007. NK cell survival mediated through the regulatory synapse with human DCs requires IL-15Ralpha. *J Clin Invest,* 117**,** 3316-29.

BRUMBAUGH, K. M., BINSTADT, B. A. & LEIBSON, P. J. 1998. Signal transduction during NK cell activation: balancing opposing forces. *Curr Top Microbiol Immunol,* 230**,** 103-22.
BRUNNER, K. T., MAUEL, J., CEROTTINI, J. C. & CHAPUIS, B. 1968. Quantitative assay of lytic action of immune lymphoid cells on 51Cr-labelled allogenic target cells in vitro; inhibition by isoantibody and by drugs. *Immunology,* 14**,** 181-196.
BRYCESON, Y. T., LJUNGGREN, H. G. & LONG, E. O. 2009. Minimal requirement for induction of natural cytotoxicity and intersection of activation signals by inhibitory receptors. *Blood,* 114**,** 2657-66.
BRYCESON, Y. T., MARCH, M. E., BARBER, D. F., LJUNGGREN, H. G. & LONG, E. O. 2005. Cytolytic granule polarization and degranulation controlled by different receptors in resting NK cells. *J Exp Med,* 202**,** 1001-12.
BRYCESON, Y. T., MARCH, M. E., LJUNGGREN, H. G. & LONG, E. O. 2006. Synergy among receptors on resting NK cells for the activation of natural cytotoxicity and cytokine secretion. *Blood,* 107**,** 159-66.
BUECHELE, C., BAESSLER, T., SCHMIEDEL, B. J., SCHUMACHER, C. E., GROSSE-HOVEST, L., RITTIG, K. & SALIH, H. R. 2012. 4-1BB ligand modulates direct and Rituximab-induced NK-cell reactivity in chronic lymphocytic leukemia. *Eur J Immunol,* 42**,** 737-48.
BURKHARDT, J. K., HESTER, S. & ARGON, Y. 1989. Two proteins targeted to the same lytic granule compartment undergo very different posttranslational processing. *Proc Natl Acad Sci U S A,* 86**,** 7128-32.
BURSHTYN, D. N., SHIN, J., STEBBINS, C. & LONG, E. O. 2000. Adhesion to target cells is disrupted by the killer cell inhibitory receptor. *Curr Biol,* 10**,** 777-80.
CAMPBELL, J. J., QIN, S., UNUTMAZ, D., SOLER, D., MURPHY, K. E., HODGE, M. R., WU, L. & BUTCHER, E. C. 2001. Unique Subpopulations of CD56+ NK and NK-T Peripheral Blood Lymphocytes Identified by Chemokine Receptor Expression Repertoire. *The Journal of Immunology,* 166**,** 6477-6482.
CARLSTEN, M., NORELL, H., BRYCESON, Y. T., POSCHKE, I., SCHEDVINS, K., LJUNGGREN, H. G., KIESSLING, R. & MALMBERG, K. J. 2009. Primary human tumor cells expressing CD155 impair tumor targeting by down-regulating DNAM-1 on NK cells. *J Immunol,* 183**,** 4921-30.
CASTRICONI, R., DONDERO, A., BELLORA, F., MORETTA, L., CASTELLANO, A., LOCATELLI, F., CORRIAS, M. V., MORETTA, A. & BOTTINO, C. 2013. Neuroblastoma-derived TGF-beta1 modulates the chemokine receptor repertoire of human resting NK cells. *J Immunol,* 190**,** 5321-8.
CATALONA , W. J., SMITH , D. S., RATLIFF , T. L., DODDS , K. M., COPLEN , D. E., YUAN , J. J. J., PETROS , J. A. & ANDRIOLE , G. L. 1991. Measurement of Prostate-Specific Antigen in Serum as a Screening Test for Prostate Cancer. *New England Journal of Medicine,* 324**,** 1156-1161.
CHAN, C. J., MARTINET, L., GILFILLAN, S., SOUZA-FONSECA-GUIMARAES, F., CHOW, M. T., TOWN, L., RITCHIE, D. S., COLONNA, M., ANDREWS, D. M. & SMYTH, M. J. 2014. The receptors CD96 and CD226 oppose each other in the regulation of natural killer cell functions. *Nat Immunol,* 15**,** 431-8.
CHANG, D. T. S., CHALLACOMBE, B. & LAWRENTSCHUK, N. 2013. Transperineal biopsy of the prostate[mdash]is this the future? *Nat Rev Urol,* 10**,** 690-702.
CHEN, M. E., JOHNSTON, D. A., TANG, K., BABAIAN, R. J. & TRONCOSO, P. 2000. Detailed mapping of prostate carcinoma foci: biopsy strategy implications. *Cancer,* 89**,** 1800-9.
CHENG, I., WITTE, J. S., JACOBSEN, S. J., HAQUE, R., QUINN, V. P., QUESENBERRY, C. P., CAAN, B. J. & VAN DEN EEDEN, S. K. 2010. Prostatitis, Sexually Transmitted Diseases, and Prostate Cancer: The California Men's Health Study. *PLoS ONE,* 5**,** e8736.
CHITADZE, G., LETTAU, M., BHAT, J., WESCH, D., STEINLE, A., FURST, D., MYTILINEOS, J., KALTHOFF, H., JANSSEN, O., OBERG, H. H. & KABELITZ, D. 2013. Shedding of endogenous MHC class I-related chain molecules A and B from different human tumor

entities: heterogeneous involvement of the "a disintegrin and metalloproteases" 10 and 17. *Int J Cancer,* 133**,** 1557-66.
CHODAK, G. W., KELLER, P. & SCHOENBERG, H. W. 1989. Assessment of screening for prostate cancer using the digital rectal examination. *Journal of Urology,* 141**,** 1136-8.
COHNEN, A., CHIANG, S. C., STOJANOVIC, A., SCHMIDT, H., CLAUS, M., SAFTIG, P., JANSSEN, O., CERWENKA, A., BRYCESON, Y. T. & WATZL, C. 2013. Surface CD107a/LAMP-1 protects natural killer cells from degranulation-associated damage. *Blood,* 122**,** 1411-8.
COLOTTA, F., ALLAVENA, P., SICA, A., GARLANDA, C. & MANTOVANI, A. 2009. Cancer-related inflammation, the seventh hallmark of cancer: links to genetic instability. *Carcinogenesis,* 30**,** 1073-81.
COOPER, M. A. 2001. Human natural killer cells: a unique innate immunoregulatory role for the CD56bright subset. *Blood,* 97**,** 3146-3151.
COOPER, M. A., FEHNIGER, T. A. & CALIGIURI, M. A. 2001. The biology of human natural killer-cell subsets. *Trends in Immunology,* 22**,** 633-640
CROFT, M. 2003. Costimulation of T cells by OX40, 4-1BB, and CD27. *Cytokine & Growth Factor Reviews,* 14**,** 265-273.
CROFT, M. 2010. Control of immunity by the TNFR-related molecule OX40 (CD134). *Annu Rev Immunol,* 28**,** 57-78.
CRUK. 2013. Cancer Research UK. Available: http://www.cancerresearchuk.org/about-cancer/prostate-cancer.
CUTURI, M. C., ANEGON, I., SHERMAN, F., LOUDON, R., CLARK, S. C., PERUSSIA, B. & TRINCHIERI, G. 1989. Production of hematopoietic colony-stimulating factors by human natural killer cells. *J Exp Med,* 169**,** 569-83.
D'AMICO, A. V., DESJARDIN, A., CHUNG, A. & CHEN, M. H. 1998. Assessment of outcome prediction models for localized prostate cancer in patients managed with external beam radiation therapy. *Semin Urol Oncol,* 16**,** 153-9.
DAVIS, D. M., CHLU, I., FASSETT, M., COHEN, G. B., MANDELBOLM, O. & STROMINGER, J. L. 1999. The human natural killer cell immune synapse. *PNAS,* 96**,** 15062-15067.
DEGLIANTONI, G., MURPHY, M., KOBAYASHI, M., FRANCIS, M. K., PERUSSIA, B. & TRINCHIERI, G. 1985. Natural killer (NK) cell-derived hematopoietic colony-inhibiting activity and NK cytotoxic factor. Relationship with tumor necrosis factor and synergism with immune interferon. *J Exp Med,* 162**,** 1512-30.
DEMURA, T., HIOKA, T., FURUNO, T., KANETA, T., GOTODA, H., MURAOKA, S., SATO, T., MOCHIZUKI, T., NAGAMORI, S. & SHINOHARA, N. 2005. Differences in tumor core distribution between palpable and nonpalpable prostate tumors in patients diagnosed using extensive transperineal ultrasound-guided template prostate biopsy. *Cancer,* 103**,** 1826-1832.
DENNING, S. M., DUSTIN, M. L., SPRINGER, T. A., SINGER, K. H. & HAYNES, B. F. 1988. Purified lymphocyte function-associated antigen-3 (LFA-3) activates human thymocytes via the CD2 pathway. *J Immunol,* 141**,** 2980-5.
DIMERY, I. W., ROSS, D. D., TESTA, J. R., GUPTA, S. K., FELSTED, R. L., POLLAK, A. & BACHUR, N. R. 1983. Variation amongst K562 cell cultures. *Experimental hematology,* 11**,** 601-610.
DIMMEN, M., VLATKOVIC, L., HOLE, K.-H., NESLAND, J. M., BRENNHOVD, B. & AXCRONA, K. 2012. Transperineal prostate biopsy detects significant cancer in patients with elevated prostate-specific antigen (PSA) levels and previous negative transrectal biopsies. *BJU International,* 110**,** E69-E75.
DUNN, G. P., BRUCE, A. T., IKEDA, H., OLD, L. J. & SCHREIBER, R. D. 2002. Cancer immunoediting: from immunosurveillance to tumor escape. *Nat Immunol,* 3**,** 991-8.
DUNN, G. P., OLD, L. J. & SCHREIBER, R. D. 2004a. The Immunobiology of Cancer Immunosurveillance and Immunoediting. *Immunity,* 21**,** 137-148.
DUNN, G. P., OLD, L. J. & SCHREIBER, R. D. 2004b. The three Es of cancer immunoediting. *Annu Rev Immunol,* 22**,** 329-60.

DUSTIN, M. L. & SPRINGER, T. A. 1989. T-cell receptor cross-linking transiently stimulates adhesiveness through LFA-1. *Nature,* 341**,** 619-624.

EBELT, K., BABARYKA, G., FRANKENBERGER, B., STIEF, C. G., EISENMENGER, W., KIRCHNER, T., SCHENDEL, D. J. & NOESSNER, E. 2009. Prostate cancer lesions are surrounded by FOXP3+, PD-1+ and B7-H1+ lymphocyte clusters. *Eur J Cancer,* 45**,** 1664-72.

EISSMANN, P. & DAVIS, D. M. 2010. Inhibitory and regulatory immune synapses. *Curr Top Microbiol Immunol,* 340**,** 63-79.

EL-HAKIM, A. & MOUSSA, S. 2010. CUA guidelines on prostate biopsy methodology. *Canadian Urological Association Journal,* 4**,** 89-94.

EL-SHERBINY, Y. M., MEADE, J. L., HOLMES, T. D., MCGONAGLE, D., MACKIE, S. L., MORGAN, A. W., COOK, G., FEYLER, S., RICHARDS, S. J., DAVIES, F. E., MORGAN, G. J. & COOK, G. P. 2007. The requirement for DNAM-1, NKG2D, and NKp46 in the natural killer cell-mediated killing of myeloma cells. *Cancer Res,* 67**,** 8444-9.

EPSTEIN, J. I., EGEVAD, L., AMIN, M. B., DELAHUNT, B., SRIGLEY, J. R. & HUMPHREY, P. A. 2016. The 2014 International Society of Urological Pathology (ISUP) Consensus Conference on Gleason Grading of Prostatic Carcinoma: definition of grading patterns and proposal for a new grading system. *Am J Surg Pathol,* 40.

FAURIAT, C., LONG, E. O., LJUNGGREN, H. G. & BRYCESON, Y. T. 2010. Regulation of human NK-cell cytokine and chemokine production by target cell recognition. *Blood,* 115**,** 2167-76.

FAWCETT, J., HOLNESS, C. L. L., NEEDHAM, L. A., TURLEY, H., GATTERT, K. C., MASON, D. Y. & SIMMONS, D. L. 1992. Molecular cloning of ICAM-3, a third ligand for LFA-1, constitutively expressed on resting leukocytes. *Nature,* 360**,** 481-484.

FEBBRAIO, M. & SILVERSTEIN, R. L. 1990. Identification and characterisation of LAMP-1 as an activation-dependent platelet surface glycoprotein. *The Journal of Biological Chemistry,* 265**,** 18531-18537.

FEHNIGER, T. A., SHAH, M. H., TURNER, M. J., VANDEUSEN, J. B., WHITMAN, S. P., COOPER, M. A., SUZUKI, K., WECHSER, M., GOODSAID, F. & CALIGIURI, M. A. 1999. Differential cytokine and chemokine gene expression by human NK cells following activation with IL-18 or IL-15 in combination with IL-12: implications for the innate immune response. *J Immunol,* 162**,** 4511-20.

FERRIS, R. L., JAFFEE, E. M. & FERRONE, S. 2010. Tumor antigen-targeted, monoclonal antibody-based immunotherapy: clinical response, cellular immunity, and immunoescape. *J Clin Oncol,* 28**,** 4390-9.

FESKE, S., SKOLNIK, E. Y. & PRAKRIYA, M. 2012. Ion channels and transporters in lymphocyte function and immunity. *Nat Rev Immunol,* 12**,** 532-47.

FITZPATRICK, J. M., BELLMUNT, J., FIZAZI, K., HEIDENREICH, A., STERNBERG, C. N., TOMBAL, B., ALCARAZ, A., BAHL, A., BRACARDA, S., DI LORENZO, G., EFSTATHIOU, E., FINN, S. P., FOSSA, S., GILLESSEN, S., KELLOKUMPU-LEHTINEN, P. L., LECOUVET, F. E., OUDARD, S., DE REIJKE, T. M., ROBSON, C. N., DE SANTIS, M., SERUGA, B. & DE WIT, R. 2014. Optimal management of metastatic castration-resistant prostate cancer: highlights from a European Expert Consensus Panel. *Eur J Cancer,* 50**,** 1617-27.

FREGNI, G., MESSAOUDENE, M., FOURMENTRAUX-NEVES, E., MAZOUZ-DORVAL, S., CHANAL, J., MAUBEC, E., MARINHO, E., SCHEER-SENYARICH, I., CREMER, I., AVRIL, M. F. & CAIGNARD, A. 2013. Phenotypic and functional characteristics of blood natural killer cells from melanoma patients at different clinical stages. *PLoS One,* 8**,** e76928.

FRIDLENDER, Z. G. & ALBELDA, S. M. 2012. Tumor-associated neutrophils: friend or foe? *Carcinogenesis,* 33**,** 949-955.

GABRILOVICH, D. I., OSTRAND-ROSENBERG, S. & BRONTE, V. 2012. Coordinated regulation of myeloid cells by tumours. *Nat Rev Immunol,* 12**,** 253-268.

GANNON, P. O., POISSON, A. O., DELVOYE, N., LAPOINTE, R., MES-MASSON, A. M. & SAAD, F. 2009. Characterization of the intra-prostatic immune cell infiltration in androgen-deprived prostate cancer patients. *J Immunol Methods,* 348**,** 9-17.

GHIRINGHELLI, F., MENARD, C., TERME, M., FLAMENT, C., TAIEB, J., CHAPUT, N., PUIG, P. E., NOVAULT, S., ESCUDIER, B., VIVIER, E., LECESNE, A., ROBERT, C., BLAY, J. Y., BERNARD, J., CAILLAT-ZUCMAN, S., FREITAS, A., TURSZ, T., WAGNER-BALLON, O., CAPRON, C., VAINCHENCKER, W., MARTIN, F. & ZITVOGEL, L. 2005. CD4+CD25+ regulatory T cells inhibit natural killer cell functions in a transforming growth factor-beta-dependent manner. *J Exp Med,* 202**,** 1075-85.

GLEASON, D. F. & MELLINGER, G. T. 1974. Prediction of prognosis for prostatic adenocarcinoma by combined histological grading and clinical staging. *Journal of Urology* 111**,** 58-64.

GLEASON, M. K., ROSS, J. A., WARLICK, E. D., LUND, T. C., VERNERIS, M. R., WIERNIK, A., SPELLMAN, S., HAAGENSON, M. D., LENVIK, A. J., LITZOW, M. R., EPLING-BURNETTE, P. K., BLAZAR, B. R., WEINER, L. M., WEISDORF, D. J., VALLERA, D. A. & MILLER, J. S. 2014. CD16xCD33 bispecific killer cell engager (BiKE) activates NK cells against primary MDS and MDSC CD33+ targets. *Blood,* 123**,** 3016-26.

GOLLAPUDI, K., GALET, C., GROGAN, T., ZHANG, H., SAID, J. W., HUANG, J., ELASHOFF, D., FREEDLAND, S. J., RETTIG, M. & ARONSON, W. J. 2013. Association between tumor-associated macrophage infiltration, high grade prostate cancer, and biochemical recurrence after radical prostatectomy. *Am J Cancer Res,* 3**,** 523-9.

GORDETSKY, J. & EPSTEIN, J. 2016. Grading of prostatic adenocarcinoma: current state and prognostic implications. *Diagnostic Pathology,* 11**,** 1-8.

GOSSELAAR, C., ROOBOL, M. J., ROEMELING, S. & SCHRÖDER, F. H. 2008. The Role of the Digital Rectal Examination in Subsequent Screening Visits in the European Randomized Study of Screening for Prostate Cancer (ERSPC), Rotterdam. *European Urology,* 54**,** 581-588.

GRAKOUI, A., BROMLEY, S. K., SUMEN, C., DAVIS, M. M., SHAW, A. S., ALLEN, P. M. & DUSTIN, M. L. 1999. The Immunological Synapse: A Molecular Machine Controlling T Cell Activation. *Science,* 285**,** 221-227.

GRÉGOIRE, C., CHASSON, L., LUCI, C., TOMASELLO, E., GEISSMANN, F., VIVIER, E. & WALZER, T. 2007. The trafficking of natural killer cells. *Immunological Reviews,* 220**,** 169-182.

GRIFFIN, J. D., HERCEND, T., BEVERIDGE, R. & SCHLOSSMAN, S. F. 1983. Characterization of an antigen expressed by human natural killer cells. *J Immunol,* 130**,** 2947-51.

GRIFFITH, J. W., SOKOL, C. L. & LUSTER, A. D. 2014. Chemokines and chemokine receptors: positioning cells for host defense and immunity. *Annu Rev Immunol,* 32**,** 659-702.

GROH, V., BAHRAM, S., BAUER, S., HERMAN, A., BEAUCHAMP, M. & SPIES, T. 1996. Cell stress-regulated human major histocompatibility complex class I gene expressed in gastrointestinal epithelium. *Proc Natl Acad Sci U S A,* 93**,** 12445-50.

GROH, V., STEINLE, A., BAUER, S. & SPIES, T. 1998. Recognition of stress-induced MHC molecules by intestinal epithelial gammadelta T cells. *Science,* 279**,** 1737-40.

GROH, V., WU, J., YEE, C. & SPIES, T. 2002. Tumour-derived soluble MIC ligands impair expression of NKG2D and T-cell activation. *Nature,* 419**,** 734-738.

GRZYWACZ, B., KATARIA, N. & VERNERIS, M. R. 2007. CD56(dim)CD16(+) NK cells downregulate CD16 following target cell induced activation of matrix metalloproteinases. *Leukemia,* 21**,** 356-9; author reply 359.

HANABUCHI, S., WATANABE, N., WANG, Y. H., WANG, Y. H., ITO, T., SHAW, J., CAO, W., QIN, F. X. & LIU, Y. J. 2006. Human plasmacytoid predendritic cells activate NK cells through glucocorticoid-induced tumor necrosis factor receptor-ligand (GITRL). *Blood,* 107**,** 3617-23.

HANAHAN, D. & WEINBERG, R. A. 2000. The Hallmarks of Cancer. *Cell,* 100**,** 57-70.

HANAHAN, D. & WEINBERG, R. A. 2011. Hallmarks of cancer: the next generation. *Cell,* 144**,** 646-74.

HANKEY, B. F., FEUER, E. J., CLEGG, L. X., HAYES, R. B., LEGLER, J. M., PROROK, P. C., RIES, L. A., MERRILL, R. M. & KAPLAN, R. S. 1999. Cancer Surveillance Series: Interpreting Trends in Prostate Cancer—Part I: Evidence of the Effects of Screening in Recent Prostate

Cancer Incidence, Mortality, and Survival Rates. *Journal of the National Cancer Institute,* 91**,** 1017-1024.

HARRIS, A. L. 2002. Hypoxia--a key regulatory factor in tumour growth. *Nat Rev Cancer,* 2**,** 38-47.

HASMIM, M., MESSAI, Y., ZIANI, L., THIERY, J., BOUHRIS, J. H., NOMAN, M. Z. & CHOUAIB, S. 2015. Critical Role of Tumor Microenvironment in Shaping NK Cell Functions: Implication of Hypoxic Stress. *Front Immunol,* 6**,** 482.

HAZELDINE, J., HAMPSON, P. & LORD, J. M. 2012. Reduced release and binding of perforin at the immunological synapse underlies the age-related decline in natural killer cell cytotoxicity. *Aging Cell,* 11**,** 751-759.

HEIDENREICH, A., BASTIAN, P. J., BELLMUNT, J., BOLLA, M., JONIAU, S., VAN DER KWAST, T., MASON, M., MATVEEV, V., WIEGEL, T., ZATTONI, F. & MOTTET, N. 2014a. EAU guidelines on prostate cancer. part 1: screening, diagnosis, and local treatment with curative intent-update 2013. *Eur Urol,* 65**,** 124-37.

HEIDENREICH, A., BASTIAN, P. J., BELLMUNT, J., BOLLA, M., JONIAU, S., VAN DER KWAST, T., MASON, M., MATVEEV, V., WIEGEL, T., ZATTONI, F. & MOTTET, N. 2014b. EAU guidelines on prostate cancer. Part II: Treatment of advanced, relapsing, and castration-resistant prostate cancer. *Eur Urol,* 65**,** 467-79.

HERBERMAN, R. B., NUNN, M. E., HOLDEN, H. T. & LAVRIN, D. H. 1975a. Natural cytotoxic reactivity of mouse lymphoid cells against syngeneic and allogeneic tumors. II. Characterization of effector cells. *Int J Cancer,* 16**,** 230-9.

HERBERMAN, R. B., NUNN, M. E. & LAVRIN, D. H. 1975b. Natural cytotoxic reactivity of mouse lymphoid cells against syngeneic acid allogeneic tumors. I. Distribution of reactivity and specificity. *Int J Cancer,* 16**,** 216-29.

HERBERMAN, R. B. & ORTALDO, J. R. 1981. Natural killer cells: their roles in defenses against disease. *Science,* 214**,** 24-30.

HERCEND, T., GRIFFIN, J. D., BENSUSSAN, A., SCHMIDT, R. E., EDSON, M. A., BRENNAN, A., MURRAY, C., DALEY, J. F., SCHLOSSMAN, S. F. & RITZ, J. 1985. Generation of monoclonal antibodies to a human natural killer clone. Characterization of two natural killer-associated antigens, NKH1A and NKH2, expressed on subsets of large granular lymphocytes. *J Clin Invest,* 75**,** 932-43.

HOECHST, B., VOIGTLAENDER, T., ORMANDY, L., GAMREKELASHVILI, J., ZHAO, F., WEDEMEYER, H., LEHNER, F., MANNS, M. P., GRETEN, T. F. & KORANGY, F. 2009. Myeloid derived suppressor cells inhibit natural killer cells in patients with hepatocellular carcinoma via the NKp30 receptor. *Hepatology,* 50**,** 799-807.

HOLMBERG, L., BILL-AXELSON, A., STEINECK, G., GARMO, H., PALMGREN, J., JOHANSSON, E., ADAMI, H. O. & JOHANSSON, J. E. 2012. Results from the Scandinavian Prostate Cancer Group Trial Number 4: a randomized controlled trial of radical prostatectomy versus watchful waiting. *J Natl Cancer Inst Monogr,* 2012**,** 230-3.

HOPKINSON, K., WILLIAMS, E. A., FAIRBURN, B., FORSTER, S., FLOWER, D. J., SAXTON, J. M. & POCKLEY, A. G. 2007. A MitoTracker Green-based flow cytometric assay for natural killer cell activity: variability, the influence of platelets and a comparison of analytical approaches. *Exp Hematol,* 35**,** 350-7.

HOROWITZ, A., STRAUSS-ALBEE, D. M., LEIPOLD, M., KUBO, J., NEMAT-GORGANI, N., DOGAN, O. C., DEKKER, C. L., MACKEY, S., MAECKER, H., SWAN, G. E., DAVIS, M. M., NORMAN, P. J., GUETHLEIN, L. A., DESAI, M., PARHAM, P. & BLISH, C. A. 2013. Genetic and environmental determinants of human NK cell diversity revealed by mass cytometry. *Sci Transl Med,* 5**,** 208ra145.

HORTON, N. C. & MATHEW, P. A. 2015. NKp44 and Natural Cytotoxicity Receptors as Damage-Associated Molecular Pattern Recognition Receptors. *Front Immunol,* 6**,** 31.

HOUCHINS, J. P., YABE, T., MCSHERRY, C. & BACH, F. H. 1991. DNA sequence analysis of NKG2, a family of related cDNA clones encoding type II integral membrane proteins on human natural killer cells. *The Journal of Experimental Medicine,* 173**,** 1017-1020.

HOUCHINS, J. P., YABE, T., MCSHERRY, C., MIYOKAWA, N. & BACH, F. H. 1990. Isolation and characterisation of NK cell or NK/T cell specific cDNA clone *Journal of Molecular and Cellular Immunology,* 4**,** 295-306.

HROMADNIKOVA, I., PIRKOVA, P. & SEDLACKOVA, L. 2013. Influence of in vitro IL-2 or IL-15 alone or in combination with Hsp-70-derived 14-mer peptide (TKD) on the expression of NK cell activatory and inhibitory receptors. *Mediators Inflamm,* 2013**,** 405295.

HSING, A. W., TSAO, L. & DEVESA, S. S. 2000. International trends and patterns of prostate cancer incidence and mortality. *Int J Cancer,* 85**,** 60-7.

HUDSON, M. A., BAHNSON, R. R. & CATALONA, W. J. 1989. Clinical use of prostate specific antigen in patients with prostate cancer. *Journal of Urology,* 142**,** 1011-7.

HUMPHREY, P. A. 2004. Gleason grading and prognostic factors in carcinoma of the prostate. *Mod Pathol,* 17**,** 292-306.

IDORN, M., KOLLGAARD, T., KONGSTED, P., SENGELOV, L. & THOR STRATEN, P. 2014. Correlation between frequencies of blood monocytic myeloid-derived suppressor cells, regulatory T cells and negative prognostic markers in patients with castration-resistant metastatic prostate cancer. *Cancer Immunol Immunother,* 63**,** 1177-87.

IMAI, K., MATSUYAMA, S., MIYAKE, S., SUGA, K. & NAKACHI, K. 2000. Natural cytotoxic activity of peripheral-blood lymphocytes and cancer incidence: an 11-year follow-up study of a general population. *The Lancet,* 356**,** 1795-1799.

ITOH, K., TILDEN, A. B., KUMAGAI, K. & BALCH, C. M. 1985. Leu-11+ lymphocytes with natural killer (NK) activity are precursors of recombinant interleukin 2 (rIL 2)-induced activated killer (AK) cells. *J Immunol,* 134**,** 802-7.

JU, S., JU, S., GE, Y., QIU, H., LU, B., QIU, Y., FU, J., LIU, G., WANG, Q., HU, Y., SHU, Y. & ZHANG, X. 2009. A novel approach to induce human DCs from monocytes by triggering 4-1BBL reverse signaling. *International Immunology,* 21**,** 1135-1144.

JU, S. W., JU, S. G., WANG, F. M., GU, Z. J., QIU, Y. H., YU, G. H., MA, H. B. & ZHANG, X. G. 2003. A functional anti-human 4-1BB ligand monoclonal antibody that enhances proliferation of monocytes by reverse signaling of 4-1BBL. *Hybridoma Hybridomics,* 22**,** 333-8.

KARIN, M. 2006. Nuclear factor-[kappa]B in cancer development and progression. *Nature,* 441**,** 431-436.

KARRE, K. 2008. Natural killer cell recognition of missing self. *Nat Immunol,* 9**,** 477-80.

KAUFMAN, D. S., SCHOON, R. A., ROBERTSON, M. J. & LEIBSON, P. J. 1995. Inhibition of selective signaling events in natural killer cells recognizing major histocompatibility complex class I. *Proc Natl Acad Sci U S A,* 92**,** 6484-8.

KENNEDY, J., VICARI, A. P., SAYLOR, V., ZURAWSKI, S. M., COPELAND, N. G., GILBERT, D. J., JENKINS, N. A. & ZLOTNIK, A. 2000. A molecular analysis of NKT cells: identification of a class-I restricted T cell-associated molecule (CRTAM). *Journal of Leukocyte Biology,* 67**,** 725-34.

KLOTZ, L. 2010. Active surveillance for prostate cancer: a review. *Curr Urol Rep,* 11**,** 165-71.

KLOTZ, L., ZHANG, L., LAM, A., NAM, R., MAMEDOV, A. & LOBLAW, A. 2010. Clinical results of long-term follow-up of a large, active surveillance cohort with localized prostate cancer. *J Clin Oncol,* 28**,** 126-31.

KOHRT, H. E., HOUOT, R., GOLDSTEIN, M. J., WEISKOPF, K., ALIZADEH, A. A., BRODY, J., MULLER, A., PACHYNSKI, R., CZERWINSKI, D., COUTRE, S., CHAO, M. P., CHEN, L., TEDDER, T. F. & LEVY, R. 2011. CD137 stimulation enhances the antilymphoma activity of anti-CD20 antibodies. *Blood,* 117**,** 2423-32.

KOTTARIDIS, P. D., NORTH, J., TSIROGIANNI, M., MARDEN, C., SAMUEL, E. R., JIDE-BANWO, S., GRACE, S. & LOWDELL, M. W. 2015. Two-Stage Priming of Allogeneic Natural Killer Cells for the Treatment of Patients with Acute Myeloid Leukemia: A Phase I Trial. *PLoS One,* 10**,** e0123416.

KRZEWSKI, K., CHEN, X. & STROMINGER, J. L. 2008. WIP is essential for lytic granule polarization and NK cell cytotoxicity. *Proc Natl Acad Sci U S A,* 105**,** 2568-73.

KUPFER, A., DENNERT, G. & SINGER, S. J. 1983. Polarization of the Golgi apparatus and the microtubule-organizing center within cloned natural killer cells bound to their targets. *Proc Natl Acad Sci U S A,* 80**,** 7224-8.

KURIYAMA, M., WANG, M. C., PAPSIDERO, L. D., KILLIAN, C. S., SHIMANO, T., VALENZUELA, L., NISHIURA, T., MURPHY, G. P. & CHU, T. M. 1980. Quantitation of Prostate-specific Antigen in Serum by a Sensitive Enzyme Immunoassay. *Cancer Research,* 40**,** 4658-4662.

LANCIOTTI, M., MASIERI, L., RASPOLLINI, M. R., MINERVINI, A., MARI, A., COMITO, G., GIANNONI, E., CARINI, M., CHIARUGI, P. & SERNI, S. 2014. The role of M1 and M2 macrophages in prostate cancer in relation to extracapsular tumor extension and biochemical recurrence after radical prostatectomy. *Biomed Res Int,* 2014**,** 486798.

LANE, B. R., ZIPPE, C. D., ABOUASSALY, R., SCHOENFIELD, L., MAGI-GALLUZZI, C. & JONES, J. S. 2008. Saturation Technique Does Not Decrease Cancer Detection During Followup After Initial Prostate Biopsy. *The Journal of Urology,* 179**,** 1746-1750.

LANGSTEIN, J., MICHEL, J., FRITSCHE, J., KREUTZ, M., ANDREESEN, R. & SCHWARZ, H. 1998. CD137 (ILA/4-1BB), a member of the TNF receptor family, induces monocyte activation via bidirectional signaling. *J Immunol,* 160**,** 2488-94.

LANIER, L. L. 2005. NK cell recognition. *Annu Rev Immunol,* 23**,** 225-74.

LANIER, L. L., BENIKE, C. J., PHILLIPS, J. H. & ENGLEMAN, E. G. 1985. Recombinant interleukin 2 enhanced natural killer cell-mediated cytotoxicity in human lymphocyte subpopulations expressing the Leu 7 and Leu 11 antigens. *J Immunol,* 134**,** 794-801.

LANIER, L. L., LE, A. M., CIVIN, C. I., LOKEN, M. R. & PHILLIPS, J. H. 1986. The relationship of CD16 (Leu-11) and Leu-19 (NKH-1) antigen expression on human peripheral blood NK cells and cytotoxic T lymphocytes. *J Immunol,* 136**,** 4480-6.

LANIER, L. L., LE, A. M., PHILLIPS, J. H., WARNER, N. L. & BABCOCK, G. F. 1983. Subpopulations of human natural killer cells defined by expression of the Leu-7 (HNK-1) and Leu-11 (NK-15) antigens. *J Immunol,* 131**,** 1789-96.

LANIER, L. L., TESTI, R., BINDL, J. & PHILLIPS, J. H. 1989. Identity of Leu-19 (CD56) leukocyte differentiation antigen and neural cell adhesion molecule. *J Exp Med,* 169**,** 2233-8.

LAWRENCE, M. B. & SPRINGER, T. A. 1991. Leukocytes roll on a selectin at physiologic flow rates: distinction from and prerequisite for adhesion through integrins. *Cell,* 65**,** 859-73.

LE DREAN, E., VELY, F., OLCESE, L., CAMBIAGGI, A., GUIA, S., KRYSTAL, G., GERVOIS, N., MORETTA, A., JOTEREAU, F. & VIVIER, E. 1998. Inhibition of antigen-induced T cell response and antibody-induced NK cell cytotoxicity by NKG2A: association of NKG2A with SHP-1 and SHP-2 protein-tyrosine phosphatases. *Eur J Immunol,* 28**,** 264-76.

LEE, F., TORP-PEDERSEN, S. T. & SIDERS, D. B. 1989. The role of transrectal ultrasound in the early detection of prostate cancer. *CA Cancer J Clin,* 39**,** 337-60.

LI, H., HAN, Y., GUO, Q., ZHANG, M. & CAO, X. 2009. Cancer-expanded myeloid-derived suppressor cells induce anergy of NK cells through membrane-bound TGF-beta 1. *J Immunol,* 182**,** 240-9.

LI, T., YANG, Y., HUA, X., WANG, G., LIU, W., JIA, C., TAI, Y., ZHANG, Q. & CHEN, G. 2012. Hepatocellular carcinoma-associated fibroblasts trigger NK cell dysfunction via PGE2 and IDO. *Cancer Letters,* 318**,** 154-161.

LIU, C. C., PERUSSIA, B., COHN, Z. A. & YOUNG, J. D. 1986. Identification and characterization of a pore-forming protein of human peripheral blood natural killer cells. *J Exp Med,* 164**,** 2061-76.

LIU, D., BRYCESON, Y. T., MECKEL, T., VASILIVER-SHAMIS, G., DUSTIN, M. L. & LONG, E. O. 2009. Integrin-dependent organization and bidirectional vesicular traffic at cytotoxic immune synapses. *Immunity,* 31**,** 99-109.

LIU, D., MARTINA, J. A., WU, X. S., HAMMER, J. A., 3RD & LONG, E. O. 2011. Two modes of lytic granule fusion during degranulation by natural killer cells. *Immunol Cell Biol,* 89**,** 728-38.

LIU, D., PETERSON, M. E. & LONG, E. O. 2012. The adaptor protein Crk controls activation and inhibition of natural killer cells. *Immunity,* 36**,** 600-11.

LIU, G., LU, S., WANG, X., PAGE, S. T., HIGANO, C. S., PLYMATE, S. R., GREENBERG, N. M., SUN, S., LI, Z. & WU, J. D. 2013a. Perturbation of NK cell peripheral homeostasis accelerates prostate carcinoma metastasis. *J Clin Invest,* 123**,** 4410-22.

LIU, L., CHAHROUDI, A., SILVESTRI, G., WERNETT, M. E., KAISER, W. J., SAFRIT, J. T., KOMORIYA, A., ALTMAN, J. D., PACKARD, B. Z. & FEINBERG, M. B. 2002. Visualization and quantification of T cell-mediated cytotoxicity using cell-permeable fluorogenic caspase substrates. *Nat Med,* 8**,** 185-9.

LIU, S., ZHANG, H., LI, M., HU, D., LI, C., GE, B., JIN, B. & FAN, Z. 2013b. Recruitment of Grb2 and SHIP1 by the ITT-like motif of TIGIT suppresses granule polarization and cytotoxicity of NK cells. *Cell Death Differ,* 20**,** 456-64.

LJUNGGREN, H. G. & KARRE, K. 1985. Host resistance directed selectively against H-2-deficient lymphoma variants. Analysis of the mechanism. *J Exp Med,* 162**,** 1745-59.

LORENTE, D. & DE BONO, J. S. 2014. Molecular alterations and emerging targets in castration resistant prostate cancer. *Eur J Cancer,* 50**,** 753-64.

MABJEESH, N. J., LIDAWI, G., CHEN, J., GERMAN, L. & MATZKIN, H. 2012. High detection rate of significant prostate tumours in anterior zones using transperineal ultrasound-guided template saturation biopsy. *BJU Int,* 110**,** 993-7.

MACE, E. M., DONGRE, P., HSU, H. T., SINHA, P., JAMES, A. M., MANN, S. S., FORBES, L. R., WATKIN, L. B. & ORANGE, J. S. 2014. Cell biological steps and checkpoints in accessing NK cell cytotoxicity. *Immunol Cell Biol,* 92**,** 245-55.

MACE, E. M., MONKLEY, S. J., CRITCHLEY, D. R. & TAKEI, F. 2009. A Dual Role for Talin in NK Cell Cytotoxicity: Activation of LFA-1-Mediated Cell Adhesion and Polarization of NK Cells. *The Journal of Immunology,* 182**,** 948-956.

MACE, E. M. & ORANGE, J. S. 2011. Multiple distinct NK-cell synapses. *Blood,* 118**,** 6475-6.

MAMESSIER, E., SYLVAIN, A., BERTUCCI, F., CASTELLANO, R., FINETTI, P., HOUVENAEGHEL, G., CHARAFFE-JAUFRET, E., BIRNBAUM, D., MORETTA, A. & OLIVE, D. 2011a. Human Breast Tumor Cells Induce Self-Tolerance Mechanisms to Avoid NKG2D-Mediated and DNAM-Mediated NK Cell Recognition. *Cancer Research,* 71**,** 6621-6632.

MAMESSIER, E., SYLVAIN, A., THIBULT, M. L., HOUVENAEGHEL, G., JACQUEMIER, J., CASTELLANO, R., GONCALVES, A., ANDRE, P., ROMAGNE, F., THIBAULT, G., VIENS, P., BIRNBAUM, D., BERTUCCI, F., MORETTA, A. & OLIVE, D. 2011b. Human breast cancer cells enhance self tolerance by promoting evasion from NK cell antitumor immunity. *J Clin Invest,* 121**,** 3609-22.

MANDELBOIM, O., LIEBERMAN, N., LEV, M., PAUL, L., ARNON, T. I., BUSHKIN, Y., DAVIS, D. M., STROMINGER, J. L., YEWDELL, J. W. & PORGADOR, A. 2001. Recognition of haemagglutinins on virus-infected cells by NKp46 activates lysis by human NK cells. *Nature,* 409**,** 1055-1060.

MANIAR, A., ZHANG, X., LIN, W., GASTMAN, B. R., PAUZA, C. D., STROME, S. E. & CHAPOVAL, A. I. 2010. Human gammadelta T lymphocytes induce robust NK cell-mediated antitumor cytotoxicity through CD137 engagement. *Blood,* 116**,** 1726-33.

MANTOVANI, A., ALLAVENA, P., SICA, A. & BALKWILL, F. 2008. Cancer-related inflammation. *Nature,* 454**,** 436-444.

MARIANI, E., RODA, P., MARIANI, A. R., VITALE, M., DEGRASSI, A., PAPA, S. & FACCHINI, A. 1990. Age-associated changes in CD8+ and CD16+ cell reactivity: clonal analysis. *Clin Exp Immunol,* 81**,** 479-84.

MARKEL, G., SEIDMAN, R., BESSER, M. J., ZABARI, N., ORTENBERG, R., SHAPIRA, R., TREVES, A. J., LOEWENTHAL, R., ORENSTEIN, A., NAGLER, A. & SCHACHTER, J. 2009. Natural killer lysis receptor (NKLR)/NKLR-ligand matching as a novel approach for enhancing anti-tumor activity of allogeneic NK cells. *PLoS One,* 4**,** e5597.

MARTEN, A., VON LILIENFELD-TOAL, M., BUCHLER, M. W. & SCHMIDT, J. 2006. Soluble MIC is elevated in the serum of patients with pancreatic carcinoma diminishing gammadelta T cell cytotoxicity. *Int J Cancer,* 119**,** 2359-65.

MARTINET, L. & SMYTH, M. J. 2015. Balancing natural killer cell activation through paired receptors. *Nat Rev Immunol,* 15**,** 243-54.

MATHEW, S. O., RAO, K. K., KIM, J. R., BAMBARD, N. D. & MATHEW, P. A. 2009. Functional role of human NK cell receptor 2B4 (CD244) isoforms. *Eur J Immunol,* 39**,** 1632-41.

MAZZUCCHELLI, R., LOPEZ-BELTRAN, A., CHENG, L., SCARPELLI, M., KIRKALI, Z. & MONTIRONI, R. 2008. Rare and unusual histological variants of prostatic carcinoma: clinical significance. *BJU Int,* 102**,** 1369-74.

MCCANN, F. E., VANHERBERGHEN, B., ELEME, K., CARLIN, L. M., NEWSAM, R. J., GOULDING, D. & DAVIS, D. M. 2003. The Size of the Synaptic Cleft and Distinct Distributions of Filamentous Actin, Ezrin, CD43, and CD45 at Activating and Inhibitory Human NK Cell Immune Synapses. *The Journal of Immunology,* 170**,** 2862-2870.

MCNEAL, J. E. 1969. Origin and development of carcinoma in the prostate. *Cancer,* 23**,** 24-34.

MELERO, I., HIRSCHHORN-CYMERMAN, D., MORALES-KASTRESANA, A., SANMAMED, M. F. & WOLCHOK, J. D. 2013. Agonist antibodies to TNFR molecules that costimulate T and NK cells. *Clin Cancer Res,* 19**,** 1044-53.

MENTLIK, A. N., SANBORN, K. B., HOLZBAUR, E. L. & ORANGE, J. S. 2010. Rapid Lytic Granule Convergence to the MTOC in Natural Killer Cells Is Dependent on Dynein But Not Cytolytic Commitment. *Molecular Biology of the Cell,* 21**,** 2241-2256.

MENTLIK JAMES, A., COHEN, A. D. & CAMPBELL, K. S. 2013. Combination immune therapies to enhance anti-tumor responses by NK cells. *Front Immunol,* 4**,** 481.

MEYER, D., SETH, S., ALBRECHT, J., MAIER, M. K., DU PASQUIER, L., RAVENS, I., DREYER, L., BURGER, R., GRAMATZKI, M., SCHWINZER, R., KREMMER, E., FOERSTER, R. & BERNHARDT, G. 2009. CD96 interaction with CD155 via its first Ig-like domain is modulated by alternative splicing or mutations in distal Ig-like domains. *J Biol Chem,* 284**,** 2235-44.

MILLER, J. S., SOIGNIER, Y., PANOSKALTSIS-MORTARI, A., MCNEARNEY, S. A., YUN, G. H., FAUTSCH, S. K., MCKENNA, D., LE, C., DEFOR, T. E., BURNS, L. J., ORCHARD, P. J., BLAZAR, B. R., WAGNER, J. E., SLUNGAARD, A., WEISDORF, D. J., OKAZAKI, I. J. & MCGLAVE, P. B. 2005. Successful adoptive transfer and in vivo expansion of human haploidentical NK cells in patients with cancer. *Blood,* 105**,** 3051-7.

MOCCHEGIANI, E. & MALAVOLTA, M. 2004. NK and NKT cell functions in immunosenescence. *Aging Cell,* 3**,** 177-84.

MOCCHEGIANI, E., MUZZIOLI, M., GIACCONI, R., CIPRIANO, C., GASPARINI, N., FRANCESCHI, C., GAETTI, R., CAVALIERI, E. & SUZUKI, H. 2003. Metallothioneins/PARP-1/IL-6 interplay on natural killer cell activity in elderly: parallelism with nonagenarians and old infected humans. Effect of zinc supply. *Mech Ageing Dev,* 124**,** 459-68.

MONKS, C. R. F., FREIBERG, B. A., KUPFER, H., SCIAKY, N. & KUPFER, A. 1998. Three-dimensional segregation of supramolecular activation clusters in T cells. *Nature,* 395**,** 82-86.

MONTALDO, E., DEL ZOTTO, G., DELLA CHIESA, M., MINGARI, M. C., MORETTA, A., DE MARIA, A. & MORETTA, L. 2013. Human NK cell receptors/markers: a tool to analyze NK cell development, subsets and function. *Cytometry A,* 83**,** 702-13.

MORETTA, A., BOTTINO, C., PENDE, D., TRIPODI, G., TAMBUSSI, G., VIALE, O., ORENGO, A., BARBARESI, M., MERLI, A., CICCONE, E. & ET AL. 1990a. Identification of four subsets of human CD3-CD16+ natural killer (NK) cells by the expression of clonally distributed functional surface molecules: correlation between subset assignment of NK clones and ability to mediate specific alloantigen recognition. *J Exp Med,* 172**,** 1589-98.

MORETTA, A., TAMBUSSI, G., BOTTINO, C., TRIPODI, G., MERLI, A., CICCONE, E., PANTALEO, G. & MORETTA, L. 1990b. A novel surface antigen expressed by a subset of human CD3-

CD16+ natural killer cells. Role in cell activation and regulation of cytolytic function. *J Exp Med,* 171**,** 695-714.
MORGADO, S., SANCHEZ-CORREA, B., CASADO, J. G., DURAN, E., GAYOSO, I., LABELLA, F., SOLANA, R. & TARAZONA, R. 2011. NK cell recognition and killing of melanoma cells is controlled by multiple activating receptor-ligand interactions. *J Innate Immun,* 3**,** 365-73.
NAFIE, S., MELLON, J. K., DORMER, J. P. & KHAN, M. A. 2014a. The role of transperineal template prostate biopsies in prostate cancer diagnosis in biopsy naive men with PSA less than 20 ng ml(-1.). *Prostate Cancer Prostatic Dis,* 17**,** 170-3.
NAFIE, S., PAL, R. P., DORMER, J. P. & KHAN, M. A. 2014b. Transperineal template prostate biopsies in men with raised PSA despite two previous sets of negative TRUS-guided prostate biopsies. *World J Urol,* 32**,** 971-5.
NAGLER, A., LANIER, L. L., CWIRLA, S. & PHILLIPS, J. H. 1989. Comparative studies of human FcRIII positive and negative NK cells. *Immunology,* 143**,** 3183-3191.
NAKAMURA, K., NAKAYAMA, M., KAWANO, M., AMAGAI, R., ISHII, T., HARIGAE, H. & OGASAWARA, K. 2013. Fratricide of natural killer cells dressed with tumor-derived NKG2D ligand. *Proc Natl Acad Sci U S A,* 110**,** 9421-6.
NARAYAN, V. M., KONETY, B. R. & WARLICK, C. 2017. Novel biomarkers for prostate cancer: An evidence-based review for use in clinical practice. *Int J Urol*.
NAUGHTON, C. K., MILLER, D. C., MAGER, D. E., ORNSTEIN, D. K. & CATALONA, W. J. 2000. A prospective randomized trial comparing 6 verus 12 prostate biopsy cores: Impact on cancer detection. *The Journal of Urology,* 164**,** 388-392.
NESBIT, M., SCHAIDER, H., MILLER, T. H. & HERLYN, M. 2001. Low-Level Monocyte Chemoattractant Protein-1 Stimulation of Monocytes Leads to Tumor Formation in Nontumorigenic Melanoma Cells. *The Journal of Immunology,* 166**,** 6483-6490.
NICE. 2014. *Prostate cancer: diagnosis and managment* [Online]. National Institute for Health and Care Excellence. Available: https://www.nice.org.uk/guidance/cg175.
NISHIMURA, M., MITSUNAGA, S., AKAZA, T., MITOMI, Y., TADOKORO, K. & JUJI, T. 1994. Protection against natural killer cells by interferon-gamma treatment of K562 cells cannot be explained by augmented major histocompatibility complex class I expression. *Immunology,* 83**,** 75-80.
NITTA, T., YAGITA, H., SATO, K. & OKUMURA, K. 1989. Involvement of CD56 as an adhesion molecule in NK target cell interation. *Journal of Experimental Medicine,* 170**,** 1757-1761.
NONOMURA, N., TAKAYAMA, H., NAKAYAMA, M., NAKAI, Y., KAWASHIMA, A., MUKAI, M., NAGAHARA, A., AOZASA, K. & TSUJIMURA, A. 2011. Infiltration of tumour-associated macrophages in prostate biopsy specimens is predictive of disease progression after hormonal therapy for prostate cancer. *BJU Int,* 107**,** 1918-22.
NORTH, J., BAKHSH, I., MARDEN, C., PITTMAN, H., ADDISON, E. G., NAVARRETE, C., ANDERSON, R. & LOWDELL, M. W. 2007. Tumor-primed human NK cells lyse NK resistant tumor targets evidence of a two stage process in resting NK cell activation. *Immunology,* 178**,** 85-94.
OGATA, K., YOKOSE, N., TAMURA, H., AN, E., NAKAMURA, K., DAN, K. & NOMURA, T. 1997. Natural killer cells in the late decades of human life. *Clin Immunol Immunopathol,* 84**,** 269-75.
OKOTIE, O. T., ROEHL, K. A., HAN, M., LOEB, S., GASHTI, S. N. & CATALONA, W. J. Characteristics of Prostate Cancer Detected by Digital Rectal Examination Only. *Urology,* 70**,** 1117-1120.
ORANGE, J. S. 2008. Formation and function of the lytic NK-cell immunological synapse.pdf>. *Nature Review Immunology,* 8**,** 713-725.
ORANGE, J. S., HARRIS, K. E., ANDZELM, M. M., VALTER, M. M., GEHA, R. S. & STROMINGER, J. L. 2003. The mature activating natural killer cell immunologic synapse is formed in distinct stages. *Proc Natl Acad Sci U S A,* 100**,** 14151-6.

ORANGE, J. S., RAMESH, N., REMOLD-O'DONNELL, E., SASAHARA, Y., KOOPMAN, L., BYRNE, M., BONILLA, F. A., ROSEN, F. S., GEHA, R. S. & STROMINGER, J. L. 2002. Wiskott-Aldrich syndrome protein is required for NK cell cytotoxicity and colocalizes with actin to NK cell-activating immunologic synapses. *Proc Natl Acad Sci U S A,* 99**,** 11351-6.

OZER, H., STRELKAUSKAS, A. J., CALLERY, R. T. & SCHLOSSMAN, S. F. 1979. The functional dissection of human peripheral null cells with respect to antibody-dependent cellular cytotoxicity and natural killing. *Eur J Immunol,* 9**,** 112-8.

PAGEON, S. V., CORDOBA, S. P., OWEN, D. M., ROTHERY, S. M., OSZMIANA, A. & DAVIS, D. M. 2013. Superresolution microscopy reveals nanometer-scale reorganization of inhibitory natural killer cell receptors upon activation of NKG2D. *Sci Signal,* 6**,** ra62.

PAL, R. P., ELMUSSAREH, M., CHANAWANI, M. & KHAN, M. A. 2012. The role of a standardized 36 core template-assisted transperineal prostate biopsy technique in patients with previously negative transrectal ultrasonography-guided prostate biopsies. *BJU International,* 109**,** 367-371.

PARHAM, P. 2005. MHC class I molecules and KIRs in human history, health and survival. *Nat Rev Immunol,* 5**,** 201-14.

PASERO, C., GRAVIS, G., GRANJEAUD, S., GUERIN, M., THOMASSIN-PIANA, J., ROCCHI, P., SALEM, N., WALZ, J., MORETTA, A. & OLIVE, D. 2015. Highly effective NK cells are associated with good prognosis in patients with metastatic prostate cancer. *Oncotarget,* 6**,** 14360-73.

PCUK. 2013. Prostate Cancer UK. Available: http://prostatecanceruk.org/.

PENDE, D., PAROLINI, S., PESSINO, A., SIVORI, S., AUGUGLIARO, R., MORELLI, L., MARCENARO, E., ACCAME, L., MALASPINA, A., BIASSONI, R., BOTTINO, C., MORETTA, L. & MORETTA, A. 1999. Identification and molecular characterization of NKp30, a novel triggering receptor involved in natural cytotoxicity mediated by human natural killer cells. *J Exp Med,* 190**,** 1505-16.

PEREZ-VILLAR, J. J., MELERO, I., NAVARRO, F., CARRETERO, M., BELLON, T., LLANO, M., COLONNA, M., GERAGHTY, D. E. & LOPEZ-BOTET, M. 1997. The CD94/NKG2-A inhibitory receptor complex is involved in natural killer cell-mediated recognition of cells expressing HLA-G1. *J Immunol,* 158**,** 5736-43.

PERUSSIA, B., ACUTO, O., TERHORST, C., FAUST, J., LAZARUS, R., FANNING, V. & TRINCHIERI, G. 1983a. Human natural killer cells analyzed by B73.1, a monoclonal antibody blocking Fc receptor functions. II. Studies of B73.1 antibody-antigen interaction on the lymphocyte membrane. *J Immunol,* 130**,** 2142-8.

PERUSSIA, B., STARR, S., ABRAHAM, S., FANNING, V. & TRINCHIERI, G. 1983b. Human natural killer cells analyzed by B73.1, a monoclonal antibody blocking Fc receptor functions. I. Characterization of the lymphocyte subset reactive with B73.1. *J Immunol,* 130**,** 2133-41.

PERUSSIA, B., TRINCHIERI, G., JACKSON, A., WARNER, N. L., FAUST, J., RUMPOLD, H., KRAFT, D. & LANIER, L. L. 1984. The Fc receptor for IgG on human natural killer cells: phenotypic, functional, and comparative studies with monoclonal antibodies. *J Immunol,* 133**,** 180-9.

PETERS, P. J., BORST, J., OORSCHOT, V., FUKUDA, M., KRAHENBUHL, O., TSCHOPP, J., SLOT, J. W. & GEUZE, H. J. 1991. Cytotoxic T lymphocyte granules are secretory lysosomes, containing both perforin and granzymes.pdf>. *Journal of Experimental Medicine,* 173**,** 1099-1109.

PETERS, P. M., ORTALDO, J. R., SHALABY, M. R., SVEDERSKY, L. P., NEDWIN, G. E., BRINGMAN, T. S., HASS, P. E., AGGARWAL, B. B., HERBERMAN, R. B., GOEDDEL, D. V. & ET AL. 1986. Natural killer-sensitive targets stimulate production of TNF-alpha but not TNF-beta (lymphotoxin) by highly purified human peripheral blood large granular lymphocytes. *J Immunol,* 137**,** 2592-8.

PHILLIPS, J. H. & LANIER, L. L. 1986. Dissection of the lymphokine-activated killer phenomenon. Relative contribution of peripheral blood natural killer cells and T lymphocytes to cytolysis. *J Exp Med,* 164**,** 814-25.

PIETRA, G., MANZINI, C., RIVARA, S., VITALE, M., CANTONI, C., PETRETTO, A., BALSAMO, M., CONTE, R., BENELLI, R., MINGHELLI, S., SOLARI, N., GUALCO, M., QUEIROLO, P., MORETTA, L. & MINGARI, M. C. 2012. Melanoma cells inhibit natural killer cell function by modulating the expression of activating receptors and cytolytic activity. *Cancer Res,* 72**,** 1407-15.

PLATONOVA, S., CHERFILS-VICINI, J., DAMOTTE, D., CROZET, L., VIEILLARD, V., VALIDIRE, P., ANDRE, P., DIEU-NOSJEAN, M. C., ALIFANO, M., REGNARD, J. F., FRIDMAN, W. H., SAUTES-FRIDMAN, C. & CREMER, I. 2011. Profound coordinated alterations of intratumoral NK cell phenotype and function in lung carcinoma. *Cancer Research,* 71**,** 5412-22.

POGGE VON STRANDMANN, E., SIMHADRI, V. R., VON TRESCKOW, B., SASSE, S., REINERS, KATRIN S., HANSEN, H. P., ROTHE, A., BÖLL, B., SIMHADRI, V. L., BORCHMANN, P., MCKINNON, P. J., HALLEK, M. & ENGERT, A. 2007. Human Leukocyte Antigen-B-Associated Transcript 3 Is Released from Tumor Cells and Engages the NKp30 Receptor on Natural Killer Cells. *Immunity,* 27**,** 965-974.

PRADEU, T., JAEGER, S. & VIVIER, E. 2013. The speed of change: towards a discontinuity theory of immunity? *Nat Rev Immunol,* 13**,** 764-9.

PROCOPIO, A. D., ALLAVENA, P. & ORTALDO, J. R. 1985. Noncytotoxic functions of natural killer (NK) cells: large granular lymphocytes (LGL) produce a B cell growth factor (BCGF). *J Immunol,* 135**,** 3264-71.

RAJA, S. M., WANG, B., DANTULURI, M., DESAI, U. R., DEMELER, B., SPIEGEL, K., METKAR, S. S. & FROELICH, C. J. 2002. Cytotoxic cell granule-mediated apoptosis. Characterization of the macromolecular complex of granzyme B with serglycin. *J Biol Chem,* 277**,** 49523-30.

RITZ, J., SCHMIDT, R. E., MICHON, J., HERCEND, T. & SCHLOSSMAN, S. F. 1988. Characterization of functional surface structures on human natural killer cells. *Adv Immunol,* 42**,** 181-211.

RODA-NAVARRO, P., VALES-GOMEZ, M., CHISHOLM, S. E. & REYBURN, H. T. 2006. Transfer of NKG2D and MICB at the cytotoxic NK cell immune synapse correlates with a reduction in NK cell cytotoxic function. *Proc Natl Acad Sci U S A,* 103**,** 11258-63.

RODA, J. M., JOSHI, T., BUTCHAR, J. P., MCALEES, J. W., LEHMAN, A., TRIDANDAPANI, S. & CARSON, W. E., 3RD 2007. The activation of natural killer cell effector functions by cetuximab-coated, epidermal growth factor receptor positive tumor cells is enhanced by cytokines. *Clin Cancer Res,* 13**,** 6419-28.

ROSENBERG, E. B., HERBERMAN, R. B., LEVINE, P. H., HALTERMAN, R. H., MCCOY, J. L. & WUNDERLICH, J. R. 1972. Lymphocyte cytotoxicity reactions to leukemia-associated antigens in identical twins. *Int J Cancer,* 9**,** 648-58.

ROSENTAL, B., BRUSILOVSKY, M., HADAD, U., OZ, D., APPEL, M. Y., AFERGAN, F., YOSSEF, R., ROSENBERG, L. A., AHARONI, A., CERWENKA, A., CAMPBELL, K. S., BRAIMAN, A. & PORGADOR, A. 2011. Proliferating cell nuclear antigen is a novel inhibitory ligand for the natural cytotoxicity receptor NKp44. *J Immunol,* 187**,** 5693-702.

ROTHLEIN, R., DUSTIN, M. L., MARLIN, S. D. & SPRINGER, T. A. 1986. A human intercellular adhesion molecule (ICAM-1) distinct from LFA-1. *J Immunol,* 137**,** 1270-4.

ROTHLEIN, R. & SPRINGER, T. A. 1986. The requirement for lymphocyte function-associated antigen 1 in homotypic leukocyte adhesion stimulated by phorbol ester. *J Exp Med,* 163**,** 1132-49.

RUMPOLD, H., KRAFT, D., OBEXER, G., BOCK, G. & GEBHART, W. 1982. A monoclonal antibody against a surface antigen shared by human large granular lymphocytes and granulocytes. *J Immunol,* 129**,** 1458-64.

SABRY, M. & LOWDELL, M. W. 2013. Tumor-primed NK cells: waiting for the green light. *Front Immunol,* 4**,** 408.

SABRY, M., TSIROGIANNI, M., BAKHSH, I. A., NORTH, J., SIVAKUMARAN, J., GIANNOPOULOS, K., ANDERSON, R., MACKINNON, S. & LOWDELL, M. W. 2011. Leukemic priming of resting NK cells is killer Ig-like receptor independent but requires CD15-mediated CD2 ligation and natural cytotoxicity receptors. *J Immunol,* 187**,** 6227-34.

SARHAN, D., PALMA, M., MAO, Y., ADAMSON, L., KIESSLING, R., MELLSTEDT, H., ÖSTERBORG, A. & LUNDQVIST, A. 2015. Dendritic cell regulation of NK-cell responses involves lymphotoxin-α, IL-12, and TGF-β. *European Journal of Immunology,* 45**,** 1783-1793.

SCHRÖDER, F. H., KRUGER, A. B., RIETBERGEN, J., KRANSE, R., MAAS, P. V. D., BEEMSTERBOER, P. & HOEDEMAEKER, R. 1998. Evaluation of the Digital Rectal Examination as a Screening Test for Prostate Cancer. *Journal of the National Cancer Institute,* 90**,** 1817-1823.

SCOTT, A. M., WOLCHOK, J. D. & OLD, L. J. 2012. Antibody therapy of cancer. *Nat Rev Cancer,* 12**,** 278-287.

SELIGER, B., STOEHR, R., HANDKE, D., MUELLER, A., FERRONE, S., WULLICH, B., TANNAPFEL, A., HOFSTAEDTER, F. & HARTMANN, A. 2010. Association of HLA class I antigen abnormalities with disease progression and early recurrence in prostate cancer. *Cancer Immunol Immunother,* 59**,** 529-40.

SERVAIS, C. & EREZ, N. 2013. From sentinel cells to inflammatory culprits: cancer-associated fibroblasts in tumour-related inflammation. *J Pathol,* 229**,** 198-207.

SHANKARAN, V., IKEDA, H., BRUCE, A. T., WHITE, J. M., SWANSON, P. E., OLD, L. J. & SCHREIBER, R. D. 2001. IFNgamma and lymphocytes prevent primary tumour development and shape tumour immunogenicity. *Nature,* 410**,** 1107-11.

SHAW, S. & LUCE, G. E. 1987. The lymphocyte function-associated antigen (LFA)-1 and CD2/LFA-3 pathways of antigen-independent human T cell adhesion. *J Immunol,* 139**,** 1037-45.

SHEEHY, M. E., MCDERMOTT, A. B., FURLAN, S. N., KLENERMAN, P. & NIXON, D. F. 2001. A novel technique for the fluorometric assessment of T lymphocyte antigen specific lysis. *J Immunol Methods,* 249**,** 99-110.

SHEN, M. M. & ABATE-SHEN, C. 2010. Molecular genetics of prostate cancer: new prospects for old challenges. *Genes Dev,* 24**,** 1967-2000.

SHIBUYA, A., CAMPBELL, D., HANNUM, C., YSSEL, H., FRANZ-BACON, K., MCCLANAHAN, T., KITAMURA, T., NICHOLL, J., SUTHERLAND, G. R., LANIER, L. L. & PHILLIPS, J. H. 1996. DNAM-1, a novel adhesion molecule involved in the cytolytic function of T lymphocytes. *Immunity,* 4**,** 573-81.

SHIBUYA, K., LANIER, L. L., PHILLIPS, J. H., OCHS, H. D., SHIMIZU, K., NAKAYAMA, E., NAKAUCHI, H. & SHIBUYA, A. 1999. Physical and functional association of LFA-1 with DNAM-1 adhesion molecule. *Immunity,* 11**,** 615-23.

SIVORI, S., VITALE, M., MORELLI, L., SANSEVERINO, L., AUGUGLIARO, R., BOTTINO, C., MORETTA, L. & MORETTA, A. 1997. p46, a novel natural killer cell-specific surface molecule that mediates cell activation. *J Exp Med,* 186**,** 1129-36.

SMITH, D. S. & CATALONA, W. J. 1995. Interexaminer variability of digital examination in detecting prostate cancer *Urology,* 45**,** 70-4.

SRIVASTAVA, R. M., LEE, S. C., ANDRADE FILHO, P. A., LORD, C. A., JIE, H. B., DAVIDSON, H. C., LOPEZ-ALBAITERO, A., GIBSON, S. P., GOODING, W. E., FERRONE, S. & FERRIS, R. L. 2013. Cetuximab-activated natural killer and dendritic cells collaborate to trigger tumor antigen-specific T-cell immunity in head and neck cancer patients. *Clin Cancer Res,* 19**,** 1858-72.

STAMEY , T. A., YANG , N., HAY , A. R., MCNEAL , J. E., FREIHA , F. S. & REDWINE , E. 1987. Prostate-Specific Antigen as a Serum Marker for Adenocarcinoma of the Prostate. *New England Journal of Medicine,* 317**,** 909-916.

STANIETSKY, N., SIMIC, H., ARAPOVIC, J., TOPORIK, A., LEVY, O., NOVIK, A., LEVINE, Z., BEIMAN, M., DASSA, L., ACHDOUT, H., STERN-GINOSSAR, N., TSUKERMAN, P., JONJIC, S. & MANDELBOIM, O. 2009. The interaction of TIGIT with PVR and PVRL2 inhibits human NK cell cytotoxicity. *Proc Natl Acad Sci U S A,* 106**,** 17858-63.

STAUNTON, D. E., DUSTIN, M. L. & SPRINGER, T. A. 1989. Functional cloning of ICAM-2, a cell adhesion ligand for LFA-1 homologous to ICAM-1. *Nature,* 339**,** 61-4.

STEWART, C. S., LEIBOVICH, B. C., WEAVER, A. L. & LIEBER, M. M. 2001. Prostate cancer diagnosis using a saturation needle biopsy technique after previous negative sextant biopsies. *The Journal of Urology,* 166**,** 86-92.

STRASNER, A. & KARIN, M. 2015. Immune Infiltration and Prostate Cancer. *Frontiers in Oncology,* 5.

STRAUSS, L., BERGMANN, C., SZCZEPANSKI, M., GOODING, W., JOHNSON, J. T. & WHITESIDE, T. L. 2007. A Unique Subset of CD4+CD25high Foxp3+T Cells Secreting Interleukin-10 and Transforming Growth Factor-β1 Mediates Suppression in the Tumor Microenvironment. *Clinical Cancer Research,* 13**,** 4345-4354.

SUN, D., WANG, X., ZHANG, H., DENG, L. & ZHANG, Y. 2011. MMP9 mediates MICA shedding in human osteosarcomas. *Cell Biology International,* 35**,** 569-574.

SUTHERLAND, C. L., CHALUPNY, N. J., SCHOOLEY, K., VANDENBOS, T., KUBIN, M. & COSMAN, D. 2002. UL16-binding proteins, novel MHC class I-related proteins, bind to NKG2D and activate multiple signaling pathways in primary NK cells. *J Immunol,* 168**,** 671-9.

TALLERICO, R., TODARO, M., DI FRANCO, S., MACCALLI, C., GAROFALO, C., SOTTILE, R., PALMIERI, C., TIRINATO, L., PANGIGADDE, P. N., LA ROCCA, R., MANDELBOIM, O., STASSI, G., DI FABRIZIO, E., PARMIANI, G., MORETTA, A., DIELI, F., KARRE, K. & CARBONE, E. 2013. Human NK cells selective targeting of colon cancer-initiating cells: a role for natural cytotoxicity receptors and MHC class I molecules. *J Immunol,* 190**,** 2381-90.

TANGYE, S. G., CHERWINSKI, H., LANIER, L. L. & PHILLIPS, J. H. 2000. 2B4-mediated activation of human natural killer cells. *Mol Immunol,* 37**,** 493-501.

TIGUERT, R., GHEILER, E. L., TEFILLI, M. V., BANERJEE, M., GRIGNON, D. J., SAKR, W., WOOD, D. P., JR., POWELL, I. J. & PONTES, J. E. 1998. Racial differences and prognostic significance of tumor location in radical prostatectomy specimens. *Prostate,* 37**,** 230-5.

TIMONEN, T., SAKSELA, E., VIRTANEN, I. & CANTELL, K. 1980. Natural killer cells are responsible for the interferon production induced in human lymphocytes by tumor cell contact. *European Journal of Immunology,* 10**,** 422-427.

TORRE, L. A., BRAY, F., SIEGEL, R. L., FERLAY, J., LORTET-TIEULENT, J. & JEMAL, A. 2015. Global cancer statistics, 2012. *CA Cancer J Clin,* 65**,** 87-108.

TORTORA, G. J. & GRABOWSKI, S. R. 2003. *Principles of Anatomy and Physiology*, John Wiley & Sons, Inc.

TRINCHIERI, G. 1989. Biology of natural killer cells. *Adv Immunol,* 47**,** 187-376.

TRINCHIERI, G., MATSUMOTO-KOBAYASHI, M., CLARK, S. C., SEEHRA, J., LONDON, L. & PERUSSIA, B. 1984. Response of resting human peripheral blood natural killer cells to interleukin 2. *J Exp Med,* 160**,** 1147-69.

TROWSDALE, J. 2001. Genetic and functional relationships between MHC and NK receptor genes. *Immunity,* 15**,** 363-74.

VALDMAN, A., JARAJ, S. J., COMPERAT, E., CHARLOTTE, F., ROUPRET, M., PISA, P. & EGEVAD, L. 2010. Distribution of Foxp3-, CD4- and CD8-positive lymphocytic cells in benign and malignant prostate tissue. *Apmis,* 118**,** 360-5.

VAN KOOYK, Y., VAN DE WIEL-VAN KEMENADE, P., WEDER, P., KUIJPERS, T. W. & FIGDOR, C. G. 1989. Enhancement of LFA-1-mediated cell adhesion by triggering through CD2 or CD3 on T lymphocytes. *Nature,* 342**,** 811-813.

VITALE, M., BOTTINO, C., SIVORI, S., SANSEVERINO, L., CASTRICONI, R., MARCENARO, E., AUGUGLIARO, R., MORETTA, L. & MORETTA, A. 1998. NKp44, a novel triggering surface

molecule specifically expressed by activated natural killer cells, is involved in non-major histocompatibility complex-restricted tumor cell lysis. *J Exp Med,* 187**,** 2065-72.
VITALE, M., CANTONI, C., PIETRA, G., MINGARI, M. C. & MORETTA, L. 2014. Effect of tumor cells and tumor microenvironment on NK-cell function. *European Journal of Immunology,* 44**,** 1582-1592.
VIVIER, E., TOMASELLO, E., BARATIN, M., WALZER, T. & UGOLINI, S. 2008. Functions of natural killer cells. *Nat Immunol,* 9**,** 503-10.
VOLLGER, L. W., TUCK, D. T., SPRINGER, T. A., HAYNES, B. F. & SINGER, K. H. 1987. Thymocyte binding to human thymic epithelial cells is inhibited by monoclonal antibodies to CD-2 and LFA-3 antigens. *J Immunol,* 138**,** 358-63.
VRAL, A., MAGRI, V., MONTANARI, E., GAZZANO, G., GOURVAS, V., MARRAS, E. & PERLETTI, G. 2012. Topographic and quantitative relationship between prostate inflammation, proliferative inflammatory atrophy and low-grade prostate intraepithelial neoplasia: a biopsy study in chronic prostatitis patients. *Int J Oncol,* 41**,** 1950-8.
VYAS, Y. M., MANIAR, H. & DUPONT, B. 2002. Cutting edge: differential segregation of the SRC homology 2-containing protein tyrosine phosphatase-1 within the early NK cell immune synapse distinguishes noncytolytic from cytolytic interactions. *J Immunol,* 168**,** 3150-4.
WATANABE, H., KAIHO, H. & TANAKA, M. 1971. Diagnostic application of ultrasonotomography *Investigative Urology* 8**,** 548-549.
WELCH, H. G., FISHER, E. S., GOTTLIEB, D. J. & BARRY, M. J. 2007. Detection of Prostate Cancer via Biopsy in the Medicare–SEER Population During the PSA Era. *Journal of the National Cancer Institute,* 99**,** 1395-1400.
WESTDORP, H., SKÖLD, A. E., SNIJER, B. A., FRANIK, S., MULDER, S. F., MAJOR, P. P., FOLEY, R., GERRITSEN, W. R. & DE VRIES, I. J. M. 2014. Immunotherapy for Prostate Cancer: Lessons from Responses to Tumor-Associated Antigens. *Frontiers in Immunology,* 5.
WHITESIDE, T. L. 2008. The tumor microenvironment and its role in promoting tumor growth. *Oncogene,* 27**,** 5904-5912.
WHO. 2014. *United Kingdom Cancer Country Profile* [Online]. World Health Organisation. Available: http://www.who.int/cancer/country-profiles/gbr_en.pdf?ua=1.
WILLIAMS, G. S., COLLINSON, L. M., BRZOSTEK, J., EISSMANN, P., ALMEIDA, C. R., MCCANN, F. E., BURSHTYN, D. & DAVIS, D. M. 2007. Membranous structures transfer cell surface proteins across NK cell immune synapses. *Traffic,* 8**,** 1190-204.
WILSON, E. B., EL-JAWHARI, J. J., NEILSON, A. L., HALL, G. D., MELCHER, A. A., MEADE, J. L. & COOK, G. P. 2011. Human tumour immune evasion via TGF-beta blocks NK cell activation but not survival allowing therapeutic restoration of anti-tumour activity. *PLoS One,* 6**,** e22842.
WU, J., SONG, Y., BAKKER, A. B., BAUER, S., SPIES, T., LANIER, L. L. & PHILLIPS, J. H. 1999. An activating immunoreceptor complex formed by NKG2D and DAP10. *Science,* 285**,** 730-2.
WU, J. D., HIGGINS, L. M., STEINLE, A., COSMAN, D., HAUGK, K. & PLYMATE, S. R. 2004. Prevalent expression of the immunostimulatory MHC class I chain-related molecule is counteracted by shedding in prostate cancer. *J Clin Invest,* 114**,** 560-8.
YOSSEPOWITCH, O. 2008. Digital Rectal Examination Remains an Important Screening Tool for Prostate Cancer. *European Urology,* 54**,** 483-484.
YU, H., KORTYLEWSKI, M. & PARDOLL, D. 2007. Crosstalk between cancer and immune cells: role of STAT3 in the tumour microenvironment. *Nat Rev Immunol,* 7**,** 41-51.
YU, X., HARDEN, K., GONZALEZ, L. C., FRANCESCO, M., CHIANG, E., IRVING, B., TOM, I., IVELJA, S., REFINO, C. J., CLARK, H., EATON, D. & GROGAN, J. L. 2009. The surface protein TIGIT suppresses T cell activation by promoting the generation of mature immunoregulatory dendritic cells. *Nat Immunol,* 10**,** 48-57.

YUASA, T., TSUCHIYA, N., KUMAZAWA, T., INOUE, T., NARITA, S., SAITO, M., HORIKAWA, Y., SATOH, S. & HABUCHI, T. 2008. Characterization of prostate cancer detected at repeat biopsy. *BMC Urology,* 8**,** 1-7.

ZITVOGEL, L., TESNIERE, A. & KROEMER, G. 2006. Cancer despite immunosurveillance: immunoselection and immunosubversion. *Nat Rev Immunol,* 6**,** 715-727.